STRUCTURAL RESPONSE AND DESIGN CRITERIA OF FOOTBRIDGES WITH TUNED MASS DAMPERS

A thesis submitted to Imperial College London

for the degree of Doctor of Philosophy by

Natividad Leonor Garcia-Troncoso

Department of Civil and Environmental Engineering

Imperial College of Science, Technology and Medicine

London SW7 2AZ, United Kingdom

January 2020

This work is dedicated to my parents and brother

Natividad and Guillermo[2]

Declaration of Originality

I herewith certify that the work presented in this thesis is my own work. All material in this thesis which is not my own work has been properly acknowledged.

Natividad Leonor Garcia-Troncoso

January 2020, London

Copyright declaration

The copyright of this thesis rests with the author and is made available under a Creative Commons Attribution Non-Commercial No Derivatives licence. Researchers are free to copy, distribute or transmit the thesis on the condition that they attribute it, that they do not use it for commercial purposes and that they do not alter, transform or build upon it. For any reuse or redistribution, researchers must make clear to others the licence terms of this work.

Abstract

During the last decades, the mitigation of the effects of human-induced vibrations has been one of the most critical aspects of footbridges construction. Unexpected vibrations of footbridges under pedestrian actions have shown the necessity of developing more realistic representations of loads transmitted by pedestrians, to obtain an accurate dynamic response. This representation should include all the energy introduced at each step and that their amplitude in the lateral direction is related to the dynamic response of the bridge. The London Millennium Bridge in the UK, the Passerelle Léopold-Sédar-Senghor in Paris, France and the Toda Park cable-stayed footbridge in Japan are some of the famous structures which have been experienced unexpected vibrations. These footbridges required the use of supplemental damping devices to control the human-induced vibrations after their construction. However, there are not guidelines or research work so far which account a realistic representation of pedestrian loads whilst considering these devices. Especially for the cases where the serviceability criteria cannot be fulfilled by using conventional approaches.

Therefore, this research work includes a detailed literature review of studies concerning to footbridges typologies, pedestrian actions, serviceability criteria and supplemental damping devices. The main emphasis given here is to reduce human-induced vibrations in the vertical and lateral direction. As a result, on an exhaustive analysis of the literature review, girder and cable-stayed footbridges using tuned mass dampers under a stochastic pedestrian load model are selected for further parametric studies. For this purpose, a set of footbridges are used to study the benefits of the tuned mass dampers under different pedestrian densities (0.2, 0.6 and 1.0 ped/m^2) and two activities, leisure and commuting. This work has been carried out combining Abaqus, Matlab, Python and Fortran software packages. The main purposes of this study are to improve the understanding of the response of these bridges when TMDs are implemented and to provide design recommendations of optimal locations and properties of these devices. This is to mitigate the dynamic response in girder and cable-stayed footbridges under pedestrian actions.

In this thesis, a methodology of implementation of TMDs and a detail design procedure are given as a guide to select tuned mass dampers when the maximum comfort is not achieved. The design procedure is complemented by the definition of a comprehensive set of design criteria on how to

use supplemental damping devices at the design stage according to the comfort level, mean or maximum, to control the dynamic response in girder and cable-stayed footbridges under pedestrian actions. Based on the parametric studies in both typologies (girder and cable-stayed footbridges), it is shown that tuned mass dampers can be employed at the design stage with efficiencies up to 85% in the reduction of the dynamic response. This can only be achieved if the TMDs are correctly located. For this, it is required to represent and to check the structural accelerations according to the comfort limits. If these responses do not fulfil the serviceability criteria, it is necessary to identify the mode that has a larger contribution to that response. This mode can be identified by representing the response in the frequency domain. Afterwards, the TMD needs to be located at the maximum nodal coordinate where the modal shape dominates the response. In the case that the TMD location is not adequately selected, the TMD efficiency will be decreased, i.e. TMD efficiency $\leq$ 37%. In most of the cases, one tuned mass damper is enough to control human-induced vibration. However, there are some cases where it can be required to consider more than one damper, e.g. for handling reasons due to one damper being bulky or due to the existence of other structural elements. For these cases, the tuned mass dampers employed at the same location have similar efficiency as when one TMD was employed. Besides, for girder footbridges, one vertical TMD can be split into more dampers as long as the location is the maximum nodal coordinates of those modal shapes dominating the response, having flexibility within the ±15% of the span length from that point (with variations of the efficiency around 1.0%). For cable-stayed footbridges with one and two towers, the location will be the maximum nodal coordinates, having a flexibility to shift them along the span, from that location, by ± 10%, and ±6%, with variations in the efficiency of around 9% and 2%, respectively. Likewise, for the lateral direction, the TMD can be split into more devices as long as the location corresponds to the maximum nodal coordinates of those modal shapes dominating the response, with a flexibility of locating the TMDs ±5% along the length from that location.

In conclusion, several design recommendations including TMD mass ratio in accordance with the comfort level, span lengths, pylon shapes, pedestrian densities and activities are provided. Given that the characteristics of both typologies were obtained as representative of the built footbridges, this research work may facilitate the construction of similar footbridges structures whilst avoiding serviceability problems when a TMD is considered at the design stage.

Acknowledgments

Firstly, I would like to express my sincere gratitude to my supervisors Dr Ana M. Ruiz-Teran and Dr Peter J. Stafford, for their continuous encouragement, invaluable guidance in technical and life aspects. Their clear support, patient, discussions, and meetings have contributed to the successful completion of this thesis. I will be forever grateful. I think that this PhD would not have been possible without their support. Dr Ruiz-Teran although it was a really busy season (Christmas and New Year 2019) you have found some time for me in your holidays. I will never be able to thank you for this valuable time. I just can say that you are the best supervisor that someone can have. I hope you can visit me one day in Ecuador.

I am also grateful to Caterina Ramos-Moreno, my colleague and friend, for her guidance, suggestions, and support to complete this study. Your help is very much appreciated. Thanks Caterina. I hope that you and Oscar can visit me in Ecuador.

The financial support of Ecuadorian government (SENECYT) and Escuela Superior Politécnica del Litoral (ESPOL) are gratefully acknowledged.

I would like to thank the academic and staff support, in particular, Fionnuala Ni Dhonnabhain, Callum Munro and Dimitrios Papadakos. I would also like to thank all my friends from the Civil Engineering Department and from the office #429, for being part of my life during these years. They have made my PhD experience much more meaningful. Also, I would like to thank all my closest Ecuadorian friends for the support that they brought me during this time. Even though they are far away, they are an important part of my life. Thanks also for visiting me. Although London is far from my hometown Guayaquil, you have managed to visit me. I will never forget it. In addition, Dr Cecilia Paredes Verduga thanks for encouraging me to pursue this PhD. Your invaluable guidance to consider this big step in my life is very grateful.

And finally, but most importantly, I would like to thank my parents and my brother (Ñanito). They provided huge support, self-discipline, moral support and encouragement to finish this research. Dad and mom thanks for being there for me always, thanks for give me everything

including the high-level education that I have received since I was a kid. Ñanito, thank you for being on this long journey with me and thanks for your support. Thanks for running with me the half-marathon and all the parkruns every Saturday. London has been our home from 2016. We have been very far from our parents but at least I had part of our family here. I will miss you. I just can say this work is dedicated to them. Thanks for everything.

Table of contents

Abstract ..... **v**

Acknowledgments ..... **vii**

List of figures ..... **xiii**

List of tables ..... **xxviii**

Notation ..... **xxxi**

1 Introduction **1**

1.1 General background 1

1.2 Aims and objectives 4

1.3 Thesis outline 7

2 State of the art **10**

2.1 Introduction 10

2.2 Typologies and materials for the footbridges studied in this thesis 10

2.3 Pedestrian actions 16

2.3.2 Dynamic effect of pedestrians in structures 17

2.3.3 Vertical and Lateral loads 18

2.3.4 Pedestrian - structure interaction 22

2.3.5 Deterministic and probabilistic models to represent pedestrians loads 23

2.4 Damping characteristics of footbridges structures 25

2.4.1 Structural damping 26

2.4.2 Supplemental damping devices 29

2.5 Vibration control in footbridges 30

2.5.1 Tuned mass damper design and approaches 33

2.5.2 Built footbridges with supplemental damping devices 42

2.5.3 Current research: inherent drawbacks 43

2.6 Comfort criteria in footbridges 45

2.6.1 Evaluation of the comfort related to vertical vibration 46

2.6.2 Evaluation of the comfort related to lateral vibration 47

2.7 Design, standards, regulations and guidelines 47

2.8 Footbridge dynamics 51

2.9 Concluding remarks 53

3 Research methodology and preliminary analyses 55
3.1 Introduction 55
3.2 Model to represent pedestrian actions 56
3.2.1 Description of the vertical and lateral direction 56
3.2.2 Parameters of the pedestrian load model 58
3.2.3 Description to consider the crowd behaviour 62
3.3 Description of footbridges 63
3.3.1 Girder footbridges 64
3.3.2 Cable-stayed footbridges 66
3.4 Finite element analysis: assumption and representation 69
3.4.1 Finite element representation of girder footbridges 69
3.4.2 Finite element representation of cable-stayed footbridges 76
3.5 Automation of functions to evaluate the dynamic response 82
3.6 Serviceability criteria 83
3.7 Supplemental damping devices 84
3.7.1 Problem formulation 84
3.7.2 Method to choose properties and placement of damping devices 86
3.7.3 Criteria to determine the parameters of tuned mass dampers 87
3.8 Concluding remarks 96
4 Dynamic response of girder footbridges 98
4.1 Introduction 98
4.2 Python versus Abaqus models 98
4.3 Dynamic response in the vertical direction 99
4.3.1 Single tuned mass damper 100
4.3.2 Multiple tuned mass dampers (MTMDs) 103
4.3.3 Cost analysis 107
4.3.4 Design recommendations 110
4.4 Dynamic response in the lateral direction 117
4.5 Concluding remarks 121
5 Dynamic response of cable-stayed footbridges with a single tower 124

5.1 Introduction 124
5.2 Benchmark case for cable-stayed footbridges with a single pylon 125
5.2.1 Modelling characteristics 125
5.2.2 Modal analysis 126
5.2.3 Distribution of step frequencies of the pedestrians 129
5.3 Cable-stayed footbridges with an I-shaped pylon without tuned mass dampers 131
5.3.1 Parametric studies with a span length of 50 m 132
5.3.2 Parametric studies with a span length of 100 m 135
5.3.3 Parametric studies with a span length of 150 m 138
5.4 Cable-stayed footbridges with an I-shaped pylon with tuned mass dampers 141
5.4.1 Parametric studies for 50 m span cable-stayed footbridges 141
5.4.2 Parametric studies for 100 m span cable-stayed footbridges 148
5.4.3 Parametric studies for 150 m span cable-stayed footbridges 153
5.5 Parametric analysis with H-, and A-shaped pylons 156
5.5.1 Dynamic response in the vertical direction 157
5.5.2 Dynamic response in the lateral direction 159
5.6 Cost analysis 161
5.7 Main conclusions and design recommendations 163
6 Dynamic response of cable-stayed footbridges with two towers 173
6.1 Introduction 173
6.2 Benchmark case for cable-stayed footbridges with two pylons 174
6.2.1 Modelling characteristics 174
6.2.2 Modal analysis 175
6.2.3 Distribution of step frequencies of the pedestrians 178
6.3 Cable-stayed footbridges with an I-shaped pylon without tuned mass dampers 180
6.3.1 Parametric studies with a span length of 50 m 180
6.3.2 Parametric studies with a span length of 100 m 184
6.3.3 Parametric studies with a span length of 150 m 187
6.4 Cable-stayed footbridges with an I-shaped pylon with tuned mass dampers 191
6.4.1 Parametric studies with a span length of 50 m 191

6.4.2 Parametric studies with a span length of 100 m 198
6.4.3 Parametric studies with a span length of 150 m 206
6.5 Cable-Stayed footbridges with different pylon's shapes 211
6.6 Cost analysis 216
6.7 Main conclusions and design recommendations 219
7 Conclusions and further research work 229
7.1 Conclusions 229
7.2 Future research 235
Annex A Girder footbridge dataset 237
Annex B Cable-stayed footbridge dataset 239
Annex C Footbridge dataset with supplemental damping devices 241
References 245

List of figures

Figure 1.1: Pedestrians in the Toda Park Bridge in Japan (Nakamura, 2004) 2
Figure 1.2 Pedro e Inés footbridge in Coimbra, Portugal (Structurae, 2015) 3
Figure 1.3: Pedestrian test in the West Bromwich footbridge in the United Kingdom (Caetano & Cunha, 2014) 4
Figure 2.1: (a) Forcheim footbridge in Germany (Seiler et al., 2002). (b) Passerelle du Stade de France (Setra, 2006). (c) The Footbridge at Rotterdam Central Station in the Netherlands (Breman et al., 2011). (d) The T-bridge in Japan (Nakamura & Kawasaki, 2006). (e) The Footbridge Skoda in Poland (Kala et al., 2010) 12
Figure 2.2: (a) Occurrence of girder footbridges according to the number of spans based in a dataset of this typology (Annex A). (b) Span length for one, two, three four and five spans girder footbridges 13
Figure 2.3: (a) Occurrence of cable-stayed footbridges according to the number of spans based in a dataset of these footbridges (Annex B). (b) Span length for one, two and three span cable-stayed footbridges 13
Figure 2.4 Cable arrangements (a) modified fan arrangement, (b) Harp arrangement (Wells & Clash, 2008) 14
Figure 2.5: (a) Occurrence of cable-stayed footbridges according to the pylon shape (Annex B). (b) A-, I- and H-shaped pylons 15
Figure 2.6: Relationship between main span length of cable-stayed footbridges with (a) pylon height above the deck h_p and main span length, and (b) deck depth 15
Figure 2.7 Representation of human-induced forces in (a) vertical, (b) lateral, and (c) longitudinal direction (Živanović et al., 2005) 18
Figure 2.8: Parameters required to define the vertical load introduced by each step (Butz et al., 2007) 20
Figure 2.9: Inverted pendulum (IP) model (Macdonald, 2009) 22
Figure 2.10 Pedestrian load model proposed by Ramos et al. (2014) 25
Figure 2.11: Percentage of footbridges from a dataset of 54 footbridges compiled with supplemental damping devices to reduce human-induced vibrations 31
Figure 2.12: Amplification Factor R as a function of the frequency ratio β 34

Figure 2.13: Frequency response function of (a, b) structural displacement (H_s); and (c, d) TMD relative displacement (H_d)..... 37
Figure 2.14 (a) Steel girder footbridge; (b) Absorber (Weber & Feltrin, 2010)..... 38
Figure 2.15: The London Millennium Bridge (Structurae, 2015) 43
Figure 2.16 (a) Vertical and (b) Lateral critical accelerations as a function of the structural frequencies 50
Figure 2.17 Structural frequencies as a function of the span length..... 53
Figure 3.1 Parameters to define the amplitude of the vertical load 56
Figure 3.2: Vertical human force for step frequencies from 1.3 to 2.4 Hz..... 58
Figure 3.3 Step frequency distribution following a MCMC sampling for a distribution in a footbridge with a span length of 22.5 m for leisure and commuting activities. The value adopted for the standard deviation of the step frequency is 0.15 (Butz et al. 2008) 61
Figure 3.4: Ramos' pedestrian model (Ramos-Moreno, 2015) 62
Figure 3.5: Mesh convergence study (a) Accelerations (m/s^2) vs Number of elements, (b) Error based on the results obtained with 40 elements vs Number of elements, and (c) Vertical acceleration (blue line) and solve time in minutes (orange line) vs the number of elements at mid-span 71
Figure 3.6 Plan views of the decks at certain instants, with the centre of masses of the different pedestrians represented in blue and red circles for those pedestrians entering the structure from the left and the right abutments, respectively. The percentages of pedestrians entering the footbridge from each side, and across the width, have been also represented 73
Figure 3.7 RMS vertical accelerations for a 1-second interval at midspan in a simply supported prestressed concrete footbridge (L= 22.5 m, section type 1) under a pedestrian density of 0.6 ped/m^2 for commuting activities. The average of the 10 simulations is highlighted with a diamond marker. Cases are defined through Figure 3.6 74
Figure 3.8: Normalized vertical accelerations versus the simulation time normalized to t_{ap} 75
Figure 3.9 Normalized vertical accelerations vs the number of simulations..... 76
Figure 3.10 Structural frequencies for beam and shell elements for a cable-stayed footbridge with a span length of 50 m..... 77

Figure 3.11 (a) Differences in deflections for beam and shell elements for a cable-stayed footbridge with a span length of 50 m at different positions along the length of the bridge, (b) Lateral view of the cable-stayed footbridge..... 77
Figure 3.12 Differences in % in peak vertical accelerations at different positions along the length of the bridge for (a) Tower element analysis (b) Deck mesh sensitivity 78
Figure 3.13: Maximum vertical accelerations in the whole deck versus the simulation time for cable-stayed footbridges 79
Figure 3.14: RMS normalized accelerations versus the number of simulations for cable-stayed footbridges without TMDs..... 80
Figure 3.15 Vertical RMS accelerations along the length before and after a tuned mass damper (μ = 0.01) was employed at the first mode in the vertical direction in a cable-stayed footbridge of a 60 m span length considering a pedestrian density of 0.2 ped/m^2 for leisure activities 80
Figure 3.16: Cable-stayed representation in Abaqus (2014) 81
Figure 3.17: Representation of the user amplitude subroutine (UAMP) in Abaqus (2014) 83
Figure 3.18: Summary of the serviceability criteria analysis 84
Figure 3.19 Summary of the dynamic analysis in footbridges under pedestrian loads (Garcia-Troncoso et al., 2017) 86
Figure 3.20: (a) Natural frequencies (b) Peak accelerations for one pedestrian walking with a velocity of 1.4 m/s..... 88
Figure 3.21: Maximum peak accelerations in the vertical direction: a) in a rectangular beam; b) in a T-beam 88
Figure 3.22: Maximum peak vertical accelerations for a set of prestressed concrete girder footbridges with spans ranging from 10 to 45 meters for commuting traffic considering different TMD design criteria under pedestrian densities of 0.6 ped/m^2..... 89
Figure 3.23: Maximum peak vertical accelerations for a set of prestressed concrete girder footbridges ranging from10 to 45 meters for leisure traffic considering different TMD design criteria under pedestrian densities of 0.6 ped/m^2 89
Figure 3.24 Maximum peak accelerations (m/s^2) with and without tuned mass dampers for (a and c) commuting, and (b and d) leisure activities under pedestrian densities of 0.6 ped/m^2..... 91

Figure 3.25: Maximum peak accelerations in a T-beam for (a) commuting and (b) leisure activities under pedestrian densities of 0.6 ped/m^2 92
Figure 3.26: Vertical RMS accelerations with and without tuned mass dampers of a 50 m cable-stayed footbridge with one pylon under pedestrian densities of 0.6 ped/m^2 93
Figure 3.27: (a) Acceleration (m/s^2) and (b) displacement (m) before and after the tuned mass damper is installed in a T-beam for a pedestrian density of 0.6 ped/m^2 for commuting activities94
Figure 3.28 Vertical peak accelerations vs mass ratio (μ) normalized by the values proposed by Asami for a prestressed concrete footbridge with a 22.5 m span under pedestrian densities of 0.6 ped/m^2 for commuting activities..... 95
Figure 3.29 Vertical peak accelerations vs frequency ratio (α_{opt}) and damping ratio (ξ_{opt}) normalized by the values proposed by Asami for a prestressed concrete footbridge with a 22.5 m span under pedestrian densities of 0.6 ped/m^2 for commuting activities..... 96
Figure 4.1: Peak accelerations for a girder footbridge with a 20 m span and a 4 m width using Abaqus a) in the time domain, b) in the frequency domain..... 99
Figure 4.2: Peak accelerations for a girder footbridge with a 20 m span and a 4 m width using Python a) in the time domain, b) in the frequency domain..... 99
Figure 4.3: Simply-supported prestressed concrete (section type 1) footbridge with a 22.5 m span under pedestrian densities of 0.6 ped/m^2 for commuting activities: (a) peak vertical accelerations at mid-span when a TMD (μ= 0.05) is located at different positions along the length of the bridge, (b) Frequency amplitude spectrum of the peak vertical accelerations at mid-span when a TMD (μ= 0.05) located at 0.35 L and 0.5L and when no supplemental damping is implemented..... 101
Figure 4.4: Maximum vertical peak accelerations for a set of prestressed concrete footbridges (section type 1 in Table 3.3) with spans ranging from 10 up to 45 meters for leisure activities under pedestrian densities of 0.6 ped/m^2 102
Figure 4.5: Maximum dynamic sagging bending moments along the length before and after a TMD (μ= 0.04) was employed at mid-span in a prestressed concrete footbridge of a 25 m span length considering a pedestrian density of 0.6 ped/m^2 for leisure activities. The static bending moment induced by the weight of the pedestrians is also represented 103
Figure 4.6: (a) Distribution of pedestrian frequencies for leisure (red) and commuting (blue) activities for pedestrian densities of 0.6 ped/m^2 for the UK population (b) Structural frequency

versus the span length for a prestressed concrete (cross-section type 1) footbridge where the blue lines represent the range of vertical frequencies that can be excited by pedestrians 104
Figure 4.7: Maximum vertical peak accelerations for prestressed concrete (section type 1 in Table 3-3) footbridges with and without TMDs (each of them with $\mu = 0.05$) (see Table 4.1), under pedestrian densities of 0.6 ped/m^2 (commuters) for spans ranging from 10 m (a) up to 45 meters, (b) up to 100 m..... 105
Figure 4.8 Cost analysis for different slab depth (m) when one or multiple TMDs are employed in the design of a prestressed concrete footbridge with a 11.25 m span length, for different TMD expected lives of 20, 25, 33.3, 50 and 100 years, with pedestrian densities of 0.6 ped/m^2 (commuters) 109
Figure 4.9 Maximum vertical accelerations for Section Types 2, 3, and 4 (Table 3.3), when one, two, three or four TMDs are implemented at the maximum nodal coordinate of the modal shape with a larger contribution in the dynamic response, under pedestrian densities of 0.6 ped/m^2 (commuting activities) 111
Figure 4.10 Maximum vertical accelerations for Section Types 5, 6, and 7 (Table 3.3), when one, two, three or four TMDs are implemented at the maximum nodal coordinate of the modal shape with a larger contribution in the dynamic response, under pedestrian densities of 0.6 ped/m^2 (commuting activities) 113
Figure 4.11: Maximum vertical accelerations for Section Types 8, 9, and 10 (Table 3.3), when one, two, three or four TMDs are implemented at the maximum nodal coordinate of the modal shape with a larger contribution in the dynamic response, under pedestrian densities of 0.6 ped/m^2 (commuting activities) 115
Figure 4.12 Maximum lateral peak accelerations in prestressed (section type 1 in Table 3.3) footbridges with spans ranging from 20 up to 100 m under pedestrian densities of 0.6 ped/m^2 for commuting traffic..... 117
Figure 4.13 Structural lateral frequencies versus the span length for a slab depth of L/10 under a pedestrian density of 0.6 ped/m^2 for commuting activities where the green lines represent the range of lateral frequencies that can be excited by pedestrians 118

Figure 4.14: Maximum lateral peak accelerations for prestressed (section type 1 in Table 3.3) footbridges with spans ranging from 20 up to 100 m under pedestrian densities of 0.6 ped/m^2 (commuters) for width/span ratios of 1/20 118
Figure 4.15 Maximum lateral accelerations for Section Types 4, 5 and 6 (Table 3.3) under pedestrian densities of 0.6 ped/m^2 (commuters and leisure activities) with and without TMDs 120
Figure 5.1 Geometry and plan view of the 50 m benchmark cable-stayed footbridge with a single pylon. Dimensions in meters (m) (Ramos-Moreno, 2015) 125
Figure 5.2 Modal frequencies of 50 m span cable-stayed footbridge with an I-shaped pylon considering a pedestrian density of 0.6 ped/m^2 126
Figure 5.3 Modal frequencies of 100 m span cable-stayed footbridge with an I-shaped pylon considering a pedestrian density of 0.6 ped/m^2 127
Figure 5.4 Modal frequencies of 150 m span cable-stayed footbridge with an I-shaped pylon considering a pedestrian density of 0.6 ped/m^2 128
Figure 5.5 Distribution of pedestrian frequencies for commuting (blue) and leisure (red) activities for pedestrian densities of 0.2, 0.6 and 1.0 ped/m^2 for the UK population in a 50 m span cable-stayed footbridge 130
Figure 5.6 Structural (a) vertical, (b) lateral and (c and d) torsional frequencies versus the span length in cable-stayed footbridges with one tower under a pedestrian density of 0.6 ped/m^2 for commuting activities 131
Figure 5.7 Peak and 1s-RMS vertical accelerations for a CSF of a span length of 50 m under a pedestrian density of 0.6 ped/m^2 for commuting activities 132
Figure 5.8 Frequency domain analysis at (a) 18.5 m, and (b) 25 m (L/2) from the pylon for a CSF of a span length of 50 m with one tower under a pedestrian density of 0.6 ped/m^2 for commuting activities in the vertical direction 133
Figure 5.9 Peak and 1s-RMS lateral accelerations for a CSF of a span length of 50 m under a pedestrian density of 0.6 ped/m^2 for commuting activities 134
Figure 5.10 Frequency domain analysis at (a) 18.5 m, and (b) 25 m (L/2) from the pylon for a CSF of a span length of 50 m with one tower under a pedestrian density of 0.6 ped/m^2 for commuting activities in the lateral direction 134

Figure 5.11 Maximum vertical and lateral peak accelerations for cable-stayed footbridges with a span length of 50 m under different pedestrian densities for commuting and leisure activities. 135
Figure 5.12 Peak and 1s-RMS vertical accelerations for a CSF of a span length of 100 m under a pedestrian density of 0.6 ped/m^2 for commuting activities..... 136
Figure 5.13 Frequency domain analysis at (a) at 25 m, and (b) 50 m (L/2) from the pylon for a CSF of a span length of 100 m with one tower under a pedestrian density of 0.6 ped/m^2 for commuting activities in the vertical direction..... 136
Figure 5.14 Peak and 1s-RMS lateral accelerations for a cable-stayed footbridge with a span length of 100 m under a pedestrian density of 0.6 ped/m^2 for commuting activities 137
Figure 5.15 Frequency domain analysis at (a) at 25 m, and (b) 50 m (L/2) from the pylon in the lateral direction for a cable-stayed footbridge with a span length of 100 m with one tower under a pedestrian density of 0.6 ped/m^2 for commuting activities..... 137
Figure 5.16 Maximum vertical and lateral peak accelerations for cable-stayed footbridges with a span length of 100 m under different pedestrian densities for commuting and leisure activities138
Figure 5.17 Peak and 1s-RMS vertical accelerations for a CSF of a span length of 150 m under a pedestrian density of 0.6 ped/m^2 for commuting activities..... 139
Figure 5.18 Frequency domain analysis at (a) 45 m, and (b) 75 m (L/2) from the pylon in the vertical direction for a cable-stayed footbridge with a span length of 150 m with one tower under a pedestrian density of 0.6 ped/m^2 for commuting activities..... 139
Figure 5.19 Peak and 1s-RMS lateral accelerations for a cable-stayed footbridge with a span length of 150 m under a pedestrian density of 0.6 ped/m^2 for commuting activities..... 140
Figure 5.20 Frequency domain analysis at (a) 45 m and, (b) 75 m (L/2) from the pylon in the lateral direction for a cable-stayed footbridge with a span length of 150 m with one tower under a pedestrian density of 0.6 ped/m^2 for commuting activities..... 140
Figure 5.21 Maximum vertical and lateral peak accelerations for cable-stayed footbridges with a span length of 150 m under different pedestrian densities for commuting and leisure activities141
Figure 5.22 Peak vertical accelerations for a cable-stayed footbridge with a span length of 50 m under a pedestrian density of 0.6 ped/m^2 when different TMD mass ratios (0.05 and 0.07) are employed for commuting activities 142

Figure 5.23 Peak lateral accelerations for a cable-stayed footbridge with a span length of 50 m under a pedestrian density of 0.6 ped/m^2 when different TMD mass ratios (0.01 and 0.03) are employed for commuting activities 143
Figure 5.24 Peak vertical accelerations for cable-stayed footbridges with a span length of 50 m under pedestrian densities of 0.2, 0.6 and 1.0 ped/m^2 when different TMD mass ratios are employed for (a) commuting and (b) leisure activities 144
Figure 5.25 Peak lateral accelerations for cable-stayed footbridges with a span length of 50 m under pedestrian densities of 0.2, 0.6 and 1.0 ped/m^2 when different TMD mass ratios are employed for (a) commuting and (b) leisure activities 145
Figure 5.26 Plan view for a CSF with a span length of 50 with one tower where the red dot #5 corresponds to the nodal coordinates of those modal shapes with a larger contribution (V2) in vertical direction located at 28 m from the left support 145
Figure 5.27 Plan view for a CSF with a span length of 50 m with one tower where the red dot # 5 corresponds to the nodal coordinates of those modal shapes with a larger contribution in the lateral direction (L1) located at 25 m (L/2) from the pylon 147
Figure 5.28 Sagging and hogging bending moments along the length before and after a TMD (μ= 0.05) was employed at 18 m from the pylon in a 50 m span cable-stayed footbridge considering a pedestrian density of 0.6 ped/m^2 for commuting activities 148
Figure 5.29 Vertical modes 1 and 2 for a cable-stayed footbridge with a span length of 100 m 150
Figure 5.30 Maximum vertical peak accelerations for a CSF with a span length of 100 m when a TMD was employed in different locations based on Table 5.6 for a pedestrian density of 0.6 ped/m^2 for commuting activities 151
Figure 5.31 Peak vertical accelerations for cable-stayed footbridges with a span length of 100 m under pedestrian densities of 0.2, 0.6 and 1.0 ped/m^2 when different TMD mass ratios are employed for (a) commuting and (b) leisure activities 152
Figure 5.32 Peak lateral accelerations for cable-stayed footbridges with a span length of 100 m under pedestrian densities of 0.2, 0.6 and 1.0 ped/m^2 when different TMD mass ratios are employed for (a) commuting and (b) leisure activities 153
Figure 5.33 Maximum nodal coordinates for modal shapes with a larger contribution in the critical acceleration where the TMDs were located in (a) vertical and (b) lateral direction 154

Figure 5.34 Peak vertical accelerations for cable-stayed footbridges with a span length of 150 m under pedestrian densities of 0.2, 0.6 and 1.0 ped/m^2 when different TMD mass ratios are employed for (a) commuting and (b) leisure activities 155
Figure 5.35 Peak lateral accelerations for cable-stayed footbridges with a span length of 150 m under pedestrian densities of 0.2, 0.6 and 1.0 ped/m^2 when different TMD mass ratios are employed for (a) commuting and (b) leisure activities 156
Figure 5.36 Structural (a) vertical, (b) lateral and (c and d) torsional frequencies versus the span length in cable-stayed footbridges with different pylon's shapes under a pedestrian density of 0.6 ped/m^2 for commuting activities 157
Figure 5.37 Vertical peak accelerations (m/s^2) for a cable-stayed footbridge with a span length of 50 m for (a) commuting and (b) leisure activities for different pylon shapes 158
Figure 5.38 Vertical peak accelerations (m/s^2) for a cable-stayed footbridge with a span length of 100 m for (a) commuting and (b) leisure activities for different pylon shapes 159
Figure 5.39 Vertical peak accelerations (m/s^2) for a cable-stayed footbridge with a span length of 150 m for (a) commuting and (b) leisure activities for different pylon shapes 159
Figure 5.40 Lateral peak accelerations (m/s^2) for a cable-stayed footbridge with a span length of 50 m for (a) commuting and (b) leisure activities for different pylon shapes 160
Figure 5.41 Lateral peak accelerations (m/s^2) for a cable-stayed footbridge with a span length of 100 m for (a) commuting and (b) leisure activities for different pylon shapes 160
Figure 5.42 Lateral peak accelerations (m/s^2) for a cable-stayed footbridge with a span length of 150 m for (a) commuting and (b) leisure activities for different pylon shapes 161
Figure 5.43 (a) Vertical and (b) lateral peak accelerations according to the span length for CSF with one tower with a slab depth of 0.2 and 0.3 m for pedestrian densities of 0.6 ped/m^2 (commuters) 162
Figure 5.44 Cost analysis for different slab thickness (0.2 and 0.3 m) when one TMD is employed in the design of cable-stayed footbridges with 50, 100 and 150 span lengths with pedestrian densities of 0.6 ped/m^2 (commuters) 163
Figure 5.45 Vertical peak accelerations according to the span length for different pedestrian densities without TMDs according to the envelope of the I-, A-, and H-shaped pylons for CSFs with one tower 166

Figure 5.46 Lateral peak accelerations according to the span length for different pedestrian densities without TMDs according to the envelope of the I- and A-shaped pylon for CSFs with one tower 166
Figure 5.47 Lateral peak accelerations according to the span length for different pedestrian densities without TMDs according to the H-shaped pylon for CSFs with one tower 167
Figure 5.48 Vertical peak accelerations and comfort levels for different TMD mass ratios (μ), active in the vertical direction, and for different span lengths under pedestrian densities of a) 0.2, b) 0.6 and c) 1.0 ped/m^2 according to the envelope of the I- A, and H-shaped pylons for CSFs with one tower..... 168
Figure 5.49 Lateral peak accelerations and comfort levels for different TMD mass ratios (μ), active in the lateral direction, and for different span lengths under pedestrian densities of a) 0.2, b) 0.6 and c) 1.0 ped/m^2 according to the envelope of the I- and A-shaped pylons for CSFs with one tower 169
Figure 5.50 Lateral peak accelerations and comfort levels for different TMD mass ratios (μ), active in the lateral direction, and for different span lengths under pedestrian densities of a) 0.2, b) 0.6 and c) 1.0 ped/m^2 according to the H-shaped pylon for CSFs with one tower..... 170
Figure 5.51 TMD implementation: a flowchart to include TMDs in cable-stayed footbridges with one tower..... 172
Figure 6.1 Geometry, support configurations and plan view of the cable-stayed footbridges with two pylons. Dimensions in meters (m) (Ramos-Moreno, 2015) 174
Figure 6.2 Modal frequencies of 50 m span cable-stayed footbridge with two towers considering a pedestrian density of 0.6 ped/m^2..... 175
Figure 6.3 Modal frequencies of cable-stayed footbridges with a span length of 100 m with two towers considering a pedestrian density of 0.6 ped/m^2..... 176
Figure 6.4 Modal frequencies of cable-stayed footbridges with a span length of 150 m with two towers considering a pedestrian density of 0.6 ped/m^2..... 177
Figure 6.5 Distribution of pedestrian frequencies for commuting (blue) and leisure (red) activities for pedestrian densities of 0.2, 0.6 and 1.0 ped/m^2 in a 50 m span cable-stayed footbridge with two towers..... 179

Figure 6.6 Structural (a) vertical, (b) lateral and (c, d) torsional frequencies versus the span length in cable-stayed footbridges with two towers under a pedestrian density of 0.6 ped/m^2 for commuting activities 180
Figure 6.7 Peak and 1s-RMS vertical accelerations for a CSF of a span length of 50 m with two towers under a pedestrian density of 0.6 ped/m^2 for commuting activities 181
Figure 6.8 Peak and 1s-RMS lateral accelerations for a CSF with a span length of 50 m with two towers under a pedestrian density of 0.6 ped/m^2 for commuting activities 182
Figure 6.9 Frequency domain analysis at (a) 12.5 m (L/4) and (b) 25.0 m (L/2) from the pylon for a CSF of a span length of 50 m with two towers under a pedestrian density of 0.6 ped/m^2 for commuting activities in the vertical direction 182
Figure 6.10 Frequency domain analysis at (a) 12.5 m (L/4) and (b) 25.0 m (L/2) from the pylon for a CSF of a span length of 50 m with two towers under a pedestrian density of 0.6 ped/m^2 for commuting activities in the lateral direction 183
Figure 6.11 Maximum (a) vertical and (b) lateral peak accelerations at mid-span for cable-stayed footbridges with a span length of 50 m for commuting and leisure activities 184
Figure 6.12 Peak and 1s-RMS vertical accelerations for a CSF of a span length of 100 m with two towers under a pedestrian density of 0.6 ped/m^2 for commuting activities 185
Figure 6.13 Peak and 1s-RMS lateral accelerations for a CSF of a span length of 100 m with two towers under a pedestrian density of 0.6 ped/m^2 for commuting activities 185
Figure 6.14 Frequency domain analysis at (a) 25 m (L/4) and (b) 50 m (L/2) from the pylon for a CSF of a span length of 100 m with two towers under a pedestrian density of 0.6 ped/m^2 for commuting activities in the vertical direction 186
Figure 6.15 Frequency domain analysis at (a) 25 m (L/4) and (b) 50 m (L/2) from the pylon for a CSF of a span length of 100 m with two towers under a pedestrian density of 0.6 ped/m^2 for commuting activities in the lateral direction 186
Figure 6.16 Maximum (a) vertical and (b) lateral peak accelerations at mid-span for cable-stayed footbridges with a span length of 100 m with two towers for commuting and leisure activities 187
Figure 6.17 Peak and 1s-RMS vertical accelerations for a CSF of a span length of 150 m with two towers under a pedestrian density of 0.6 ped/m^2 for commuting activities 188

Figure 6.18 Peak and 1s-RMS lateral accelerations for a CSF with a span length of 150 m with two towers under a pedestrian density of 0.6 ped/m^2 for commuting activities 189
Figure 6.19 Frequency domain analysis at (a) 37.5 (L/4) and (b) 75.0 m (L/2) from the pylon for a CSF of a span length of 150 m with two towers under a pedestrian density of 0.6 ped/m^2 for commuting activities in the vertical direction..... 189
Figure 6.20 Frequency domain analysis at (a) 37.5 (L/4) and (b) 75.0 m (L/2) from the pylon for a CSF of a span length of 150 m with two towers under a pedestrian density of 0.6 ped/m^2 for commuting activities in the lateral direction..... 190
Figure 6.21 Maximum (a) vertical and (b) lateral peak accelerations at mid-span for cable-stayed footbridges with a span length of 150 m with two towers for commuting and leisure activities 191
Figure 6.22 Plan view for a CSF with a span length of 50 m with two towers where the red dot #5 corresponds to the nodal coordinates of those modal shapes with a greater contribution (V1) located at 25.0 m (L/2) from the pylon 192
Figure 6.23 Maximum nodal coordinates for modal shapes dominating the response where the tuned mass damper is located in the vertical and lateral direction for a cable-stayed footbridge with a span length of 50 m with two towers 194
Figure 6.24 Peak vertical accelerations for a cable-stayed footbridge with a span length of 50 m with two towers under a pedestrian density of 0.6 ped/m^2 when a TMD (μ= 0.06) located at 25 m (L/2) from the pylon is employed for commuting activities..... 195
Figure 6.25 Peak lateral accelerations for a cable-stayed footbridge with a span length of 50 m with two towers under a pedestrian density of 0.6 ped/m^2 when a TMD (μ= 0.03) located at 25 m (L/2) from the pylon is employed for commuting activities..... 195
Figure 6.26 Peak vertical accelerations for cable-stayed footbridges with a span length of 50 m with two towers under pedestrian densities of 0.2, 0.6 and 1.0 ped/m^2 when different TMD mass ratios are considered for (a) commuting and (b) leisure activities..... 197
Figure 6.27 Peak lateral accelerations for cable-stayed footbridges with a span length of 50 m with two towers under pedestrian densities of 0.2, 0.6 and 1.0 ped/m^2 when different TMD mass ratios are considered for (a) commuting and (b) leisure activities 197

Figure 6.28 Sagging bending moments along the length before and after a TMD (μ= 0.06) is employed at 25 m (L/2) from the pylon in a 50 m span cable-stayed footbridge with two towers considering a pedestrian density of 0.6 ped/m^2 for commuting activities 198
Figure 6.29 Peak vertical accelerations for a cable-stayed footbridge with a span length of 100 m with two towers under a pedestrian density of 0.6 ped/m^2 for commuting activities when TMDs are employed according to Table 6.6 200
Figure 6.30 Peak vertical accelerations for cable-stayed footbridges with a span length of 100 m with two towers under pedestrian densities of 0.2, 0.6 and 1.0 ped/m^2 when different TMD mass ratios are considered for (a) commuting and (b) leisure activities 201
Figure 6.31 Comparison of the vertical peak accelerations using a slab depth of 0.2 and 0.3 m for cable-stayed footbridges with a span length of 100 m with two towers using different pedestrian scenarios for a) commuting and b) leisure activities 202
Figure 6.32 Vertical peak accelerations with tuned mass dampers using a slab depth of 0.3 m for cable-stayed footbridges with a span length of 100 m with two towers using different pedestrian scenarios for (a)commuting and (b) leisure activities 203
Figure 6.33 Peak lateral accelerations for cable-stayed footbridges with a span length of 100 m with two towers under pedestrian densities of 0.2, 0.6 and 1.0 ped/m^2 when different TMD mass ratios are considered for (a) commuting and (b) leisure activities 204
Figure 6.34 Comparison of the lateral peak accelerations using a slab depth of 0.2 and 0.3 m for cable-stayed footbridges with a span length of 100 m with two towers using different pedestrian scenarios for a) commuting and b) leisure activities 205
Figure 6.35 Lateral peak accelerations with tuned mass dampers using a slab depth of 0.3 m for cable-stayed footbridges with a span length of 100 m with two towers using different pedestrian scenarios for (a) commuting and (b) leisure activities 205
Figure 6.36 Maximum nodal coordinates for modal shapes with a larger contribution in the critical acceleration for the (a) third vertical mode (V3) and, the (b) first lateral mode (L1) 206
Figure 6.37 Peak vertical accelerations for cable-stayed footbridges with a span length of 150 m with two towers under pedestrian densities of 0.2, 0.6 and 1.0 ped/m^2 when different TMD mass ratios are considered for (a) commuting and (b) leisure activities 207

Figure 6.38 Peak lateral accelerations for cable-stayed footbridges with a span length of 150 m with two towers under pedestrian densities of 0.2, 0.6 and 1.0 ped/m^2 when different TMD mass ratios are considered for (a) commuting and (b) leisure activities..... 208
Figure 6.39 Comparison of the vertical peak accelerations using a slab depth of 0.2 and 0.3 m for cable-stayed footbridges with a span length of 150 m with two towers using different pedestrian scenarios for (a) commuting and (b) leisure activities..... 209
Figure 6.40 Comparison of the lateral peak accelerations using a slab depth of 0.2 and 0.3 m for cable-stayed footbridges with a span length of 150 m with two towers using different pedestrian scenarios for (a) commuting and (b) leisure activities..... 209
Figure 6.41 Vertical peak accelerations with tuned mass dampers using a slab depth of 0.3 m for cable-stayed footbridges with a span length of 150 m with two towers using different pedestrian scenarios for (a) commuting and (b) leisure activities..... 210
Figure 6.42 Lateral peak accelerations with tuned mass dampers using a slab depth of 0.3 m for cable-stayed footbridges with a span length of 150 m with two towers using different pedestrian scenarios for (a) commuting and (b) leisure activities..... 211
Figure 6.43 Structural (a) vertical, (b) lateral and (c) torsional frequencies versus the span length in cable-stayed footbridges with different pylon's shapes under a pedestrian density of 0.6 ped/m^2 for commuting activities 212
Figure 6.44 Vertical peak accelerations for cable-stayed footbridges with a span length of 50 m with two towers for (a)commuting and (b) leisure activities using different pylon shapes..... 213
Figure 6.45 Lateral peak accelerations for cable-stayed footbridges with a span length of 50 m with two towers for (a)commuting and (b) leisure activities using different pylon shapes..... 213
Figure 6.46 Vertical peak accelerations for cable-stayed footbridges with a span length of 100 m with two towers for (a) commuting and (b) leisure activities using different pylon shapes..... 214
Figure 6.47 Lateral peak accelerations for cable-stayed footbridges with a span length of 100 m with two towers for (a) commuting and (b) leisure activities using different pylon shapes..... 215
Figure 6.48 Vertical peak accelerations for cable-stayed footbridges with a span length of 150 m with two towers for (a) commuting and (b) leisure activities using different pylon shapes..... 215
Figure 6.49 Lateral peak accelerations for cable-stayed footbridges with a span length of 150 m with two towers for (a) commuting and (b) leisure activities using different pylon shapes..... 216

Figure 6.50 (a) Vertical and (b) lateral peak accelerations according to the span length for CSF with two towers with a slab depth of 0.2 and 0.3 m for pedestrian densities of 0.6 ped/m^2 (commuters) 217
Figure 6.51 Cost analysis for different slab thickness (m) when one TMD is employed in the design of cable-stayed footbridges with a span length of 50 m with two towers for pedestrian densities of 0.6 ped/m^2 (commuters) 218
Figure 6.52 Vertical peak accelerations according to the span length for different pedestrian densities without TMDs according to the envelope of the I-, A- and H-shaped pylons for CSFs with two towers 221
Figure 6.53 Lateral peak accelerations according to the span length for different pedestrian densities without TMDs according to the envelope of the I- and H-shaped pylons for CSFs with two towers 222
Figure 6.54 Lateral peak accelerations according to the span length for different pedestrian densities without TMDs according to the A-shaped pylon for CSFs with two towers 222
Figure 6.55 Vertical peak accelerations and comfort levels for different TMD mass ratios (μ), active in the vertical direction, and for different span lengths under pedestrian densities of a) 0.2, b) 0.6 and c) 1.0 ped/m^2 according to the envelope of the I-, A- and H-shaped pylons for CSFs with two towers 224
Figure 6.56 Lateral peak accelerations and comfort levels for different TMD mass ratios (μ), active in the lateral direction, and for different span lengths under pedestrian densities of a) 0.2, b) 0.6 and c) 1.0 ped/m^2 according to the envelope of the I- and H-shaped pylons for CSFs with two towers 225
Figure 6.57 Lateral peak accelerations and comfort levels for different TMD mass ratios (μ), active in the lateral direction, and for different span lengths under pedestrian densities of a) 0.2, b) 0.6 and c) 1.0 ped/m^2 according to the A-shaped pylon for CSFs with two towers 226
Figure 6.58 TMD implementation: a flowchart to include TMDs in cable-stayed footbridges with two towers 228

List of tables

Table 2.1: Footbridges with supplemental damping devices 11
Table 2.2 Step frequencies of pedestrians (Ingólfsson et al., 2012) 19
Table 2.3: Properties shown in Figure 2.8 to define the vertical loads for different step frequencies 21
Table 2.4 Common values of damping ratio ξ according to the structural material 28
Table 2.5: Structural protective systems (Soong & Dargush, 1997) 29
Table 2.6: Optimum damping ratio (α_{opt}) and optimum frequency ratio (ξ_{opt}) according to Den Hartog, Warburton, Krenk and Asami criteria 36
Table 2.7: Vertical accelerations on the girder footbridge (Weber & Feltrin, 2010) 38
Table 2.8: Common values of damping ratio ξ for footbridges recommended by BSI (2003) 48
Table 2.9: Damping ratios according to the material's structure (ISO 2005) 48
Table 2.10: Acceleration range for vertical and lateral vibration (Setra, 2006) 49
Table 2.11 Frequency ranges in the vertical, longitudinal and lateral direction (Setra, 2006) 49
Table 2.12 Damping ratios for different material's structure (Setra, 2006) 50
Table 3.1: Median values of the parameters to define the vertical load amplitude (Ramos-Moreno, 2015) 57
Table 3.2: Values of the factor φj according to the purpose of the journey 60
Table 3.3: The most common cross-sections and materials in girder footbridges (Ramos-Moreno, 2015) 65
Table 3.4: Structural materials characteristics of girder footbridges (Ramos-Moreno, 2015) 66
Table 3.5: Geometric characteristics of cable-stayed footbridges for the parametric studies (Ramos-Moreno, 2015) 67
Table 3.6: Structural materials used for the deck and pylons of the cable-stayed footbridges in this thesis 68
Table 3.7: Steel characteristics of the stays in the cable-stayed footbridges 68
Table 3.8: Footbridges that will be evaluated for further parametric studies 82
Table 3.9: Tuned mass damper properties required to mitigate the human-induced vibrations in the footbridges considered in Figure 3.22 and Figure 3.23 90
Table 3.10: Design values for the tuned mass damper according to the different TMD's criteria 92

Table 4.1 Tuned mass damper properties (all with μ=0.05) required to mitigate the human-induced vibrations in the footbridges considered in Figure 4.7 106
Table 4.2: Material unit costs used in this analysis 107
Table 4.3 Cost analysis for different slab depth (m) when one or multiple tuned mass dampers are employed for a prestressed concrete footbridge based on Figure 4.8 for different TMD expected lives of 20, 25, 33.3, 50 and 100 years 109
Table 4.4 Tuned mass damper properties according to the span length under pedestrian densities of 0.6 ped/m^2 for commuting and leisure traffic 112
Table 4.5 Tuned mass damper properties according to the span length under pedestrian densities of 0.6 ped/m^2 for commuting and leisure traffic 114
Table 4.6: Tuned mass damper properties according to the span length under pedestrian densities of 0.6 ped/m^2 for commuting and leisure traffic. For those cases in which the accelerations do not satisfy the comfort criterion, the value of the TMD efficiency is not included(-) 116
Table 4.7 Tuned mass damper properties according to the structural section under 0.6 ped/m^2 for commuting and leisure activities based on Figure 4.14 119
Table 4.8 Tuned mass damper properties according to the structural section under 0.6 ped/m^2 for commuting and leisure activities based on Figure 4.15 121
Table 5.1 Frequencies (in Hz) of 50 m span cable-stayed footbridge when the bridge is empty and when it is loaded with different pedestrian densities 127
Table 5.2 Frequencies (in Hz) of 100 m span cable-stayed footbridge when the bridge is empty and when it is loaded with different pedestrian densities 128
Table 5.3 Frequencies (in Hz) of 150 m span cable-stayed footbridge when the bridge is empty and when it is loaded with different pedestrian densities 129
Table 5.4 Peak vertical accelerations and TMD efficiency along the deck for a CSF with a span length of 50 m with one tower under pedestrian densities of 0.6 ped/m^2 for commuting activities when a TMD (μ= 0.07) is located at different abscises along the length 146
Table 5.5 Peak lateral accelerations and TMD efficiency along the deck for a CSF with a span length of 50 m with one tower under pedestrian densities of 0.6 ped/m^2 for commuting activities when a TMD (μ= 0.03) is located at different abscises along the length 147

Table 5.6 Location where the tuned mass dampers were employed for the parametric studies for a CSF with a span length of 100 m 149
Table 5.7 Structural vertical, lateral and torsional modes dominating the response in cable-stayed footbridges with different pylon's shapes under a pedestrian density of 0.6 ped/m^2 for commuting activities based on Figure 5.36 164
Table 6.1 Frequencies (Hz) of 50 m span cable-stayed footbridge with two towers when the bridge is empty and when it is loaded with different pedestrian densities 176
Table 6.2 Frequencies (Hz) of 100 m span cable-stayed footbridge with two towers when the bridge is empty and when it is loaded with different pedestrian densities 177
Table 6.3 Frequencies (Hz) of 150 m span cable-stayed footbridge with two towers when the bridge is empty and when it is loaded with different pedestrian densities 178
Table 6.4 Peak vertical accelerations and TMD efficiency along the deck for a CSF with a span length of 50 m with two towers under pedestrian densities of 0.6 ped/m^2 for commuting activities when a TMD (μ= 0.06) is located at different abscises along the length 193
Table 6.5 Peak lateral accelerations and TMD efficiency along the deck for a CSF with a span length of 50 m (L/2) with two towers under pedestrian densities of 0.6 ped/m^2 for commuting activities when a TMD (μ= 0.03) is located at different abscises along the length 193
Table 6.6 Location where the tuned mass dampers were employed for the parametric studies for a CSF with two towers with a span length of 100 m 199
Table 6.7: TMD cost used in this analysis according to Maurer supplier (Benicke, 2019) 218
Table 6.8 Structural vertical, lateral and torsional modes dominating the response in cable-stayed footbridges with different pylon's shapes under a pedestrian density of 0.6 ped/m^2 for commuting activities based on Figure 6.43 219

Notation

Abbreviations

DAF	Dynamic amplification factor
CSF	Cable-stayed footbridges
GFRP	Glass-fibre reinforced polymers
TMD	Tuned mass damper
MCMC	Markov chain Monte Carlo simulation
MTMD	Multiple tuned mass dampers
CoM	Pedestrian's centre of mass
RMS	Root-mean-square accelerations
UAMP	User Amplitude subroutine in FORTRAN

Symbols

$\ddot{u}$	Acceleration
$\ddot{y}$	Acceleration of the CoM of pedestrian
ϕ_j	Aim of the journey factor
Ω_p	Angular frequency of the lateral movements of the CoM
$p(t)$	Applied loading in time
t_{ap}	Average time required by a pedestrian to cross the bridge
L	Cable-stayed footbridge main span length
L_k	Cable-stayed footbridge side span length
f_{ck}	Compressive strength of concrete
ρ_c	Concrete density
ν_c	Concrete Poisson's ratio
E_c	Concrete Young's modulus
c	Damping matrix
D_p	Distance between abutment and first cable anchorage
ϕ_d	Flow density factor

$\boldsymbol{F}_p$	Force due to the interaction with other pedestrians
$\boldsymbol{F}_b$	Force due to the interaction with boundaries
ω_a	Frequency of the tuned mass damper
g	Gravity acceleration
u_s	Lateral displacement of the structure
F_l	Lateral force applied on the structure
M	Mass matrix
μ	Mass ratio
u_o	Maximum dynamic displacement
$f_{y,b}$	Maximum stress of bars
g_N	Normal components of the gravity acceleration
g_L	Parallel components of the gravity acceleration
a_p	Pedestrian age
$\boldsymbol{F}_D$	Pedestrian driving force
v_f	Pedestrian free velocity
w_s	Pedestrian half-step width
h_{pd}	Pedestrian height
$f_{l,p}$	Pedestrian lateral step frequency
f_p	Pedestrian step frequency
T_p	Pedestrian step period
v_p	Pedestrian velocity
f_p	Pedestrian vertical step frequency
W_p	Pedestrian weight
h_p	Pylon height above the deck
H_i	Pylon height below the deck
α_{opt}	Ratio between the TMD and the structural frequencies
$\boldsymbol{F}_T$	Resultant social force
ρ_p	Stay cable density (prestressed steel)
f_y	Stay cable maximum stress

E_p	Stay cable Young's Modulus (prestressed steel)
ρ_s	Steel density
ν_s	Steel Poisson's ratio
E_s	Steel Young's modulus
k	Stiffness matrix
ξ	Structural damping ratio
f_s	Structural frequency
y	Time position of the CoM of pedestrian
ξ_{opt}	TMD damping ratio
t	Time
H_{Tp}	Total pylon height
t_T	Total time duration of footstep load
ω_i	Undamped natural circular frequency of the i_{th} mode
$\dot{u}$	Velocity
$f_{s,y}$	Yield strength of structural steel

1 Introduction

1.1 General background

Nowadays, the bridge engineering community is addressing the challenge of designing more slender footbridges, some of them with longer spans. This challenge can cause vibration problems in footbridges due to pedestrian traffic. If one of the footbridge frequencies lies near the step frequency of pedestrians, resonance effects can occur, amplifying the dynamic response, and could cause discomfort to users. In many cases, supplemental damping devices are required to mitigate human-induced vibrations in footbridges.

In recent years, various studies have focused on developing methods to either avoid or mitigate human-induced vibrations in pedestrian bridges, with more emphasis on the vertical direction. However, excessive lateral vibrations registered at the Toda Park Bridge (T-bridge) in Japan (Figure 1.1) (Fujino et al., 1993; Nakamura, 2004), the London Millennium Bridge (Dallard et al., 2001), and The Pont de Solferino, which is now known as Passerelle Léopold-Sédar-Senghor, in Paris (Danbon & Grillaud, 2005), brought as a consequence a more intense research attention on the analysis of lateral vibrations. The London Millennium Bridge and the Passerelle Léopold-Sédar-Senghor were closed immediately after their inauguration in 1999 and 2000 respectively due to the unexpected vibrations in the lateral direction. After these serviceability failures, the assessment of the dynamic response in the lateral direction has been included in the design of footbridges (Brownjohn et al., 2004; Nakamura & Kawasaki, 2006; Setra, 2006; Butz et al., 2007). For lateral vibrations, researchers have been focusing on the lock-in effect, which is also called synchronous lateral excitation. This effect is caused when pedestrians synchronize their step frequencies with the frequency associated with the lateral vibration of the structure.



Figure 1.1: Pedestrians in the Toda Park Bridge in Japan (Nakamura, 2004)

Many studies have proposed deterministic models for simulating human-induced vibrations in both directions (vertical and lateral) through a periodic force defined using Fourier series. Nevertheless, pedestrians will not produce the same force in each step and its value will depend on various parameters, such as the biomechanical properties of each pedestrian (weight, height, age, gender), parameters describing pedestrian's walking (speed, and step frequency), the acceleration registered in the bridge at a particular time and location, the pedestrian density, and the route followed by pedestrians as a consequence of pedestrian-pedestrian interactions. Ramos-Moreno (2015) proposed a stochastic load model considering all of these effects, compiling previous research outcomes from different fields.

When evaluating the effects of pedestrian-induced vibrations, taking into consideration that each step does not produce the same force (intra-variability), the different anthropometric characteristics across the population leading to different actions induced by each pedestrian (inter-variability), and the interaction between pedestrians crossing the bridge at the same time (pedestrian-pedestrian interaction or crowd flow), is critical for the design and assessment of footbridges. By controlling the accelerations within the comfort limits, serviceability problems can be avoided. After performing the dynamic analyses under pedestrian loads, when excessive accelerations are obtained, supplemental damping devices may be considered as an optimal solution to control the dynamic response. In recent years, experimental studies based upon field analysis as well as numerical studies employing finite element methods have provided useful information about how designers' can reduce human-induced vibrations in footbridges using

supplemental damping devices, such as tuned mass dampers (TMD), tuned liquid dampers (TLD) and visco-elastic dampers (Setra, 2006). These supplemental damping devices are being more frequently incorporated into footbridges after construction has finished, as a way to reduce unexpected human-induced vibrations, such as the three-span steel box girder footbridge over the River Wharfe at Wetherby in Yorkshire, England (Jones & Pretlove, 1981), and the Pedro e Inés footbridge in Coimbra, Portugal (Caetano et al., 2010a) (Figure 1.2).



Figure 1.2 Pedro e Inés footbridge in Coimbra, Portugal (Structurae, 2015)

Many of the studies related to the control of human-induced vibrations in footbridges released to date have been conducted using supplemental damping devices in existing structures. These studies have analysed the forces induced by a certain number of walking, running or jogging pedestrians (Figure 1.3) (Moutinho et al., 2007; Caetano et al., 2010a; Caetano & Cunha, 2014). In some cases, when the damping system is introduced once the bridge is in use, after construction, the available space to deploy the supplemental damping devices is limited, and it is necessary to design special dampers (Meinhardt et al., 2008). Tuned mass dampers have many applications in existing footbridges due to their low cost, reliability and high efficiency in the mitigation of the vibration under pedestrian loads (fib, 2006). Over the last few years, research has been developed to optimize the placement and properties of multiple tuned mass dampers through deterministic approaches to reduce human-induced vibration in pedestrian bridges (Krenk et al., 2005; Daniel et al., 2011).



Figure 1.3: Pedestrian test in the West Bromwich footbridge in the United Kingdom (Caetano & Cunha, 2014)

However, a rigorous methodology that focusses on the optimal location and the properties of the tuned mass dampers in footbridges, considering the non-linearities induced by the pedestrian loads in the vertical and lateral directions, is not available yet. Most studies to date focus on using one or multiple TMDs and optimizing its parameters after construction through experimental tests. It is noticeable that there are not proper standards, regulations or guidelines to help designers with the implementation of supplemental damping devices to mitigate human-induced vibrations in footbridges during the design stage. In addition, these existing guidelines do not consider the intra- and inter-variability in the load action, the pedestrian-pedestrian interactions within the crowd flow, as well as the non-linearities of the pedestrian action in the vertical and lateral directions.

1.2 Aims and objectives

The main purpose of this study is defining a methodology to implement tuned mass dampers at the design stage in footbridges under a stochastic pedestrian load model in order to minimize the dynamic response in service, complying with the serviceability limit state, and demonstrating the benefits of the TMD implementation, as well as the limitations of this approach. This research will be addressed through numerical analyses, using the finite element method to represent girder and cable-stayed footbridges under a stochastic pedestrian load model with and without supplemental

damping devices. This work will look for a way to facilitate the design of slender girder and cable-stayed footbridges through an efficient damping arrangement avoiding serviceability problems.

The current research work aims to evaluate the dynamic response of girder and cable-stayed footbridges under pedestrian actions with tuned mass dampers, optimizing their parameters and their proper location within the design stage. The reasons to choose both typologies are that:

- The girder footbridge is the most common typology. A previous PhD thesis (Ramos-Moreno, 2015) has demonstrated that, for certain materials and spans, the accelerations cannot be kept under certain thresholds by altering the geometrical and mechanical properties without attempting the implementation of supplemental damping devices.

- Cable-stayed footbridges are very slender structures prone to vibrate under dynamic excitations and are one of the most efficient schemes to cross long spans. The aforementioned previous PhD thesis has also demonstrated that the vertical and lateral accelerations cannot be controlled under certain comfort thresholds by altering the geometrical and mechanical properties without attempting the implementation of supplemental damping devices (Ramos-Moreno, 2015).

The aims of this research will be fulfilled through the development of the following objectives:

a) To define the current state of the art through an extensive literature review. This methodology includes:

  - Analysing the state of art in terms of understanding the structural response and design criteria of girder and cable-stayed footbridges under pedestrian actions.

  - Defining the current state of the art of pedestrian loads based on human-induced vibration in footbridges choosing an optimal representation of these loads for the fulfilment of the serviceability requirements.

- Defining the current state of the art of supplemental damping devices proposed by guidelines, codes and researchers considering that these devices should have been employed to mitigate human-induced vibrations. Selecting and describing the type of supplemental damping devices used in footbridges. This includes operation principles, design considerations, functionality, and implementation issues. It is also important to remark that nowadays, the implementation of these devices is done when they are already built, but this research will consider the implementation of them at the design stage.

b) To implement a stochastic pedestrian load model (developed by Ramos-Moreno, 2015) in Python. This pedestrian model considers that each step does not produce the same force (intra-subject variability), the different anthropometric characteristics (inter-subject variability), the interaction between pedestrians crossing the bridge at the same time (leading to change of trajectories followed by pedestrians), and the influence of the parapets. This model will be used to evaluate the dynamic response in girder and cable-stayed footbridges.

c) To represent and analyse girder footbridges under a stochastic pedestrian load model with and without tuned mass dampers to gain understanding about the structural response and appropriate design criteria for the TMDs in these bridges. These analyses will be performed through finite element models developed in Python using representative cases (benchmark cases).

d) To investigate the dynamic response of cable-stayed footbridges under a stochastic pedestrian load model by using benchmark cases. For this purpose, Python, FORTRAN and Abaqus will be used to represent the pedestrian actions, the equilibrium forces of the pedestrians in the lateral direction and the Finite Element Analysis, respectively. The nature of the pedestrian actions is defined as stochastic with Python while the forces required to achieve the equilibrium of the pedestrians in the lateral direction is implemented

by using a special subroutine in FORTRAN. Both are combined into several numerical FE models in order to understand the structural behaviour, with and without TMDs.

e) To develop a methodology that shows how to employ supplemental damping devices in girder and cable-stayed footbridges under a stochastic pedestrian traffic.

f) To develop a set of design recommendations to construct slender girder and cable-stayed footbridges without serviceability problems considering the implementation of tuned mass dampers.

1.3 Thesis outline

The thesis comprises the following chapters:

Chapter 1, Introduction (this chapter), which introduces the thesis structure and summarizes the contents of this research work.

Chapter 2, State of the art, which introduces a comprehensive literature review of the background of this research. This includes footbridge typologies and materials, pedestrian actions considering deterministic and probabilistic models proposed to represent pedestrian loads. Furthermore, it includes the damping characteristics of footbridges structures, different supplemental damping devices for the mitigation of human-induced vibrations in footbridges, and the comfort criteria proposed by codes, standards and guidelines.

Chapter 3, Research methodology and preliminary analyses, which details the methodology for the fulfilment of the objectives of this work. This chapter presents the description of the girder and cable-stayed footbridges, the pedestrian load model, the serviceability requirements and the supplemental damping device that will be used in this research work. Furthermore, it includes some preliminary analyses to determine the TMD criteria that will be used

to define the parameters of these devices in footbridges. This chapter also includes initial sensitivity analyses to define the framework of this research work.

Chapter 4, Dynamic response of girder footbridges, which provides the numerical work performed to analyse the fulfilment of the serviceability criteria in girder footbridges with and without tuned mass dampers. This chapter shows the evaluation of the dynamic response in the vertical and lateral direction under a probabilistic pedestrian load model with and without single or multiple tuned mass dampers of a broad range of footbridges. The location where the TMDs can be employed, the different number of dampers, and their efficiency are analysed. In addition, a comparison of the relative cost of changing structural parameters or employing TMDs to mitigate the human-induced vibrations is presented. The chapter aims to present a comprehensive set of design criteria for the implementation of tuned mass dampers.

Chapter 5, Dynamic response of cable-stayed footbridges with one tower, which provides parametric analyses of the cable-stayed footbridges with a single pylon considering the most common structural parameters identified in built structures with this typology. After the evaluation of the dynamic response, in cases where the maximum comfort is not achieved, tuned mass dampers will be implemented until the comfort criteria is fulfilled. Different location and numbers of tuned mass dampers are considered showing how the dynamic response in the vertical and lateral direction can be reduced. The effect in the dynamic response after changing the pylon shape is presented. Furthermore, a cost analysis of changing structural parameters or employing TMDs to mitigate the human-induced vibrations is shown. Finally, design recommendations that may facilitate an efficient design of CSFs with tuned mass dampers at the design stage avoiding serviceability problems are provided.

Chapter 6, Dynamic response of cable-stayed footbridges with two towers, which describes parametric analyses of the cable-stayed footbridges with two pylons, considering the most common structural characteristics. This chapter shows how the implementation of tuned mass dampers can mitigate the human-induced vibrations in the vertical and lateral direction. Once a detailed analysis of the dynamic response is presented, a list of design recommendations is

provided to facilitate the construction of these footbridges while neither avoiding nor mitigating serviceability problems. Recommendations are presented in terms of (1) modes dominating the response; (2) dynamic response achieved and expected without TMDs; (3) optimum location for TMDs; (4) dynamic response and required TMD mass ratio according the degree of comfort; and (5) cost comparison between either changing structural parameters (without implementing supplemental damping devices) or employing TMDs.

Chapter 7, Conclusions, recommendations and further research work, which provides the findings, benefits, and conclusions of this research. This chapter finishes by providing recommendations for future research work in this field.

2 State of the art

2.1 Introduction

The design and construction of pedestrian bridges is increasingly driven towards slenderer (and therefore lighter) and longer schemes. Therefore, the modal properties of footbridges, such as structural frequencies, tend to decrease, whereas there is an increase of the dynamic response under pedestrian action as a consequence of the mass reduction. In order to obtain an accurate dynamic response, a pedestrian load model is required that represents the forces in the vertical and lateral direction, with time and space variation, simulating the discontinuous nature of the human walking forces. The longitudinal actions induced by pedestrians are usually neglected in these structural types. The dynamic response needs to be compared to appropriate comfort levels according to standards, guidelines and regulations in order to analyse whether or not the kinematic magnitudes (deflections and accelerations, given the range of fundamental frequencies) of the footbridge satisfy the serviceability criteria. When accelerations exceed limits, supplemental damping devices can be employed to mitigate human-induced vibrations.

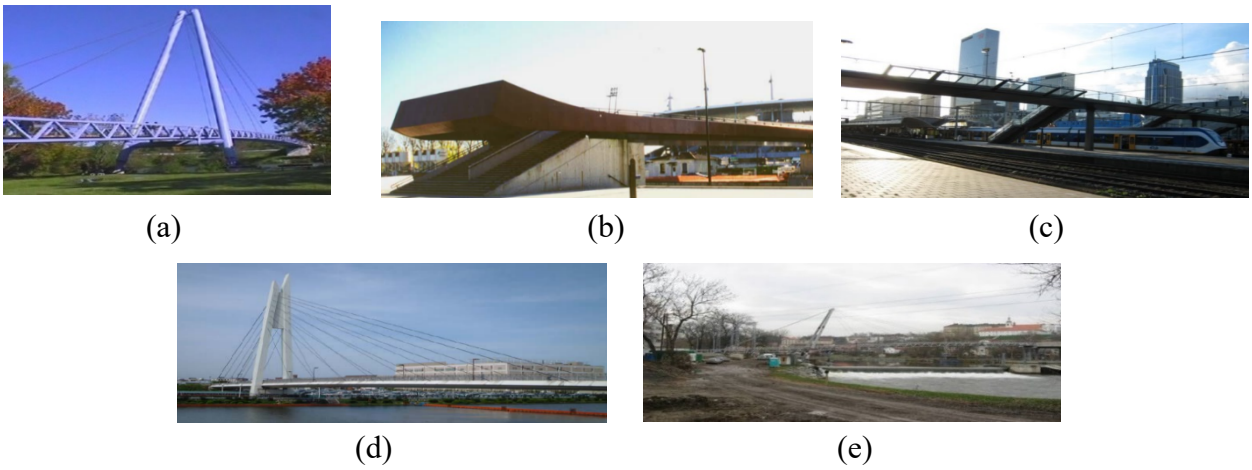
This chapter represents a comprehensive literature review of the structural characteristics and materials of girder and cable-stayed footbridges, the deterministic and probabilistic models to represent the pedestrian actions in the vertical and lateral direction, the damping characteristics of footbridges according to the structural material, the availability of supplemental damping devices to mitigate human-induced vibrations, and the serviceability criteria according to codes of practice, standards and guidelines. The chapter finishes with some concluding remarks.

2.2 Typologies and materials for the footbridges studied in this thesis

Footbridge construction has experienced noticeable changes over the last century leading to the construction of lighter and slenderer decks, with more efficient use of materials and longer spans. As a result of these changes, some of the footbridges have shown serviceability problems due to pedestrian activities. In these cases, supplemental damping devices were employed to satisfy the serviceability criteria (Table 2.1 and Figure 2.1), but they were implemented after construction, when there is less flexibility than during the design stage.

Name	Country	Structure	Total length (m)	Direction of the supplemental damping devices	Reference
Bellagio Bridge in Las Vegas	USA	Box girder	46.0	Vertical	(Breukleman et al., 2002)
Forchheim footbridge	Germany	Cable-stayed	117.5	Vertical – Lateral	(Seiler et al., 2002)
Langelinie footbridge	Denmark	Box girder	169.8	Vertical	(Krenk et al., 2005)
Passerelle du Stade de France	France	Box girder	180.0	Vertical	(Setra, 2006)
Rotterdam central Station	The Netherlands	Box girder	136.0	Vertical	(Breman et al., 2011)
T-bridge	Japan	Cable-stayed	179.0	Vertical – Lateral	(Nakamura & Kawasaki, 2006)
The Footbridge Skoda	Poland	Cable-stayed	94.8	Vertical	(Kala et al., 2010)
The London Millennium Bridge	United Kingdom	Suspension	325.0	Lateral	(Dallard et al., 2001)
The Pilsen footbridge	Czech Republic	Cable-stayed	65.0	Vertical	(Karásek et al., 2005)

Table 2.1: Footbridges with supplemental damping devices



(a) (b) (c)

(d) (e)

Figure 2.1: (a) Forcheim footbridge in Germany (Seiler et al., 2002). (b) Passerelle du Stade de France (Setra, 2006). (c) The Footbridge at Rotterdam Central Station in the Netherlands (Breman et al., 2011). (d) The T-bridge in Japan (Nakamura & Kawasaki, 2006). (e) The Footbridge Skoda in Poland (Kala et al., 2010)

The most common pedestrian bridges according to structural forms are beams and girders, trusses, frames, arches, cable-stayed and suspensions footbridges. This research work will focus on the implementation of supplemental damping devices in girder and cable-stayed footbridges, as these are two of the most frequent structural types. Girder footbridges are the most common type of footbridges. They may have a single or multiple spans. Most of the footbridges with a beam deck use box girders or I-beams as part of the cross-section. The deck can be made of different structural materials, such as stainless steel, reinforced concrete, prestressed concrete, timber, structural glass fibre reinforced polymers, aluminium, or a combination of them.

Figure 2.2 represents the number of spans and the span length of the girder's footbridges. These characteristics are extracted from a dataset of 39 footbridges found in literature and compiled by the author (Annex A). It can be seen that, most common girder footbridges have one, two and three spans. Their average span lengths are approximately 43, 57 and 100 m for one, two and three spans, respectively. The data in Annex A shows that the average deck width is 4 meters.

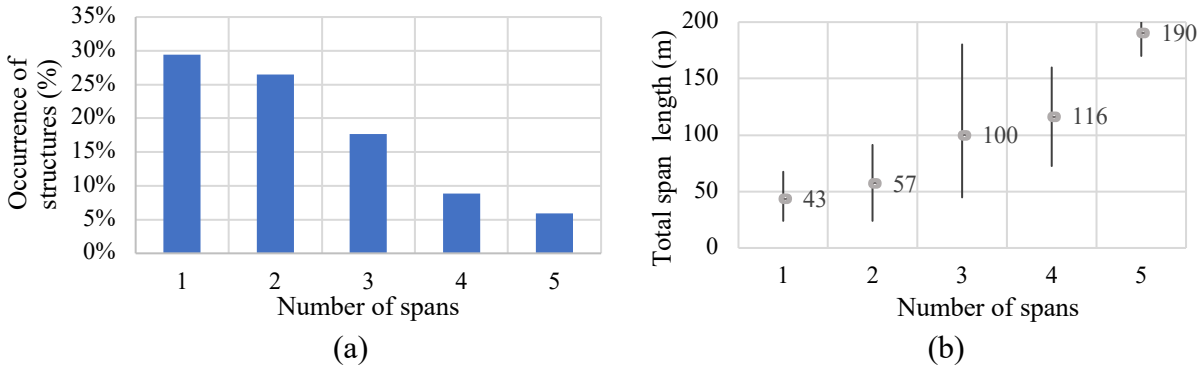


Figure 2.2: (a) Occurrence of girder footbridges according to the number of spans based in a dataset of this typology (Annex A). (b) Span length for one, two, three four and five spans girder footbridges

The second bridge typology that this thesis is going to study in detail is the cable-stayed footbridge. A cable-stayed footbridge is considered an efficient and economical structure with stay cables supporting the deck from one or more pylons or towers. The most common footbridges are steel girders with a reinforced concrete slab (composite deck), steel box girders or steel girders with timber decking. According to data found in the literature and compiled by the author (Annex B), the most common cable-stayed footbridges have two and three spans (Figure 2.3 (a)). The number of footbridges that have been considered for this dataset is 32. Their main span lengths are approximately 50, 60 and 130 for one, two and three spans, respectively (Figure 2.3 (b)).

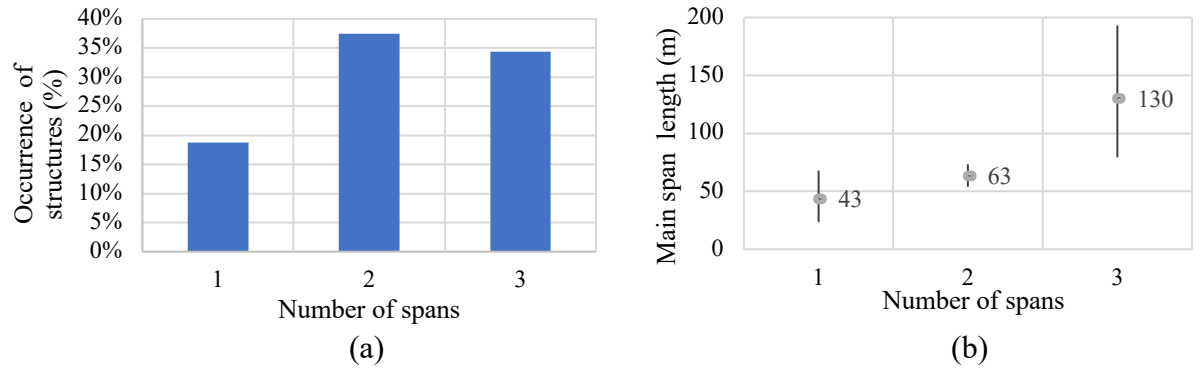


Figure 2.3: (a) Occurrence of cable-stayed footbridges according to the number of spans based in a dataset of these footbridges (Annex B). (b) Span length for one, two and three span cable-stayed footbridges

The stay cables are made of steel, either strands or locked cables. The cable system arrangement can be as a harp or as a fan. The best arrangement of cable-stayed footbridges is the modified fan arrangement, also known as a semi-fan arrangement (Wells & Clash, 2008). This is an alteration of the fan configuration. On this arrangement, each cable is anchored near the top of the pylon making the cable slopes steeper. As a result, the axial force in the girder is smaller (Figure 2.4(a)). On top of this, the optimal ratio between the side and the main span is from 0.20 to 0.40 for the modified fan arrangement and 0.30 to 0.45 L for the harp arrangement (Strasky, 2011; Gimsing et al., 2012) (Figure 2.4).

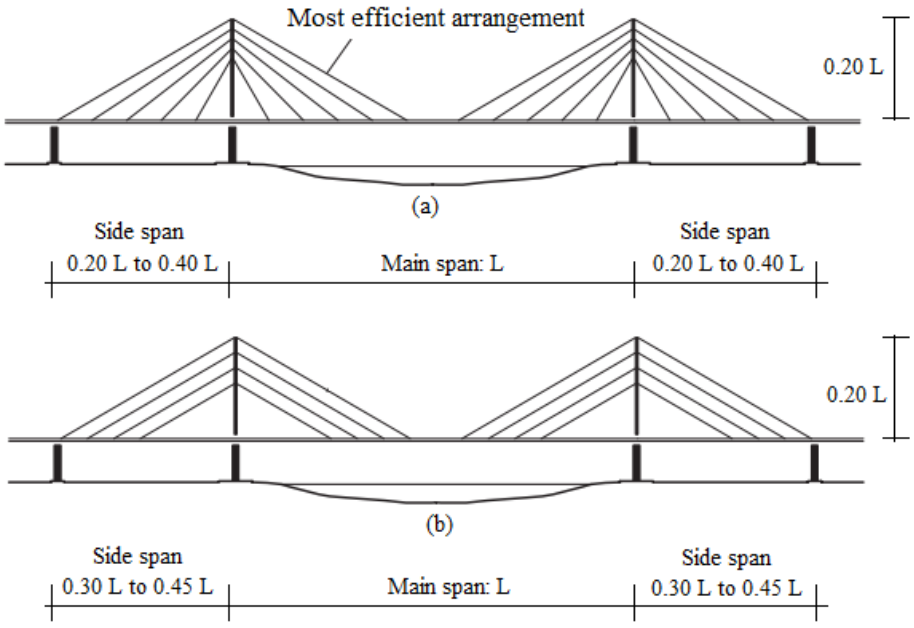
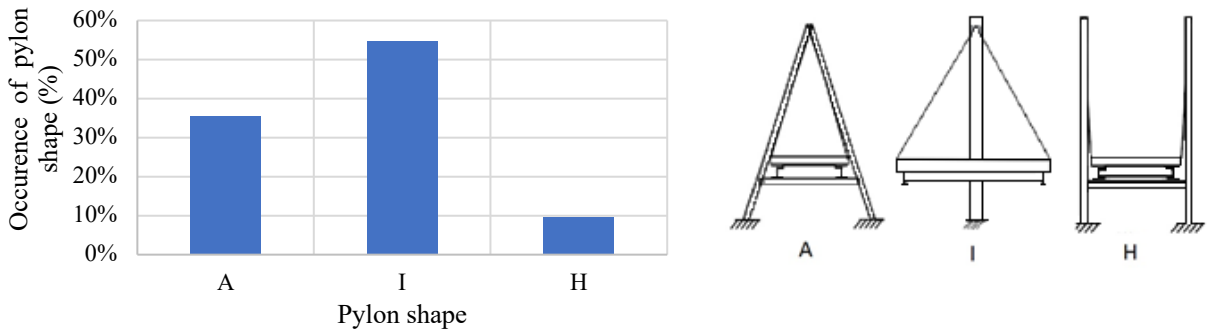


Figure 2.4 Cable arrangements (a) modified fan arrangement, (b) Harp arrangement (Wells & Clash, 2008)

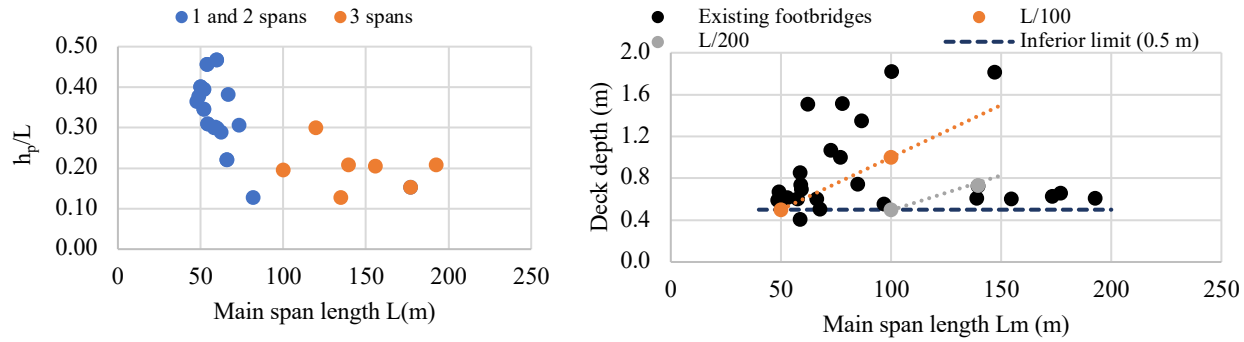
The pylon is frequently made of concrete or steel and the shape can be I (single pylon), H, A, inverted Y and diamond. The most common shapes found in the literature review are the I and A and the least used is the H-shaped pylon (Figure 2.5) (Annex B). In an A-shaped pylon, the foundations are usually connected to avoid transmitting a large horizontal action to the ground.



(a) (b)

Figure 2.5: (a) Occurrence of cable-stayed footbridges according to the pylon shape (Annex B). (b) A-, I- and H-shaped pylons

The ratios between the tower height (h_p) and deck depth for the built database are shown in Figure 2.6. The average of these ratios is approximately 0.36 for one and two spans, and 0.20 for three spans. These values are consistent with those for cable-stayed road bridges, and lead to a minimum inclination of stay cables over the deck alignment of 20 degrees. The ratio between the span length and the deck depth is equivalent to 1/100. This ratio corresponds to the geometries adopted by designers according to the build database.



(a) (b)

Figure 2.6: Relationship between main span length of cable-stayed footbridges with (a) pylon height above the deck h_p and main span length, and (b) deck depth

2.3 Pedestrian actions

A dynamic load, which has vertical, lateral and longitudinal components, is induced when pedestrians step on a footbridge. Serviceability problems can occur to any type of footbridges under pedestrian actions with vertical and lateral frequencies under 5.0 Hz. For several years, researchers have tried to predict human characteristics in different activities such as walking, running or jogging. Focusing on the civil engineering area, many experimental studies have been performed in order to find the link between human-induced vibrations and the dynamic response of the structures (Matsumoto et al., 1978; Pedersen et al., 2010). This connection has been proved using experimental cases as the five footbridges in Tokyo, analysed by Matsumoto et al. (1978) where the arrival time of pedestrians corresponded to a Poisson distribution. Despite the vast research about the dynamic response in footbridges under pedestrian actions, there is not an accurate model that is applied in codes, standards and guidelines where the anthropometric characteristics, speed, step frequency, and the nonlinearity of the lateral loads transmitted of each pedestrian are considered. This section focuses on describing pedestrian characteristics, and the vertical and lateral load effects applied to footbridges. It also presents deterministic and probabilistic models available to represent pedestrian actions.

2.3.1 Pedestrian characteristics

It is well known that different pedestrian's activities will produce a structural response in footbridges. All these activities (standing, walking, jogging or running) transmit loads onto the deck of the footbridge. This implies that the performance in service of footbridges depends on these activities. Therefore, running activities can be found in BSI (2008) considering that this is one of the least likely real activities in footbridges performed by pedestrians as Caetano et al. (2011) mentioned. On the other hand, walking constitutes the main consecutive action of placing people's foot on the ground overlapping in time (T_p). The step frequency of pedestrians is given by $f_p = 1/T_p$. The parameters to define the pedestrian actions while walking in the vertical direction are the speed, step frequency, and step length which are related to the pedestrian anthropometric characteristics (weight, height, age, and gender) (Rose & Gamble, 1994). Some

other important considerations that should be described are the gait of a pedestrian which is given by the representation of individual loads, the step frequency and the speed, both describing the movement of the user. In the lateral direction, it is necessary to consider the lateral step width which has a strong relationship with the lateral movement of the CoM (pedestrian's centre of mass) (Townsend, 1985). It is important to remark that one of the most significant considerations, when it refers to pedestrian characteristics, is their weight. It should be noted that the average pedestrian weight in codes and guidelines is a constant value of 700 N (Setra, 2006). For this research work, a uniform weight of 780 N has been used which represent the average weight of the UK population (Ramos-Moreno, 2015, Ramos-Moreno et al., 2019).

2.3.2 Dynamic effect of pedestrians in structures

According to ISO (2005) to assess the comfort of a pedestrian who walks over a footbridge three factors should be considered; these are the vibration source, the transmission path and the receiver. It mentions that if the vibration source is the same as the receiver (in this case pedestrian actions) and it changes in time and space, then the dynamic response is harder to solve analytically with traditional approaches; therefore, designers try to solve them using an empirical method. The footbridge is the transmission path from the vibration source to the receiver. The dynamic response of footbridges induced by the vibration source is calculated with the equation of motion in time according to the d'Alembert's principle (Equation (2.1)) (Clough & Penzien, 1993), where the external loads $p(t)$ that are acting on the structure are resisted by the inertial, damping and elastic forces (Equation (2.1)). The properties of the system are its mass (m), stiffness (k) and damping (c). The vibration source is given by the dynamic force induced by pedestrians in the vertical and lateral direction.

Figure 2.7 shows the vertical, lateral and longitudinal forces produced by a walking pedestrian. The forces transmitted in the longitudinal direction (Figure 2.7(c)) are neglected in this study, as the longitudinal accelerations induced are very small for many common structures (Ramos-Moreno, 2015).

$$m\ddot{u}(t) + c\dot{u}(t) + ku(t) = p(t) \tag{2.1}$$

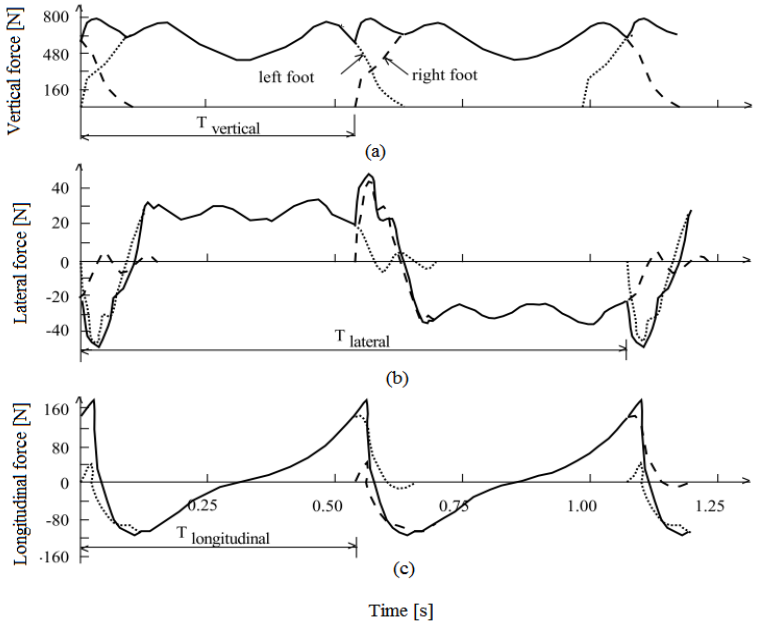


Figure 2.7 Representation of human-induced forces in (a) vertical, (b) lateral, and (c) longitudinal direction (Živanović et al., 2005)

2.3.3 Vertical and Lateral loads

Pedestrian's vertical frequencies are generally in ranges of 1.6 Hz to 2.4 Hz and in the lateral direction is half of these values. These ranges have been proposed in many studies through experimental tests. Table 2.2 shows the average frequencies in the vertical direction. Different frequency ranges have been proposed according to the nature of the activity. For instance, walking has a suggested frequency range of 1.6 to 2.4 Hz and running has a suggested frequency range of 2.0 to 3.5 Hz. Footbridges critical ranges for vertical and lateral structural frequencies are $1.3\ Hz \leq f_i \leq 2.3\ Hz$ and $0.5\ Hz \leq f_i \leq 1.2$, respectively (Butz et al., 2007).

Author	Number of pedestrians	Average frequencies (Hz)
Matsumoto et al., 1978	505	1.99
Živanović et al., 2005	1976	1.87
Pizzimenti et al., 2007	116	1.84
Sahnaci & Kasperski, 2005	251	1.82
Pachi & Ji, 2005	400	1.83
Živanović et al., 2007	939	1.94
Butz et al., 2006	98	1.84

Table 2.2 Step frequencies of pedestrians (Ingólfsson et al., 2012)

The average contact time between the foot and the ground varies depending on the speed and frequency of pedestrians. The resultant shape for the vertical direction can be seen in Figure 2.7(a). It can be characterized by a double hump separated by a trough e.g. lower amplitude. The most common model to evaluate vertical loads (p_v) induced by pedestrians is representing the pedestrian's loads as a periodic force using a Fourier series (Equation (2.2)) (Bachmann & Ammann, 1987). This equation considers the pedestrian weight (W_p) and a set of harmonics, defined by three parameters (b_n, ω_n, ϕ_n). As it is known, the total vertical load introduced by both feet could be given by this series considering the step frequency as the main gait parameter (Wheeler, 1982; Živanović et al., 2007).

$$p_v(t) = W_p \left[1 + \sum_{n=1}^{\infty} b_n \sin(\omega_n t - \phi_n)\right] \tag{2.2}$$

Many researchers have focused on finding these harmonic parameters. However, this model is not as accurate as it should be, because it does not consider the nonlinear behaviour of the pedestrian actions in the lateral direction and the variation of human-induced loads on distance, time, velocity, step distance and step frequency. For this reason, it is necessary to simulate the pedestrian loads considering these uncertainties to obtain a more realistic representation of the pedestrian action and therefore a more accurate dynamic response. There are some studies that describe the human-induced loads in the vertical direction, such as Brownjohn & Omenzetter (2004). This study

showed, through experimental measurements using a treadmill, the difference between the periodic sinusoidal load and the real forces. They claimed that pedestrian loads need to be simulated through a stochastic model. A similar experimental measurement using a treadmill was developed by Racic & Brownjohn (2011) in which they claimed that, a realistic model for vertical forces could be adopted in the design of structures used by pedestrians. This is because the dynamic response can be obtained in an accurate manner when realistic pedestrian's models are adopted.

Another way to represent the vertical loads is to define pedestrian's real foot loads according to the closest temporal variation. Butz et al. (2007) define the vertical force based on a set of parameters shown in Figure 2.8. These are included in Table 2.3, for step frequencies from 1.2 to 2.4 Hz, where t_{end} is the total time for the pedestrian step, m_A is the gradient of the force at the beginning of the step (Equation (2.3)), $F_{max,1}/G$ is the first peak for the step, F_{min}/G is the minimum value for the transition, $F_{max,2}/G$ is the second peak value when the pedestrian foot pushes off the ground and m_B is the gradient of the force when the foot is pushing off the ground (Equation (2.4)).

$$m_A = \frac{F_{min}/G - 0.1}{t_2 - t_1} \tag{2.3}$$

$$m_B = \frac{0.1 - F_{min}/G}{t_4 - t_3} \tag{2.4}$$

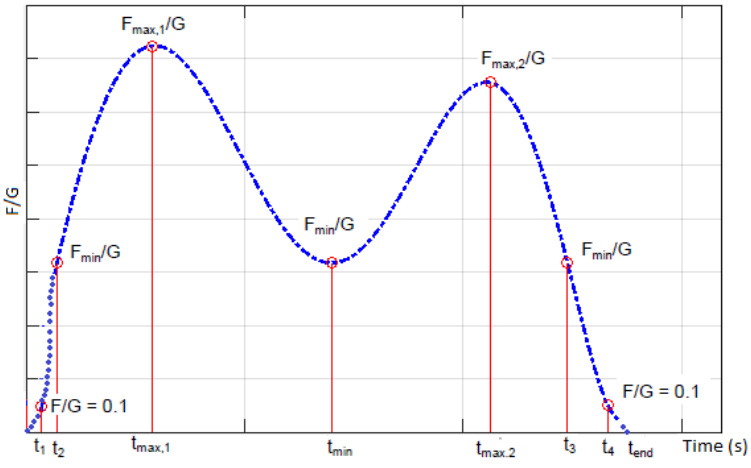


Figure 2.8: Parameters required to define the vertical load introduced by each step (Butz et al., 2007)

Frequencies (Hz)	t_1(s)	t_2(s)	$t_{max,1}$(s)	t_{min}(s)	$t_{max,2}$(s)	t_3(s)	t_4(s)	t_{end}(s)	m_A	$F_{max,1}/G$	F_{min}/G	$F_{max,2}/G$	m_B
1.30	0.0390	0.279	0.325	0.560	0.710	0.775	0.984	1.000	4.470	1.130	1.040	1.080	-4.520
1.50	0.0196	0.146	0.240	0.440	0.645	0.741	0.858	0.890	6.180	1.110	0.870	1.140	-6.650
1.80	0.0119	0.076	0.170	0.355	0.535	0.626	0.688	0.700	10.410	1.240	0.770	1.270	-10.830
2.00	0.0013	0.048	0.140	0.310	0.470	0.548	0.593	0.600	12.710	1.330	0.690	1.280	-13.150
2.20	0.0010	0.028	0.115	0.280	0.425	0.496	0.533	0.550	19.520	1.450	0.630	1.310	-14.380
2.40	0.0012	0.027	0.110	0.265	0.390	0.457	0.499	0.500	19.330	1.590	0.590	1.320	-11.740

Table 2.3: Properties shown in Figure 2.8 to define the vertical loads for different step frequencies

Lateral loads have smaller magnitude and frequency ($f_{l,p} = f_p/2$) than those in the vertical direction. This shape can be seen in Figure 2.7 (b). Lateral loads follow the same pattern of vertical loads, variating the real-time by a model which describes the Center of Mass (CoM) movement. The Fourier series in lateral loads are given by Equation (2.5). Many authors have focused on describing the parameters of these series (Bachmann & Ammann, 1987; Fujino et al., 1993).

$$p_l(t) = W_p \left[\sum_{n=1}^{\infty} b_n \sin(\omega_n t - \phi_n) \right] \tag{2.5}$$

Even if these lateral forces are small, the real problem is that pedestrians could synchronize their frequency steps with the frequency of the bridge introducing larger dynamic response (resonance effects). In order to counteract this shortcoming researchers started to modify them by the implementation of the inverted pendulum (IP) model. This model represents pedestrian's movement in time as a function of the CoM (Townsend, 1985; Bauby et al., 2000; Bocian et al., 2012; Carroll et al., 2013). This IP model (Figure 2.9) shows that the CoM movement has a relationship between the gait, the stride width, the anthropometric characteristics of the person and the lateral acceleration of the structure. The position in time of the next step and the CoM can be defined by knowing the previous foot position, and the acceleration of the structure. Equations (2.6), (2.7) and (2.8) are used to define the resulting lateral force applied on the structure (F_l) introduced by the pedestrian on the structure on that particular step. The following parameters are required to define the inverted pendulum, L_{eq} represents the distance from the centre of pressure

(CoP) to the CoM, m_p is the mass of the pedestrian, g is the gravity acceleration, u_s is the lateral displacement of the structure (therefore $\ddot{u}$ is the lateral acceleration of the structure in global axes), ω_s is the position of the foot in local axis, y is the position of the CoM in local axis (therefore $\ddot{y}$ is the acceleration of the CoM in the local axes), g_L and g_N are the parallel and normal components of the gravity acceleration. Ω_p is defined as the natural frequency of the lateral movements of the CoM and is given by $\Omega_p = \sqrt{\frac{g}{L_{eq}}}$.

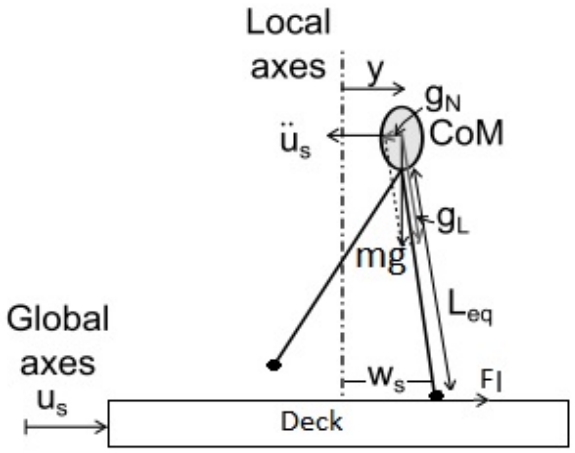


Figure 2.9: Inverted pendulum (IP) model (Macdonald, 2009)

$$g_N = \frac{g}{L_{eq}}(\omega_s - y) \tag{2.6}$$

$$\ddot{u}_s + \ddot{y} = -g_N = -\frac{g}{L_{eq}}(\omega_s - y) \tag{2.7}$$

$$F_l = m_p(\ddot{u}_s + \ddot{y}) = m_p\Omega_p^2(\omega_s - y) \tag{2.8}$$

2.3.4 Pedestrian - structure interaction

During footbridge vibration, a human-structure synchronization can occur which is called lock-in effect (Fujino et al., 1993; Fujino & Siringoringo, 2015) or synchronous lateral excitation (SLE) (Dallard et al., 2001). In the vertical direction, pedestrians have better balance than in the lateral direction because their legs and joints provide an amount of damping (Butz et al., 2007). Hence,

this effect is not common in this direction and not many studies have been performed. On the other hand, this effect can be seen in the lateral direction and it was the reason why unexpected vibrations in the London Millennium Bridge (Dallard et al., 2001) and in the Solferino Footbridge in Paris (Danbon & Grillaud, 2005) happened.

This effect occurs when pedestrians match the frequency of their steps with the frequencies of the structure (Živanović et al., 2005). A general procedure to check the lock-in effect in footbridges has been shown in Butz et al. (2007). Many authors have made different assumptions in relation to the number of pedestrians who are synchronized to the structure. Fujino et al. (1993) and Danbon & Grillaud (2005) are examples of these assumptions. The first one considers a 20% of synchronization while the second assumes a 100% synchronization if the lateral displacement is larger than 6 mm. However, the inverted pendulum model can represent the interaction human-structure depending on the acceleration of the deck at the location where the pedestrian steps. Nevertheless, this model does not take into account any previous assumptions.

2.3.5 Deterministic and probabilistic models to represent pedestrians loads

Based on vertical and lateral human-induced vibrations of footbridges, many researchers (such as Nakamura, 2004; Nakamura & Kawasaki, 2006; Fujino & Siringoringo, 2015) highlighted the importance of evaluating the dynamic behaviour of footbridges under pedestrian loads. Many of them proposed deterministic models to evaluate human-induced vibrations in both directions. However, the induced force by pedestrians cannot be modelled in a deterministic manner as each step does not introduce the same force and it is demonstrated that human-induced force depends on many parameters such as anthropometric characteristics (height, age and weight), step frequency, etc.

Human-induced forces change over time and position within each step depending on the step width, gait, weight, height, gender, age, speed, etc. There are deterministic and probabilistic force models. A deterministic model through a periodic force states that pedestrians introduce the same force in each step, and that pedestrians are walking one immediately after the other. While the

probabilistic model considers non-deterministic parameters, such as step length, velocity, and pedestrian frequency to represent the human-induced force. To evaluate human-induced vibrations in footbridges it is required to simulate these forces in both vertical and lateral direction, to obtain an accurate dynamic response. In the biomechanical, physics and transport field, there are multiple studies on how to model human loads and the considerations for modelling this type of loads. Andriacchi et al. (1977) showed the relation between the ground reaction force and the walking speed which can be normal, fast and slow. Keller et al. (1996) showed the correlation between gait, speed and vertical ground force during human activities through an experimental study on a platform considering men and women. Helbing (1998) presented a macroscopic model for high density traffic in which pedestrians are be represented through a fluid dynamic model and this highlighted the importance of the human interaction analysis.

A social force model for humans, which is a microscopic model, was proposed by Helbing & Molnar (1995) based on three conditions which are: the person choose the destination so that the desired speed is calculated, the distance from another pedestrian which depends on the pedestrian density so that a new speed is calculated, and finally the possibility to form pedestrian groups is evaluated. However, it is noticeable that this type of representation cannot be totally adopted to evaluate human-induced vibrations in footbridges due to the limitations (such as that it cannot consider the pedestrian-structure interaction, and the inter- and intra-subject variability) that it possesses referring to both directions which are required to evaluate footbridge's serviceability.

Despite the vast research about human-induced vibration in the civil engineering field, it is noticeable that there is not a guideline on how to represent human-induced forces in both directions in terms of their speed, frequency, velocity, anthropometric characteristics in a temporal variation in time and distance. A model to evaluate the dynamic response on footbridges based on an exhaustive analysis of the inter- and intra-subject variability in the vertical and lateral direction has been proposed by Ramos et al. (2014). Inter-subject variability refers to the anthropometric characteristics already defined during the literature and the intra-subject variability refers to how pedestrians are unable to repeat monotonous activities involving step length and frequency (Figure 2.10).

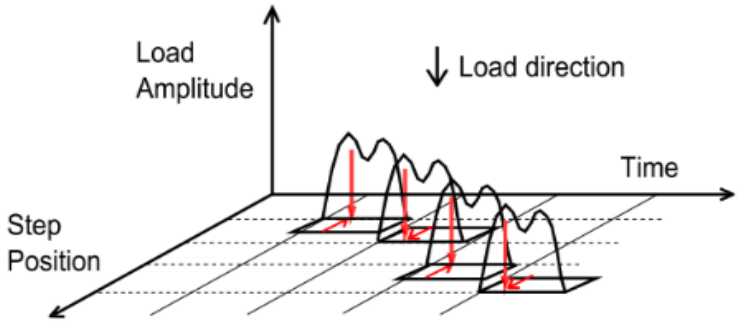


Figure 2.10 Pedestrian load model proposed by Ramos et al. (2014)

In Ramos' work, human loads are described as anthropogenic loads considering their anthropometric characteristics, the representation of the forces induced by pedestrians in time and distance depending on the activity, and the interaction between some pedestrians that are crossing the bridge at the same time. For representing vertical loads, definition of the step frequency and pedestrian mass is required, and for the lateral loads, the step frequency, step width, the pedestrian anthropometric characteristics such as the pedestrian height and mass, and the lateral acceleration of the deck at the point where the pedestrian steps are required definitions. This model is divided into three main stages which are the initial data flow (traffic type), the anthropometric characteristics of pedestrians and the gait data (to calculate the walking speed of each pedestrian, the mean step frequency, and the initial half-step width). Then an algorithm is used to simulate the interaction between pedestrians. The model can be used for any analysis of the dynamic response of girder and cable-stayed footbridges in the vertical and lateral direction. This methodology will be adopted for the evaluation of the serviceability criteria in this research. More details about this model will be defined in Section 3.2.

2.4 Damping characteristics of footbridges structures

The dynamic response of a footbridge depends on many factors such as the structural mass, the stiffness, the material's properties, the damping and the span length. For example, based on dynamic tests on footbridges, Tilly et al. (1984) highlighted that the dynamic response depends on the stiffness and damping. Many techniques such as modifying appropriately the stiffness and the

mass have been proposed in order to improve the dynamic response of footbridges (Matsumoto et al., 1978; Bachmann & Ammann, 1987; Setra, 2006). These techniques can be applied either during the design stage or post-construction stage (once the footbridge has been constructed). However, the technique in which the stiffness is modified results in an expensive procedure without a clear effect on the reduction of the dynamic response, whereas the technique based on changing the mass can be very limited in some cases. An effective measure to control the dynamic response due to human-induced vibration in footbridges could be to increase the damping ratio. The damping ratio is a property of the structures ability to dissipate the energy of their dynamic response. The damping ratio depends on different parameters such as the materials, the structure type, and the friction in connections and supports.

Damping can be increased by installing supplemental damping devices on the structure. The most useful supplemental damping devices to reduce pedestrian-induced vibrations in footbridges are tuned mass dampers (TMDs), tuned liquid dampers (TLDs) and viscous dampers. A tuned mass damper is a mass with spring-dashpot that is attached to the footbridge and it is tuned to the frequency that will be controlled in order to mitigate undesired vibrations (Jones & Pretlove, 1981; Tilly et al., 1984; Hatanaka & Kwon, 2002; Venuti & Bruno, 2007). A tuned liquid damper uses a large mass of liquid and the effectiveness of this device happens when the forcing frequency is near the natural frequency of the structure (Setra, 2006). A viscous damper converts the kinetic energy into heat increasing the damping of the structure (Dallard et al., 2001).

2.4.1 Structural damping

Different approaches are used to evaluate the damping ratio, such as the free-vibration decay method, the resonant amplification method, half-power (band-width) method and the resonance energy loss per cycle (Clough & Penzien, 1993). In addition, more studies investigated the values of damping ratio for footbridges under pedestrian actions. Tilly et al. (1984) showed that it is common to find footbridges having equivalent viscous damping ratios lower than 1.0 % based on several footbridges' tests under pedestrian actions. The work of Bachmann & Weber (1995) showed minimum, maximum and mean damping ratio according to structural materials of the

footbridge. Some guidelines recommend values of 0.2-0.4% for steel structures, 0.8-1.3% for reinforced concrete, 1.0-1.5% for timber, and 0.5-1.0 % for prestressed concrete, and 0.3-0.6% for composite structures (Setra, 2006; Hivoss, 2008).

Heinmeyer et al. (2009) summarised the variation of the structural frequency and measured damping ratios under service loads on several footbridges. They found that numerous steel bridges had damping ratios lower than 0.5% when the pedestrian's frequencies are in ranges of 1.6 to 2.4 Hz. As a result, they recommended using the minimum damping values for short span bridges and the mean value for longer ones (Heinmeyer & Feldmann, 2008). Van Nimmen et al. (2014a) also found that damping ratios measured in steel structures were below the minimum range given by guidelines.

Table 2.4 shows a summary of the structural damping proposed by different authors. Based on these studies, it is difficult to define unique values for footbridge damping. For that reason, the recommendations made by Bachmann & Weber (1995) are still used by structural designers (Heinemeyer et al., 2009; Živanović et al., 2014). As a recommendation, some researchers and guidelines suggested to not overestimate the structural damping. This is to ensure a conservative analysis of the dynamic response avoiding under-dimensioning (Setra, 2006; Heinemeyer et al., 2009; Van Nimmen et al., 2014a). Besides, these damping ratios are normal for traffic loads under service conditions, but significantly smaller than those activated under other dynamic actions inducing larger demands in the structure, closer to ultimate limit state.

Structural material	Suggested damping values (ξ)	References
Reinforced concrete	0.8 - 1.5%	Bachmann & Weber (1995)
	0.8 - 1.3%	Setra (2006), Hivoss (2008), Heinmeyer et al. (2009)
	0.8%	Blanchard et al. (1977), ISO (2005)
	1.5%	BSI (2003)
Prestressed concrete	0.5 -1.0%	Bachmann & Weber (1995), Setra (2006), Heinmeyer et al. (2009)
	0.8%	Blanchard et al. (1977), ISO (2005)
Composite (steel and concrete)	0.3 - 0.6%	Bachmann & Weber (1995), Setra (2006), Heinmeyer et al. (2009)
	0.5%	BSI (2003)
	0.6%	Blanchard et al. (1977), ISO (2005)
Steel	0.2 -0.5%	Bachmann & Weber (1995)
	0.2 - 0.4%	Setra (2006), Heinmeyer et al. (2009)
	0.5%	Blanchard et al. (1977), BSI (2003), ISO (2005), Heinemeyer et al. (2009)
Timber	0.4 - 1.5%	Labonnote et al. (2013 a)
	0.5%	Schubert et al. (2010)
	1.0 - 1.5%	Hivoss (2008), Heinmeyer et al. (2009)
	1.5 - 3.0 %	Setra (2006)
Aluminium	0.4%	Umashankar et al. (2009), Mevada & Patel (2016)
GRFP	0.3 -1.2%	Živanović et al. (2014)
	0.4%	Cadei et al. (2002)

Table 2.4 Common values of damping ratio ξ according to the structural material

2.4.2 Supplemental damping devices

Supplemental damping devices are used in structures, such as buildings, bridges and footbridges, for controlling unexpected vibrations caused by wind, waves, earthquakes and pedestrian traffic. These devices absorb part of the energy before it can be transmitted to the structure so that the vibrations on the structure will be reduced. According to Soong & Dargush (1997), supplemental damping devices are divided into three groups as shown in the following Table 2.5.

Seismic Isolation	Passive Energy Dissipation	Semi-active and Active control
Elastomeric bearings	Metallic dampers	Active bracing systems
Lead rubber bearings	Friction dampers	Active mass dampers
Sliding friction pendulum	Viscoelastic dampers	Variable stiffness or damping systems
	Viscous fluid dampers	Smart materials
	Tuned mass dampers	
	Tuned liquid dampers	

Table 2.5: Structural protective systems (Soong & Dargush, 1997)

Seismic Isolation damping devices are usually placed at the foundation of a structure to mitigate the dynamic response. The semi-active and active control damping devices have higher costs and require sophisticated technology which is still being developed so that there is very little implementation yet. Tuned Mass Dampers (TMDs) are the most used supplemental damping devices to mitigate the pedestrian-induced vibrations in footbridges. Others passive dampers, such as Viscous Fluid Dampers (VFDs) or Tuned Liquid Dampers (TLDs) are less used in footbridges.

2.5 Vibration control in footbridges

It has been a general practice to increase damping employing supplemental damping devices when vibration problems arise in structures under pedestrian actions. In the past thirty years, supplemental damping devices, including tuned mass dampers, viscous dampers and tuned liquid column dampers, used for the reduction of the dynamic response under pedestrian actions have been used for a variety of applications in footbridges. Among them, tuned mass dampers have played a prevailing role in the mitigation of human-induced vibrations. A tuned mass damper has positive characteristics such as reliability, efficiency and low cost (fib, 2006; Low A, 2008).

A variety of supplemental damping devices has been developed and widely used in footbridges to mitigate the vertical and lateral vibrations (Figure 2.11). This data comes from a database compiled by the author from studies found in the literature (further details are shown in Annex C). The control of human-induced vibrations using supplemental damping devices had led to significant theoretical, experimental, and analytic studies. Many of the studies undertaken until now employ supplemental damping devices after the construction of footbridges so that it is necessary to consider the limited space available and the aesthetic requirements. Nevertheless, supplemental damping devices can be used within the design stage facilitating the design of more slender footbridges. However, the use of these devices at the design stage is only mentioned and unfortunately, it does not have a defined procedure either in codes or in guidelines. Eurocode 1993-2 Part 2 mentions that dampers can be employed to mitigate human-induced vibrations, but it does not have a procedure on how to employ them. There are other types of damping devices used to mitigate human-induced vibrations in footbridges such as fluid viscous damper, semi-active damper (Seiler et al., 2002), and the tuned liquid column dampers, which were employed in Toda-Park footbridge in Japan reducing the lateral displacement from 8.3 mm to 2.9 mm (Nakamura & Fujino, 2002). Despite the higher cost and high energy consumption, Moutinho et al. (2007) employed an active mass which is controlled by sensors and actuators (external damping devices) to control the vibrations in a footbridge. These sensors and actuators showed a decrease in accelerations going from 0.30 to 0.19 m/s². This reduction can also be achieved if the selection of the properties and the location of the passive devices are chosen properly.

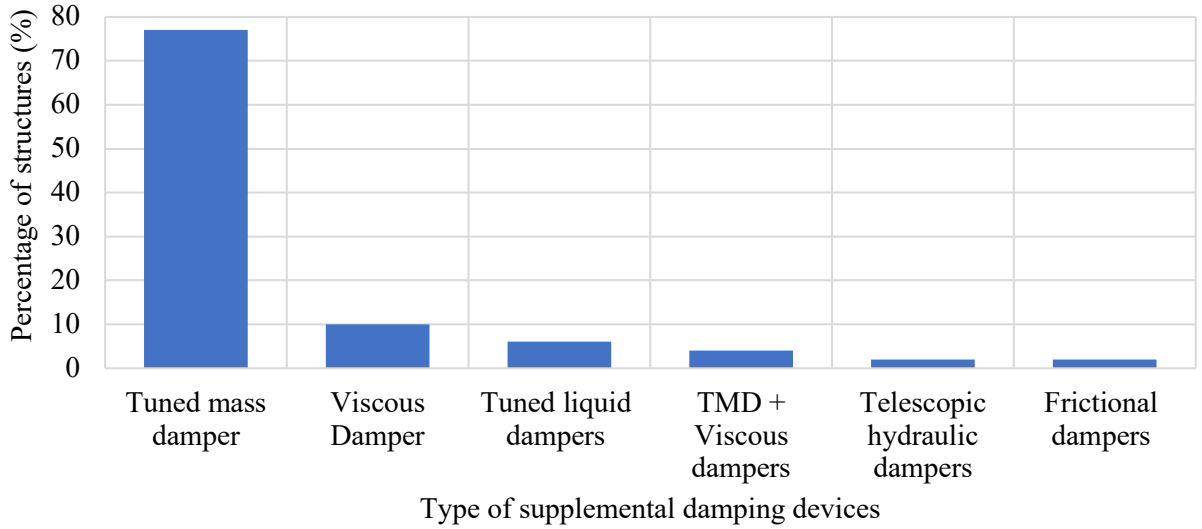


Figure 2.11: Percentage of footbridges from a dataset of 54 footbridges compiled with supplemental damping devices to reduce human-induced vibrations

The characteristics of supplemental damping devices in footbridges will be presented herein. It is noticeable that each one of these alternatives has positive and negative characteristics. As a result, the following features can be listed:

- **Frictional damping device**

  These are infrequently used in footbridges. It is useful to damp several modes. It has a high capacity to dissipate energy. However, the non-linear behaviour makes their numerical evaluation harder. Besides, it can have oxide layers on the surface.

- **Telescopic hydraulic damper**

  These are infrequently used in footbridges. It can be used to damp vertical or lateral vibrations. It has a high capacity to dissipate energy based on its force versus velocity characteristic. However, it is expensive to employ in footbridges.

- **Tuned sloshing damper**

  These are infrequently used in footbridges. It is not required sophisticated components. Therefore, it is considered as a cheap device. However, the frequency and damping ratio

of this type of device increases nonlinearly with the amplitude of the excitation force so that it is hard to tune them to their optimal parameters.

- **Tuned liquid column damper**

  These are infrequently used in footbridges. It is easy to tune the natural frequency and damping. It has a low cost of design and maintenance. However, in many cases, numerical and experimental investigations are required for the design and implementation of this damper.

- **Tuned mass damper**

  This device is widely used. It is easy and quick to install. Therefore, an additional operator is not required. Besides footbridges have sometimes few modes to be damped out. In this case, a single TMD can be employed to mitigate vibrations. Furthermore, if it is required to damp out more than one mode it is necessary to design as a multiple tuned mass dampers (MTMDs).

- **Viscous damper**

  This approach is not used often. It has high reliability. It has a high capacity to dissipate energy. It is useful to damp out several modes. However, the non-linear behaviour makes their numerical evaluation harder.

It is noticeable that each device has positive and negative attributes. Considering that the TMD has been widely used in the mitigation of dynamic response in footbridges, this section shows previous research work for the state of the art on TMDs and methodologies focusing on how to use them and how to minimize the dynamic response in footbridges, considering that TMDs have been widely used as a way to reduce human-induced pedestrian vibrations.

2.5.1 Tuned mass damper design and approaches

The objective of this section is to provide an overview of the development of an optimum methodology for the design of more slender footbridges. Maximizing the advantages of a TMD requires an accurate analysis of the dynamic response of the footbridge under dynamic forces, and an optimal selection of the TMD properties and location according to the dynamic analysis. Therefore, it is imperative that these factors are considered when implementing the TMD in footbridges in order to satisfy the serviceability criteria in an efficient manner.

Multiple researchers have proposed different procedures in order to determine the optimum parameters of supplemental damping devices in different structures. The conventional procedure for determining the optimum characteristics of the TMD that minimize the displacement was developed by Den Hartog (Soong & Dargush, 1997), in case of harmonic excitation $f(t)$ of amplitude f_o and of pulsation ω, when the structural system is undamped ($C = 0$). The dynamic amplification factor R, defined as the ratio between the maximum dynamic amplitude y_{max} and the static displacement y_{st}, is calculated from Equation (2.9).

$$R = \frac{y_{max}}{y_{st}} = \sqrt{\frac{(\alpha^2 - \beta^2)^2 + (2\xi\alpha\beta)^2}{[(\alpha^2 - \beta^2)(1 - \beta^2) - \alpha^2\beta^2\mu]^2 + (2\xi_a\alpha\beta)^2(1 - \beta^2 - \beta^2\mu)^2}} \tag{2.9}$$

$$\beta = \frac{\omega}{\omega_s} \tag{2.10}$$

$$\alpha = \frac{\omega_a}{\omega_s} \tag{2.11}$$

$$\omega_a^2 = \frac{k}{m} \tag{2.12}$$

$$\omega_s^2 = \frac{K}{M} \tag{2.13}$$

$$\xi_a = \frac{c}{c_c} = \frac{c}{2m\omega_a} \tag{2.14}$$

$$\mu = \frac{m}{M} \tag{2.15}$$

Where β is the forced frequency ratio, α is the frequency ratio, ω_a is the natural frequency of the TMD, ω_s is the natural frequency of the structural system, ξ_a is the damping ratio of TMD (c/c_c the optimum damping of the absorber), k is the stiffness and μ is the mass ratio (ratio between absorber mass, m, and modal mass, M). These parameters are defined in Equations (2.10), (2.11), (2.12), (2.13), (2.14), and (2.15) respectively. Figure 2.12 shows the amplification factor as a function of the frequency ratio β for five different damping ratio ($\xi = 0.00, 0.05, 0.10, 0.20, 0.70$).

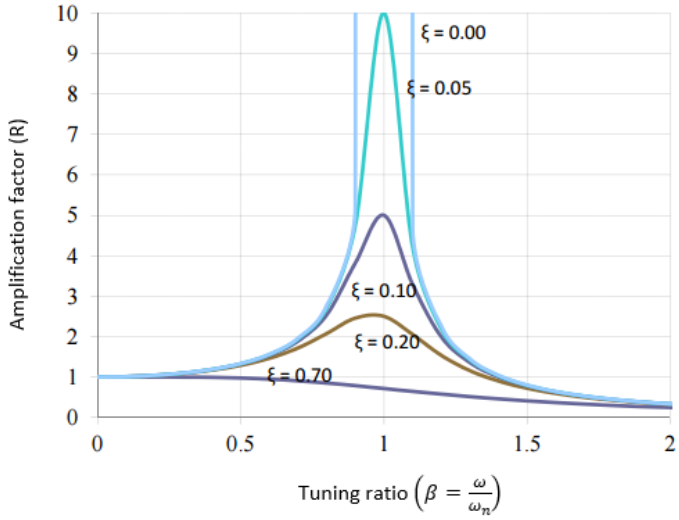


Figure 2.12: Amplification Factor R as a function of the frequency ratio β

According to Den Hartog criteria, the parameters of the TMD (frequency ratio α_{opt} and damping ratio ξ_{opt}) are used to minimize the displacement which can be determined as seen in Equations (2.16) and (2.17) (Soong & Dargush, 1997).

$$\alpha_{opt} = \frac{1}{1+\mu} \tag{2.16}$$

$$\xi_{opt} = \sqrt{\frac{3}{8}\frac{\mu}{(1+\mu)^3}} \tag{2.17}$$

Warburton (1982) focused on finding the optimal TMD parameters for structures under white noise excitation minimizing the acceleration of the structure. The TMD parameters of an undamped structure according to Warburton are given by Equations (2.18) and (2.19).

$$\alpha_{opt} = \frac{\sqrt{1-\frac{\mu}{2}}}{1+\mu} \tag{2.18}$$

$$\xi_{opt} = \sqrt{\frac{\mu * (1-\frac{\mu}{4})}{4(1+\mu)(1-\frac{\mu}{2})}} \tag{2.19}$$

Another alternative to calculate the damping ratio for the TMD has been proposed by Krenk et al. (2005) with the aim of minimizing the structural accelerations. The optimum damping ratio of an undamped primary structure is given by Equation (2.20).

$$\xi_{opt} = \sqrt{\frac{1}{2}\frac{\mu}{(1+\mu)}} \tag{2.20}$$

In relation to these formulas, Asami et al. (2002) proposed other equations to calculate the optimum frequency ratio considering structures with a low damping ratio such as footbridges. The analytical approximations (2.21) and (2.22) were obtained in order to calculate the optimal damping frequency and damping ratio by minimizing the acceleration.

$$\alpha_{opt} = \sqrt{\frac{1}{1+\mu}} \tag{2.21}$$

$$\xi_{opt} = \sqrt{\frac{3\mu}{8(1+\mu)}}\sqrt{1+\frac{27\mu}{32}} \tag{2.22}$$

Table 2.6 provides a comparison for the typical values of mass ratio (0.01 to 0.05) found in footbridges according to the previous equations. It can be seen that the values of the optimum frequency ratio α_{opt} are similar for undamped and damped structures, while the values for the damping ratio ξ_{opt} are different. The damping ratio calculated by Den Hartog for an undamped structure is similar to those values calculated by Asami for a damped structure.

μ	Den Hartog (1956)		Warburton (1982)		Krenk (2005)	Asami et al. (2002)	
	α_{opt}	ξ_{opt}	α_{opt}	ξ_{opt}	ξ_{opt}	α_{opt}	ξ_{opt}
0.01	0.9901	0.0609	0.9926	0.0498	0.0704	0.9950	0.0612
0.02	0.9804	0.0857	0.9853	0.0702	0.0990	0.9901	0.0865
0.03	0.9709	0.1045	0.9781	0.0856	0.1207	0.9853	0.1058
0.04	0.9615	0.0144	0.9711	0.0985	0.1387	0.9806	0.1221
0.05	0.9524	0.1336	0.9642	0.1098	0.1543	0.9759	0.1364

Table 2.6: Optimum damping ratio (α_{opt}) and optimum frequency ratio (ξ_{opt}) according to Den Hartog, Warburton, Krenk and Asami criteria

Figure 2.13 shows the frequency response of structural displacement and TMD relative displacement for a structural damping ratio of 0.06 (Section 2.4.1) for both cases undamped and damped structures. It can be seen that while the mass ratio μ increases, the frequency response function of the structural displacement (H_s), and TMD relative displacement (H_d) decrease. The relative displacement of the TMD and the bridge deck must be limited because of the small space

that the TMD might have, considering the fact that these devices are usually located in the deck of the bridge.

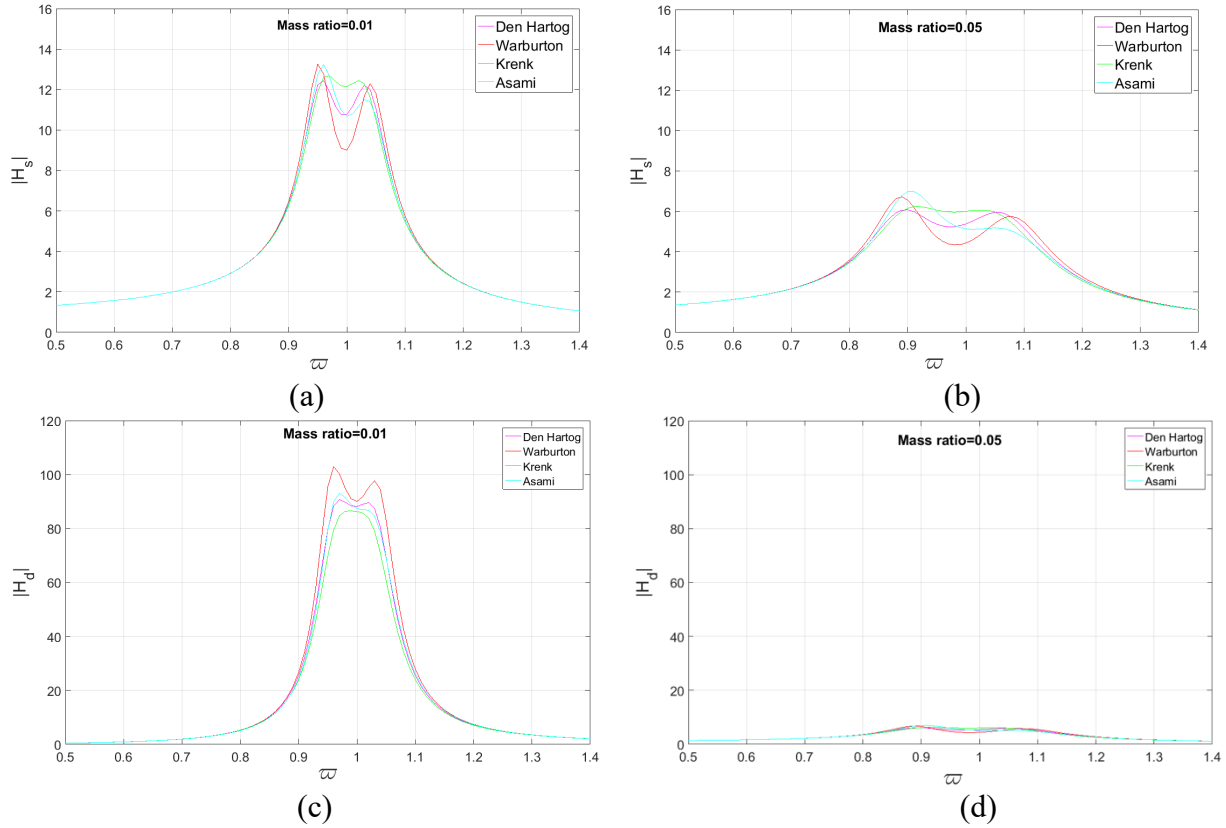
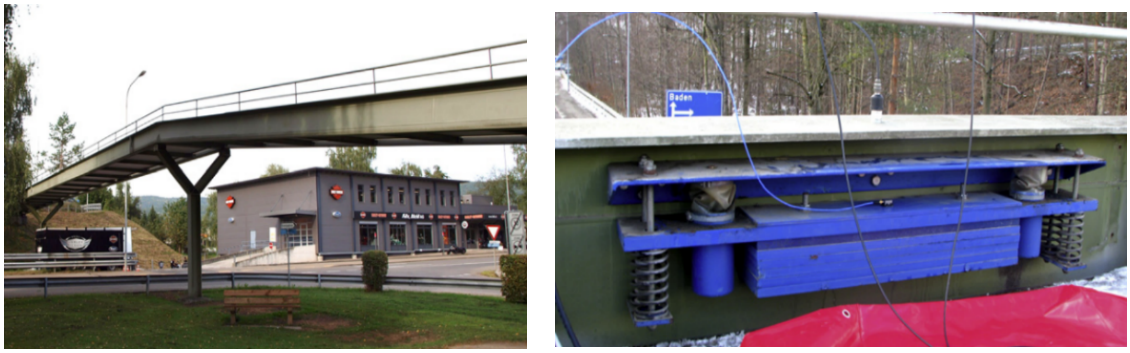


Figure 2.13: Frequency response function of (a, b) structural displacement (H_s); and (c, d) TMD relative displacement (H_d)

Regarding the tuned mass dampers systems, several research studies in footbridges with these devices have been conducted to clarify the benefits of these systems in the mitigation of human-induced vibrations. Jones & Pretlove (1981) employed vibration absorbers in two footbridges in order to control the maximum structural response. As a result, they highlighted that tuned mass dampers were an effective method to reduce human-induced vibrations. Setareh & Hanson (1992) proposed a component mode synthesis method to reduce vibration using TMD based on an equivalent single degree of freedom (SDOF) of one mode with a TMD. This study was applied to a two-dimensional model and as a result, the optimum parameters of the TMD were obtained which were close to the natural frequencies of the main system. Bachmann (1992) highlighted that activities such as walking, running and jumping affect the dynamic response of the structures such

as footbridges, buildings, sports halls, etc. and for mitigating these vibrations the tuned mass damper could be employed.

Bachmann & Weber (1995) presented curves for damped structures based on numerical analysis that could be employed in the design of the TMD to reduce accelerations. They explained that excessive vibrations are caused when the frequency due to pedestrian loads matches with the structural frequencies of the footbridge. In this study in order to reduce the excessive vibrations, tuned vibration absorbers supported by four springs were employed after the footbridge construction. Posterior studies in the same footbridge (Figure 2.14) show that the damper was working efficiently (Weber & Feltrin, 2010). Table 2.7 shows that the efficiency of the absorbers in the reduction of the accelerations under a pedestrian walking does not change over time. The high efficiency of the damping devices in the reduction of the dynamic response is a remarkable issue to point out.



(a) (b)

Figure 2.14 (a) Steel girder footbridge; (b) Absorber (Weber & Feltrin, 2010)

Test	Accelerations (m/s²)			
	Summer 1992		Summer 2008	
	Locked	Unlocked	Locked	Unlocked
Jumping	9.00	0.48		
Walking	1.20	0.24	1.30	0.25
Running	1.70	0.59		

Table 2.7: Vertical accelerations on the girder footbridge (Weber & Feltrin, 2010)

Based on studies on the London Millennium Bridge, Dallard et al. (2001) mentioned that human-induced force in the lateral direction is proportional to the footbridge lateral velocity; for that reason, it is necessary to increase damping. The required damping (c) was proposed through Equation (2.23) in which k is the lateral walking force coefficient (Ns/m), ϕ_i is the modal shape coordinate, f is the natural frequency in Hz and M is the modal mass.

$$c > \frac{k \sum_{i=1}^{i=N} \phi_i^2}{4\pi f_1 M_1} \tag{2.23}$$

Multiple experimental tests on footbridges, such as Hatanaka & Kwon (2002) showed that the reduction of the dynamic response is a consequence of the incremental of damping through a TMD attached in the footbridge. Collette (2002) observed that vibrations were reduced using damping devices through preliminary studies on finite element and then it was confirmed with field measurements. Brownjohn et al. (2004) analysed the dynamic response through finite element analysis and experimental tests in the Changi Mezzanine Bridge which had vibration problems. This bridge is a shallow arch bridge with a main span length of 140 m and side spans length of 30 m which had lateral, torsional and vertical frequencies below 2.0 Hz. They compared the frequencies and modal mass numerically and experimentally, and they highlighted that the numerical results were close to the measured values. Tuned mass dampers were employed in the locations that showed larger displacements, as a result, induced vibration by pedestrians was mitigated. However, this study did not mention a procedure on how to employ these tuned mass dampers. Other studies, such as Živanović et al. (2006) and Caetano et al. (2007) showed the reduction of dynamic response employing tuned mass damper and highlighted the importance of modelling footbridges considering realistic boundary conditions, material properties, non-structural elements, etc., as a way to obtain the most accurate dynamic response.

Meinhardt (2008) performed an experimental study on two footbridges, a girder footbridge with a vertical frequency of 2.0 Hz and a cable-stayed footbridge with a vertical and lateral frequency of 1.6 and 0.8 Hz, respectively. This experiment showed that if the calculations of the damper

parameters are wrong, then the TMD efficiency will be reduced. In this case, it was necessary to design a special tuned mass damper due to the reduced available space for the installation of it. Fiebig (2010) mentioned that the use of tuned mass damper is an economical strategy to mitigate vibrations based on the experimental studies of those two footbridges. He also claimed that these devices should be planned at the design stage.

Studies to minimize vibration of a footbridge in Portugal were based on numerical methods, and field measurements, these showed that the large reduction in the displacement on this footbridge was the result of employing tuned mass dampers (Caetano et al., 2010 b). Nevertheless, they highlighted that due to the limited available space for the tuned mass damper, it was necessary to split it into multiples one, hence the efficiency of the damper was reduced. If supplemental damping devices are split, then their efficiency is reduced. A satisfactory relation between accelerations with and without tuned mass dampers has been developed by Tubino & Piccardo (2015) using a spectral approach to simulate pedestrian vibration in the vertical direction considering pedestrian arrivals, velocities, step frequencies and pedestrian weights. In this work the response in the frequency domain of a footbridge employing a TMD and the frequency of the TMD, connected to a structure represented by a single degree of freedom, was implemented at the location where the vibration mode has the larger displacement. However, this study did not show a procedure when more than one TMD might be required.

The TMD has been considered as one of the most valuable devices for mitigating human-induced vibrations because of the multiple advantages that they have such as: how easy it is to build and install, low cost of maintenance and high performance.
It can be seen from previous studies (Brownjohn et al., 2004; Caetano et al., 2010 b) that tuning the TMD in critical modes reduce effectively the vibrations; however, this effectiveness will be reduced when the TMD is split in multiple TMDs. In these studies, each TMD is capable of dampening one structural frequency. Nevertheless, such performance results require an exhaustive procedure to select the parameters and placement of multiple damping devices. It is well known that a footbridge might have a multi-modal vibration problem in which more than one TMD will be required.

Multiple studies have been developed in order to employ multiple tuned mass dampers (MTMDs) to mitigate vibration due to harmonically forces, random external forces or wind (Yamaguchi & Harnpornchai, 1993; Gu & Chang, 2001). Li et al. (2010) proposed a random optimization method for MTMDs based on the minimization of the maximum root-mean-square (RMS) acceleration where $a(t)$ is the time acceleration, and t_1 and t_2 are the time intervals (Equation (2.24)).

$$RMS = \sqrt{\frac{\int_{t_1}^{t_2} a^2(t)dt}{t_2 - t_1}} \tag{2.24}$$

As a result, the maximum RMS accelerations were reduced in approximately 20% in a range of critical frequencies that the structure shown resulting from the human-induced vibration. Daniel et al. (2011) proposed a method based on the reduction of the accelerations under pedestrian loads with multiple critical modes. This research focused on minimizing the accelerations placing one TMD in each peak of the mode shape. They showed that the use of damping devices reduced in a significant proportion the accelerations produced by pedestrians. Nevertheless, the limitation of this research work is that the pedestrian mass was simulated as a uniform distributed load with constant magnitude moving at a constant velocity, while it is known that the pedestrian load varies in time and space.

The performance related to both parameters: properties and location, applied simultaneously in tuned mass damper in order to mitigate vibration under pedestrian actions in footbridges is scarce. In some research works, it is noted that the multi-objective method is a robust method which can be employed to obtain more accurate parameters than the traditional methods. The firefly method is a multi-objective method which can be applied to solve optimizations (Yang, 2009). An example of this can be found in Miguel et al. (2014) where the force and placement of friction dampers in footbridges under human-induced vibrations are fully described. Nevertheless, the pedestrian action was considered using a deterministic model.

Genetic algorithm is another multi-objective method that has been used to optimize problems and it is based on the natural selection process. This methodology has been used to solve optimization problems in order to ensure an optimal and robust design. Many studies have focused on the

optimization of TMD parameters through the genetic algorithm such as Marano et al. (2009) to reduce vibrations in a structure under random vibrations, and Mohebbi et al. (2013) to reduce white noise excitation. An application of this method was employed in footbridges under a deterministic pedestrian model (only vertical direction) to optimize the mass, stiffness and damping of the TMD through an objective function subjected to three conditions (mass ratio from 0.01 to 0.10, optimum frequency from 0.85 to 1.15 and optimum damping from 0.05 to 0.20). The result was compared with the Den Hartog criteria (Section 2.5.1) showing a slight reduction of the TMD parameters in comparison to the results obtained with the genetic algorithm methodology (Jiménez-Alonso & Sáez, 2015).

Despite the related studies on tuned mass dampers previously cited, it is noticeable that a methodology to optimize parameters and placement of tuned mass dampers in footbridges with the aim of reducing the dynamic response under pedestrian loads should be developed. This methodology should use a reliable finite element model (FE model) which can be capable to consider the human-induced vibration in the vertical direction and to capture the non-linear behaviour of the pedestrian loads in the lateral direction in order to obtain an accurate dynamic response, and in the cases where the serviceability criterion is not fulfilled, supplemental damping devices can be employed to design more slender footbridges.

2.5.2 Built footbridges with supplemental damping devices

There are many cases in which supplemental damping devices have been employed to mitigate the human-induced vibration in footbridges, such as the London Millennium Bridge (Figure 2.15) and the examples shown in Section 2.2. The London Millennium Bridge, which crosses the Thames River, has very low lateral frequencies. It has frequencies near 0.8 Hz in the south span, 0.5 Hz in the central span and 0.9 Hz in the north span. In order to satisfy the serviceability criteria viscous and tuned mass dampers were installed (Dallard et al., 2001). More cases of footbridges where supplemental damping devices were employed are shown in Annex C.



Figure 2.15: The London Millennium Bridge (Structurae, 2015)

2.5.3 Current research: inherent drawbacks

Despite recent advances of the research previously cited about pedestrian actions (Section 2.3), vibration control in footbridges (Section 2.5) and TMD design (Section 2.5.1), current models used to assess the serviceability criteria in footbridges under human-induced loads do not include these recent proposals. The main limitations of the current research are outlined as follows:

a) The human-induced force in the vertical and lateral direction cannot be modelled through a Fourier series due to the pedestrian intra- and inter-variability cannot be considered. It is highlighted that human-induced force depends on many factors such as height, weight, step frequency, speed, the interaction between pedestrians and parapets while they are crossing the bridge, etc.

b) To represent traffic flows sophisticated methods are needed including a Poisson arrival process and representing the intra-variability of each pedestrian in order to have a pedestrian load model as real as possible to ensure an accurate dynamic response.

c) A considerable amount of previous research on the mitigation of human-induced vibration in footbridges using TMD has been studied. Those studies have mainly focused on the following individual characteristics: (1) modelling and evaluating the performance of pedestrian loads in the vertical direction, (2) modelling and evaluating the performance of pedestrian loads in the lateral direction, (3) modelling and evaluating the performance of pedestrian flows in the lateral direction. However, the scarcity of research applications that integrates the three previously mentioned characteristics has become an issue. As a result, it is necessary to obtain an accurate dynamic response of the structure under an optimal pedestrian load representation, integrating the three previous characteristics. In case it is crucial, supplemental damping devices could be considered.

d) In general, analytical and experimental studies have investigated the dynamic response of the structure before and after installing the tuned mass dampers to understand their effectiveness. But, on the other hand, very little studies have been carried out regarding the implementation of tuned mass damper at the design stage, this as a measure to avoid serviceability problems after footbridge's construction. None of these studies show a methodology on how to employ this passive device to mitigate vibration in footbridges under pedestrian actions.

e) Some proposals suggest the Den Hartog criteria (traditional method) to calculate the TMD parameters. This conventional methodology focuses on obtaining the TMD parameters based on minimizing the displacement without considering the structural damping ratio. Nonetheless, this conventional methodology cannot be the most accurate way to obtain the TMD parameters because there are other methods that consider structures with a low damping ratio like footbridges (Section 2.5.1).

f) There is not a study that shows the efficiency of employing one or multiple tuned mass dampers in different locations in order to choose the best location at the design stage with accurate properties considering a stochastic pedestrian load model. It is

well known that footbridges can have more than one critical frequency, range between 0.0-5.0 Hz, that can be required to be damped (multimodal problem).

g) There is no research work which shows a detailed methodology of how TMD or MTMDs can be employed to mitigate human-induced vibrations in girder and cable-stayed footbridges under pedestrian loads to avoid serviceability problems.

2.6 Comfort criteria in footbridges

The comfort criteria of pedestrians in footbridges depends on many factors as Wheeler (1982) and Bachmann & Ammann (1987) remark on several studies. The complexity is due to the fact that humans respond differently to each situation, and that depends on the characteristics of the vibrations, the user's own characteristics and to the condition if there is only one pedestrian crossing the bridge at a time or if there are simultaneous users. The location of the structure and the surroundings also has an impact on the perception of the vibrations, as well as the pedestrian's expectations about the level of accelerations to be felt (Heinemeyer et al., 2009, Ramos-Moreno, 2015).

Considering the complexity of establishing a single criterion for human comfort, many authors have given a classification to the magnitudes of pedestrian movements according to four up to six levels of perception. But this perception was a consequence of analyzing the areas of physiological and psychological response of human beings, when they are in vehicles, in buildings, and in working areas (Gierke & Goldman, 1988). From this analysis, it was defined that people show minimum comfort at movement frequencies of 5.0 Hz for vertical movements and 1.5 Hz for lateral movements, because of the natural resonance of the human body under vibration. After many research works, Bachmann & Ammann (1987) proposed tolerance criteria for vibration exposure of humans; in which the most important characteristic is the representative acceleration value of the movement: the RMS (Equation (2.24)) and the VDV (vibration dose value) accelerations (Equation (2.25)). The lack of consideration becomes a deficiency for determining the proper values of acceleration used in RMS and VDV.

$$\mathrm{VDV} = \left[\int_{t_1}^{t_2} a^4(t)dt\right]^{\frac{1}{4}} \tag{2.25}$$

2.6.1 Evaluation of the comfort related to vertical vibration

It was previously mentioned that determining the comfort criteria for pedestrians was complex because of the variables that it represented. However, a proposal for a tolerance level has already been defined limiting the accelerations based on experimental studies considering standing, walking and standing pedestrians (Kobori & Kajikawa, 1974). Under these circumstances a proposed comfort limit for pedestrians on a bridge is limiting the acceleration to $0.5\sqrt{f_s}$, where f_s is the fundamental vertical frequency of the structure in Hz. But, some other authors were already suggesting different limits (Tilly et al., 1984; Bachmann & Ammann, 1987), based on the fact that there has been an inherent variables to the evaluation of comfort which was related to the peak dynamic deflection.

These new limits vary according to the authors. Tilly et al. (1984) suggested to increase the limit of acceptable vertical acceleration to $1.0\sqrt{\mathrm{f_s}}$, Bachmann & Ammann (1987) suggested a limit of 0.5-1.0 m/s^2 and the BSI (2003) suggests a limit of 0.7 m/s^2 (Section 2.7).

Recently published comfort limits for footbridges have proposed comfort ranges as an independent variable of the vibration frequency, this is the case of BSI (2008), based on the evaluations performed by Butz et al. (2007); Heinmeyer et al. (2009), etc. If the maximum vertical accelerations when pedestrians are walking along the footbridge are below 0.5 m/s^2 they will be a maximum comfort, if the accelerations are between 0.5-1.0 m/s^2 they will be a mean comfort, if the accelerations are between 1.0-2.5 m/s^2 it will be considered as a minimum comfort and if the footbridge has accelerations below 2.5 m/s^2 the accelerations are not acceptable.

2.6.2 Evaluation of the comfort related to lateral vibration

The comfort criteria under lateral movements has not been evaluated by many researchers. Despite this lack of research, there have been some authors who have proposed acceptable values to ensure comfort related to this direction.

ISO (2005) proposes a limit of 0.20 m/s^2 for standing pedestrians. There was an evaluation conducted at the M-bridge and the T-bridge (footbridge) detailed by Nakamura & Fujino (2002), where pedestrians found uncomfortable to walk under lateral acceleration of 0.30 m/s^2, it was highlighted the difficult to walk at a normal pace when the lateral acceleration was of 0.75 m/s^2 and it was mentioned that people would stop walking and losing balance with lateral acceleration of 1.35 m/s^2.

Based on this experiment conducted by Nakamura & Fujino (2002), it proposes to limit lateral accelerations to 0.10 m/s^2 to ensure a maximum comfort while ISO (2005) proposes to have a lateral acceleration for all possible conditions of 0.20 m/s^2. In many cases, the lateral accelerations are limited to 0.10 m/s^2 to avoid a significant fraction of the pedestrians to be syncronised with the structure (Nakamura & Fujino 2002; Setra, 2006).

2.7 Design, standards, regulations and guidelines

In this section, some of the available standards, regulations and guidelines are presented. The main focus will be on the recommended frequencies, acceleration and damping for the design and assessment of pedestrian bridges.

Design Manual for Roads and Bridges Volume 1 (BD37/01)

BD37/01: Part 2 Appendix B defines a procedure for checking structural vertical frequencies up to 5.0 Hz is defined a detailed dynamic analysis when lateral frequencies are lower than 1.5 Hz is required. In the case that the fundamental frequency of vertical vibration is ≤ 5.0 Hz, the maximum vertical acceleration must be limited to $0.5\sqrt{f_o}$ m/s^2.

Eurocodes and UK National Annexes

According to BSI (2003): Basis of Structural Design, the maximum accelerations should be 0.7 m/s^2 for vertical vibrations; for horizontal vibrations, the limit under normal use is 0.2 m/s^2 and under exceptional crowd conditions is 0.4 m/s^2. In the case that the structural frequencies are lower than 5.0 Hz for the vertical modes and lower than 2.5 Hz for lateral and torsional modes, a verification of the comfort criteria is required.

Table 2.8 shows structural damping values according to BSI (2003). Furthermore, this code suggests that supplemental damping devices can be employed to reduce vibrations.

Material	**Average damping ξ (%)**	
	Span L< 20 m	**Span L ≥ 20 m**
Steel and composite	0.5 + 0.125 (20 - L)	0.5
Prestressed concrete	1.0 + 0.07 (20 - L)	1.0
Filler beam and reinforced concrete	1.5 + 0.07 (20-L)	1.5
Timber without mechanical joints	1.0	
Timber with mechanical joints	1.5	

Table 2.8: Common values of damping ratio ξ for footbridges recommended by BSI (2003)

ISO (2005): Basis for the design of structures serviceability of buildings and walkways against vibrations

ISO (2005) recommends the following structural damping ratios according to the material's structure in structures under pedestrian loading (Table 2.9).

Material	**Damping ratio ξ (%)**
Steel with asphalt or epoxy surfacing	0.5
Composite steel/concrete	0.6
Prestressed and reinforced concrete	0.8

Table 2.9: Damping ratios according to the material's structure (ISO 2005)

Setra Technical Guide: Assessment of vibrational behaviour of footbridges under pedestrian loading

Setra (2006) gives three ranges for acceptable acceleration levels (Table 2.10). The acceleration level is considered acceptable depending on the usage of the bridge. Table 2.11 shows the four frequency ranges for vertical, longitudinal and lateral frequencies.

Acceleration ranges	Level for max acceleration (m/s^2)	
	Vertical vibration	Lateral vibration
Range 1 (Max)	≤ 0.50	≤ 0.15
Range 2 (Mean)	≤ 1.00	≤ 0.30
Range 3 (Min)	≤ 2.50	≤ 0.80

Table 2.10: Acceleration range for vertical and lateral vibration (Setra, 2006)

Frequency	Frequency ranges (Hz)	
	Vertical and longitudinal vibration	Lateral vibration
Range 1 (Maximum risk of resonance)	1.7 - 2.1	0.5 - 1.1
Range 2 (Medium risk of resonance)	1.0 - 1.7 and 2.1 - 2.6	0.3 - 0.5 and 1.1 - 1.3
Range 3 (Low risk of resonance)	2.6 – 5.0	1.3 - 2.5
Range 4 (Negligible risk of resonance)	≤ 1.0	≤ 0.3

Table 2.11 Frequency ranges in the vertical, longitudinal and lateral direction (Setra, 2006)

Setra (2006) recommends the following structural damping ratios according to the material's structure (Table 2.12).

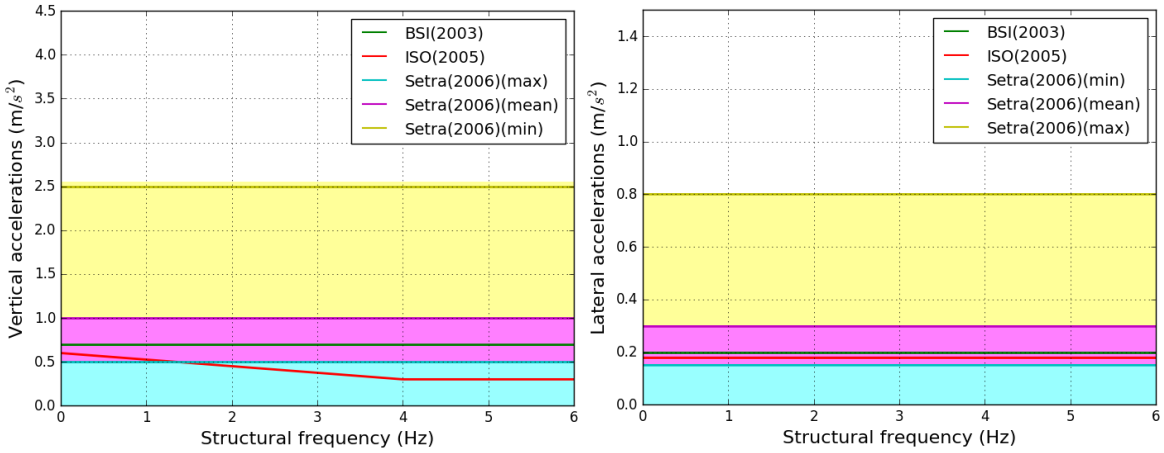
Material	Damping ratio ξ (%)
Reinforced concrete	1.30%
Prestressed concrete	1.00%
Mixed	0.60%
Steel	0.40%
Timber	1.00%

Table 2.12 Damping ratios for different material's structure (Setra, 2006)

Advanced load models for synchronous pedestrian excitation and optimized design guideline for steel footbridges (Butz et al., 2007)

This guideline (Butz et al., 2007) suggests critical frequency ranges to be considered in the dynamic design for steel footbridges under pedestrian-induced vibration. The critical structural frequencies to be considered in the vertical and longitudinal direction are $1.3 \leq f_s \leq 2.3$ Hz. And the critical structural frequencies in the lateral direction are $0.50 \leq f_s \leq 1.2$ Hz.

This guideline highlights the importance of considering the appropriate structural damping (Table 2.9 and Table 2.12) so that the accelerations of the footbridges under pedestrian loads can be calculated in an accurate way. Figure 2.16 shows a summary of the critical accelerations for vertical and lateral direction proposed by BSI (2003), ISO (2005) and Setra (2006).



(a) (b)

Figure 2.16 (a) Vertical and (b) Lateral critical accelerations as a function of the structural frequencies

2.8 Footbridge dynamics

Nowadays, pedestrian bridges are becoming more slender, leading to an amplification of the dynamic response induced by pedestrians as a consequence of the significant reduction in their structural frequencies. When any of the structural frequencies coincide with the excitation frequency, large amplitude occurs (resonance effects).

There are different factors, such as mass and structural stiffness, which affect the structural frequency and its corresponding vibration mode. If one of the footbridge frequencies lies near the step frequency of pedestrian, resonance can occur causing serviceability problems. Some authors, such as Bachmann & Weber (1995) recommended to avoid structural frequencies between 1.5 to 3.5 Hz. because these are the typical frequencies at which pedestrians do their activities. However, this is quite simplistic approach because pedestrian loading has a large impact on footbridge vibrations, not only in the range previously mentioned, but also because it depends on other factors such as intra-variability, inter-variability and others that where described in the pedestrian actions Section (2.3). These are the main factors that should be considered when referring to pedestrian actions (Ramos-Moreno, 2015):

a) In the vertical direction, the load distribution (pedestrian loads) should not be considered as a distributed load with continuous velocity; therefore, excitation in footbridges should be analysed, considering the fact that a pedestrian that crosses the footbridge has a frequency range of 1.5-3.2 Hz. This should be considered in order to evaluate in a rigorous manner the energy which is induced of each pedestrian according to the pedestrian's characteristics.

b) In the lateral direction, all the energy introduced in each step and that their amplitude is related to the dynamic response of the bridge (non-linear behaviour) should be considered because there is a relationship between the anthropometric characteristics, step width and

the characteristics of the gait of pedestrians between the lateral acceleration of the footbridge.

c) For the vertical and lateral load models, it has been claimed that anthropometric characteristics should be considered, but for this case in which both loads are combined, it is absolutely necessary to represent the weight of a pedestrian at least with the average weight of the population. Furthermore, when an average weight was examined, the accelerations were 10% greater in comparison when a constant weight was considered.

The span length is a structural parameter in footbridges which has a great effect on the vibration response under dynamic loads. Figure 2.17 shows data of structural frequencies of footbridges as a function of the span length. It can be seen from Dallard et al. (2001), Mercier et al. (2012), Oliveira (2014), and Ramos-Moreno (2015) that when the length of the span increases, the structural frequencies will be reduced. These frequencies can match with the step frequency of pedestrians, increasing the dynamic response. Based on Ramos-Moreno (2015), it is not always possible to control the human-induced vibrations by just adding additional mass. This can be seen in some cases, for both girder and cable-stayed footbridges. As a result, TMDs could be necessary to install.

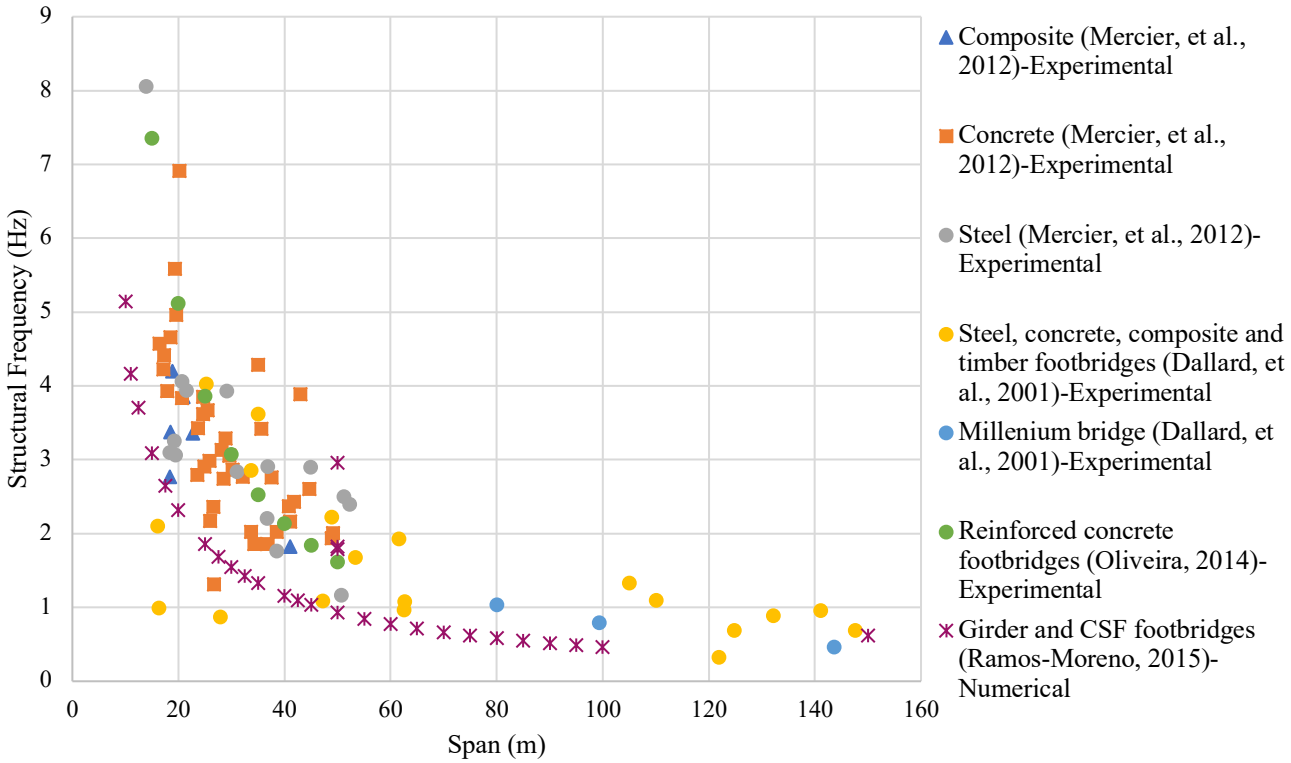


Figure 2.17 Structural frequencies as a function of the span length

2.9 Concluding remarks

The current design on pedestrian bridges is one with more slender and lighter constructions. Also, pedestrian bridges have longer spans and consequently are more prone to be excited under pedestrian traffic (see Section 2.3). In some cases, it is necessary to control undesirable accelerations by the implementation of supplemental damping devices (see Section 2.5).

Section 2.6 shows the recommended damping values, acceleration levels and frequencies according to standards, regulations and guidelines. There are several main conclusions based on this literature review that can be extracted. For instance, when a pedestrian bridge has vertical frequencies lower than 5.0 Hz, these frequencies can lie near the step frequency of pedestrian causing amplifications of vibrations. Besides, the span length has a great effect on the frequencies. Also, to represent human loads, there is a requirement to define parameters such as step length, speed, and anthropometric characteristics in a probabilistic way to simulate the most accurate force in time and space produced by them. As pedestrians do not generate the same force in each step it

is important to follow a non-deterministic approach related to the representation of pedestrian loading. In addition, an efficient method to reduce vibrations of footbridges under pedestrian loads is increasing damping by installing supplemental damping devices. The most common supplemental damping device used in footbridges is the tuned mass damper. When providing supplementary damping, the dynamic response will be reduced avoiding serviceability problems. Furthermore, footbridges need to be modelled considering boundary conditions, material's properties, etc. Finally, pedestrian loads models need to be defined through a stochastic method considering their characteristics in order to ensure an accurate dynamic response so that an optimal and robustness design of the placement and parameters of one or multiple tuned mass damper can be obtained.

It should be noted that there is a lack of research regarding the best way to employ supplemental damping devices in footbridges to mitigate human-induced vibrations. There is not a clear methodology to determine the properties of the TMDs and the best location to be implemented.

3 Research methodology and preliminary analyses

3.1 Introduction

Light footbridges are structures prone to vibrate under pedestrian loads. In some cases, conventional approaches (such as increasing the mass or shifting the structural frequencies) do not mitigate the human-induced vibrations enough and there is a requirement to employ supplemental damping devices to satisfy the serviceability criteria. To analyse the dynamic response of footbridges, an outline of a suitable methodology to evaluate the structural response of footbridges under pedestrian loads with and without supplemental damping devices is necessary. The current research work is a numerical study of the structural behaviour of girder and cable-stayed footbridges. Based on existing structures, some benchmark cases are defined as representative of the structural typology and will be taken as a reference for further analyses, i.e. parametric studies. This section provides details about the methodology for the development of the pedestrian load model which includes the vertical and lateral direction, and the interaction between pedestrians and boundaries while they are crossing the bridge (crowd modelling). It also includes the selection and the description of the structural characteristics of the girder and cable-stayed footbridges, the sensitivity analyses in order to validate the numerical models, the serviceability requirements considered and the tuned mass dampers characteristics required to mitigate the human-induced vibrations. This chapter also covers a brief description of the numerical packages employed in this study: the finite element software (ABAQUS), the code to develop a finite element model to evaluate girder footbridges (PYTHON), the code that was used to develop the input files in a parametric way (MATLAB), and the code to include the non-linear behaviour of the pedestrian loads (FORTRAN). A preliminary investigation of footbridges with and without tuned mass dampers considering different criteria to select the TMD's properties is shown at the end of the current chapter. These criteria were selected from Den Hartog, Warburton, Krenk and Asami. This investigation highlights the importance to develop design recommendations of the location and properties of tuned mass damper to reduce the human-induced vibrations in footbridges under pedestrian loads to fulfil the serviceability criteria.

3.2 Model to represent pedestrian actions

3.2.1 Description of the vertical and lateral direction

This thesis will consider the model proposed by Ramos-Moreno (2015), as it is the most comprehensive and representative model of those existing in literature so far. That model includes the vertical and lateral loads induced in each step by pedestrians. For the representation of vertical loads, knowledge of the step frequency and the pedestrian mass is required. The simulation of vertical loads will be based on the relationship between forces and weight that are transmitted by pedestrians over time. Figure 3.1 shows the parameters that are required to define the vertical load amplitude. The relationship for the median values of these parameters was defined by Ramos-Moreno (2015) based on Butz et al. (2008) where f_p is the step frequency in Hz (Table 3.1). The step by step model proposed by Butz et al. (2008) will be employed to construct the 9th order polynomial equation to describe the vertical force (Equation (3.1)). The coefficients, p_i, of the polynomial can be obtained for any step frequency, by solving a 10 x 10 system of equations which has five known points and their derivatives.

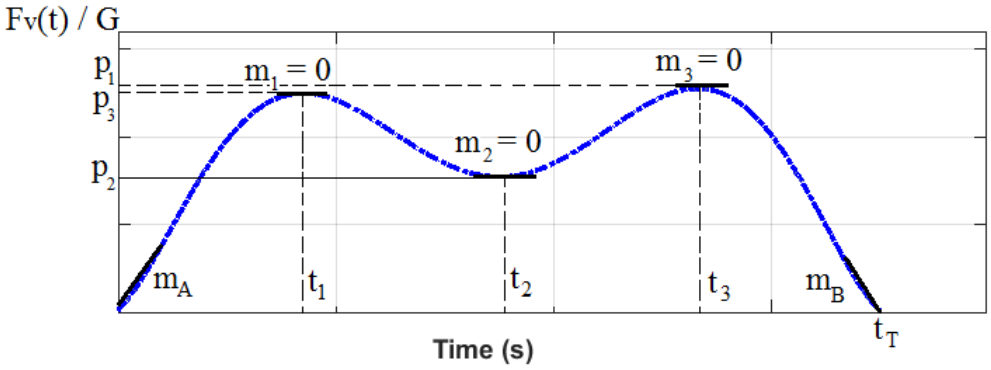


Figure 3.1 Parameters to define the amplitude of the vertical load

Parameter	Median value
p_1	$0.58 + 0.38 f_p$
p_2	$1.62 - 0.51\ f_p$
p_3	$0.74 + 0.24\ f_p$
t_1	$\left(0.46 - 0.11\ f_p\right) * t_T$
t_2	$\left(0.41 + 0.06\ f_p\right) * t_T$
t_3	$\left(0.64 + 0.06\ f_p\right) * t_T$
t_T	$1.55 - 0.46\ f_p$
m_A	$400.16 - 670.98\ f_p + 362.55\ f_p^2 - 60.41\ f_p^3$
m_B	$4.54 - 9.15\ f_p$

Table 3.1: Median values of the parameters to define the vertical load amplitude (Ramos-Moreno, 2015)

$$\frac{F_v(t)}{G} = \sum_{i=1}^{9} p_i t^i \tag{3.1}$$

Figure 3.2 plots the vertical load normalized for step frequencies from 1.3 to 2.4 Hz. The lateral load model will be simulated as an inverted pendulum (IP)(Equations (2.6), (2.7), and (2.8)) in which the pedestrian mass, half step width, lateral step frequency and the anthropometric characteristics of the pedestrian are required (Section 2.3.3)(Townsend, 1985; Bocian et al., 2012; Carroll et al., 2013). This model represents in an accurate way the lateral load in relation of the acceleration registered in the bridge at that particular time and location when the feet contact the ground according to pedestrian characteristics, such as gait, step width, and anthropometric characteristic.

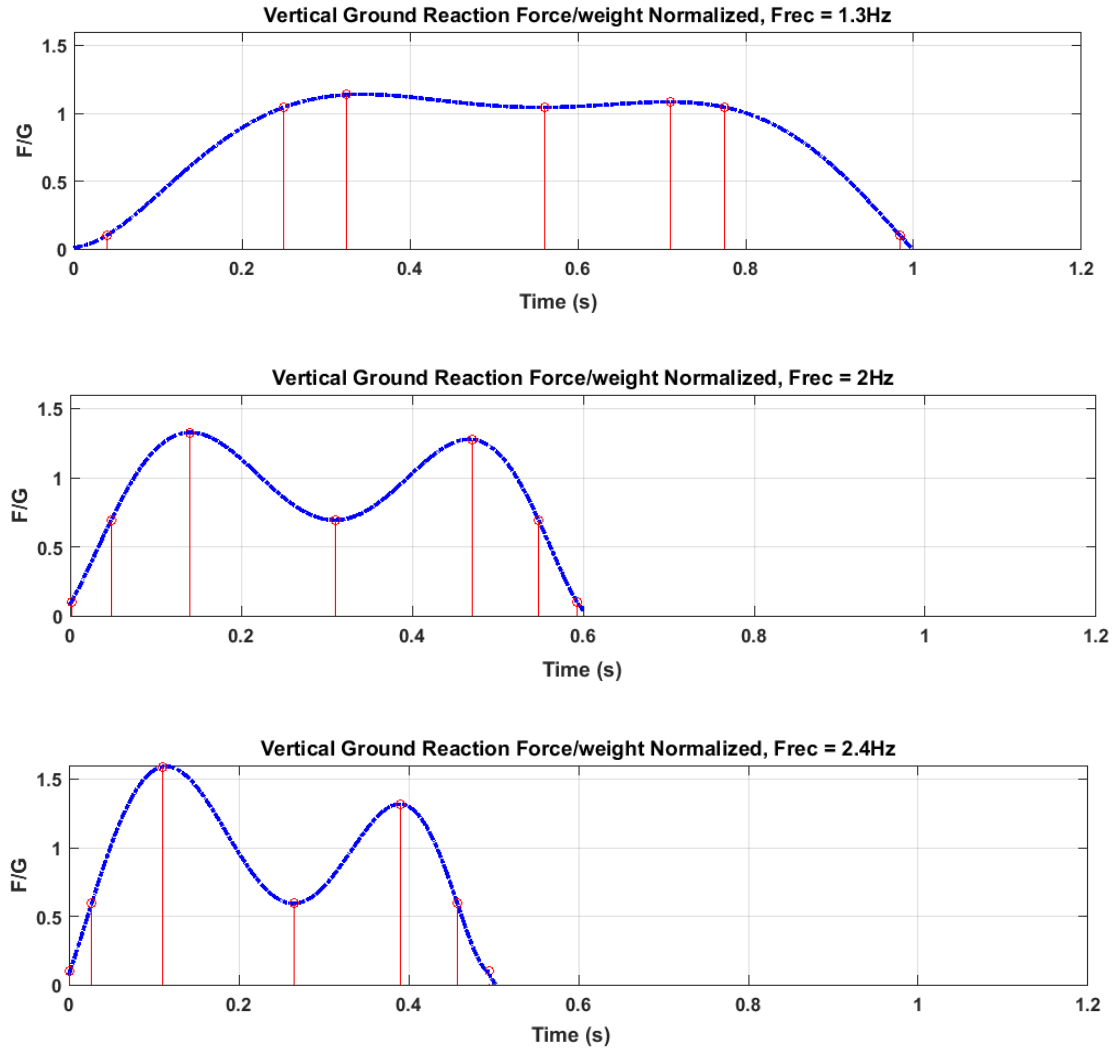


Figure 3.2: Vertical human force for step frequencies from 1.3 to 2.4 Hz

3.2.2 Parameters of the pedestrian load model

It is important to determine the specific parameters of the pedestrian load model, considering two main aspects of the vertical and lateral loads. For vertical loads, the step frequency and the pedestrian mass are most influential, while for lateral loads the pedestrian height, and step width are also important in addition to the step frequency and pedestrian mass. The parameters of the anthropometric characteristics were developed from a meta-analysis of data collected and obtained through experimental recordings found in the literature (Ramos-Moreno, 2015).

There has been plenty of research on correlating the step frequency with the speed of walking. These studies were based on 909 different subjects represented in 33 bins, resulting in the development of Ramos' model where the expected step frequency, f_p (Hz), is considered and it has been described through a quadratic function in terms of the speed v_p (m/s) (Equation (3.2)).

$$f_p = 0.11 + 2.11v_p - 0.47v_p^2 \tag{3.2}$$

Regarding the pedestrian's velocity (v_p) the model proposed the Equation (3.3). This is a function of the pedestrian free velocity, v_f , the effect of the aim of the journey , ϕ_j, and the flow density, ϕ_d. The free velocity is when external constraints do not exist and they do not have a specific aim for the journey. Hence, the pedestrians will choose their velocity based on their anthropometric characteristics and their age. To develop the Equation (3.4) data based on 1492 different subjects from Europe, USA and Japan were analysed. For this, a relationship between free velocity and pedestrian age, a_p (years), and height h_{pd} (meters) was developed. To simulate the effect of the flow density, ϕ_d, it is required to apply the Equation (3.5), where d is the density of the flow (pedestrians/m²). Equation (3.6) was developed representing the step width, w_{st} (cm) in terms of the pedestrian's velocity (m/s) and pedestrian's height (m).

$$v_p = v_f \phi_j \phi_d \tag{3.3}$$

$$v_f = 0.22 + 1.28x10^{-2}a_p - 1.71x10^{-4}a_p^2 + 0.55h_{pd} \tag{3.4}$$

$$\phi_d = 1 - exp\left[-1.913\left(\frac{1}{d} - \frac{1}{5.4}\right)\right] \tag{3.5}$$

$$w_{st} = 0.2686 - 0.3774\, v_p + 0.1337\, {v_p}^2 + 0.0492\, h_{pd} \tag{3.6}$$

Table 3.2 shows the values to represent the purpose of the journey, ϕ_j. "Business" represents pedestrians from 20 to 65 years old that cross the bridge exclusively to work. "Commuting" refers to pedestrians from 10 to 80 years old which cross the bridge repeatedly. This includes people crossing between home, study or workplace. "Leisure" refers to pedestrians who cross the bridge for leisure activities such as shopping.

Activity	ϕ_j
Business	1.20
Commuting	1.11
Leisure	0.86

Table 3.2: Values of the factor φ_j according to the purpose of the journey

Ramos' pedestrian model is capable of describing the load induced by each pedestrian in an accurate way. To represent the subject variability in the step frequency, a Markov chain Monte Carlo (MCMC) simulation is used. This approach ensures that individuals vary their step frequency according to same overall distribution, but that successive steps are autocorrelated. An example of the MCMC sampling to describe the intra-variability of four simulations can be seen in Figure 3.3. The variability in the step frequencies which are the average step frequencies that each pedestrian has while crossing the footbridge can be observed.

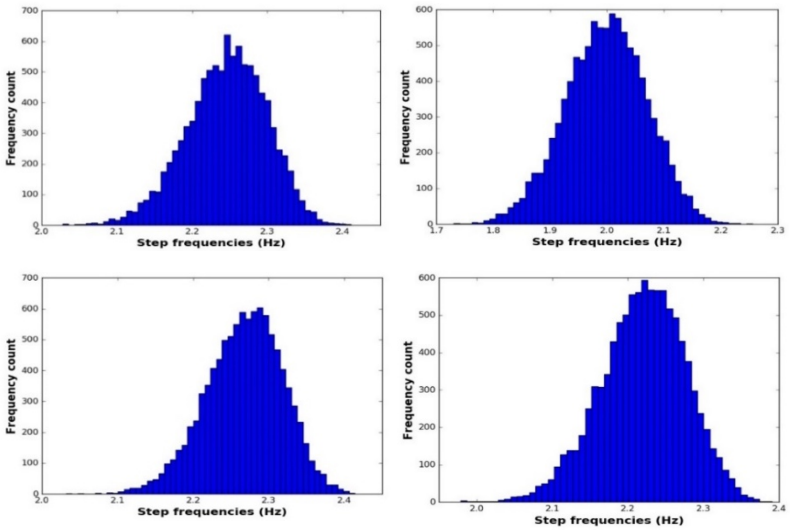


Figure 3.3 Step frequency distribution following a MCMC sampling for a distribution in a footbridge with a span length of 22.5 m for leisure and commuting activities. The value adopted for the standard deviation of the step frequency is 0.15 (Butz et al. 2008)

The step width variability is represented by the lateral movement of the CoM (centre of mass) of each pedestrian, and this depends upon the lateral bridge response. Figure 3.4 summarised the pedestrian load model in which the initial flow data which is statistically generated by the pedestrian data (anthropometric characteristics) is used to calculate the gait properties such as desired speed, mean step frequency and half-step width that are consistent with the type of journey (Equations (3.3), (3.4), (3.5), (3.6) and Table 3.2). Then, the crowd simulation is considered so that the trajectory of each pedestrian can be defined.

Each pedestrian crosses the footbridge at an arrival time according to a Poisson process and at a lateral position across the deck width. Within these considerations, an initial lateral position and velocity are defined for each pedestrian. A uniform distribution over [0.0 - 0.75], where 0.75 m represents the maximum considered value of step length, is used to represent the initial step position along the deck and for the initial step frequency of each pedestrian (mean step frequency which was previously obtained). To represent the next steps, it is important to make the following assumption: if the velocity is not affected by external constraints, then the step frequency for the next step will be done applying the MCMC simulation (and therefore considering the intra-

variability of each pedestrian). Constrains can be the presence of physical elements or other people. Otherwise, if the pedestrian's velocity is affected by other pedestrians, through the crowd model, the step frequency will be calculated through a quadratic function in terms of the speed (Equation (3.2)). Groups of pedestrians are considered by assigning similar desired speeds to the pedestrians in the group and forcing them to remain within a particular distance through the crowd model. The desired speed of pedestrians in a group corresponds to the speed of the slowest pedestrian.

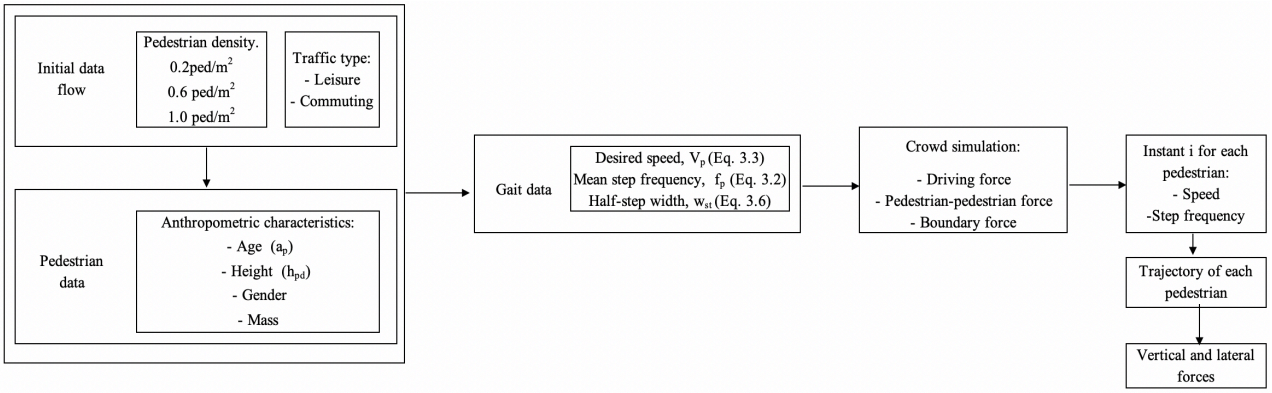


Figure 3.4: Ramos' pedestrian model (Ramos-Moreno, 2015)

3.2.3 Description to consider the crowd behaviour

In order to consider the human interaction while the pedestrians are crossing the bridge, a social force model (Section 2.3.5) was considered. This model has been applied in different studies such as transport and footbridges (Helbing and Molnar, 1995; Carroll et al., 2012; Jiménez-Alonso et al., 2016). In these studies, the parameters required to define the social force model are shown. The model is based on that the resultant force ($\boldsymbol{F}_T$), this force is needed to describe movement and direction which is the sum of the driving force ($\boldsymbol{F}_D$), the force due to the interaction with other pedestrians ($\boldsymbol{F}_p$) and the force due to the interaction with boundaries ($\boldsymbol{F}_b$) as is defined by Equation (3.7). The bold font in Equation 3.7 indicates a vector quantity.

$$\boldsymbol{F}_T = \boldsymbol{F}_D + \boldsymbol{F}_p + \boldsymbol{F}_b \tag{3.7}$$

The driving force is governed by the motivation that the person has to reach the destination (Equation (3.8)). To calculate this force, it is necessary to define the pedestrian mass (m_p), the desired velocity ($\boldsymbol{v}_d$), the actual velocity ($\boldsymbol{v}_p$) and the relaxation time (t_r = 0.50 s). The relaxation time refers to the time that is required to correct any disturbance that can occur during the movement of each pedestrian.

$$\boldsymbol{F}_D = m_p \left(\frac{\boldsymbol{v}_d - \boldsymbol{v}_p}{t_r} \right) \tag{3.8}$$

The interaction among pedestrians is based on the sum of social and physiological forces. The social force refers to when some pedestrians are crossing the bridge, a force will maintain distance between other pedestrians. The physiological force refers to the body force and sliding force, where the body force is the force to avoid physical damage from any possible physical contact with other pedestrians, and the sliding force is to avoid passing other pedestrians with more velocity when the distance is minimal. The interaction between boundaries is calculated based on the body and sliding force strength due to contact of the pedestrians with the boundaries. This force refers that the pedestrians will keep a certain distance from the boundary due to a repulsive force between the pedestrian and the boundary.

3.3 Description of footbridges

Girders are one of the most typical structural typologies for footbridges. For certain materials and for certain span ranges, vibrations cannot be mitigated in an efficient manner by adding mass (Ramos-Moreno, 2015). Cable-stayed footbridges are very slender structures which may have serviceability problems. It has been shown that both types of footbridges can be prone to vibrate with large accelerations without supplemental damping devices when certain span lengths are exceeded (Ramos-Moreno, 2015). Therefore, both typologies will be considered as part of this study. The main characteristics of both typologies have been chosen based on an exhaustive analysis of these bridges found in the literature (Ramos-Moreno, 2015).

3.3.1 Girder footbridges

The most common girder footbridges will be analysed (Table 3.3). These frequent types were identified by Ramos-Moreno (2015) through a database built from existing built footbridges and reported in the literature. The materials that will be employed are concrete (precast or cast-in-place), steel, timber, aluminium and Glass Fibre Reinforced Polymer (GRFP). The typical reinforced concrete sections are slab, T-beam and box girder. The pre-stressed concrete footbridge is more efficient. High-performance concrete allows achieving larger spans for a given depth or slenderer decks for a given span length. The typical sections are "I" girders and box girders.

The typical spans for steel-concrete composite box girders vary from 20 to 50 m. For longer spans, an orthotropic deck is usually employed. To consider the most common girder footbridges, the dynamic response will be assessed in one span for different transverse sections and materials previously mentioned (Section 2.2). Based on Ramos-Moreno (2015), there were spans for which the serviceability criterion was not fulfilled. For these cases, the impact that can have the implementation of TMDs in the dynamic response will be analysed. It will also be implemented TMDs in the other span lengths to make a comparative cost study between implementing TMDs or increasing the slab thickness.

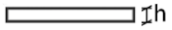
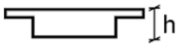
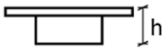
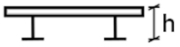
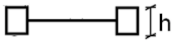
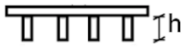
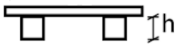
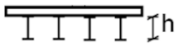
Deck cross sections		Span length (m)	Depth (m)
	Section Type 1: Prestressed concrete slab	10 < L < 45	h=L/35
	Section Type 2: Reinforced concrete slab	5 < L < 35	h=L/25
	Section Type 3: Prestressed concrete T-slab	5 < L < 35	h=L/40
	Section Type 4: Concrete box girder	12 < L < 45	h=L/40
	Section Type 5: Steel box girder with concrete slab	20 < L < 50	h=L/30
	Section Type 6: Steel I beams with concrete slab	10 < L < 45	h=L/30
	Section Type 7: H-shaped concrete section with timber decking	5 < L < 35	h=L/35
	Section Type 8: Timber beams and concrete slab	5 < L < 30	h=L/25
	Section Type 9: Aluminium box girders and concrete slab	5 < L < 25	h=L/30
	Section Type 10: GFRP beams and concrete slab	5 < L < 25	h=L/40

Table 3.3: The most common cross-sections and materials in girder footbridges (Ramos-Moreno, 2015)

The material properties of the girder footbridges are selected according to guidelines and standards (Table 3.4). The minimum recommended values for the damping factors have been considered, as it seems that the values given by the guidelines may overestimate the real magnitudes (Heinemeyer et al., 2008; Van Nimmen et al., 2014). As the minimum values given by Heinemeyer et al. (2008)

are suggested for short spans (Table 2.4), these values will be used for the damping ratio for the girder footbridges according to their structural material (Chapter 4).

Structural Material	Standard	Young Modulus (GPa)	Specific weight (kN/m^3)
Reinforced concrete	EC2(BSI,2011)	31.0	25.0
Prestressed concrete	EC2(BSI,2011)	37.0	25.0
Steel	EC3(BSI,2009) EC3(BSI,2010a)	210.0	78.5
Timber	EC5(BSI,2009; BSI,2010c)	12.0	7.0
Aluminium (Alloy EN AW 6082)	EC9 (BSI,2010b)	70.0	27.0
GFRP	Eurocomp Handbook (Clarke, 1996)	17.2	25.6

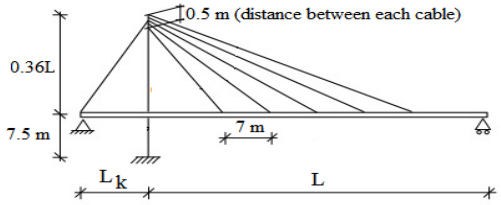
Table 3.4: Structural materials characteristics of girder footbridges (Ramos-Moreno, 2015)

3.3.2 Cable-stayed footbridges

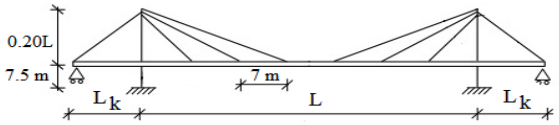
The main characteristics of the cable-stayed footbridges (CSFs) can be found in Section 2.2.1 and they will be used to assess the dynamic response under pedestrian loadsTo evaluate the dynamic performance with and without supplemental damping devices, cable-stayed footbridges with one and two pylons will be considered. The dynamic response in CSF with different pylon shapes (I, H and A) will be assessed. These are the most common pylon shapes (Figure 2.5). The deck width for the benchmark cases considered in the parametric studies is 4 meters, which is the average width in constructed CSF footbridges (Table 3.5). The deck depth is L/100 (m), which represents

the value adopted by designers (Figure 2.6). The distance between anchorages in the deck is 7 m, and the magnitude of the tower height below the deck is 7.5 m, which are the average values of existing cable-stayed footbridges (Ramos-Moreno, 2015).

Large accelerations have been obtained without supplemental damping devices when certain structural parameters have been evaluated (Ramos-Moreno, 2015). These main structural parameters are shown in Table 3.5, which represent the mean values adopted by designers in existing cable-stayed footbridges from the dataset in Annex B.



Cable-stayed footbridges with one tower



Cable-stayed footbridges with two towers

Geometric characteristics	
Main span length (L)	50,100,150 (m)
Side span length (L_k)	0.20 L (m)
Deck depth	L/100 (m)
Deck width	4 m
Cable-system arrangement	Semi-fan (with 0.5 m spacing between anchorages of stay cables at the top of the pylon)
Pylon shape	I, H and A

Table 3.5: Geometric characteristics of cable-stayed footbridges for the parametric studies (Ramos-Moreno, 2015)

The material properties of the cable-stayed footbridges are selected according to guidelines and standards (Table 3.6 and Table 3.7). The deck is a composite concrete-steel structure (in-site reinforced concrete slab) (Figure 3.16). These materials were chosen based on the most common materials adopted by designers in existing cable-stayed footbridges.

Structure concrete		Structural steel	
Compressive strength	f_{ck} = 40 MPa	Yield strength	$f_{s,y}$ = 355 MPa
Density ρ_c	2500 kg/m^3	Density ρ_s	7850 kg/m^3
Poisson's ratio ν_c	0.2	Poisson's ratio ν_s	0.3
Young's modulus E_c	35 GPa	Young's modulus E_s	210 GPa

Table 3.6: Structural materials used for the deck and pylons of the cable-stayed footbridges in this thesis

Characteristics	**Stays as stranded cables (steel)**	**Stays as bars (steel)**
Maximum stress	f_y = 1860 MPa	$f_{y,b}$ = 355 MPa
Steel density ρ_s	7850 kg/m^3	7850 kg/m^3
Cable density ρ_p	8870 kg/m^3	
Young's modulus E_p	195 GPa	210 GPa

Table 3.7: Steel characteristics of the stays in the cable-stayed footbridges

The evaluation of the dynamic response in the vertical and lateral direction will be assessed through a parametric study of the benchmark cases. This will be done by changing the location and the number of tuned mass dampers. Boundary conditions, abutments and intermediate piers play a great role in altering the dynamic response of the footbridges. For this reason, different conditions will be evaluated in the parametric studies. The time response is obtained using a step-by-step analysis which considers a non-linear step followed by a dynamic implicit analysis. The damping for these analyses is represented by an explicit damping (Rayleigh damping) (Clough & Penzien, 1993). As the mean values given by Heinemeyer et al. (2008) are suggested for longer spans (Table 2.4), a material damping ratio (ξ) of 0.4 % has been chosen for further parametric studies (Chapter 5 and 6). This value is adopted for modes with structural frequencies in the range of 2.0 - 6.0 Hz (Ramos-Moreno, 2015). The numerical models of these type of footbridges will be performed through the application of finite element (FE) package Abaqus (2014) using beam, shell and truss elements. Footbridges will include the proposed load model to represent pedestrians'

actions (Section 3.2). In the next section, the assumptions, representations and validations of the numerical models for girder and cable-stayed footbridges will be presented.

3.4 Finite element analysis: assumption and representation

3.4.1 Finite element representation of girder footbridges

To evaluate the dynamic response in the vertical and lateral direction, the girder footbridges are represented using a finite element model developed in Python (Van Rossum et al., 2010). In this representation, the time integration method (implicit) is the Hilber-Hughes-Taylor algorithms which is the same that is used in Abaqus (2014). These algorithms are also known as the alpha-method which are used for the numerical integration of the linear set of second order Ordinary Differential Equations (ODE). The alpha-method is capable to allow for energy dissipation and it is more accurate in the lower modes in comparison to other algorithms that are available in the literature (Hilber et al. 1977). This code has been used to analyse the dynamic response of a comprehensive set of girder footbridges, considering a parametric study varying: the structural characteristics (Table 3.3), the pedestrian density (0.2, 0.6 and 1.0 ped/m^2), the aim of the pedestrian journey (commuting or leisure activities) (Table 3.2), and the anthropometric characteristics of the pedestrians, which employs a sample of the UK population. This custom code also enables the relatively complex load model to be directly integrated with the structural model. To validate the numerical model in Python, a parallel implementation was made using Abaqus (2014) and both models provided essentially identical results. The numerical model with Python was preferred due to computational reasons. The simply supported girder footbridges are represented by using a detailed finite element model of the structure by using beam elements. The code developed allows to analyse the dynamic response without the necessity of a specialized software. To develop the code, the structure characteristics of the girder footbridges and the pedestrian load are defined in the vertical and lateral direction. Then the mass, stiffness and damping matrices are assembled, and the modal analysis is performed. The dynamic response was evaluated using Euler-Bernoulli (B23) elements.

3.4.1.1 Deck mesh sensitivity

It is known that with finer mesh the model will increase the structural response accuracy. However, a finer mesh (multiple degree of freedom) results in a large computational cost. A sensitivity analysis was developed to balance accuracy and computing time. A mesh sensitivity analysis in a girder footbridge of 12 m span length was conducted varying the length of elements from L/2 to L/40.

Figure 3.5 shows the error in the maximum accelerations vs the number of elements, and the maximum vertical acceleration vs. the number of elements. The maximum accelerations are represented at mi-span and at 2 meters from the left abutment (x = 2 m). Results effectively converged to a common solution from L/15 with smaller element lengths not influencing the results. The larger the number of elements, the larger the computational time (Figure 3.5 (c)). Once the mesh is fine enough, a thinner mesh increases the computational time without any numerical benefit for the results.

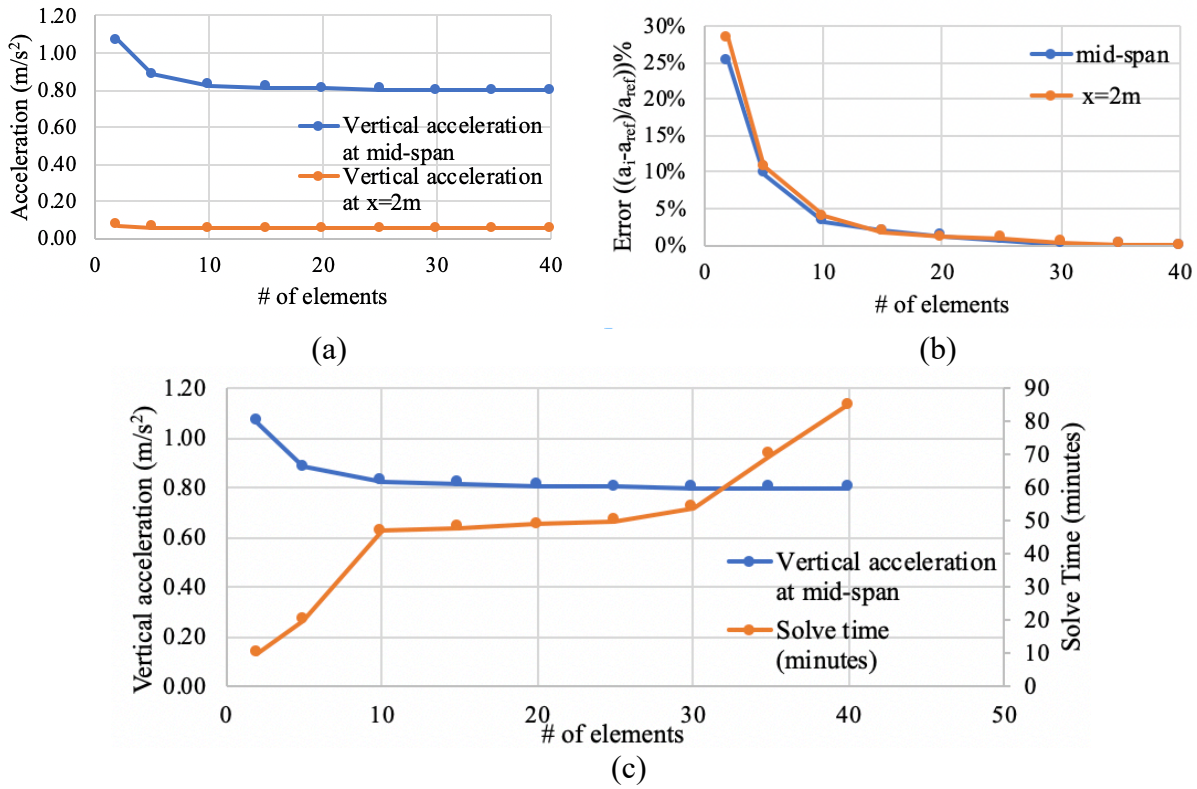


Figure 3.5: Mesh convergence study (a) Accelerations (m/s^2) vs Number of elements, (b) Error based on the results obtained with 40 elements vs Number of elements, and (c) Vertical acceleration (blue line) and solve time in minutes (orange line) vs the number of elements at mid-span

3.4.1.2 Tuned mass dampers

In the finite element models, the tuned mass damper (TMD) consists of a mass, a spring and a dashpot which is connected to the footbridge in order to reduce the dynamic response of the structure. The TMD's properties must be tuned to the footbridge's dominant mode responsible for the high dynamic response. The code includes an iteration step, where after the evaluation of the dynamic response, it automatically checks if the serviceability criterion is fulfilled. In case it is not fulfilled, the damper mass ratio will be increased until the serviceability criterion corresponds to a maximum comfort level. The properties are calculated according to the equations available in the literature (Section 2.5).

3.4.1.3 Pedestrian arrivals

The impact of assuming that pedestrians can arrive in one or two directions and the effects of the crowd interaction model were also analysed (Figure 3.6). Case 1 does not consider the interaction between pedestrians, i.e., pedestrians do not modify their trajectories due to the presence of other pedestrians around, and therefore, different pedestrians can be at the same location in time. Meanwhile, cases 2 to 5 consider the crowd interaction. Figure 3.7 shows the root mean square (RMS) vertical accelerations for a 1-second interval (Camara & Ruiz-Teran, 2015) in the different cases that were considered. The mean acceleration remains a reasonable level of consistence. However, there are some differences in the overall range of the accelerations (minimum and maximum) in the five cases. Larger responses are achieved when the pedestrians enter the footbridge with a uniform distribution across the width (cases 1, 4 and 5). The impact of the direction followed by the crowd and therefore the difference between unidirectional (Case 4) and bidirectional traffic (Case 5) is negligible. The response in cases with crowd interaction is larger and also more representative of reality. Therefore, for the rest of the analyses in this work, pedestrians will arrive in both directions and the crowd model is implemented (Case 5) in all of the simulations.

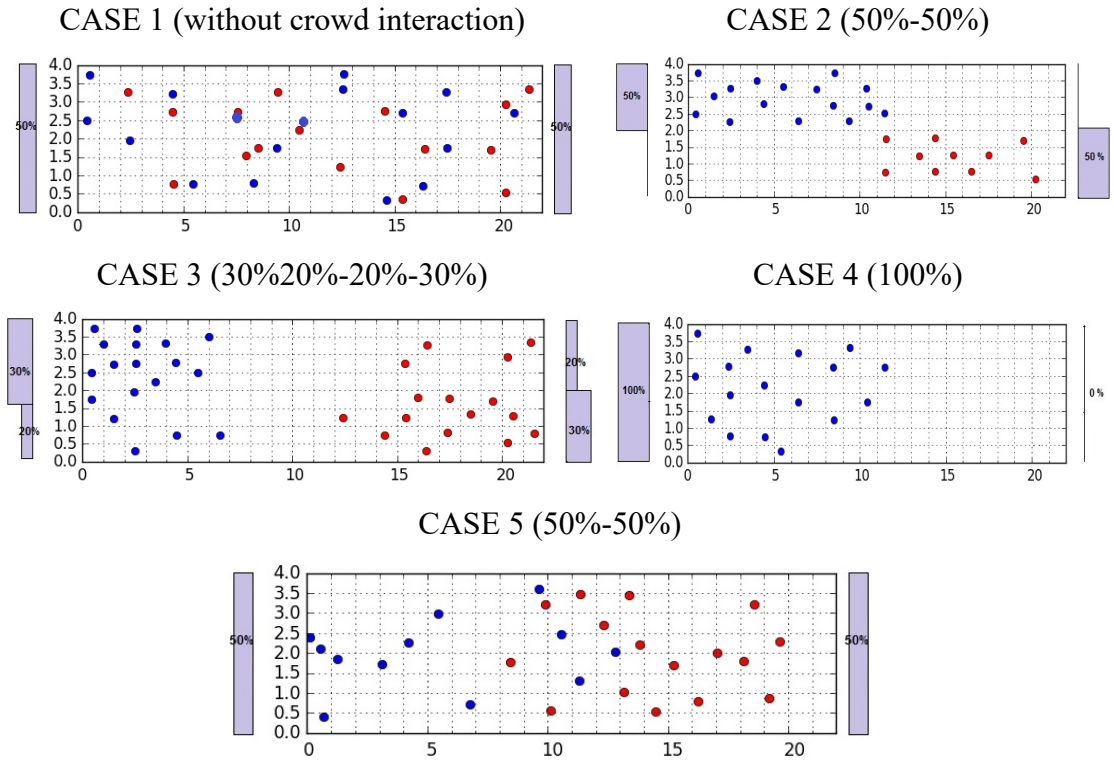


Figure 3.6 Plan views of the decks at certain instants, with the centre of masses of the different pedestrians represented in blue and red circles for those pedestrians entering the structure from the left and the right abutments, respectively. The percentages of pedestrians entering the footbridge from each side, and across the width, have been also represented

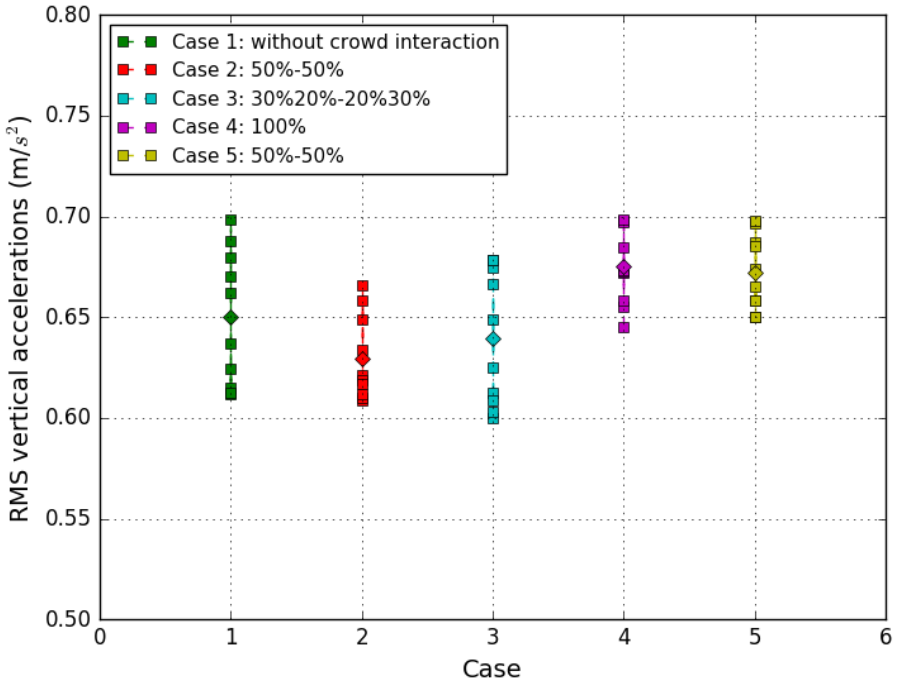


Figure 3.7 RMS vertical accelerations for a 1-second interval at midspan in a simply supported prestressed concrete footbridge (L= 22.5 m, section type 1) under a pedestrian density of 0.6 ped/m^2 for commuting activities. The average of the 10 simulations is highlighted with a diamond marker. Cases are defined through Figure 3.6

3.4.1.4 Duration of simulation events

In order to define the duration of the numerical simulations, further sensitivity analysis is conducted. After the footbridge deck is loaded with the desired pedestrian density for a while (steady-state response) the structure corresponds to a stationary ergodic process. In relation to this ergodicity[1], the structural response was obtained for simulations that extend for different intervals, from t_{ap} to nine times this time, where tap means the average time required by a pedestrian to cross the bridge. After this comparison, it was noticeable that the rms acceleration from $4t_{ap}$ is similar to the response obtained in longer events. As a result, a time event of $4t_{ap}$ was adopted to evaluate the dynamic response in girder footbridges (Figure 3.8). The vertical axis in Figure 3.8 is

[1] The analysis of different events or single events should be similar

normalized by the accelerations obtained when the simulation time is equal to t_{ap}. It is important to note that the attention needs to be paid to the RMS accelerations, and not to the peak acceleration, as longer events would lead to larger peak accelerations.

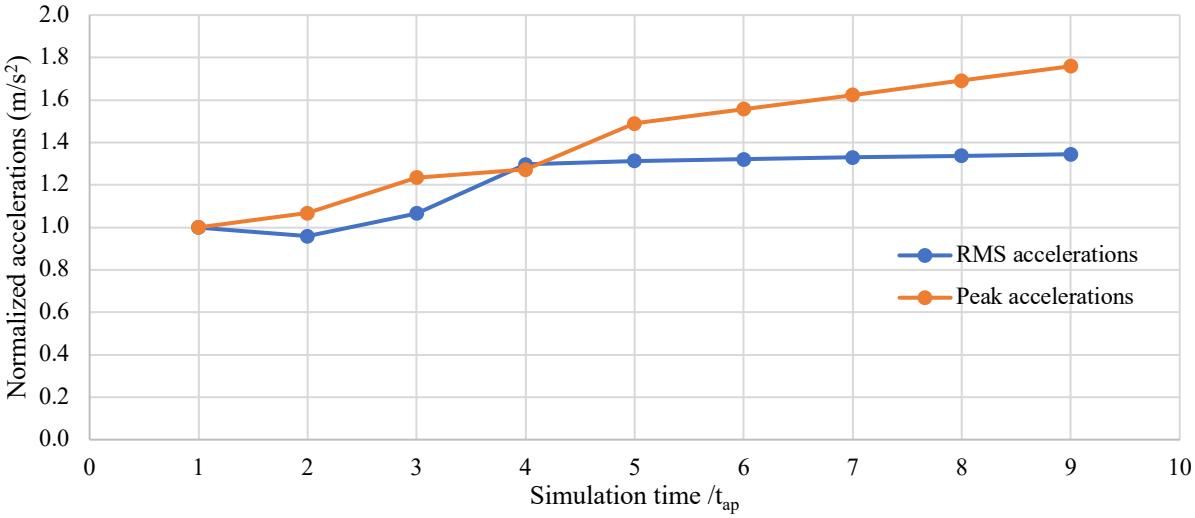


Figure 3.8: Normalized vertical accelerations versus the simulation time normalized to t_{ap}

The number of simulations required to obtain a reliable dynamic response is analysed considering in each simulation a simulation time of $4t_{ap}$ (Figure 3.9). The vertical axis in Figure 3.9 is normalized by the value obtained for one simulation. After this study, ten simulations provide reliable results without a high dispersion. Therefore, ten simulations are adopted for further parametric studies.

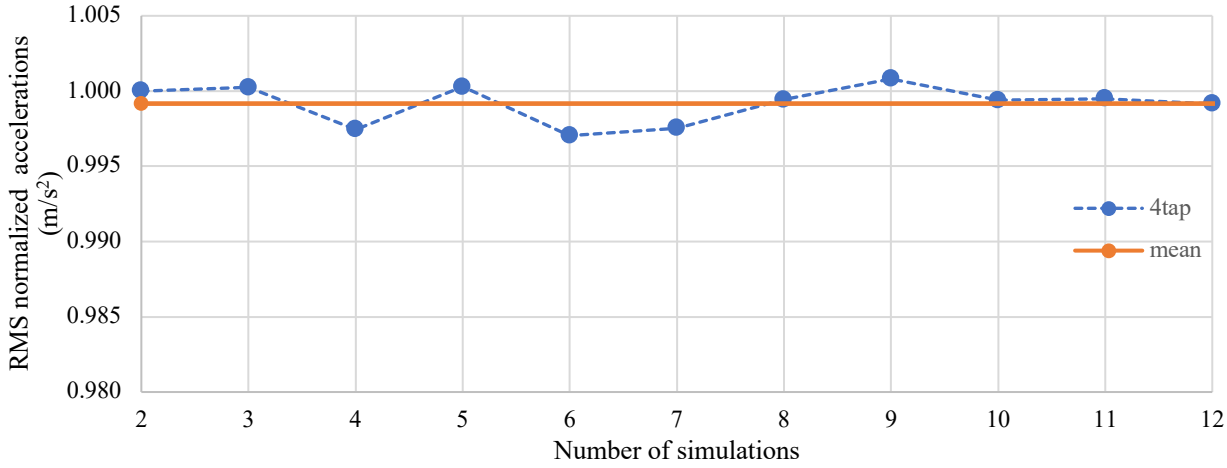


Figure 3.9 Normalized vertical accelerations vs the number of simulations

3.4.2 Finite element representation of cable-stayed footbridges

A detailed representation of the structural elements for cable-stayed footbridges is required to obtain an accurate dynamic response. Based on an exhaustive analysis of this type of footbridges under pedestrian loads showing accurate results made by Ramos-Moreno (2015), similar representations will be adopted for the design of these footbridges.

The element for the representation of the longitudinal beams, beam or shell elements, are selected based on a comparison in terms of differences between structural frequencies, vertical and lateral displacement, and stresses using both elements. Figure 3.10 and Figure 3.11 show the differences in the structural frequencies and deflections. The differences for the structural frequencies are approximately 1.9%, for vertical displacement 2.1%, for lateral displacement 3.1% and for stresses 2.4%. The computational time required for running a model with shell elements is five times that for a model with beam elements. Beam elements will be adopted to represent the longitudinal beams due to the differences between beam and shell elements is less than 5% (structural frequencies, vertical and lateral displacement, and stresses) and the computational time is reduced when is used beam elements instead of using shell elements.

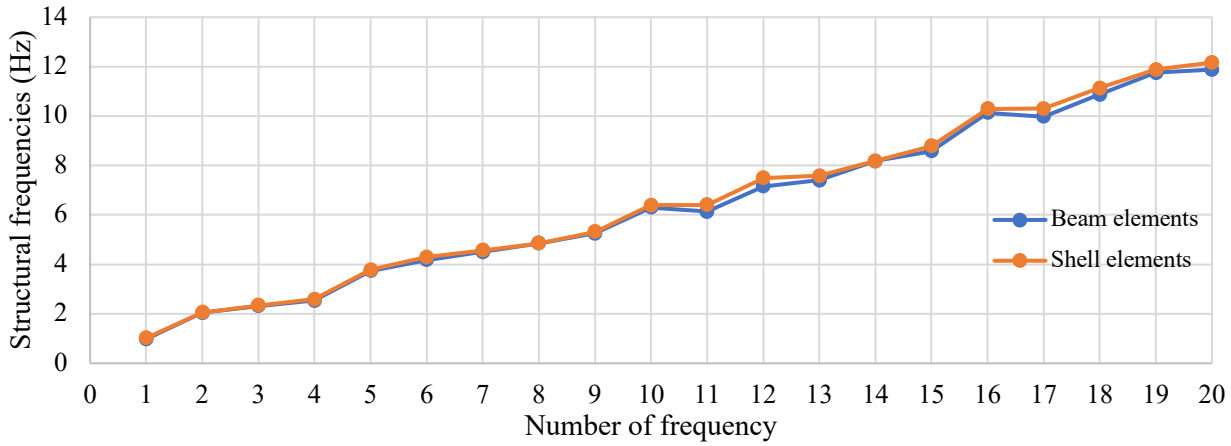
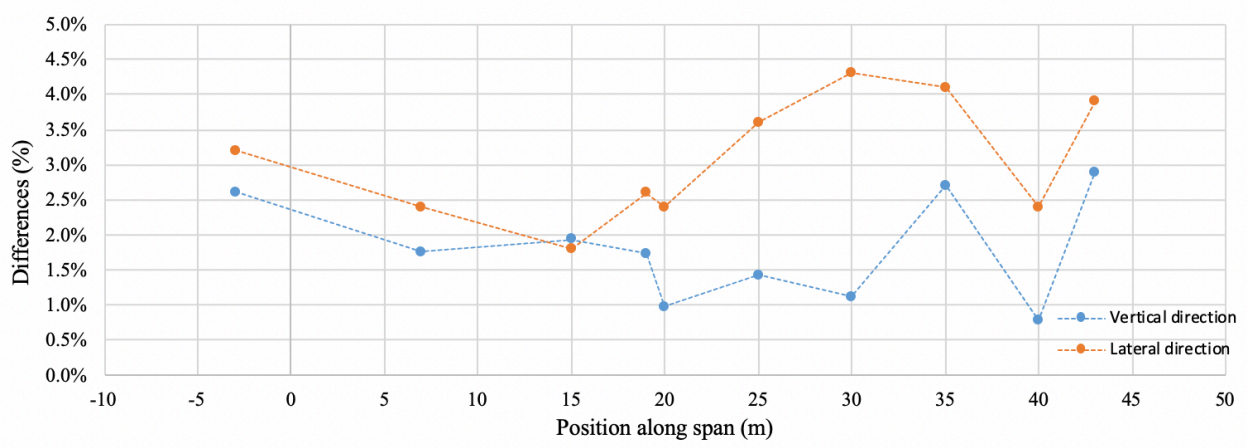
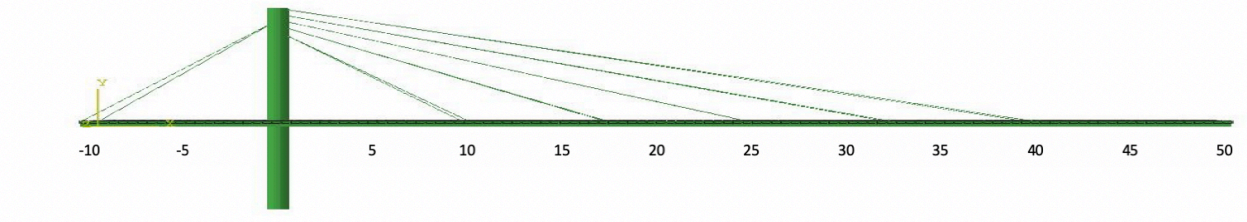


Figure 3.10 Structural frequencies for beam and shell elements for a cable-stayed footbridge with a span length of 50 m



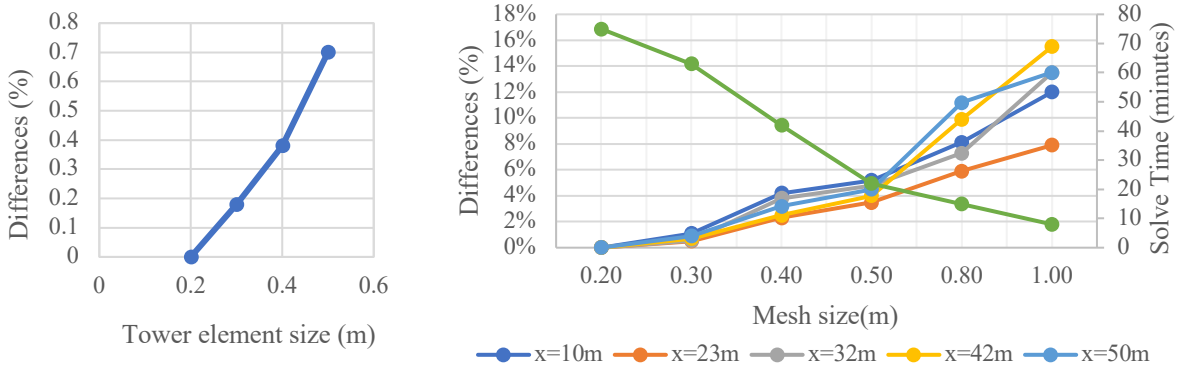
(a)



(b)

Figure 3.11 (a) Differences in deflections for beam and shell elements for a cable-stayed footbridge with a span length of 50 m at different positions along the length of the bridge, (b) Lateral view of the cable-stayed footbridge

The mesh required for the analysis has been calibrated comparing the computational time and the accelerations for different structural elements. Figure 3.12 (a) and (b) show the differences in the response after a mesh sensitivity analysis in the tower and the deck was performed. The differences are measured as the percentage of the peak accelerations at different positions along the length of the bridge with respect to the minimum mesh size of 0.2 m. In the mesh analysis of the tower, the differences between an element size of 0.2 to 0.5 m are minimum. For this reason, an element size of 0.5 m. is adopted. In Figure 3.12 (b), the results with a mesh size of 0.4 m or 0.5 m are approximately 4.4% more than those results with a smaller mesh. Therefore, a mesh size of 0.5 m is adopted for the deck.



(a) (b)

Figure 3.12 Differences in % in peak vertical accelerations at different positions along the length of the bridge for (a) Tower element analysis (b) Deck mesh sensitivity

In the same manner to the girder footbridges, sensitivity analyses are conducted to define the duration of the pedestrian loads for cable-stayed footbridges. The structural response was obtained for simulations that extend for different intervals, from t_{ap} to six times this time. After this comparison, it was noticeable that the rms acceleration from $1t_{ap}$ is similar to the response obtained in longer events. As a result, a time event of $1t_{ap}$ to evaluate the dynamic response in cable-stayed footbridges (Figure 3.13) was adopted.

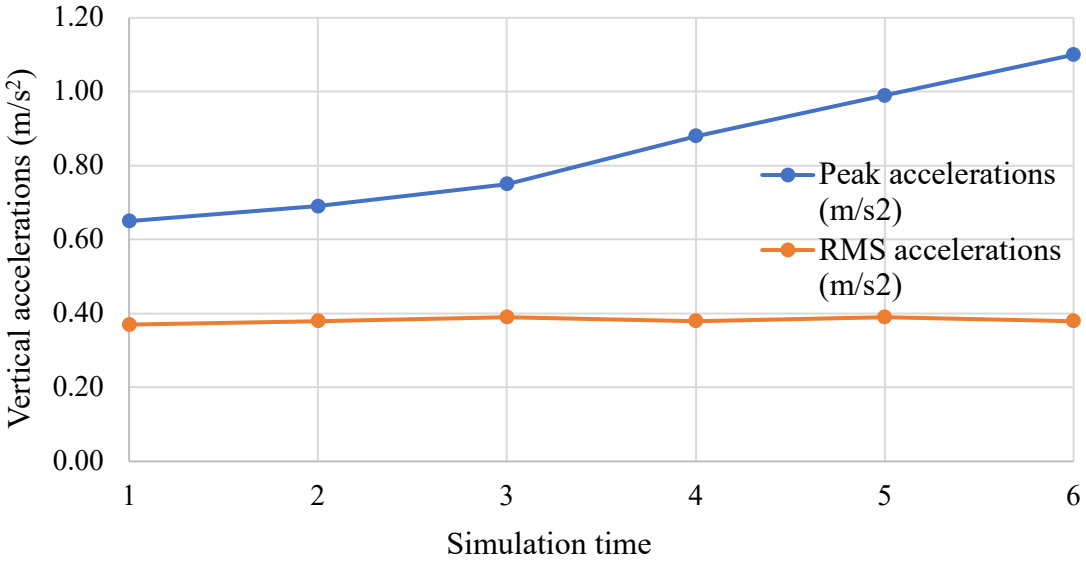


Figure 3.13: Maximum vertical accelerations in the whole deck versus the simulation time for cable-stayed footbridges

Figure 3.14 shows the number of simulations (six) that will be employed in this study to evaluate the dynamic response with and without tuned mass dampers in cable-stayed footbridges. The vertical axis is normalized by the accelerations obtained when the simulation time is equal to t_{ap}. Figure 3.15 shows an analysis considering the six simulations before and after tuned mass dampers were employed. There is a 95% chance that the true mean RMS response lies inside the dashed lines and that the ranges for the green and blue curves are completely separated –by a significant distance. Therefore, it can be concluded that the tuned mass damper is causing a reduction in the response about a factor of two.

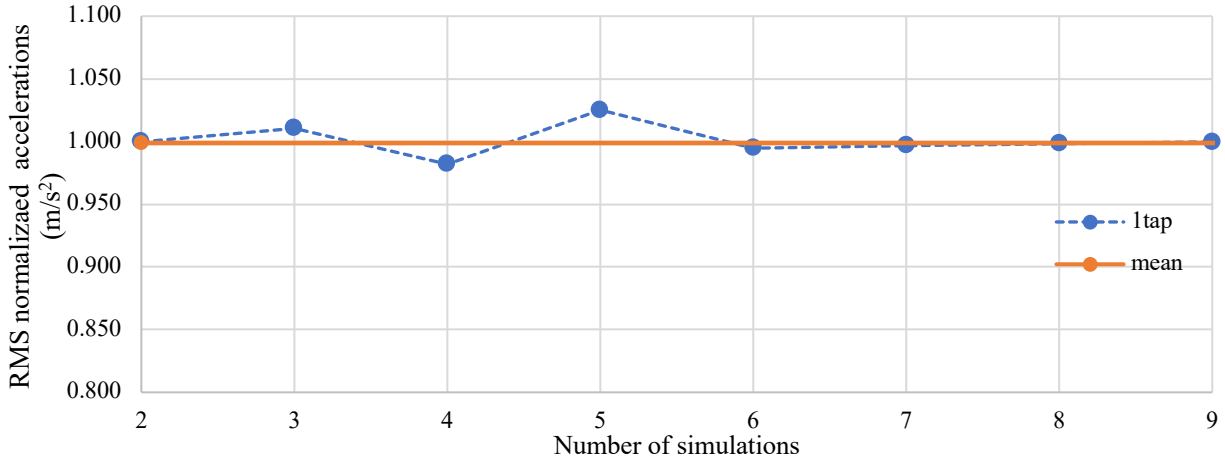


Figure 3.14: RMS normalized accelerations versus the number of simulations for cable-stayed footbridges without TMDs

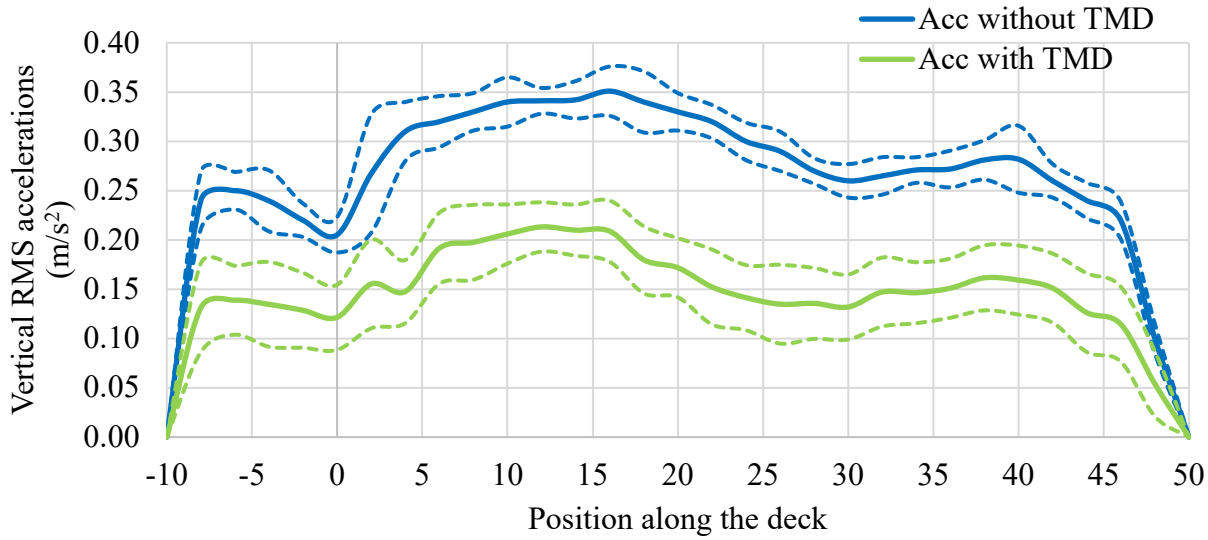


Figure 3.15 Vertical RMS accelerations along the length before and after a tuned mass damper ($\mu = 0.01$) was employed at the first mode in the vertical direction in a cable-stayed footbridge of a 60 m span length considering a pedestrian density of 0.2 ped/m^2 for leisure activities

The final finite element model was validated with previous studies (Ramos-Moreno, 2015). The final element model is characterised as follows: the deck comprises shell elements (S4R), and the transverse and longitudinal steel girders comprise beam elements. The thickness is constant for the deck. For the longitudinal girders, the thickness is based on the dimensions of flanges and web (Figure 3.16). The mesh of the deck for the evaluation of the dynamic response will be 0.5 m.

Single truss elements will be employed to represent the cables and beam elements will be employed to represent the tower. Balustrades are represented in the deck as point masses. The tuned mass dampers are represented as a mass element connecting a node in the deck connected in parallel with a spring and a dashpot. The summary of the structural characteristics and structural variables of the girder and cable-stayed footbridges that will be evaluated in this research work is schemed in Table 3.8.

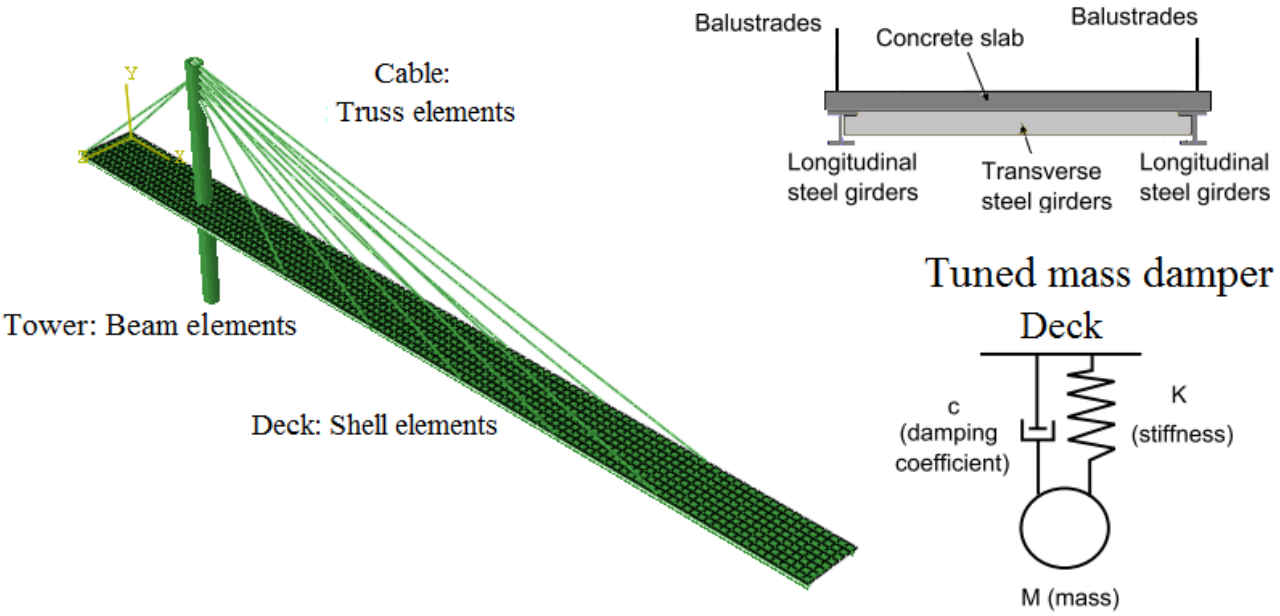


Figure 3.16: Cable-stayed representation in Abaqus (2014)

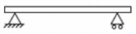
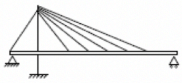
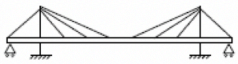
<table>
<tr><th colspan="3">Structural characteristics</th><th>Traffic</th><th>Structural variables</th><th>Chapter</th></tr>
<tr><td>Girder footbridges</td><td>1 Span</td><td>
L = up to 100 m</td><td>-0.2 ped/m² streams
-0.6 ped/m² streams
-1.0 ped/m² streams
(Commuting / Leisure)</td><td>- Cross sectional shape
-Material
- Number, properties and location of the tuned mass dampers</td><td># 4</td></tr>
<tr><td rowspan="2">Cable-stayed footbridges (CSF)</td><td>1 Tower</td><td>
L = 50 / 100 /150 m</td><td rowspan="2">-0.2 ped/m² streams
-0.6 ped/m² streams
-1.0 ped/m² streams
(Commuting / Leisure)</td><td rowspan="2">- Number, properties and location of the tuned mass dampers
-Span length
- Shape of the tower (I, H and A)</td><td># 5</td></tr>
<tr><td>2 Towers</td><td>
L = 50 / 100 /150 m</td><td># 6</td></tr>
</table>

Table 3.8: Footbridges that will be evaluated for further parametric studies

3.5 Automation of functions to evaluate the dynamic response

In order to represent the pedestrian loads in Abaqus, it is necessary to consider the human-induced vibrations in the vertical and lateral direction. The representation in the vertical direction can be defined at the beginning of the analysis, before the structural response has been obtained, defining the amplitude according to time. However, the lateral direction cannot be defined at the beginning of the analysis, before the structure response has been obtained, as the magnitude of these forces depends on the structural accelerations at the location where the pedestrian steps (see Eq. 2.8) (Section 2.3.3). The lateral force induced by pedestrians is implemented using the subroutine UAMP (User Amplitude). This is a user subroutine used to calculate the amplitudes considering the previous step in function of the time (Abaqus, 2014). This subroutine is defined in Abaqus using a script developed in FORTRAN. Figure 3.17 represents the subroutine implemented in Abaqus to evaluate the dynamic response in cable-stayed footbridges considering the induced forces in the lateral direction.

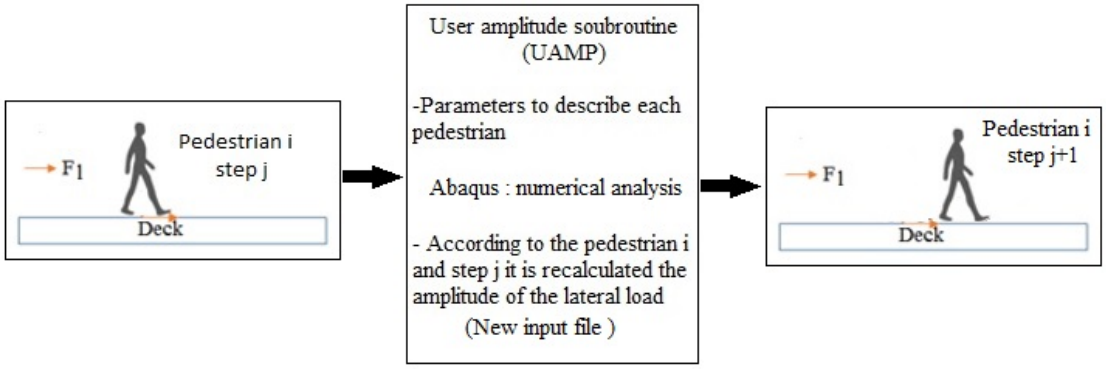


Figure 3.17: Representation of the user amplitude subroutine (UAMP) in Abaqus (2014)

The geometry and properties of the cable-stayed footbridges were parameterized to facilitate the evaluation of the dynamic response. The parameterization was developed in the commercial software package Matlab (2015) which was employed to make the input files combining Python (pedestrian load model), Fortran (subroutine) and Abaqus (FEA package).

3.6 Serviceability criteria

On basis of the maximum acceleration and displacement calculated for the girder and cable-stayed footbridges, the comfort criteria in the vertical direction will be checked according to limits proposed by BSI (2003), and Setra (2006). In the lateral direction, the response will be compared to the limits of Setra (2006) and BSI (2003) (Figure 2.17). If the calculated dynamic response does not satisfy the recommended requirements, tuned mass dampers will be implemented as a way to control the accelerations of pedestrian-induced vibration (Figure 3.18).

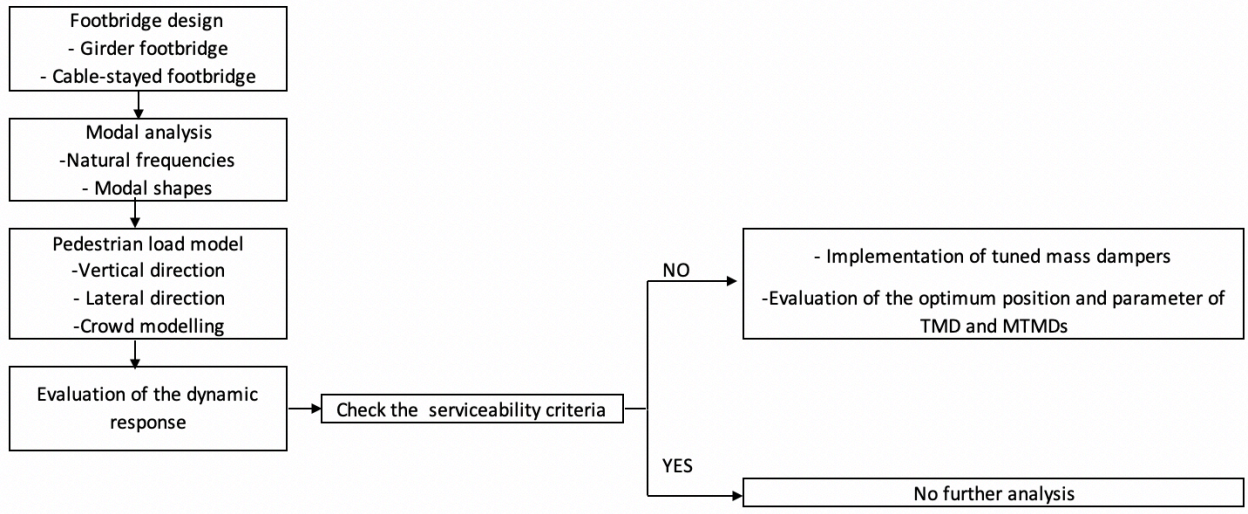


Figure 3.18: Summary of the serviceability criteria analysis

3.7 Supplemental damping devices

3.7.1 Problem formulation

A comprehensive parametric study was conducted to determine the optimal criteria to define the TMDs parameters and location. This study considers different locations and mass ratios μ (with typical values in footbridges vary from 0.01 to 0.05 - see Tubino & Piccardo (2015). An important design objective is minimizing the mass of the TMD, and therefore its size and cost, finding the minimum mass ratio that is required to fulfil the serviceability criteria. It is well known that the position of the TMD has an impact on its efficiency (Tubino & Piccardo, 2015). The TMD efficiency is measured as the percentage of the peak acceleration (prior to the implementation of this device) that would be cancelled after its installation. The design constraints set limits on the relative displacement between the TMD and the deck, as well as the deck vertical and lateral accelerations. The numerical procedure adopted in this thesis is as follows:

1. The mass, stiffness and damping matrices of the pedestrian bridges are assembled using Python for the girder footbridges. For the cable-stayed footbridges, these structures are modelled using Abaqus (2014).

2. The structural modal frequencies and mode shapes are determined. The mass of pedestrians is included on the deck of the structure to assess these modal frequencies as some guidelines suggest (Živanović et al. 2010). At this stage, potential critical modes of the footbridge under pedestrian loading can be initially identified as those with vertical frequencies in the range of the pedestrian vertical frequencies (see Table 2.3), and those with lateral and torsional frequencies in the range of the pedestrian lateral frequencies (half of the vertical pedestrian frequency) (Garcia-Troncoso et al., 2017). These modes are likely to have large contributions (point 5 below).

3. The structure is loaded considering the probabilistic pedestrian load model, which realistically simulates different pedestrians crossing the structure (Section 3.2). Different loading scenarios are considered, varying traffic conditions (such as modelling the pedestrian behaviour at peak hours, called commuting, and also during the weekends and more relaxed situations, called leisure), for different pedestrian densities (0.2, 0.6, and 1.0 ped/m^2).

4. The vertical and lateral dynamic response induced by each pedestrian flow is calculated with the equation of motion in time according to the d'Alembert's principle (Equation (2.1)) (Section 2.3.2). Multiple simulations are run, with the number of simulations determined through a sensitivity analysis.

5. If the maximum structural accelerations obtained exceed the comfort limits, and therefore do not satisfy the serviceability criteria, TMDs are deployed at the location of the maximum nodal coordinates in the modal shape for the mode that has a larger contribution for that excessive acceleration. That mode can be identified by representing the response in the frequency domain. The frequency of the TMD is tuned to damp the accelerations induced by the critical mode. The efficiency of this device depends on the ratio between the TMD and the structural modal masses (μ), the ratio between the TMD and the structural frequencies (α_{opt}), the TMD damping ratio (ξ_{opt}), and its location. The mass ratio is initially set to 1%, being incremented, if necessary, when further analyses are required after point

7. Warburton (1982), Soong & Dargush (1997), Asami et al. (2002), and Krenk et al. (2005) have provided different criteria for the optimization of the TMD frequency and damping ratio minimizing either the displacement or acceleration of the structure. In this work, all of these criteria have been used in order to select the most efficient one to improve pedestrian comfort in the footbridge types studied in this thesis.

6. The mass, stiffness and damping matrices are updated including the TMD's properties.

7. The new dynamic response, considering the damping devices, is obtained. Then the serviceability criteria are checked. If the serviceability criteria are not fulfilled, step 5 is repeated incrementing the damper mass ratio in an iterative way until the serviceability criteria is finally satisfied.

Figure 3.19 shows the summary of the proposed TMD implementation.

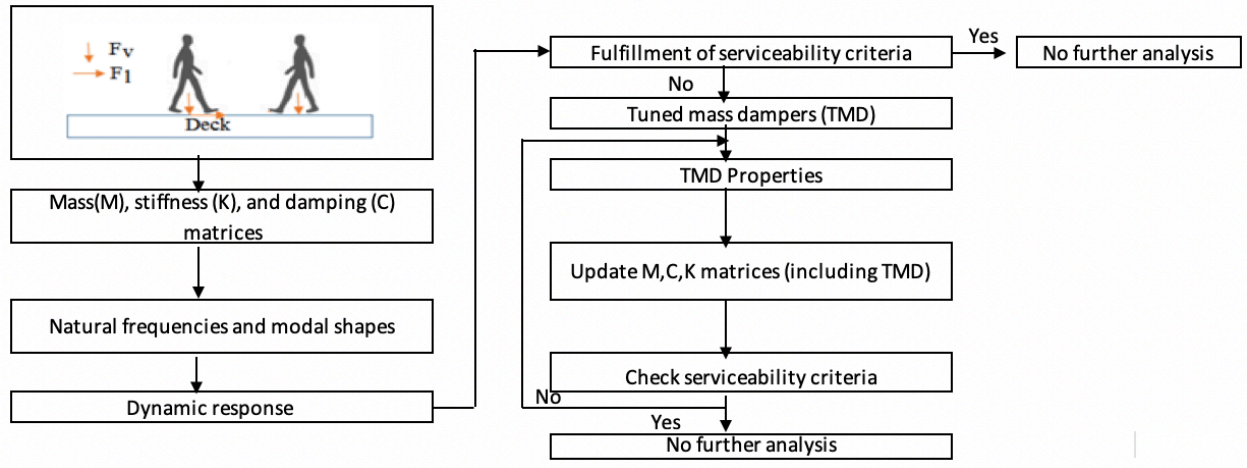


Figure 3.19 Summary of the dynamic analysis in footbridges under pedestrian loads (Garcia-Troncoso et al., 2017)

3.7.2 Method to choose properties and placement of damping devices

An automatic function was implemented in Python to employ tuned mass dampers, through the application of this function the location and properties of these devices can be found for girder

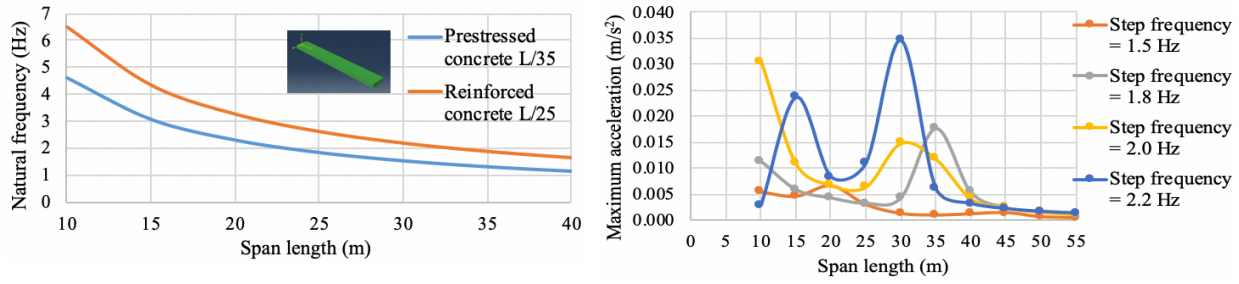
footbridges. A function implemented in Matlab is implemented to include the tuned mass dampers for cable-stayed footbridges in Abaqus. The implementation of these devices depends on the serviceability criteria, if the criteria is not fulfilled tuned mass dampers are employed; whereas, if it is satisfied these devices will not be include. In the next section, the efficiency of the tuned mass dampers for a range of girder footbridges are shown. The optimal values α_{opt} and ξ_{opt} given by Warburton (1982), Soong & Dargush (1956), Asami et al. (2002), and Krenk et al. (2005) have been used in order to select the most efficient criteria to improve the pedestrian comfort. After the implementation of the tuned mass damper, a new dynamic analysis will be made to ensure the fulfilment of the maximum comfort level.

3.7.3 Criteria to determine the parameters of tuned mass dampers

In section 2.5.1 of the literature review, four criteria were presented to obtain the design parameters of tuned mass dampers. These criteria correspond to the work available from Den Hartog, Krenk, Warburton and Asami. In this section, each of these criteria are assessed. This evaluation is developed to choose the best of them to minimize the accelerations in girder and cable-stayed footbridges for parametric studies to be carried out afterwards.

3.7.3.1 Dynamic response without tuned mass dampers

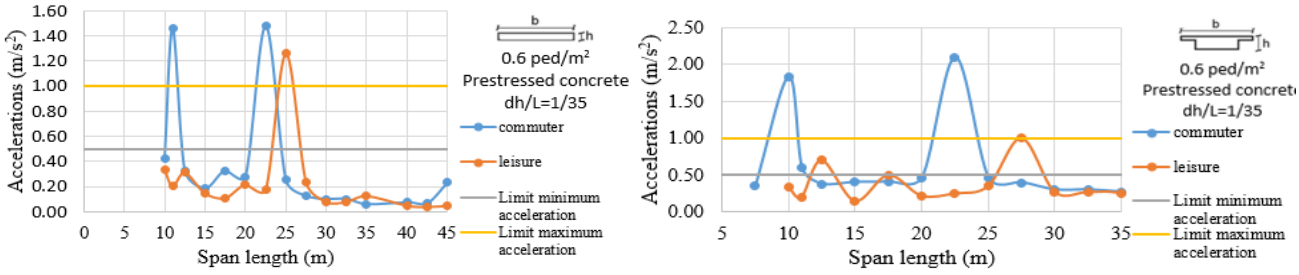
Figure 3.20 (a) shows the frequencies considering two different relations between deck depth (L/25 and L/35) and span length (10 to 40 m). It can be seen a great effect of the span length on the frequencies. These frequencies can lie near the step frequency of the pedestrians which can increase the dynamic response (Figure 3.20 (b)). When the beam has a span of 30 m, the natural frequency is 2.16 Hz which is very near to the mean step frequency of the pedestrian (2.2 Hz) the acceleration shows a peak. For the same beam with step frequencies of 1.5, 1.8, 2.0 Hz the acceleration is lower. The maximum comfort is achieved for these cases. Therefore, it is not necessary to employ tuned mass dampers.



(a) (b)

Figure 3.20: (a) Natural frequencies (b) Peak accelerations for one pedestrian walking with a velocity of 1.4 m/s

Figure 3.21 (a) shows the maximum vertical accelerations under a pedestrian stream of 0.6 ped/m^2 without supplemental damping devices. These results show that for certain span length the serviceability criterion is not fulfilled. Therefore, the implementation of tuned mass dampers will be considered for these cases.



(a) (b)

Figure 3.21: Maximum peak accelerations in the vertical direction: a) in a rectangular beam; b) in a T-beam

3.7.3.2 Dynamic response with tuned mass dampers

After the evaluation of the dynamic response in girder footbridges without supplemental damping devices, the structures which presented vibration problems in the vertical and lateral direction are identified. It has been demonstrated that for certain structural materials and span arrangement the dynamic response cannot satisfy the serviceability criteria. In these cases, tuned mass dampers are employed to mitigate the human-induced vibrations (Figure 3.22 and Figure 3.23). The properties

of these devices are analysed according to different criteria such as Den Hartog, Krenk, Warburton and Asami (Section 2.5.1).

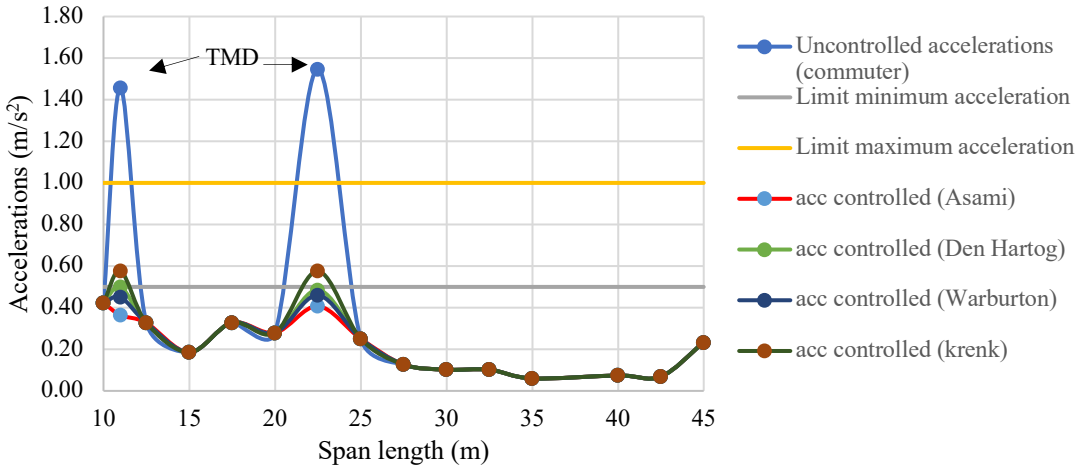


Figure 3.22: Maximum peak vertical accelerations for a set of prestressed concrete girder footbridges with spans ranging from 10 to 45 meters for commuting traffic considering different TMD design criteria under pedestrian densities of 0.6 ped/m^2

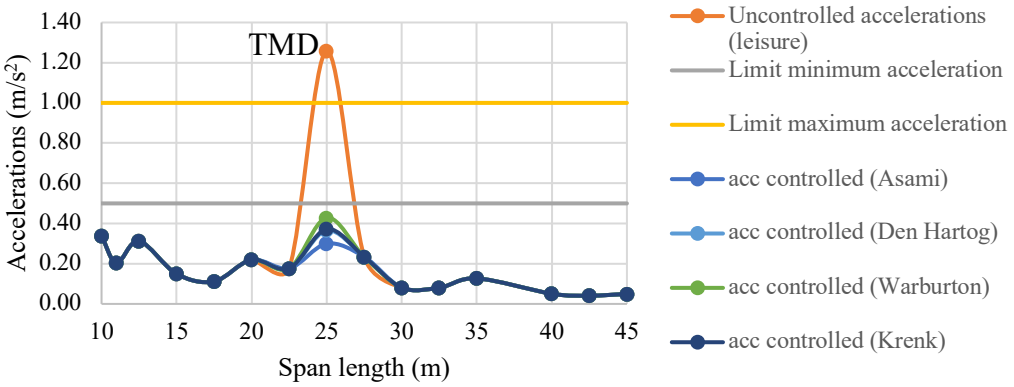


Figure 3.23: Maximum peak vertical accelerations for a set of prestressed concrete girder footbridges ranging from10 to 45 meters for leisure traffic considering different TMD design criteria under pedestrian densities of 0.6 ped/m^2

Asami's TMD design criteria led to more efficient TMDs, and therefore larger reductions in accelerations, in comparison to the other criteria. The TMD's properties according to the Asami criteria can be seen in Table 3.9. Asami's criteria gives larger efficiencies because it was set to minimise the accelerations in structures with low damping, such as in footbridges, where the comfort criteria for these structures are governed by accelerations.

Activities	Pedestrian densities (ped/m^2)	Span length (m)	TMD damping ratio (ξ)	TMD mass (kg)	Max relative displacement
Commuter	0.6	11.00	0.100	584.42	45
Commuter	0.6	22.50	0.094	1903.92	40
Leisure	0.2	25.00	0.086	1677.90	45

Table 3.9: Tuned mass damper properties required to mitigate the human-induced vibrations in the footbridges considered in Figure 3.22 and Figure 3.23

Figure 3.24 (a) shows the acceleration with and without tuned mass dampers ((a) and (b) slabs; and (c) and (d) box girders). The accelerations are reduced around 75 % for the Asami's criteria. Although the serviceability criterion corresponds to a mean comfort (range of 0.5 to 1.0 m/s^2), a tuned mass damper can be implemented to ensure the maximum comfort of the pedestrians (Figure 3.24 (b)). The evaluation for the TMD's properties has been developed using the typical values of the mass ratio. However, it can be seen in Figure 3.24 (c) that for commuting activities the accelerations do not fulfil the maximum serviceability criteria using the common values for the mass ratio. In these cases where the accelerations are higher than 1.0 m/s^2, increasing the mass ratio is required to ensure that the serviceability criteria can be fulfilled (Figure 3.24 (d)).

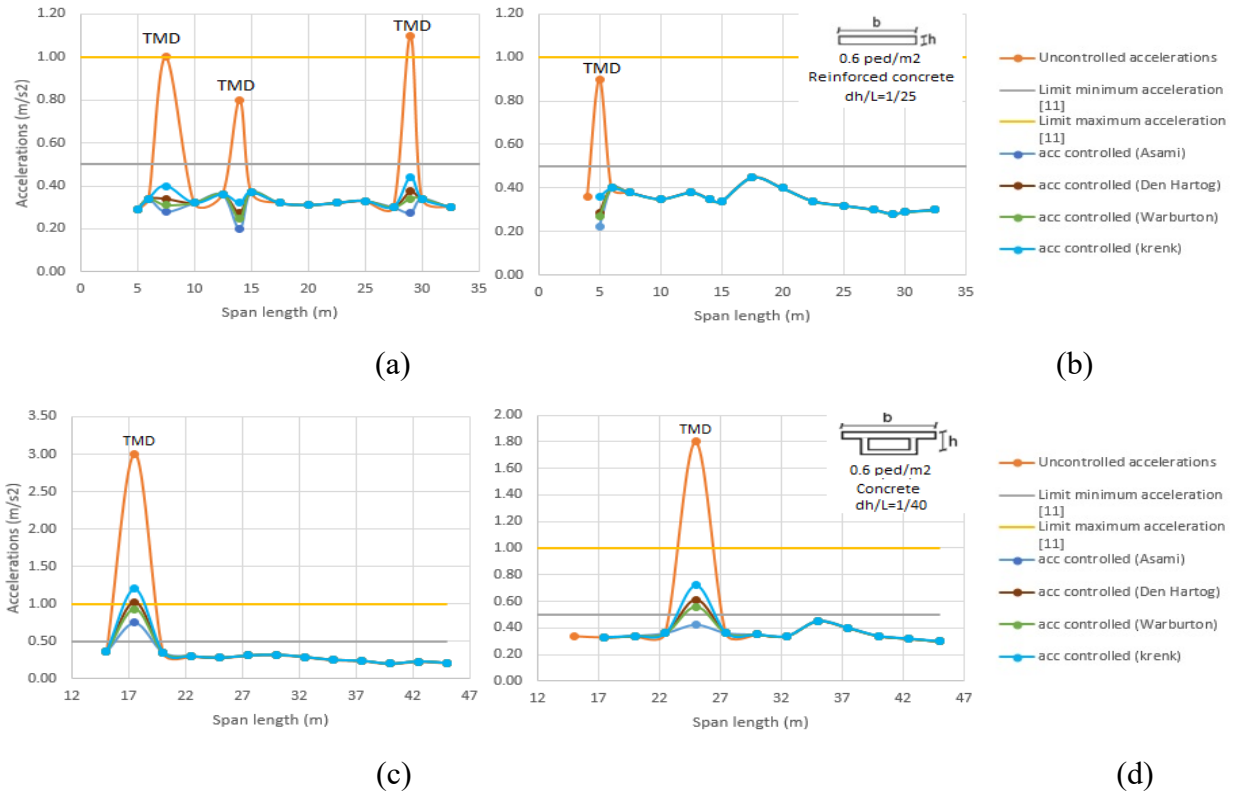
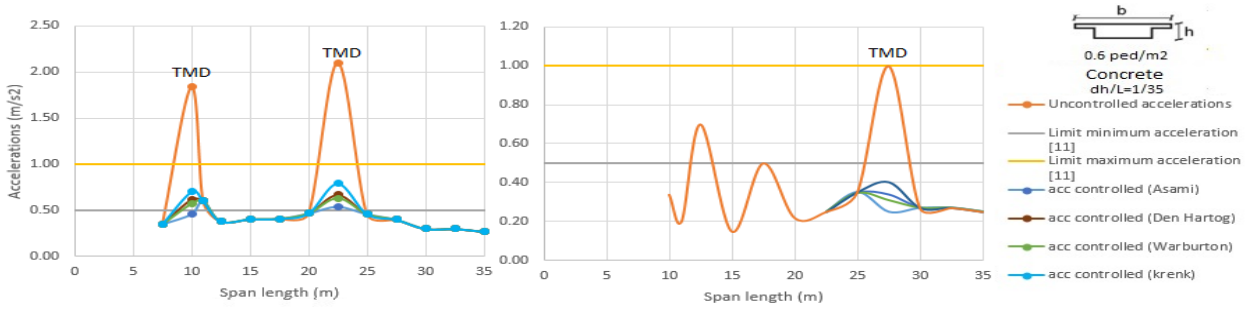


Figure 3.24 Maximum peak accelerations (m/s^2) with and without tuned mass dampers for (a and c) commuting, and (b and d) leisure activities under pedestrian densities of 0.6 ped/m^2

Figure 3.25 shows the maximum accelerations in the vertical direction in a T-beam for a pedestrian stream with a density of 0.6 ped/m^2 for commuting (a) and leisure (b) activities. In cases where the fulfilment of the maximum comfort criteria is required (commuting activities), the mass ratio needs to be more than 0.05. For leisure activities the dynamic response is fulfilled, however, a tuned mass damper is required when the beam had a span length of 27.0 m in order to fulfil the serviceability criteria. The high efficiency of the dampers in the reduction of the accelerations under a pedestrian walking is a remarkable issue to point out. This reduction is very similar to the values obtained in Weber & Feltrin (2010).



(a) (b)

Figure 3.25: Maximum peak accelerations in a T-beam for (a) commuting and (b) leisure activities under pedestrian densities of 0.6 ped/m^2

It also evaluated the different criteria to obtain the TMD's parameters in the cable-stayed footbridges. This evaluation is made to select the criteria that give the maximum reduction in the acceleration for this type of footbridge. Table 3.10 shows the design values for each criteria (Den Hartog, Asami, Warburton, Warburton and Krenk). Figure 3.26 shows that the Asami criteria gives the highest reduction in the dynamic response.

Design values for the Tuned mass damper

Modal mass	M =	230142	kg
Frequency to be damped	f_H =	2.17	Hz
Number of TMD	n_D =	1	6904 kg

1. Den Hartog	TMD		2. Asami	TMD	
	m_D = 6905	kg		m_D = 6905	kg
κ opt = 0.9709	f_D = 2.107	Hz	κ opt = 0.9853	f_D = 2.138	Hz
	k_D = 1209822	N / m		k_D = 1246116	N / m
ξ opt = 0.1015	d_D = 18547	Ns/m	ξ opt = 0.1058	d_D = 19632	Ns/m

3. Warburton	TMD		4. Krenk	TMD	
	m_D = 6905	kg		m_D = 6905	kg
κ opt = 0.9781	f_D = 2.123	Hz	κ opt = 0.9709	f_D = 2.107	Hz
	k_D = 1227969	N / m		k_D = 1209822	N / m
ξ opt = 0.0856	d_D = 15773	Ns/m	ξ opt = 0.1207	d_D = 22059	Ns/m

Table 3.10: Design values for the tuned mass damper according to the different TMD's criteria

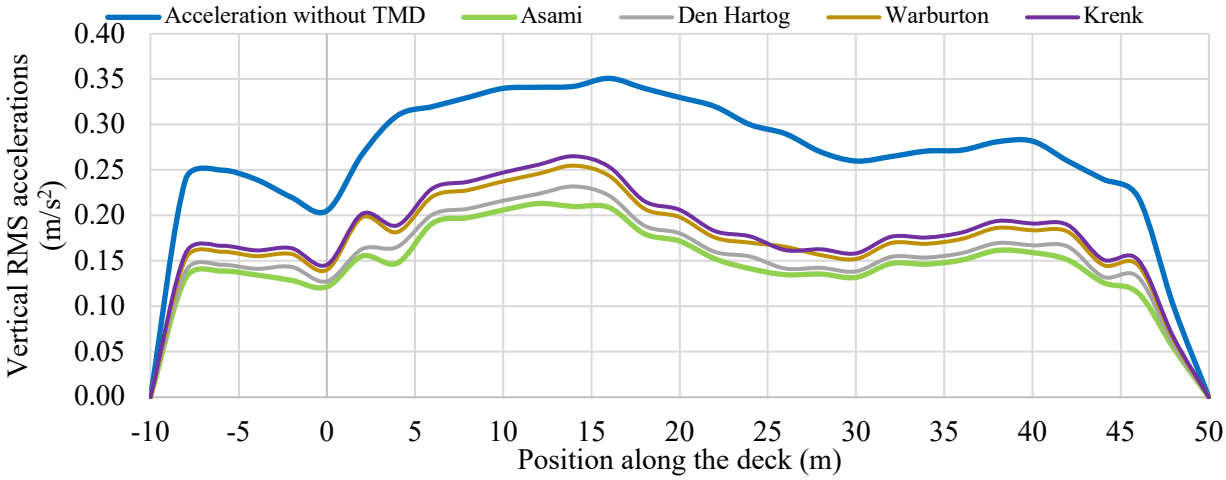
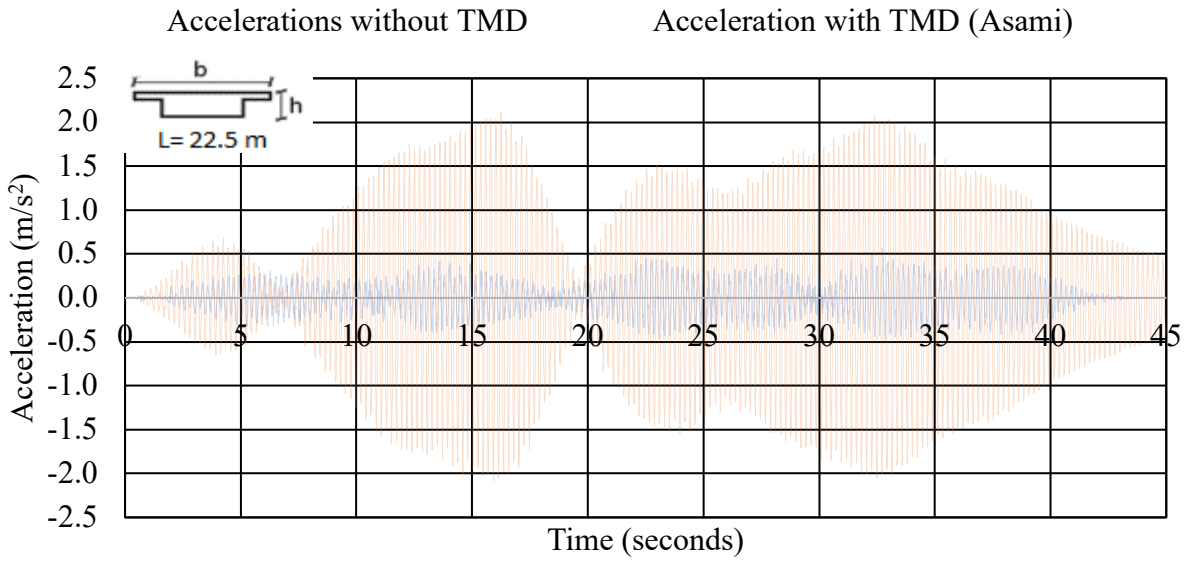
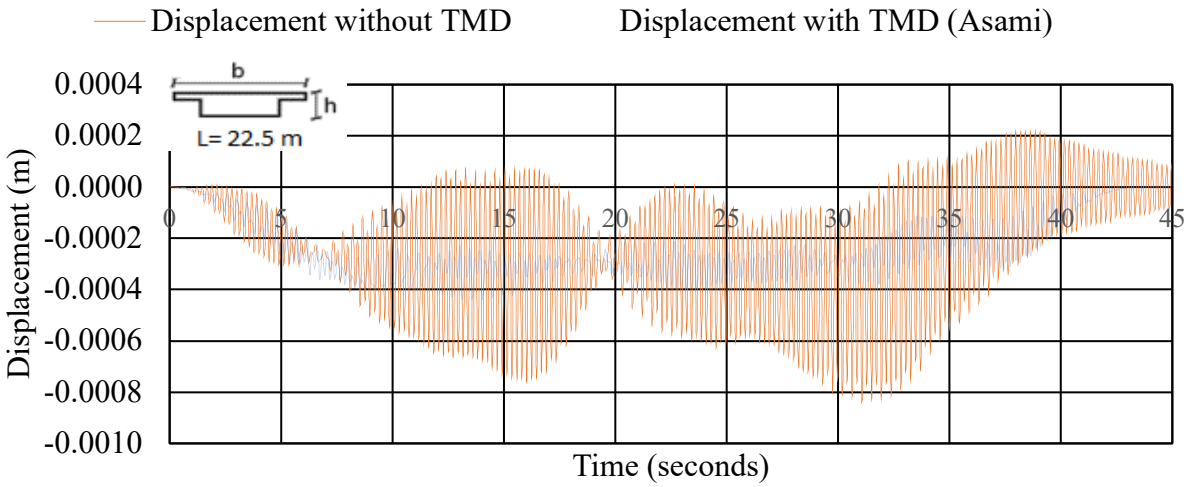


Figure 3.26: Vertical RMS accelerations with and without tuned mass dampers of a 50 m cable-stayed footbridge with one pylon under pedestrian densities of 0.6 ped/m^2

The high efficiency of the tuned mass dampers designed following Asami's criteria can be observed in the analysis in time domain in Figure 3.27. It displays the acceleration and displacement before and after the TMD was placed for different cross sections at mid-span and along the girder footbridge. When providing supplementary damping, the dynamic response is reduced in all the cases avoiding serviceability problems. Therefore, the TMD will be designed following Asami's criteria for further parametric studies for girder and cable-stayed footbridges.



(a)



(b)

Figure 3.27: (a) Acceleration (m/s^2) and (b) displacement (m) before and after the tuned mass damper is installed in a T-beam for a pedestrian density of 0.6 ped/m^2 for commuting activities

3.7.3.2.1 Impact of the TMD parameters

In the previous section, Asami criterion was found as the best option to reduce accelerations for girder and cable-stayed footbridges. This section shows a sensitivity study of the variations of the

accelerations regarding the mass ratio, damping ratio and frequency ratio (Figure 3.28 and Figure 3.29). Axis x is normalized by the parameters of damping ratio (ξ_{opt}), frequency ratio (α_{opt}) and mass ratio (μ) with respect to the values proposed by Asami (Section 2.5.1). The vertical axis represents the accelerations obtained with respect to the values that would have obtained using the same criterion. Figure 3.28 shows that with higher mass ratio values, the acceleration does not decrease. For frequency ratio (α_{opt}), once the frequency is not tuned to the frequency of the structure, the damper does not work (Figure 3.29). In addition, there is no significant reduction in the acceleration even when the damping ratio significantly increases. Therefore, the Asami criterion provides the optimum values for the reduction of accelerations.

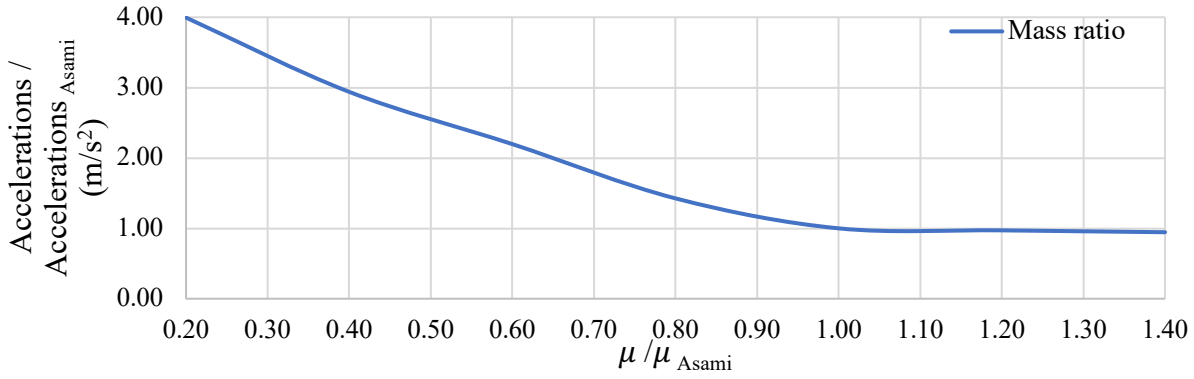


Figure 3.28 Vertical peak accelerations vs mass ratio (μ) normalized by the values proposed by Asami for a prestressed concrete footbridge with a 22.5 m span under pedestrian densities of 0.6 ped/m^2 for commuting activities

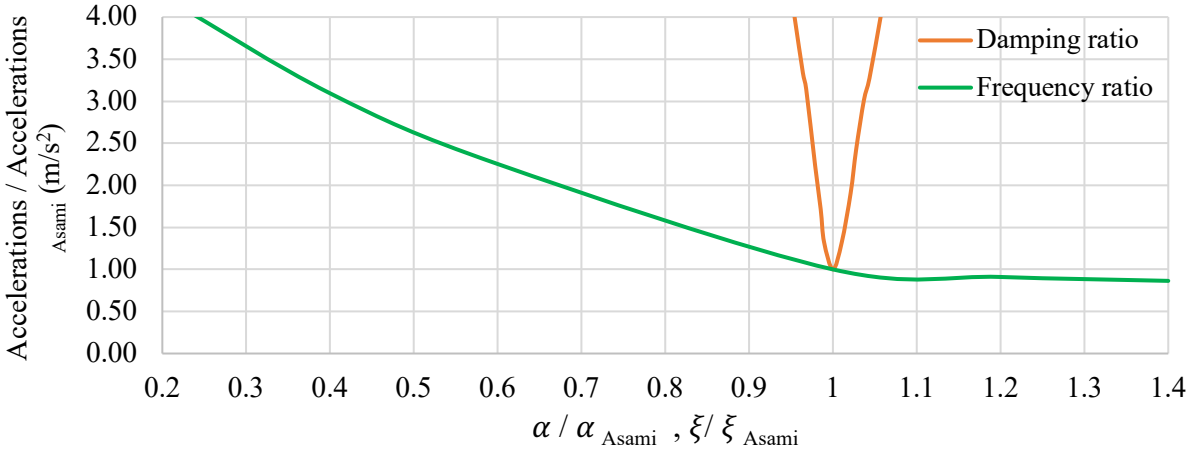


Figure 3.29 Vertical peak accelerations vs frequency ratio (α_{opt}) and damping ratio (ξ_{opt}) normalized by the values proposed by Asami for a prestressed concrete footbridge with a 22.5 m span under pedestrian densities of 0.6 ped/m^2 for commuting activities

3.8 Concluding remarks

This chapter presents the characteristics regarding the pedestrian model in the vertical and lateral direction, tuned mass dampers, and the structural characteristics of the girder and cable-stayed footbridges considered for the assessment of the serviceability criteria. It defines the probabilistic pedestrian load model that will be used in this research which is able to consider all the energy introduced in each step and that their amplitude in the lateral direction is related to the dynamic response of the bridge (non-linear behaviour). It details and identifies the numerical representation of girder and cable footbridges that will be used in the following chapters to assess the serviceability criteria with and without tuned mass dampers. Also presented are the key features of the automation of the different functions that are employed to evaluate the dynamic response. The serviceability criteria that will be used to assess the degree of comfort is presented. Furthermore, the methodology of implementing the supplemental damping devices in cases where the serviceability criterion is not fulfilled is defined. A summary of the implementation of the tuned mass dampers is also shown.

The last section of this chapter shows the evaluation of the dynamic response for girder and cable-stayed footbridges. The analyses are made considering different pedestrian loading scenarios. It is

illustrated that for certain span lengths and aim of the journey (commuting or leisure activities) of the pedestrians the serviceability criteria cannot be fulfilled using conventional approaches. In these cases, employing tuned mass dampers is required. The different criteria to obtain the parameters of the tuned mass dampers show the effectiveness in the reduction of the dynamic response. In all the cases that the tuned mass dampers are employed the structural response is reduced (efficiency ranging from 69 to 80%). The greatest efficiency of the TMDs is achieved when the TMD characteristics are determined using Asami's formulations, given the low damping in footbridges and the fact that the comfort criterion is governed by accelerations. These results justify the main goal of this research which is to give design recommendations for preliminary design in girder and cable-stayed footbridges under pedestrian loads employing TMDs to construct them without serviceability problems.

4 Dynamic response of girder footbridges

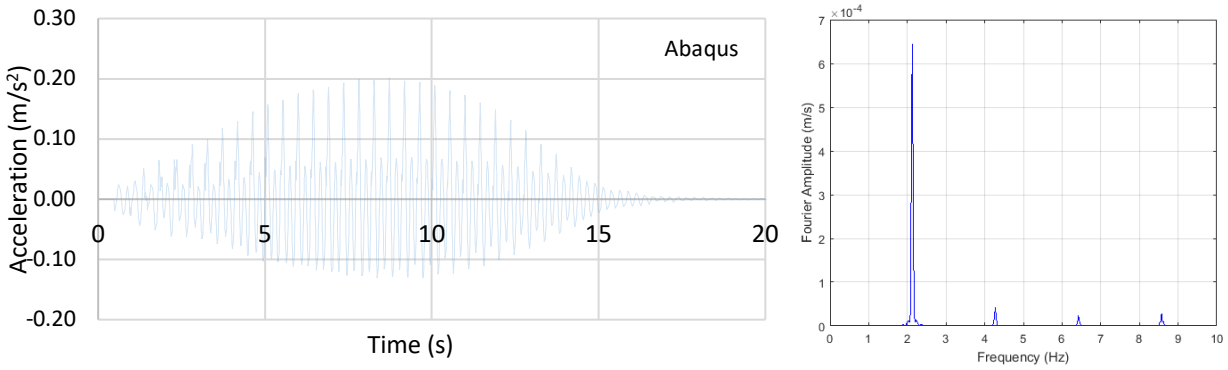
4.1 Introduction

During the last few decades, mitigating the effects of human-induced vibrations has been one of the most important aspects of vibration serviceability criteria in the construction of footbridges. Unexpected vibrations in footbridges due to pedestrian actions have shown the necessity for developing more realistic representations of transmitted loads. Some structures presented unexpected vibrations due to the lack of design criteria in codes, standards, and guidelines representing the pedestrian actions in an accurate manner. Some girder footbridges which suffered unexpected vibrations were the Langelinie footbridge in Denmark, the Passerelle Léopold-Sédar-Senghor in Paris, France, and the footbridge in Rotterdam Central Station in The Netherlands. These footbridges required the use of supplemental damping devices to control the human-induced vibrations. The evaluation of the dynamic response of a wider range of girder footbridges in the vertical and lateral direction considers the probabilistic pedestrian load model described in Section 3.2. The model includes the anthropometric characteristics of pedestrians, the force that each step transmits to the structure, the intra- and inter-subject variability, and the interaction among pedestrians crossing it at the same time. It also includes the parameters of the pedestrian load model, such as velocity and aim of the journey (Section 3.2.2). The dynamic response has been evaluated considering different pedestrian densities (0.2, 0.6, 1.0 ped/m^2). These evaluations will provide design guidance for girder footbridges employing supplemental damping devices in cases where the serviceability criterion is not fulfilled.

4.2 Python versus Abaqus models

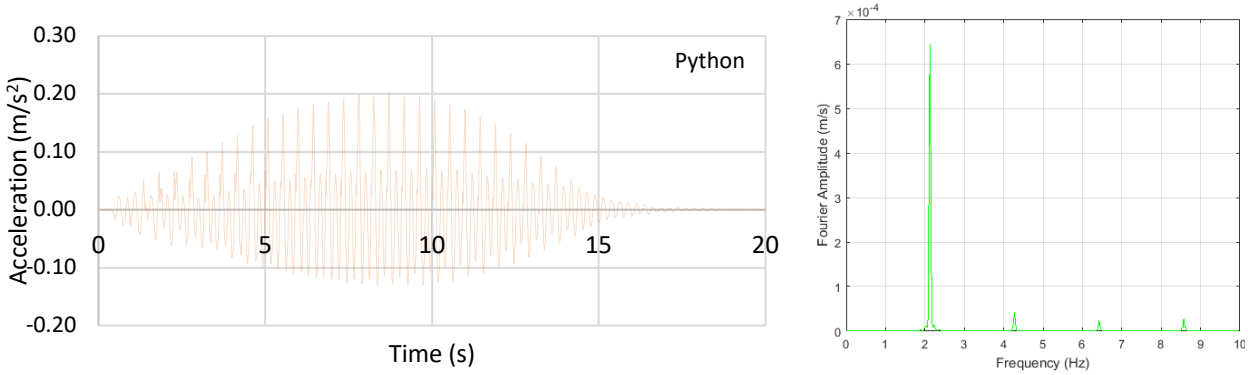
A comparison was made between the results obtained using the code developed in Python and the same model implemented using Abaqus (2014). Results for the accelerations along a girder footbridge with a 20 m span and a 4 m width, both in the time and in the frequency domains, are shown in Figure 4.1 and 4.2. The average differences obtained in Abaqus between Python for span lengths from 10 to 55 m is 0.043% and 0.167% for accelerations and displacements, respectively. Both models provided essentially identical results. The Python numerical model was preferred due

to computational reasons. Therefore, the code in Python has been employed for further parametric studies.



(a) (b)

Figure 4.1: Peak accelerations for a girder footbridge with a 20 m span and a 4 m width using Abaqus a) in the time domain, b) in the frequency domain



(a) (b)

Figure 4.2: Peak accelerations for a girder footbridge with a 20 m span and a 4 m width using Python a) in the time domain, b) in the frequency domain

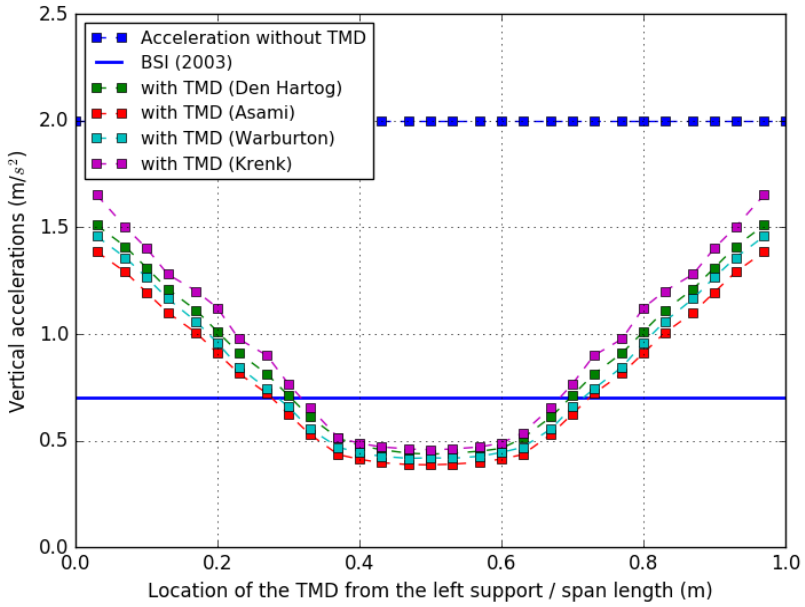
4.3 Dynamic response in the vertical direction

A set of single-span footbridges (Table 3.3), using a comprehensive set of structural materials, such as reinforced concrete, prestressed concrete, steel, steel and concrete composite sections, timber, aluminium and glass-fibre reinforced polymers (GFRP), is analysed herein, investigating the dynamic response of each of these footbridges under pedestrian loading, with and without tuned mass dampers. The span length and depth of the different sections (type 1 to 10) are shown

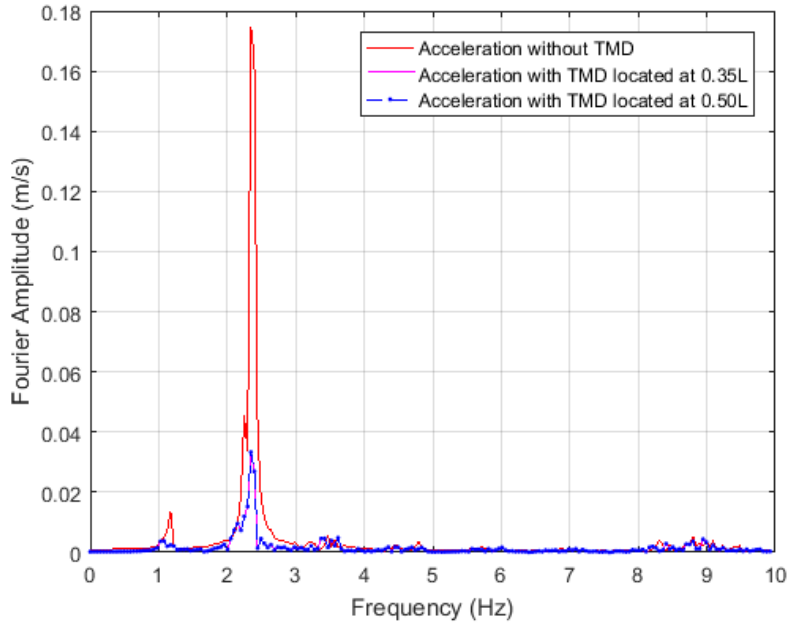
in Chapter 3 (Section 3.3.1). The structural materials for these sections are shown in Table 3.4. The footbridges are considered as simply supported structures represented by using 1-dimensional beam elements located at the sectional centroid. The modal shapes and the vibration frequencies were obtained by solving the linear eigenvalue problem. These frequencies can lie near the step frequency of the pedestrians, which can considerably increase the dynamic response (Garcia-Troncoso et al., 2017).

4.3.1 Single tuned mass damper

The greatest TMD efficiency (which is measured as the percentage of the peak acceleration prior to the implementation of this device that would be cancelled after its installation (Section 3.7.1) is achieved when the TMD is positioned at the location of the maximum nodal coordinates for the modal shape whose frequency has the largest amplitude in the representation of the excessive acceleration in the frequency domain. At that location, the efficiency of the TMD increases and therefore a smaller mass ratio is required to fulfil the serviceability criteria. For the girders considered, the maximum reduction of the dynamic response is achieved when the tuned mass damper is located at mid-span (Figure 4.3). Nevertheless, very similar efficiencies are achieved when the TMD is located in the central 30% of the span ($TMD_{efficiency}$ is equal to 74.50%, 79.40%, and 80.65%, when a TMD is located at 0.35L, 0.40L, and 0.50L respectively for the case considered in Figure 4.3). This conclusion is important for design as it gives flexibility to the designers when locating the TMDs. Nevertheless, by shifting the TMD towards the support sections, there is no benefit in reducing the vibrations linked to a second mode, or modes with a zero nodal coordinate at mid-span, as the TMD is not tuned to that modal frequency.



(a)



(b)

Figure 4.3: Simply-supported prestressed concrete (section type 1) footbridge with a 22.5 m span under pedestrian densities of 0.6 ped/m^2 for commuting activities: (a) peak vertical accelerations at mid-span when a TMD (μ= 0.05) is located at different positions along the length of the bridge, (b) Frequency amplitude spectrum of the peak vertical accelerations at mid-span when a TMD (μ= 0.05) located at 0.35 L and 0.5L and when no supplemental damping is implemented

Figure 4.4 shows the maximum vertical accelerations at mid-span for prestressed (section type 1 in Table 3.3) footbridges under pedestrian loading (leisure activities) with different span lengths. It is noticeable that for certain span lengths (close to 25 m) the serviceability criterion is not fulfilled when TMDs are not implemented, as the frequency of the structure matches the average pedestrian frequency, and a resonant effect is induced. In this case, a single TMD (μ= 0.04) was enough to mitigate the human-induced vibrations. By implementing a TMD, the accelerations were significantly reduced ($TMD_{efficiency}$=80%), down to the levels. Besides, the TMD also reduces the internal forces by mitigating the dynamic response (see Figure 4.5). At resonance, when L=25 m, the dynamic component of the bending moments at mid-span is very large, with a dynamic amplification factor (DAF) of 3.27. Nevertheless, the implementation of a TMD reduces the total, and the dynamic bending moments by 31 and 44% respectively, reducing the DAFs to 2.27. Similar values have been observed for a 12.5 m span. In this case, there is also a resonant effect, with every pedestrian step is resonant with every other vibrational modal cycle.

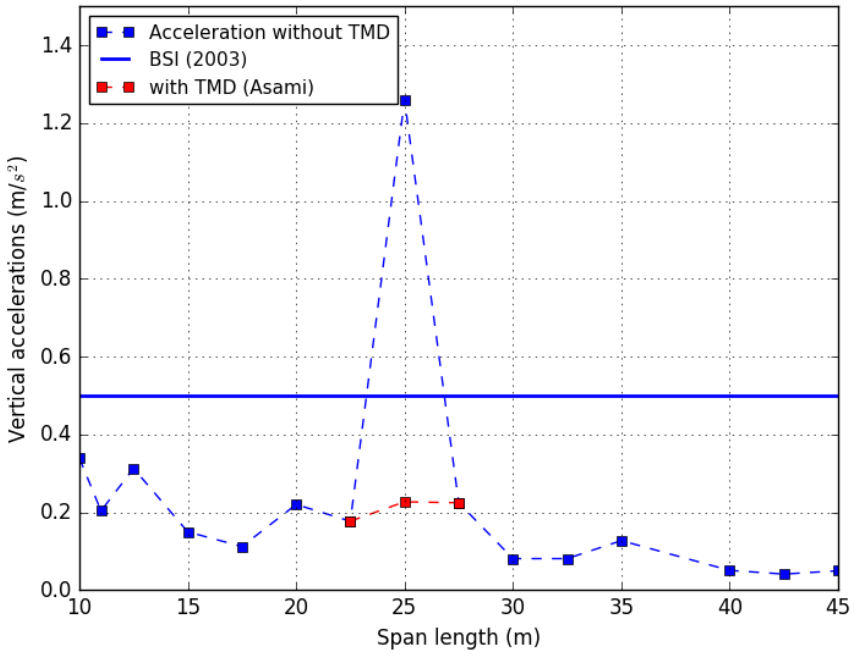


Figure 4.4: Maximum vertical peak accelerations for a set of prestressed concrete footbridges (section type 1 in Table 3.3) with spans ranging from 10 up to 45 meters for leisure activities under pedestrian densities of 0.6 ped/m^2

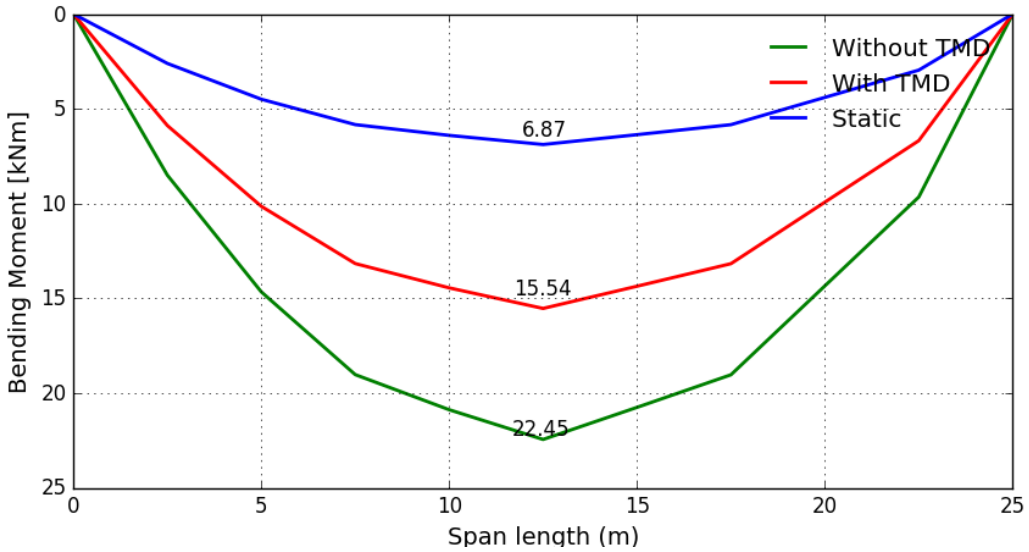
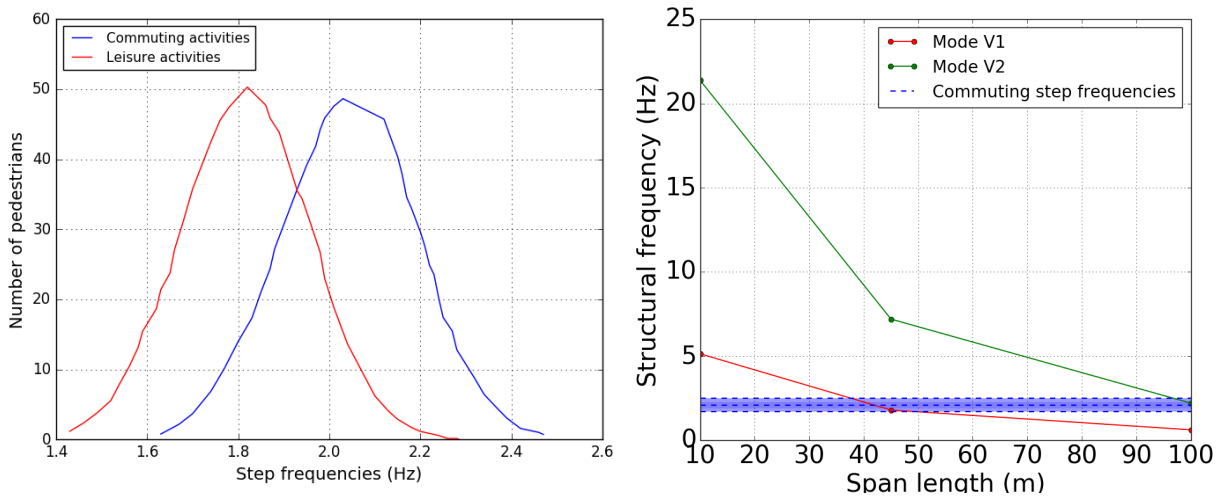


Figure 4.5: Maximum dynamic sagging bending moments along the length before and after a TMD (μ= 0.04) was employed at mid-span in a prestressed concrete footbridge of a 25 m span length considering a pedestrian density of 0.6 ped/m^2 for leisure activities. The static bending moment induced by the weight of the pedestrians is also represented

4.3.2 Multiple tuned mass dampers (MTMDs)

In the current section, the influence of splitting TMD's mass, span length, and cost in the dynamic response of a prestressed concrete footbridge for commuting activities (section type 1 in Table 3.3) is conducted. At the end of the section, design recommendations are listed for different cases, including the number of TMDs and their characteristics.

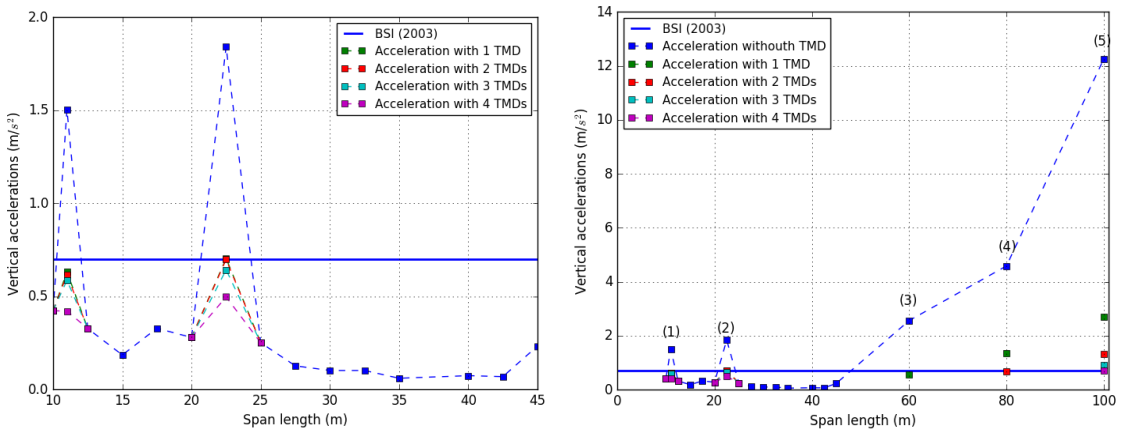
The same structural type and cross-section considered in the previous subsection is analysed herein under commuters' traffic. The main critical span is now 22.5 m, rather than 25 m, as a consequence of the increment of the pedestrian frequency (from leisure to commuting) producing resonant effects for higher fundamental structural frequencies, i.e., for smaller span lengths (See Figure 4.6). The modal shape is denoted by V followed by a number which represents the vertical mode with N-half waves.



(a) (b)

Figure 4.6: (a) Distribution of pedestrian frequencies for leisure (red) and commuting (blue) activities for pedestrian densities of 0.6 ped/m^2 for the UK population (b) Structural frequency versus the span length for a prestressed concrete (cross-section type 1) footbridge where the blue lines represent the range of vertical frequencies that can be excited by pedestrians

One tuned mass damper with a larger mass ratio ($\mu = 0.05$) located a mid-span is now required to mitigate the human-induced vibrations under the comfort limits when L=22.5 m (Figure 4.7 (a)). The increment in the mass ratio is due to the increment of the vertical forces (which are frequency related, see Table 2.3), as well as the small structural mass, leading to larger accelerations as a consequence of Newton's second law.



(a) (b)

Figure 4.7: Maximum vertical peak accelerations for prestressed concrete (section type 1 in Table 3-3) footbridges with and without TMDs (each of them with $\mu = 0.05$) (see Table 4.1), under pedestrian densities of 0.6 ped/m^2 (commuters) for spans ranging from 10 m (a) up to 45 meters, (b) up to 100 m

The serviceability criteria can be fulfilled with a single TMD located at mid-span for bridges up to 50 m long (Figure 4.7). However, for larger spans of 80 and 100 m, two and four TMDs, respectively, are required at mid-span, leading to total masses in the supplemental damping devices equal to 10% and 20% of the structural mass. For larger spans, both the structural mass and the mass increase, leading to the requirement of significantly larger TMDs (see Table 4.1).

TMD according to Figure 4.7	Number of dampers	Total mass (kg)	Length (mm)	Width (mm)	Height (mm)
(1)	1	250	600	560	275
(2)	1	1500	1000	930	325
(3)	1	5000	2560	1410	325
(4)	2	4000	2000	1410	325
(5)	4	6000	2780	1530	325

Table 4.1 Tuned mass damper properties (all with μ=0.05) required to mitigate the human-induced vibrations in the footbridges considered in Figure 4.7

In some cases, the geometrical constraints may lead to splitting the TMDs into two during a more detailed stage of the design. When a single TMD is split into two (halving the mass m, the stiffness k and the damping c, and maintaining the TMD frequency and damping ratio) shifting them longitudinally at both sides of the mid-span, the efficiency of the TMD system is barely affected, as long as they are located with a maximum spacing of 30% of the span length, and concentred at mid-span (i.e., ±15% span from the mid-span). For instance, when L=22.5 m, the maximum peak accelerations at mid-span drop from 1.886 to 0.389 m/s^2 introducing one TMD (μ=0.05) at mid-span, and to 0.411 m/s^2 when two TMDs (μ=0.025 each) are located at ± 3m from mid-span. This is consistent with the results shown in Figure 4.3 (a). Figure 4.7 (b) shows that for spans longer than 50 m, the accelerations increase dramatically without supplemental damping devices. Therefore, the number of TMDs that are required to satisfy the comfort limits also increase significantly. Nevertheless, given the size (Table 4.1) and number of TMDs (Figure 4.7 (b)), it is possible to locate all the TMDs required within that central section (i.e., ±15% span from the mid-span) guaranteeing a large efficiency of the TMD system (β=80%) and the verification of the serviceability criterion.

4.3.3 Cost analysis

Ramos-Moreno (2015) demonstrated that increasing the slab thickness (i.e., adding mass) was the most efficient way of controlling accelerations with the structural parameters (i.e., without implementing supplemental damping devices) in these types of footbridges. By adding mass, the accelerations are reduced, although this effect could be counteracted by the frequency shift if the structural frequencies get closer to the load frequencies. However, adding mass also increases the structural demands due to self-weight and seismic response, leading to increasing the capacity of several structural members. A comparative cost study between these two design alternatives (implementing TMDs or increasing the slab thickness) is included herein. The unit costs considered are shown in Table 4.2 which are those from Bourne (2013) updated through by 7.3% to reflect the cumulative effects of inflation since the publication of these costs (BBC, 2019). The TMD considered has a mass of 250 kg, a tuning range from 1.4 to 2.8 Hz, a damping ratio from 10 to 15%, and a maximum displacement range of ±40 mm, whose unit cost has been provided by a worldwide supplier (MAURER). Other costs are not considered herein, as the aim is comparing the relative deck material cost for both design alternatives.

Element	Unit costs Bourne (2013) in GBP	Cost rate (2019) in GBP
Concrete (m^3)	120	129
Reinforcement (T)	1100	1180
Prestress (T)	3000	3219
Vertical formwork (m^2)	50	54
Horizontal formwork (m^2)	125	134
Tuned mass damper (unit)		3327

Table 4.2: Material unit costs used in this analysis

The TMD would probably need to be replaced during the footbridge service life. Technical brochures of TMDs highlight that their lifetime is around twenty years (leading to 4 replacements in 100 years). However, this seems very conservative based on recent publications. Weber & Feltrin (2010) and Meinhdart et al., (2017), stated that after 16 years of setup, TMDs still showed a satisfactory performance. The TMDs installed in a footbridge at Frottmanin Subway Station, in Munich, were still working properly 21 years after, and have only required very little maintenance (cleaning and refilling the oil of the damper pot) (Benicke, 2017). Therefore, Maurer now recommends one replacement in 100 years, including two maintenance sessions (Benicke, 2017). This uncertainty in the number of TMD replacements has been considered in this study, through different TMD life lengths (20, 25, 33.3, 50 and 100 years). The same unit cost has been considered for those replacements of TMDs in future years, assuming that the investment and inflation rates would be similar, as the proper consideration of these additional uncertainties are beyond the scope of this analysis.

The cost analysis (see Figure 4.8 and Table 4.3) has been performed for a prestressed concrete (section type 1) footbridge with an 11.25 m span length, for different deck depths, considering the design scenario of pedestrian densities of 0.6 ped/m^2 (commuters). A deck depth of L/24 is required to fulfil the serviceability criterion (peak acceleration $\leq$ 0.7 m/s^2) without TMDs, leading to a material cost for the deck of 14091 GBP. From L/25 to L/35 the solutions with supplemental damping would require the installation of a single TMD at mid-span. Two TMDs would be required for the range from L/39 to L/43, and four TMDs for L/49. When TMDs are being used, regardless of the TMD expected life, the smallest material cost is achieved for deck depths of L/35. If the TMD expected life can be assumed equal to 100 years, as recommended by Benicke (2017), then the design with TMDs and deck depth of L/35 would lead to the most economical solution (12% cheaper than that for L/24 without TMDs), and very small increments would occur for deck depths down to L/43. For shorter expected lives of the TMDs of 50, 33.3, 25 and 20 years, the solutions with TMDs and deck depth of L/35 would be 2%, 16%, 35% and 45% more expensive (for the deck materials) than that for L/24 without TMDs. Nevertheless, there would be additional savings in other structural members such as bearings, abutments and foundations. For deck depths thinner than L/43 the deck material cost increases significantly.

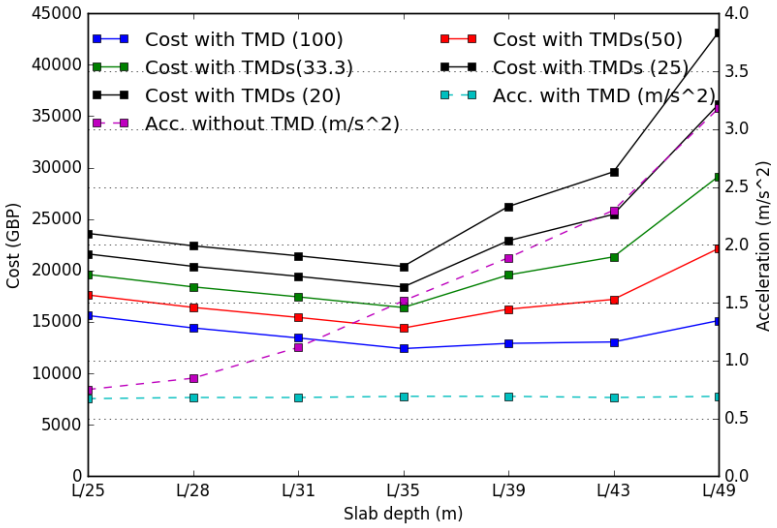


Figure 4.8 Cost analysis for different slab depth (m) when one or multiple TMDs are employed in the design of a prestressed concrete footbridge with a 11.25 m span length, for different TMD expected lives of 20, 25, 33.3, 50 and 100 years, with pedestrian densities of 0.6 ped/m^2 (commuters)

Slab depth (m)	**Acceleration without TMD (m/s^2)**	**Cost without TMD (£)**	**Acceleration with TMD (m/s^2)**	**Cost with TMD (100)**	**Cost with TMDs (50)**	**Cost with TMDs (33.3)**	**Cost with TMDs (25)**	**Cost with TMDs (20)**
L/24	0.67	14091						
L/25	0.75	13623	0.67	15619	17615	19611	21608	23604
L/28	0.85	12418	0.68	14414	16410	18406	20403	22399
L/31	1.11	11446	0.68	13442	15438	17435	19431	21427
L/35	1.51	10409	0.69	12406	14402	16398	18394	20390
L/39	1.89	9585	0.69	12912	16239	19566	22893	26220
L/43	2.30	8915	0.68	13051	17187	21324	25460	29596
L/49	3.18	8114	0.69	15128	22141	29155	36169	43182

Table 4.3 Cost analysis for different slab depth (m) when one or multiple tuned mass dampers are employed for a prestressed concrete footbridge based on Figure 4.8 for different TMD expected lives of 20, 25, 33.3, 50 and 100 years

4.3.4 Design recommendations

In this section, design recommendations are given for the different section types that have been considered in Table 3.3. In this study, one to four TMDs were located at the maximum nodal displacement of the modal shapes, i.e., at mid-span, to analyse the effect of the reduction of the dynamic response. Figure 4.9, Figure 4.10 and Figure 4.11 show the maximum acceleration in a range of footbridges in the vertical direction for leisure and commuting activities. Table 4.4, Table 4.5, and Table 4.6 show the TMD properties (minimum mass of the TMD) that can be employed for each of the resonant cases (Figure 4.9, Figure 4.10 and Figure 4.11) activated at particular span lengths. The TMD properties i.e., length and width, are selected based on the MAURER technical catalogue (Benicke, 2016). For cross-section types 1 to 8, it is enough to employ one tuned-mass damper to satisfy the serviceability criteria. In addition, when a larger number of TMDs is used, there is not a significant reduction of the accelerations. However, for cross-sections types 9 and 10, one to four TMDs are not sufficient to control the human-induced vibrations. In these ultra-light cross-sections, the serviceability limit state is not fulfilled even when a large number of TMDs are used.

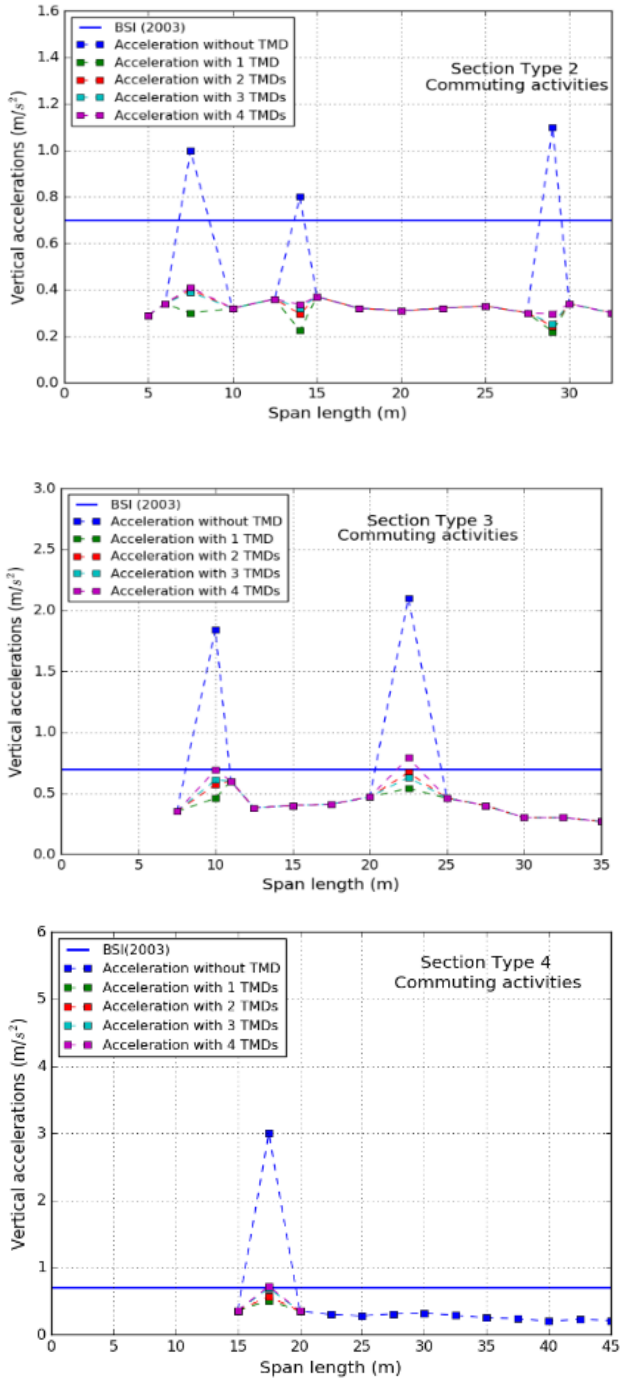


Figure 4.9 Maximum vertical accelerations for Section Types 2, 3, and 4 (Table 3.3), when one, two, three or four TMDs are implemented at the maximum nodal coordinate of the modal shape with a larger contribution in the dynamic response, under pedestrian densities of 0.6 ped/m^2 (commuting activities)

Section Type (Table 3.3)	Span length (m)	Commuting activities				Span length (m)	Leisure activities			
		Mass ratio	Length (mm)	Width (mm)	TMD efficiency (%)		Mass ratio	Length (mm)	Width (mm)	TMD efficiency (%)
2	7.5-14.0	0.01	600	560	75	5.0	0.01	600	560	78
	29.0	0.03	5.0	200	72	-	-	-	-	-
3	10.0	0.04	-	200	69	27.5	0.03	1020	200	77
	22.5	0.05	27.5	240	78	-	-	-	-	-
4	17.5	0.06	-	200	71	25.0	0.04	1420	240	69

Table 4.4 Tuned mass damper properties according to the span length under pedestrian densities of 0.6 ped/m^2 for commuting and leisure traffic

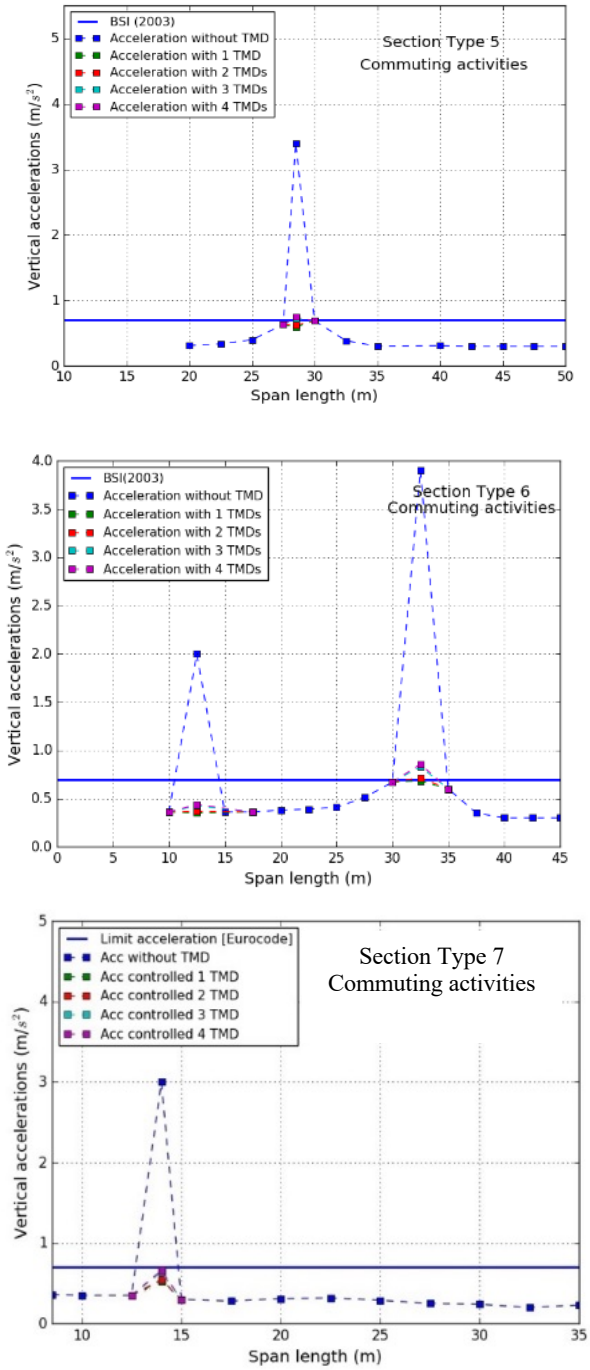


Figure 4.10 Maximum vertical accelerations for Section Types 5, 6, and 7 (Table 3.3), when one, two, three or four TMDs are implemented at the maximum nodal coordinate of the modal shape with a larger contribution in the dynamic response, under pedestrian densities of 0.6 ped/m^2 (commuting activities)

Section Type (Table 3.3)	Span length (m)	Commuting activities				Span length (m)	Leisure activities			
		Mass ratio	Length (mm)	Width (mm)	TMD efficiency (%)		Mass ratio	Length (mm)	Width (mm)	TMD efficiency (%)
5	28.5	0.06	2000	1080	77	32.5	0.05	1600	930	72
6	12.5	0.05	1220	200	72	17.5	0.03	800	556	75
	32.5	0.07	2000	1410	69	37.5	0.06	2000	1080	72
7	14.0	0.06	1220	200	74	17.5	0.04	1220	200	80

Table 4.5 Tuned mass damper properties according to the span length under pedestrian densities of 0.6 ped/m^2 for commuting and leisure traffic

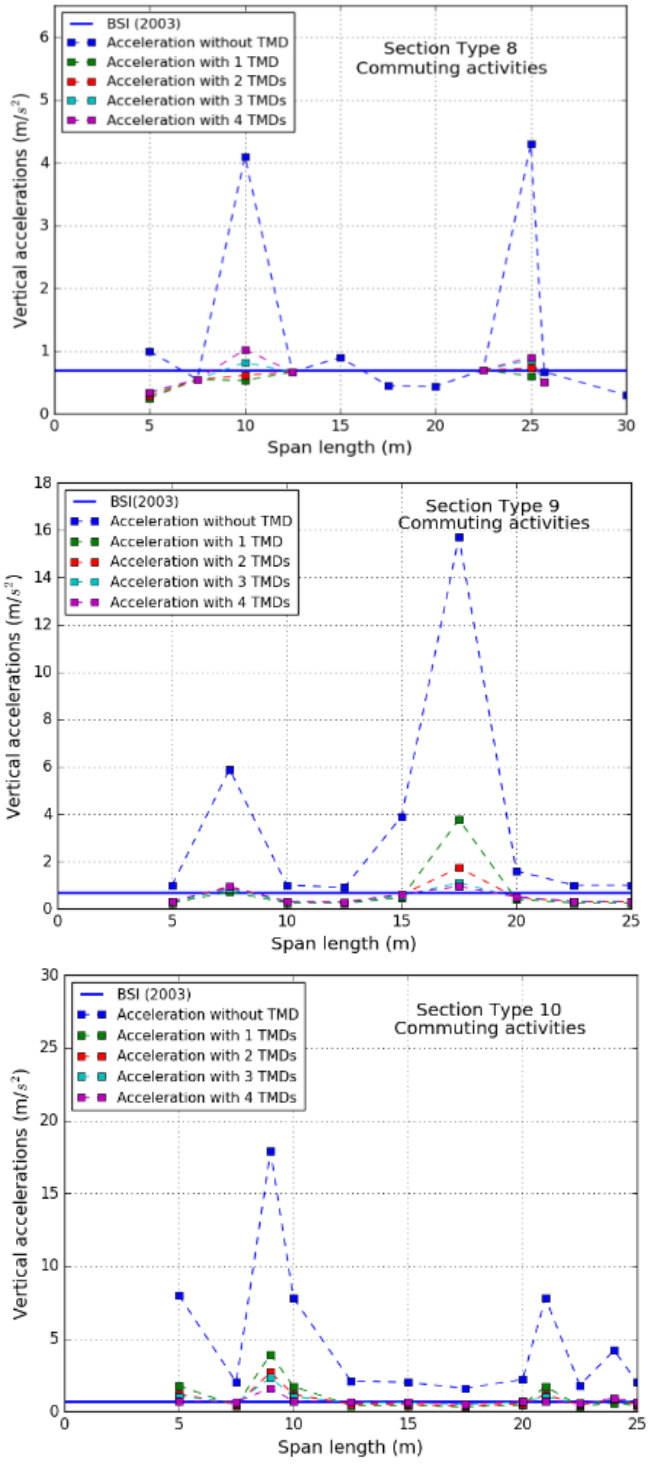


Figure 4.11: Maximum vertical accelerations for Section Types 8, 9, and 10 (Table 3.3), when one, two, three or four TMDs are implemented at the maximum nodal coordinate of the modal shape with a larger contribution in the dynamic response, under pedestrian densities of 0.6 ped/m^2 (commuting activities)

Section Type (Table 3.3)	Span length (m)	Commuting activities				Span length (m)	Leisure activities			
		Mass ratio	Length (mm)	Width (mm)	TMD efficiency (%)		Mass ratio	Length (mm)	Width (mm)	TMD efficiency (%)
8	5.0	0.03	600	560	72	7.5	0.05	600	560	79
	10.0	0.07	1250	930	78	12.5	0.05	1000	780	72
	25.0	0.07	2000	1080	75	17.5	0.04	800	556	70
9	5.0	0.04	600	560	-	6.0	0.05	600	560	-
	7.5	0.08	1250	930	-	9.0	0.06	1000	610	-
	10.0-12.5	0.03	1000	610	-	17.5	0.03	1000	750	-
	15.0	0.07	1000	750	-	20.0	0.06	2000	1410	-
	17.5	0.09	2780	1530	-	22.5-25.0	0.03-0.04	1250	930	-
	20.0-22.5-25.0	0.04	1250	930	-					
10	5.0	0.08	1600	930	-	5.0	0.06	1000	610	-
	7.5 -12.5	0.06	1000	610	-	12.5	0.05	800	556	-
	9.0	0.07	2780	1530	-	15.0	0.04	2000	1410	-
	10.0 -21.0	0.06	2000	930	-	17.5	0.04	2000	930	-
	15.0-17.5-20.0	0.07	1000	780	-	20.0	0.05	2000	930	-
	22.5	0.06	2000	1410	-	23.5-25.0	0.06-0.05	1250	930	-
	24.0-25.0	0.07-0.06	1250	930	-					

Table 4.6: Tuned mass damper properties according to the span length under pedestrian densities of 0.6 ped/m^2 for commuting and leisure traffic. For those cases in which the accelerations do not satisfy the comfort criterion, the value of the TMD efficiency is not included(-)

4.4 Dynamic response in the lateral direction

The lateral peak accelerations increase almost linearly with the span length (see Figure 4.12). For given deck widths, these footbridges will have lateral vibration problems above a certain span length (Figure 4.13). For deck widths equal to L/20, the limit accelerations are exceeded from span lengths of 20 m. Nevertheless, if the deck width is doubled up to L/10, the serviceability criteria are fulfilled for span lengths from 20 to 100 m. Supplemental damping devices are required for cases in which the deck width is equal to L/20 to mitigate the lateral human-induced vibrations (Figure 4.14 and Table 4.7). The maximum lateral peak accelerations when one lateral TMD is employed (Figure 4.14) are similar to those when the deck width is doubled and no supplemental damping is used (Figure 4.12). Furthermore, if the span length is increased beyond 100 m, the comfort limits will not be satisfied, and lock-in effect will become relevant.

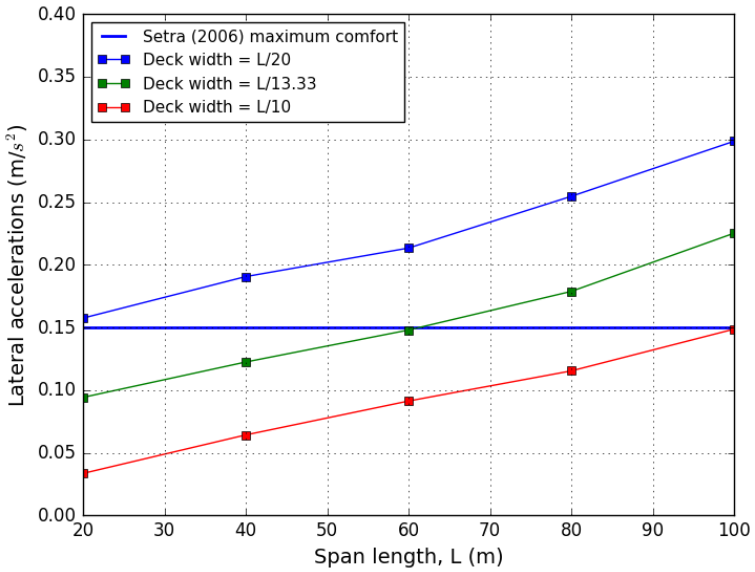


Figure 4.12 Maximum lateral peak accelerations in prestressed (section type 1 in Table 3.3) footbridges with spans ranging from 20 up to 100 m under pedestrian densities of 0.6 ped/m^2 for commuting traffic

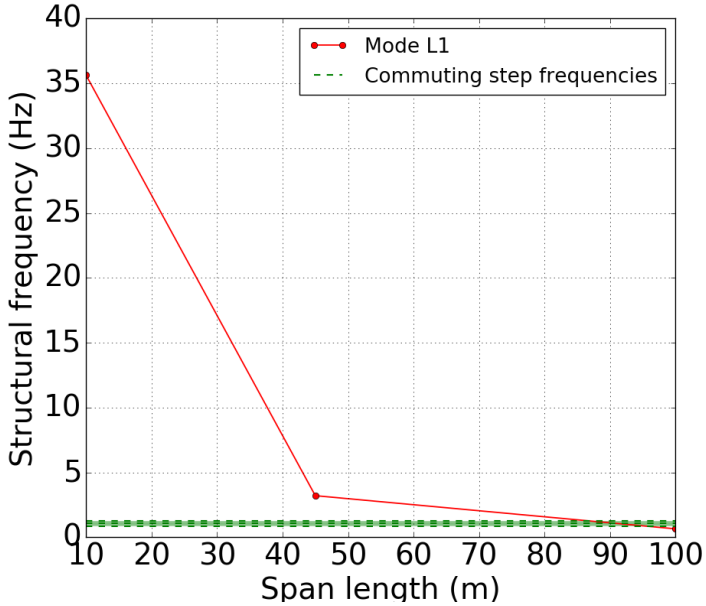


Figure 4.13 Structural lateral frequencies versus the span length for a slab depth of L/10 under a pedestrian density of 0.6 ped/m^2 for commuting activities where the green lines represent the range of lateral frequencies that can be excited by pedestrians

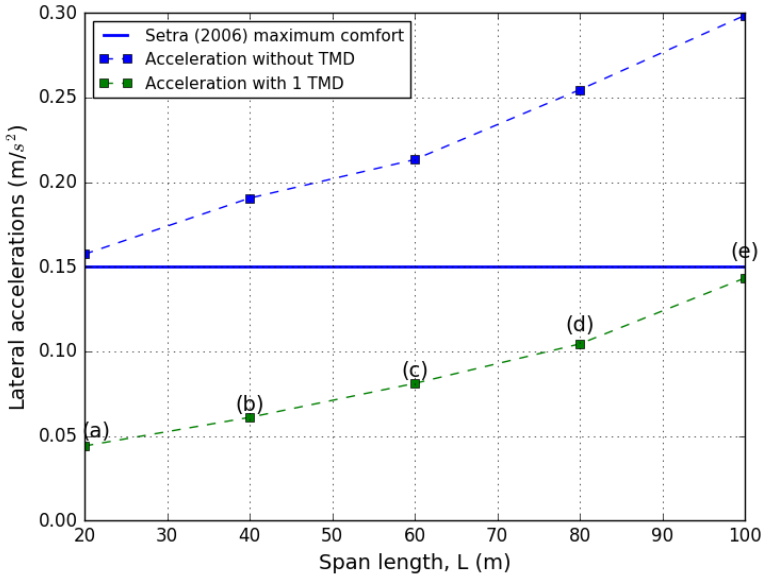


Figure 4.14: Maximum lateral peak accelerations for prestressed (section type 1 in Table 3.3) footbridges with spans ranging from 20 up to 100 m under pedestrian densities of 0.6 ped/m² (commuters) for width/span ratios of 1/20

TMD according to Figure 4.14	Mass (kg)	Length (mm)	Width (mm)	Height (mm)	TMD efficiency (%)
(a) - (b)	250	880	560	200	72
(c)	750	1330	670	210	71
(d)	2500	1530	1200	280	74
(e)	5000	2140	1780	310	70

Table 4.7 Tuned mass damper properties according to the structural section under 0.6 ped/m^2 for commuting and leisure activities based on Figure 4.14

Design recommendations are given for the different section types that have been considered in Table 3.3. In this study, one TMD was located at the maximum nodal displacement of the modal shapes, i.e. at mid-span, to analyse the effect of the reduction of the lateral accelerations. Figure 4.15 shows the maximum lateral accelerations in a range of footbridges under pedestrian densities of 0.6 ped/m^2 (commuting and leisure activities). Table 4.8 shows the TMD properties (minimum mass of the TMD) that can be employed for each of the resonant cases (Figure 4.15) activated at particular span lengths.

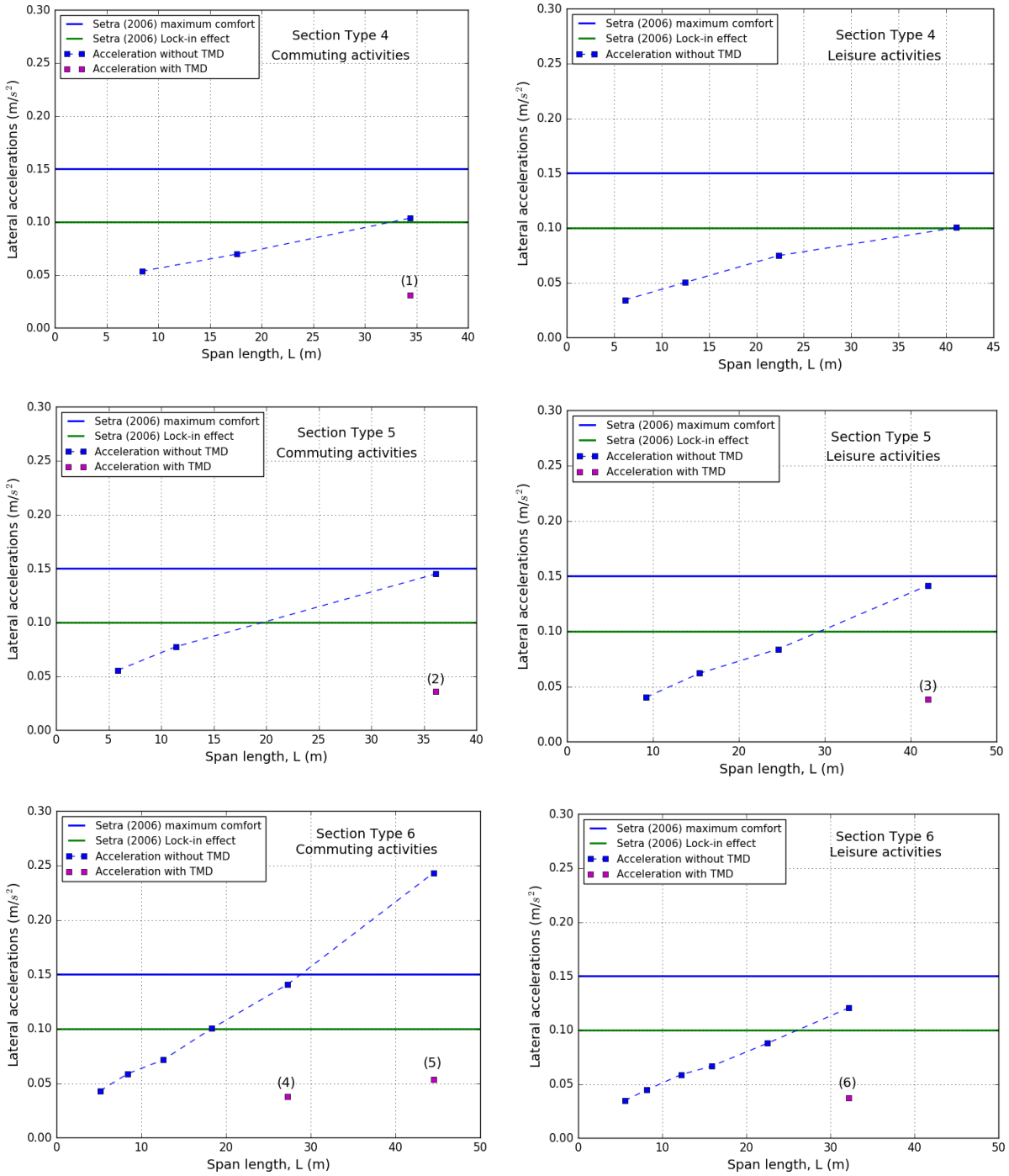


Figure 4.15 Maximum lateral accelerations for Section Types 4, 5 and 6 (Table 3.3) under pedestrian densities of 0.6 ped/m^2 (commuters and leisure activities) with and without TMDs

TMD according to Figure 4.15	Mass (kg)	Length (mm)	Width (mm)	Height (mm)	TMD efficiency (%)
(1)	250	880	560	200	70
(2) - (3)	500	1090	670	200	75
(4)	250	880	560	200	73
(5)	2500	1530	1200	280	78
(6)	250	880	560	200	69

Table 4.8 Tuned mass damper properties according to the structural section under 0.6 ped/m^2 for commuting and leisure activities based on Figure 4.15

4.5 Concluding remarks

TMDs are widely used on footbridges to mitigate excessive human-induced vibrations in the vertical and lateral direction. In this chapter, a wide range of footbridges was considered to understand their structural response through a parametric analysis. The dynamic response of girder footbridges under pedestrian actions with and without TMDs has been studied to verify the effectiveness of these devices, as well as to show design recommendations for this type of footbridge. An advantage of this study is that designers can adopt the different design recommendations to include tuned mass dampers at the design stage to avoid serviceability problems. It was evidenced that the dynamic response increased for various span lengths and the type of traffic (commuting or leisure activities). The main conclusions of this chapter are as follows:

- The comparison of the accelerations and displacement calculated for a girder footbridge using the code developed in this study (Python) vs. a specialized software (Abaqus) shows very similar results (differences in the acceleration of 0.089 %). There are several benefits of using coding as an alternative to directly using any FEA packages. Instead of becoming a software operator, developing a code allows grasping physical concepts of the problem, providing to the designer with tools and skills to understand the problem beforehand. Also, as the code normally starts from scratch, the troubleshooting sometimes is easier. However,

the time developing the code might be one of the major drawbacks of this approach, in case this is a restraint for the project. Also, deciding which programming language is time-consuming and will depend on the skills of the programmer. For this project, Python was elected as it also works very well with the selected FEA package, Abaqus. The reason why Python was chosen was, among others, it is a high-level interpreted programming language. This means a fast exploration of various ideas and fast and efficient implementation. Also, it includes many numerical tools and libraries available among open source packages. Finally, this programming language is relatively easy to learn and has a very clear and readable syntax.

- The larger efficiencies of the TMDs are achieved when they are located at the maximum nodal coordinates of those modal shapes dominating the response. Nevertheless, provided the TMD location remains with the central 30% of the span length, the high values of the efficiencies, reducing the vertical peak accelerations by up to 80% are not affected. The implementation of TMDs also reduces the dynamic component of the internal forces, to a lesser extent than for the accelerations.

- For vertical accelerations, the serviceability criteria can be fulfilled with a single TMD, with a 0.05 mass ratio, located at mid-span for bridges up to 60 m long. However, for larger spans of 80 and 100 m, two and four TMDs, respectively, are required at mid-span, leading to total masses in the supplemental damping devices equal to 10% and 20% of the structural mass. Large TMDs can be split into two, provided both remain located in the central 30% of the span length, with variations of the efficiency of 1%.

- For vertical accelerations, the most cost-effective solution is achieved for deck span ratios of 1/35 when TMDs are used. If the TMD does not need to be replaced, or is replaced only once, throughout the service life, the deck material cost would be smaller, or similar, to the case without TMDs and a deck span ratio of 1/24.

- Vertical accelerations in ultra-light footbridges, with cross-sections made of aluminium or glass fibre reinforced polymers, and conventional deck span ratios (1/30 and 1/40), do not satisfy the comfort criterion even after implementing multiple TMDs. Therefore, the slenderness and the structural masses have to be governed by the dynamic response, losing the lightness achieved by implementing these materials. For these structures, the Serviceability Limit State of Vibrations is critical for the design.

- For span lengths up to 100 m, TMDs are not required to control lateral accelerations when the width span ratios are larger than 1/10. However, TMDs are required for span lengths larger than 20 m when the width span ratios are equal or smaller than 1/20.

- Tuned mass dampers can be employed at the design stage to minimize the dynamic response in girder footbridges in the vertical and lateral direction. It is essential to highlight that the design recommendations that are shown in this chapter can be used to include tuned mass dampers in the preliminary design of girder footbridges. This is to avoid serviceability problems after the construction of footbridges.

5 Dynamic response of cable-stayed footbridges with a single tower

5.1 Introduction

Due to the recent developments in the design methodology, construction techniques, and material types, cable-stayed footbridges are becoming lighter and slenderer. However, as these improvements reduce the mass and the damping capacity, they also increase the human-induced vibration (serviceability problems). Gaining a better understanding of the structural response of footbridges with and without tuned mass dampers is necessary to identify the cases that can have serviceability problems and to propose design recommendations. Therefore, the main objective of this chapter is to analyse the structural response of cable-stayed footbridges with one tower using different span lengths, which were selected based on a database of built cable-stayed footbridges, compiled by Ramos-Moreno (2015), from existing literature. These footbridges were studied by Ramos-Moreno (2015), and it was shown that for certain span lengths, the serviceability limit state (SLS) of vibration is not satisfied without supplemental damping devices.

One of the main features of the footbridges is their long spans. The impact when the span length is increased is also investigated. Thus, Section 5.2 describes the geometry and modal analysis of the cable-stayed footbridges with a single pylon. Sections 5.3 and 5.4 show the vertical and lateral accelerations with and without tuned mass dampers in cable-stayed footbridges with an I-shaped pylon. In these sections, the tuned mass damper properties to achieve the maximum comfort criteria in both directions and also to avoid the lock-in effect in the lateral direction are defined. Section 5.5 shows a parametric study of cable-stayed footbridges with two alternative pylon shapes (H- and A-shaped). Section 5.6 shows a cost comparison between either changing structural parameters (without implementing supplemental damping devices) or employing TMDs as a strategy to mitigate the human-induced vibrations down to admissible levels. At the end of this chapter (Section 5.7), design recommendations are provided. These recommendations consider different pedestrian densities, span lengths, pylon's shapes and TMD mass ratio in the vertical and lateral direction.

5.2 Benchmark case for cable-stayed footbridges with a single pylon

5.2.1 Modelling characteristics

The geometry of the cable-stayed footbridges (CSFs) to be considered in this chapter is selected based on a dataset obtained in the literature review (Section 2.2) (Ramos-Moreno, 2015, Ramos-Moreno et al., 2017). Three different span lengths will be analysed in this thesis: CSFs with a main span of length 50, 100, and 150 m and a side span of 10, 20, and 30 respectively (always for a side to main span ratio of 0.20). The geometric characteristics such as deck depth, deck width, cable-system arrangement, and material properties of these cable-stayed footbridges were presented in Section 3.3.2. Figure 5.1 shows the geometry, boundary conditions, and deck articulation (deck plan) of the benchmark case for a 50 m main span.

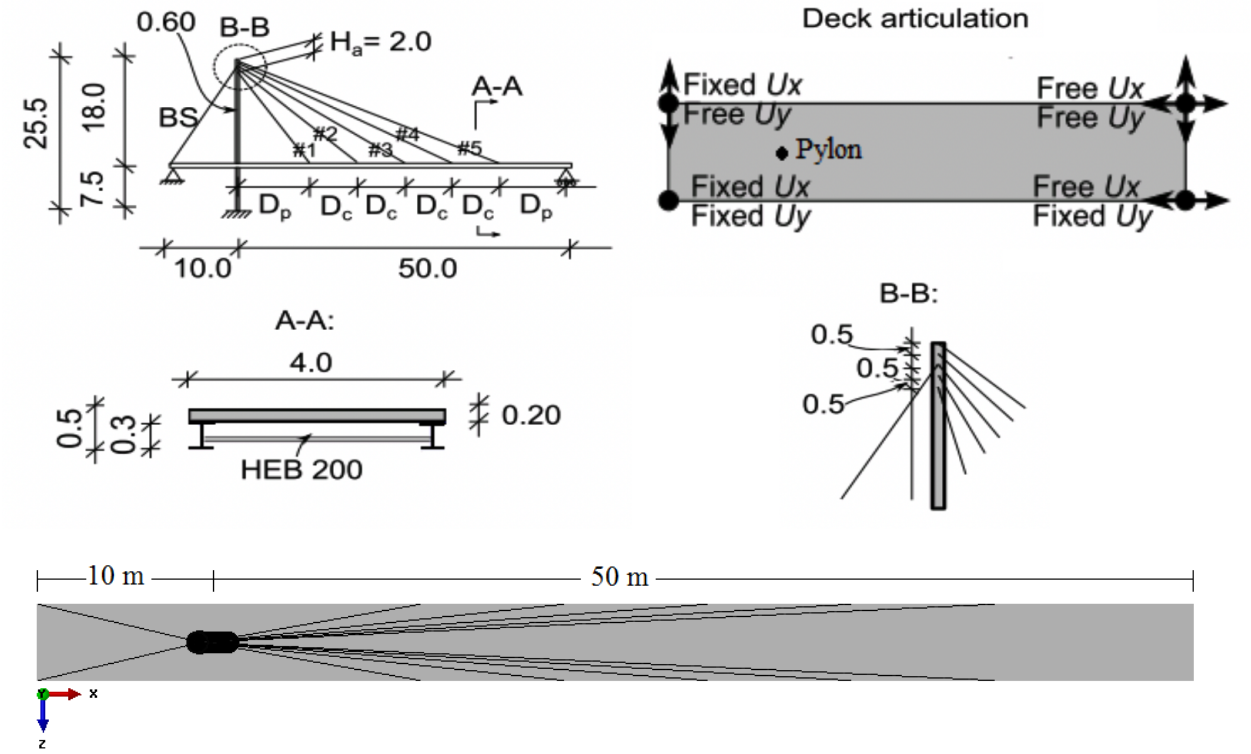


Figure 5.1 Geometry and plan view of the 50 m benchmark cable-stayed footbridge with a single pylon. Dimensions in meters (m) (Ramos-Moreno, 2015)

5.2.2 Modal analysis

Cable-stayed footbridges are characterised to have low frequencies. When these frequencies match with the range of the pedestrian frequencies, the dynamic response is amplified. In this work, a modal analysis was performed for each span length to assess if the frequencies are close to the step frequencies of the pedestrians (Figure 5.2, Figure 5.3, and Figure 5.4). Table 5.1, Table 5.2, and Table 5.3 show the vibration modes of the footbridge when it is empty and when is loaded with the different pedestrian densities in the cable-stayed footbridges with main span lengths of 50, 100, and 150 m, respectively. The mode shape description is denoted by V, L, and T followed by a number which represents the vertical, lateral and torsional modes with N-half waves. The frequencies are very similar when the bridge is empty or when it is loaded with 0.2, 0.6, or 1.0 ped/m^2. For all the cases, it was observed that the differences were smaller than 4%. As described in Section 2.8, these figures also show how the frequencies are reduced when the span length increases.

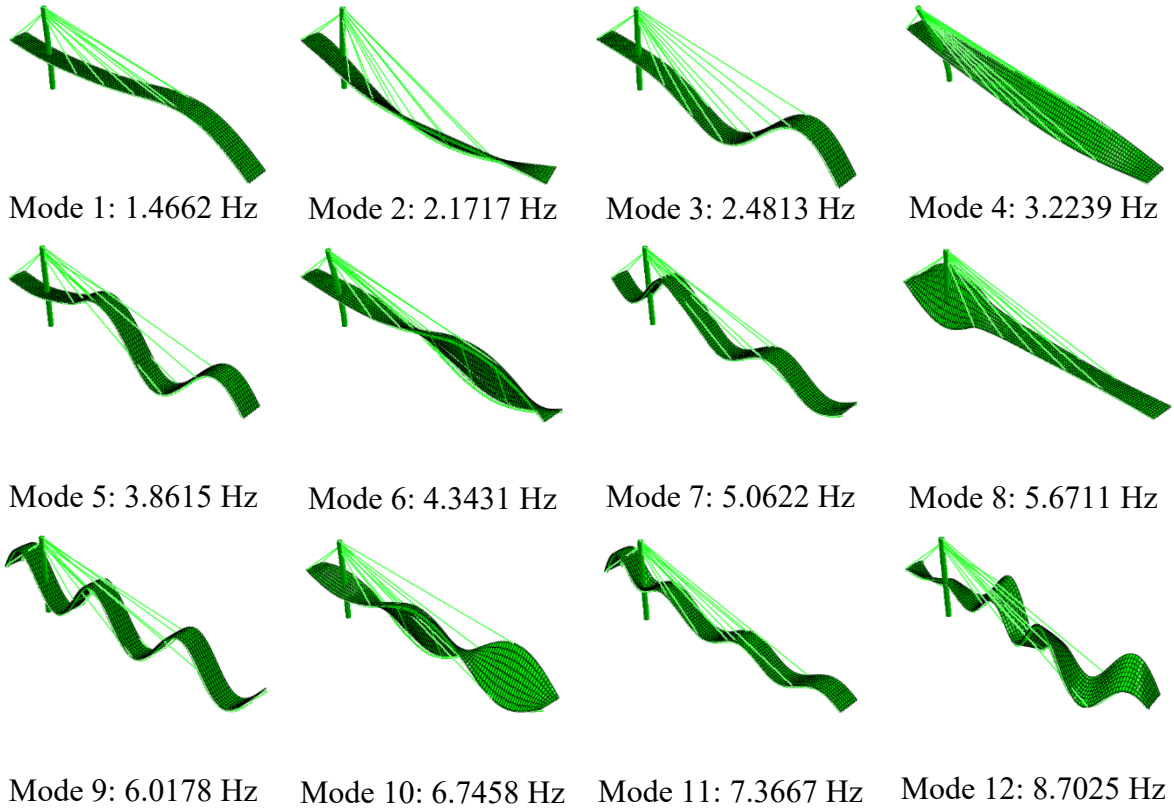


Figure 5.2 Modal frequencies of 50 m span cable-stayed footbridge with an I-shaped pylon considering a pedestrian density of 0.6 ped/m^2

Mode	Mode shape description	Footbridge empty	0.2 ped/m^2	0.6 ped/m^2	1.0 ped/m^2
1	V1	1.49	1.48	1.47	1.45
2	L1	2.18	2.16	2.17	2.15
3	V2	2.52	2.51	2.48	2.41
4	T1	3.30	3.27	3.22	3.15
5	V3	3.94	3.92	3.86	3.82
6	T2	4.40	4.37	4.34	4.28
7	V4	5.16	5.12	5.06	4.97
8	T3	5.78	5.74	5.67	5.6
9	V5	6.14	6.09	6.02	5.94
10	T4	6.85	6.81	6.75	6.66
11	V6	7.47	7.46	7.37	7.42
12	T4	8.86	8.80	8.70	8.52
Maximum differences in relation to empty structure			**0.65%**	**1.63%**	**3.01%**

Table 5.1 Frequencies (in Hz) of 50 m span cable-stayed footbridge when the bridge is empty and when it is loaded with different pedestrian densities

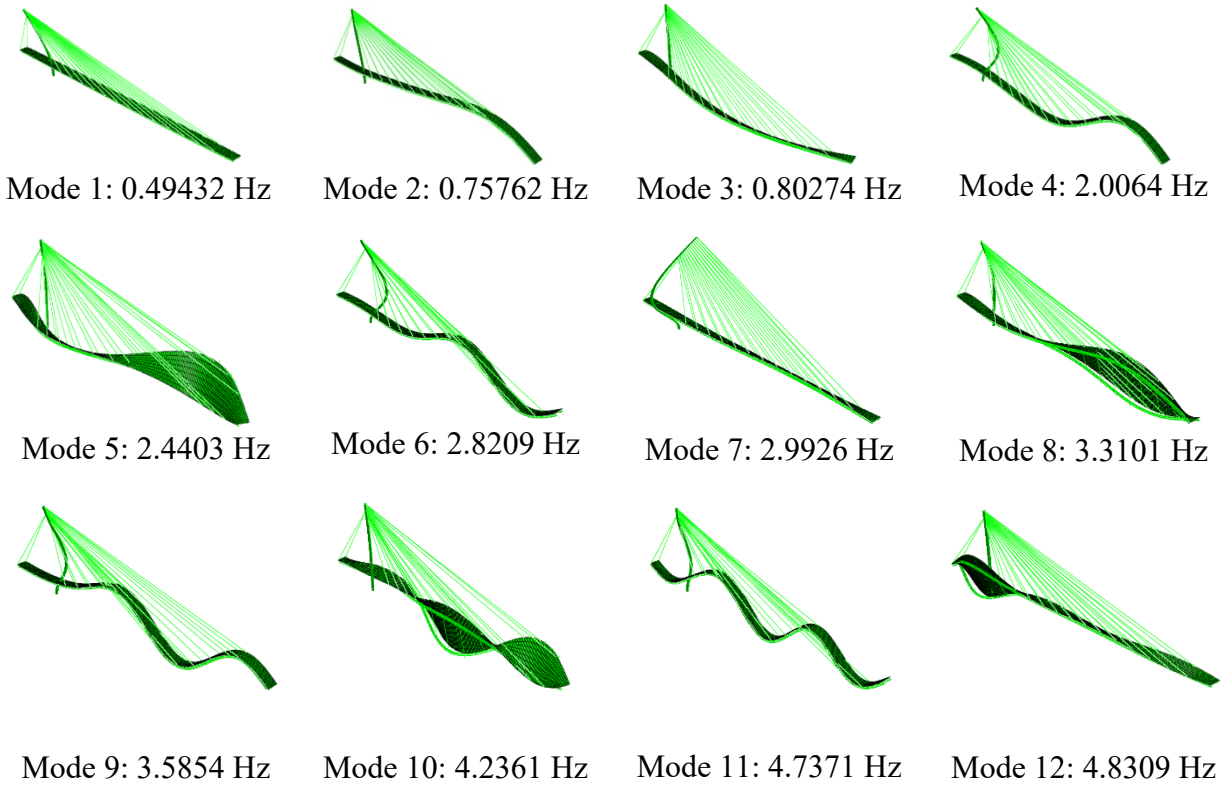


Figure 5.3 Modal frequencies of 100 m span cable-stayed footbridge with an I-shaped pylon considering a pedestrian density of 0.6 ped/m^2

Mode	Mode shape description	Footbridge empty	0.2 ped/m^2	0.6 ped/m^2	1.0 ped/m^2
1	P	0.50	0.50	0.49	0.48
2	V1	0.77	0.77	0.76	0.73
3	L1	0.80	0.80	0.80	0.80
4	V2	2.04	2.02	2.01	2.00
5	T1	2.29	2.28	2.24	2.21
6	V3	2.86	2.84	2.82	2.78
7	L3	3.05	3.04	2.99	2.94
8	T2	3.37	3.35	3.31	3.27
9	V4	3.66	3.63	3.59	3.54
10	T3	4.30	4.26	4.24	4.18
11	V5	4.80	4.80	4.72	4.77
12	T4	4.92	4.89	4.83	4.73
Maximum differences in relation to empty structure			**0.62%**	**1.70%**	**2.99%**

Table 5.2 Frequencies (in Hz) of 100 m span cable-stayed footbridge when the bridge is empty and when it is loaded with different pedestrian densities

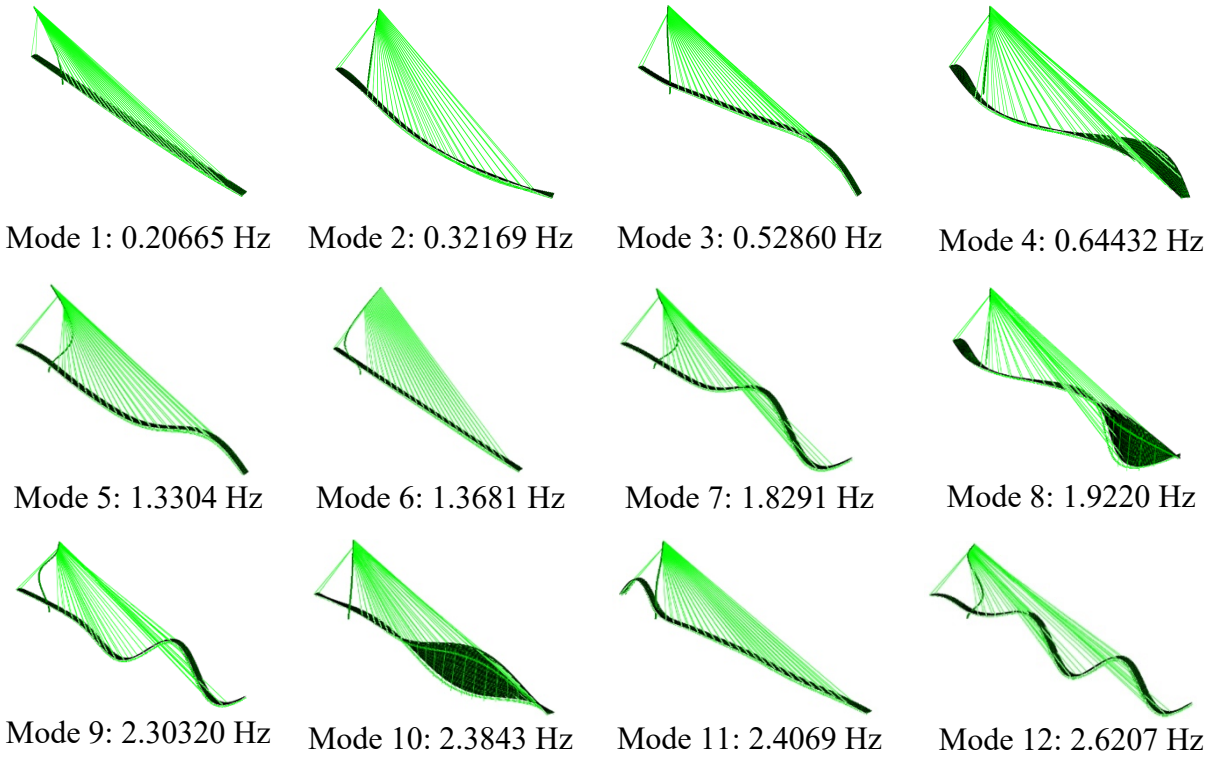


Figure 5.4 Modal frequencies of 150 m span cable-stayed footbridge with an I-shaped pylon considering a pedestrian density of 0.6 ped/m^2

Mode	Mode shape description	Footbridge empty	0.2 ped/m^2	0.6 ped/m^2	1.0 ped/m^2
1	P	0.21	0.21	0.21	0.21
2	L1	0.33	0.32	0.32	0.31
3	V1	0.53	0.52	0.53	0.53
4	T1	0.67	0.66	0.64	0.61
5	V2	1.35	1.34	1.33	1.31
6	P2	1.39	1.38	1.37	1.35
7	V3	1.86	1.85	1.83	1.80
8	T2	1.96	1.94	1.92	1.90
9	V4	2.35	2.33	2.30	2.27
10	T3	2.42	2.46	2.38	2.35
11	T4	2.44	2.43	2.40	2.43
12	V5	2.67	2.65	2.62	2.57
Maximum differences in relation to empty structure			**0.80%**	**1.66%**	**3.11%**

Table 5.3 Frequencies (in Hz) of 150 m span cable-stayed footbridge when the bridge is empty and when it is loaded with different pedestrian densities

5.2.3 Distribution of step frequencies of the pedestrians

Figure 5.5 shows the distribution of the step pedestrian frequencies for both, commuting and leisure activities. Pedestrian densities considered here are of 0.2, 0.6 and 1.0 ped/m^2, in a 50 m span cable-stayed footbridge. The distribution of step frequencies is almost identical regardless of the length of the structure, whilst the number of pedestrian changes. Guidelines such as Setra (2006) and the British code (BSI, 2008) mention that the range of the distribution of step frequencies are among 1.7 and 2.1 Hz, and 1.8 and 2.0 Hz, respectively. However, Figure 5.5 shows that the step frequencies changes depending on the pedestrian densities and the activities. The ranges suggested by these guidelines could not adequately predict the dynamic response; therefore, a more complex pedestrian model considering a wide range of step frequencies (Section 3.2) is used for the evaluation of the dynamic response. These step frequencies can lie near the structural frequencies (Figure 5.6), which can increase the dynamic response (resonance effects). The range of the vertical step frequencies is 1.3 – 2.7 and in lateral direction 0.65 to 1.35.

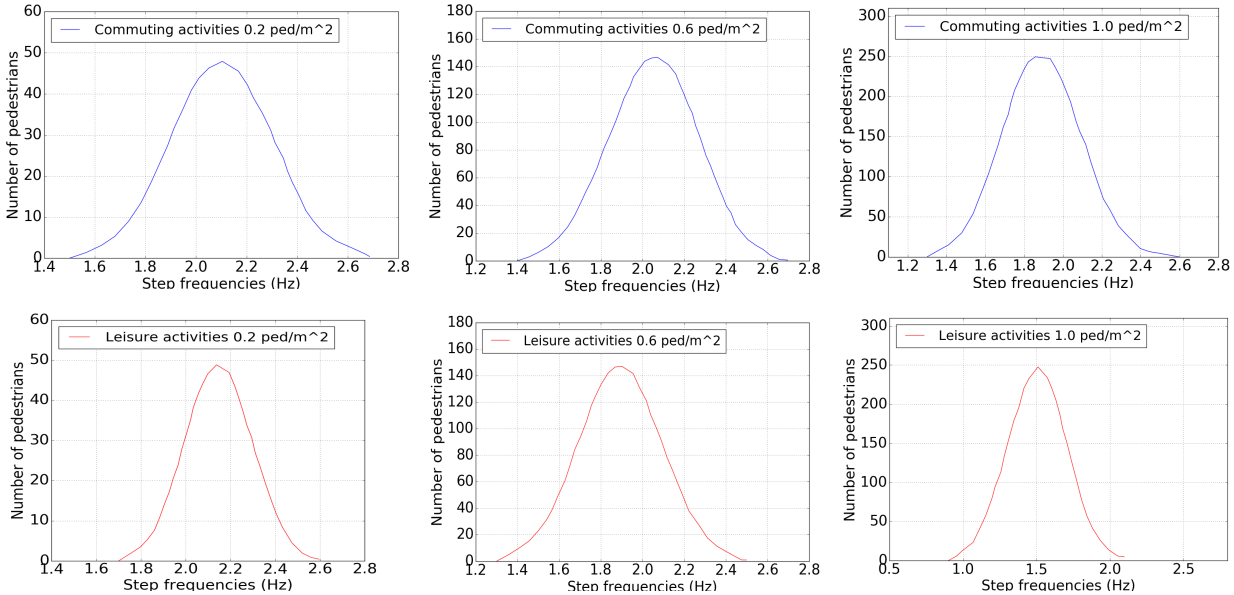


Figure 5.5 Distribution of pedestrian frequencies for commuting (blue) and leisure (red) activities for pedestrian densities of 0.2, 0.6 and 1.0 ped/m^2 for the UK population in a 50 m span cable-stayed footbridge

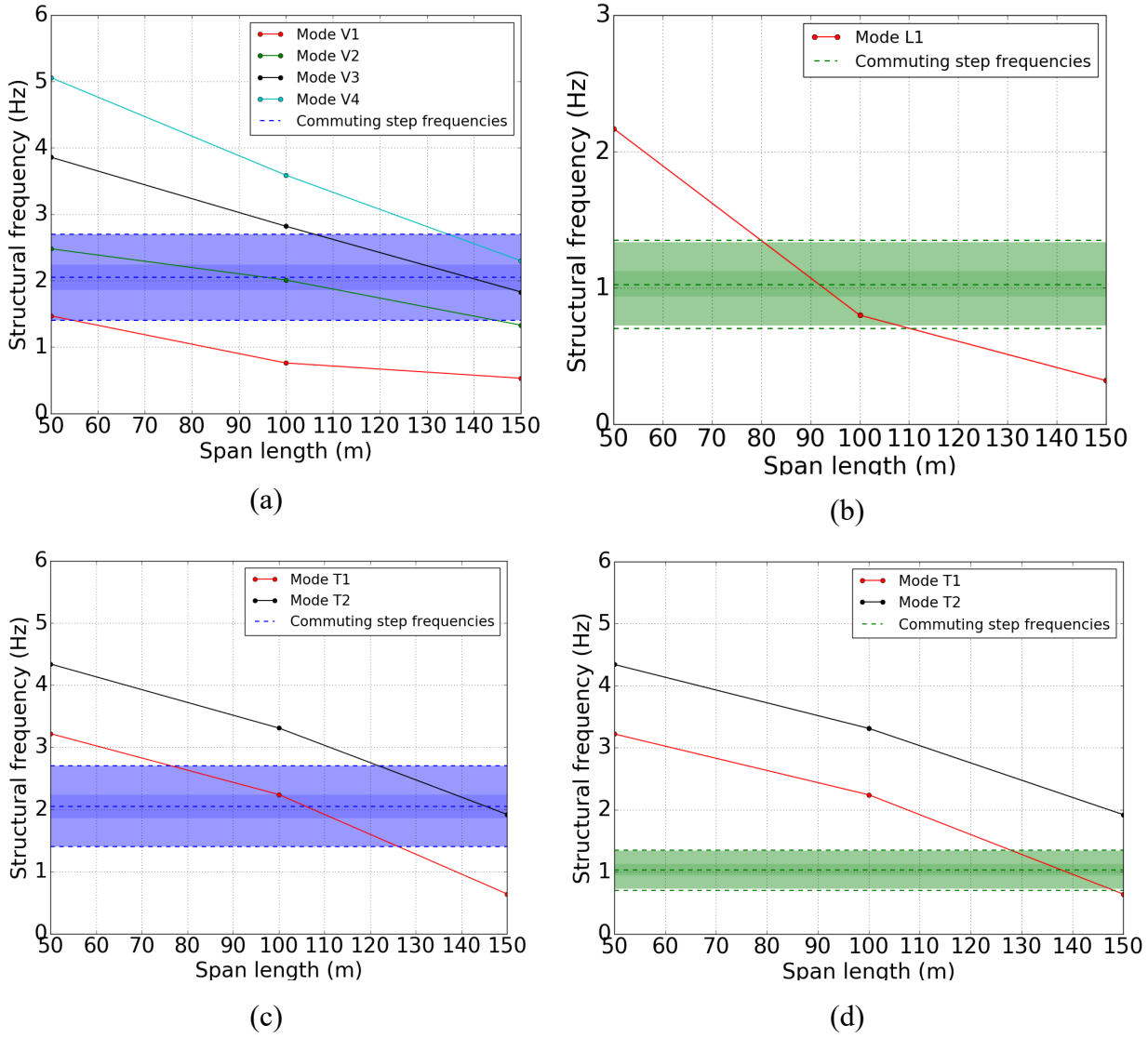


Figure 5.6 Structural (a) vertical, (b) lateral and (c and d) torsional frequencies versus the span length in cable-stayed footbridges with one tower under a pedestrian density of 0.6 ped/m^2 for commuting activities

5.3 Cable-stayed footbridges with an I-shaped pylon without tuned mass dampers

The dynamic response is checked in comparison with the comfort levels provided in codes, standards, and guidelines. This is to analyse if the serviceability criterion is fulfilled. When the serviceability criterion is not fulfilled, supplemental damping devices will be employed to evaluate the impact and efficiency of these devices in the reduction of the dynamic response. The following

sections show the accelerations of the cable-stayed footbridges without tuned mass dampers according to the three comfort levels: maximum, mean, and minimum. Cable-stayed footbridges with an I-shaped pylon were analysed under different pedestrian flow types (commuters and leisure). It also considers different pedestrian densities (0.2, 0.6, and 1.0 ped/m^2) for 50, 100 and 150 spans.

5.3.1 Parametric studies with a span length of 50 m

Figure 5.7 shows the vertical peak and 1s-RMS accelerations along the span length for commuting activities for the benchmark cable-stayed footbridge with a span length of 50 m. The comfort level corresponds to a mean comfort. According to the analysis in the frequency domain in the vertical direction in two different locations along the span length of the 50 m benchmark cable-stayed footbridge with a pedestrian density of 0.6 ped/m^2 (commuters) (Figure 5.8), the frequency of the critical mode of the footbridge is 2.48 Hz, which corresponds to the second vertical mode (see mode V2 in Table 5.1).

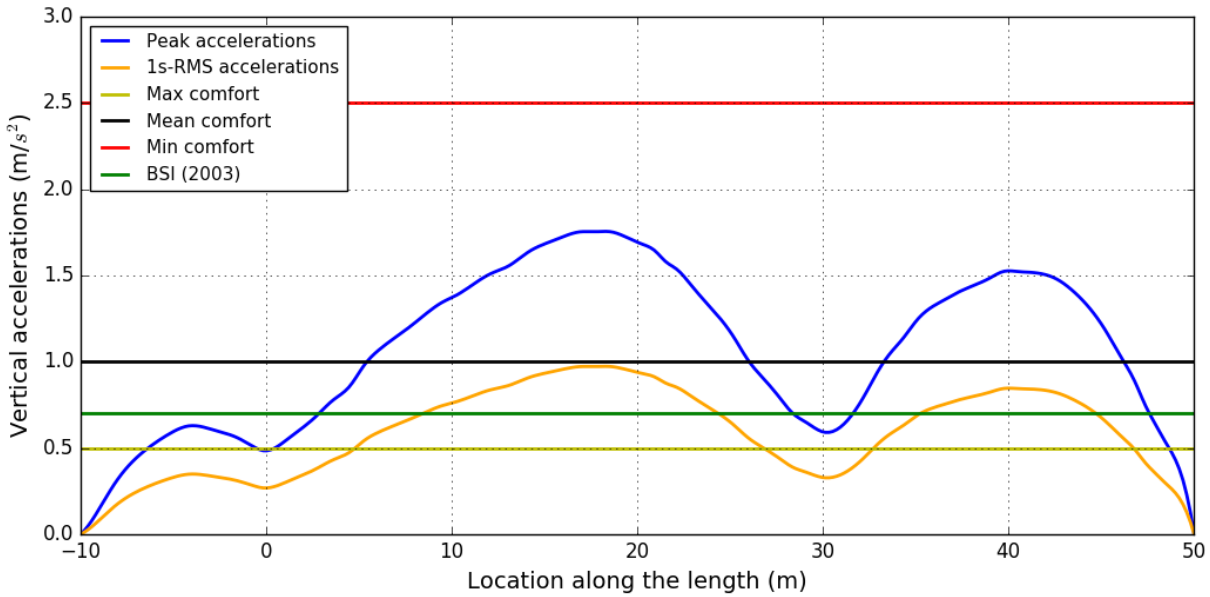


Figure 5.7 Peak and 1s-RMS vertical accelerations for a CSF of a span length of 50 m under a pedestrian density of 0.6 ped/m^2 for commuting activities

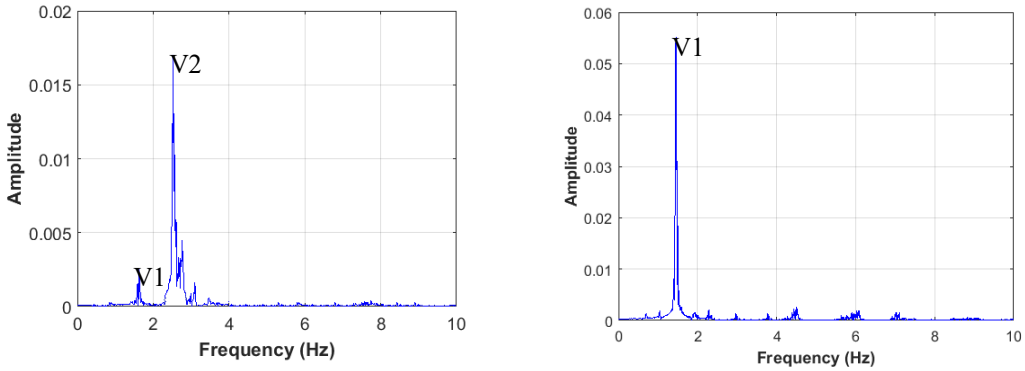


Figure 5.8 Frequency domain analysis at (a) 18.5 m, and (b) 25 m (L/2) from the pylon for a CSF of a span length of 50 m with one tower under a pedestrian density of 0.6 ped/m^2 for commuting activities in the vertical direction

Figure 5.9 shows the lateral peak and root-mean-squared (rms) accelerations along the deck, which are within the mean comfort level. The lateral accelerations are larger than the 0.1 m/s^2 limit, and pedestrians are likely to lock-in with the lateral vibration of the footbridge, inducing in turn larger lateral accelerations. According to the analysis in the frequency domain in the lateral direction for the 50 m benchmark cable-stayed footbridge with a pedestrian density of 0.6 ped/m^2 (commuters) (Figure 5.10), the frequency of the critical mode of the footbridge is 2.17 Hz, which corresponds to the first lateral mode (see mode L1 in Table 5.1). Therefore, TMDs will be implemented at the first lateral mode to mitigate the lateral accelerations and eliminate this synchronization effect.

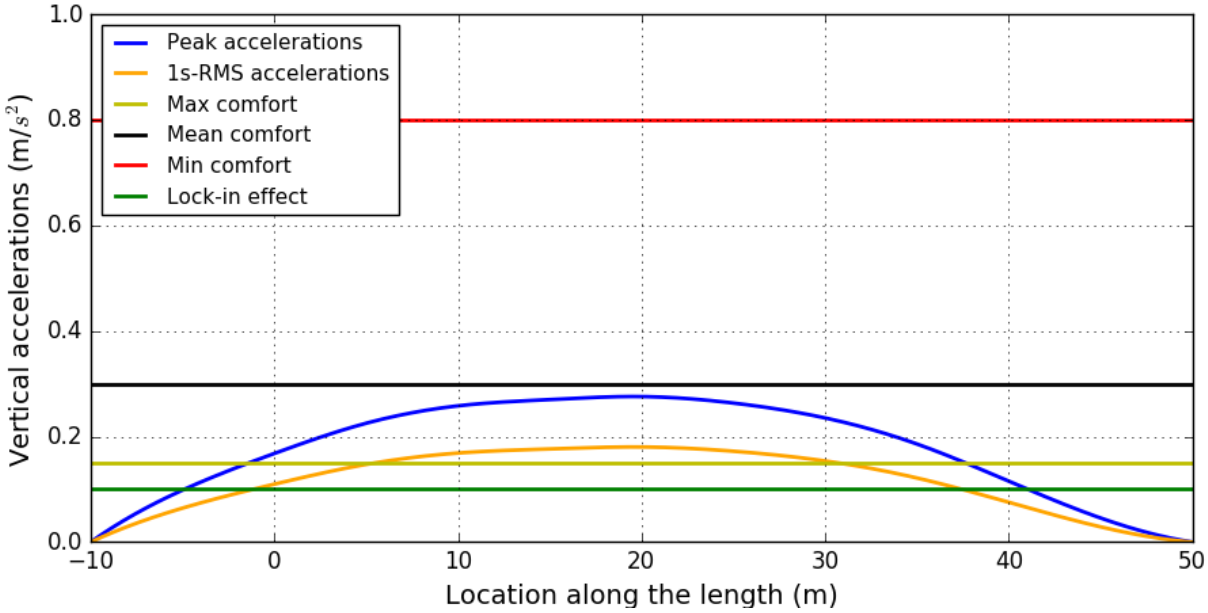
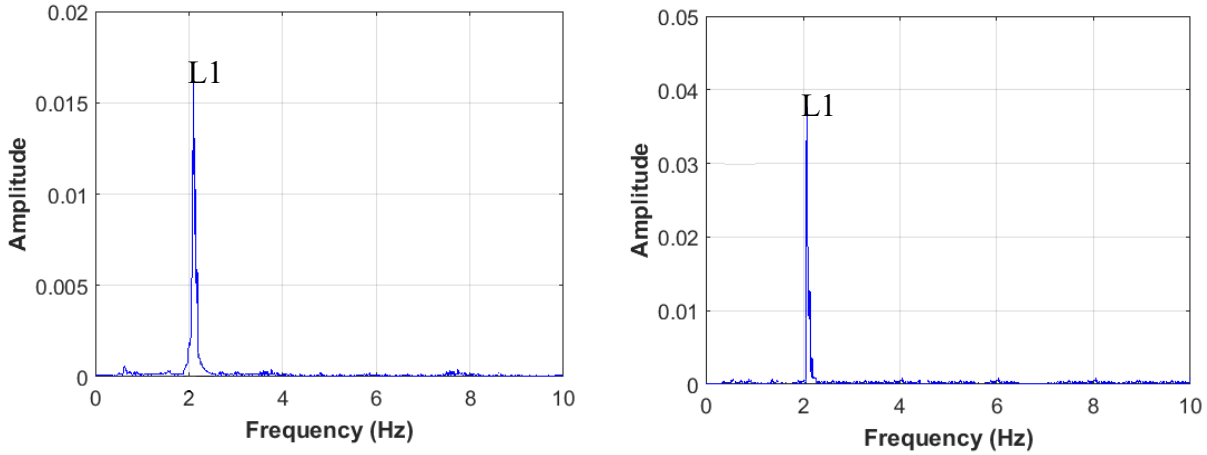


Figure 5.9 Peak and 1s-RMS lateral accelerations for a CSF of a span length of 50 m under a pedestrian density of 0.6 ped/m^2 for commuting activities



(a) (b)

Figure 5.10 Frequency domain analysis at (a) 18.5 m, and (b) 25 m (L/2) from the pylon for a CSF of a span length of 50 m with one tower under a pedestrian density of 0.6 ped/m^2 for commuting activities in the lateral direction

Figure 5.11 shows the maximum vertical and lateral peak accelerations along the length for commuting and leisure activities for the benchmark cable-stayed footbridge with a span length of

50 m. The comfort level in the vertical direction corresponds to a minimum for commuting and leisure activities for the range of the pedestrian densities, except for leisure activities with a pedestrian density of 0.2 ped/m^2, where a mean comfort was observed. In the lateral accelerations, it was identified that when the pedestrian density is 1.0 ped/m^2, the comfort level is minimum. The lateral acceleration provides a maximum and mean comfort level for pedestrian densities of 0.2 and 0.6 ped/m^2, respectively. However, in most of these cases, there is a potential risk of the pedestrians locking-in or synchronizing with the vibrations of the structure in the lateral direction, as the lateral accelerations are larger than 0.1 m/s^2.

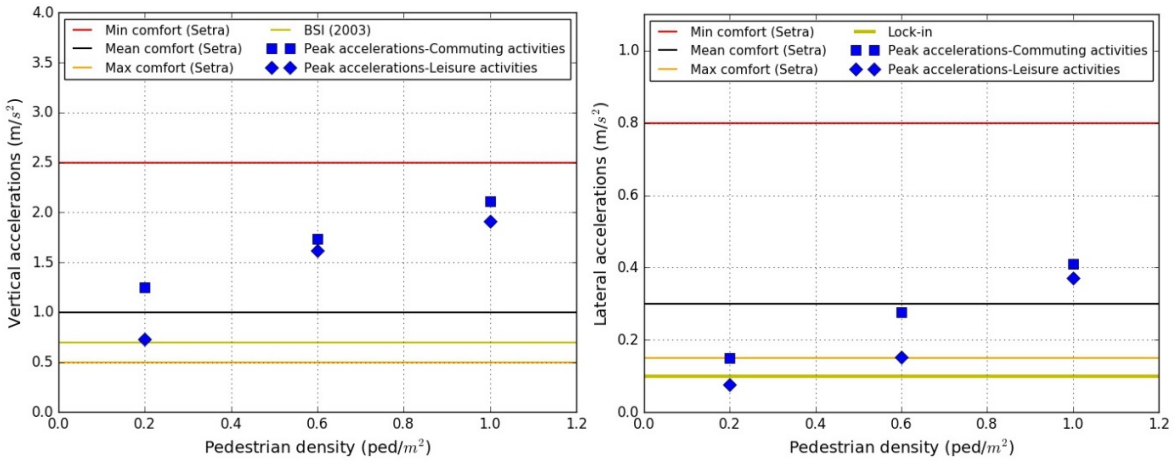


Figure 5.11 Maximum vertical and lateral peak accelerations for cable-stayed footbridges with a span length of 50 m under different pedestrian densities for commuting and leisure activities

5.3.2 Parametric studies with a span length of 100 m

Figure 5.12 shows the vertical peak and 1s-RMS acceleration along the span length for commuting activities for the benchmark cable-stayed footbridge with a span length of 100 m. The comfort level corresponds to a mean comfort. Figure 5.13 shows the frequency domain analysis for a CSF with a span length of 100 m. The frequency of the critical mode in the vertical direction of the footbridge is 2.01 Hz, which corresponds to the second vertical mode (see mode V2 in Table 5.2).

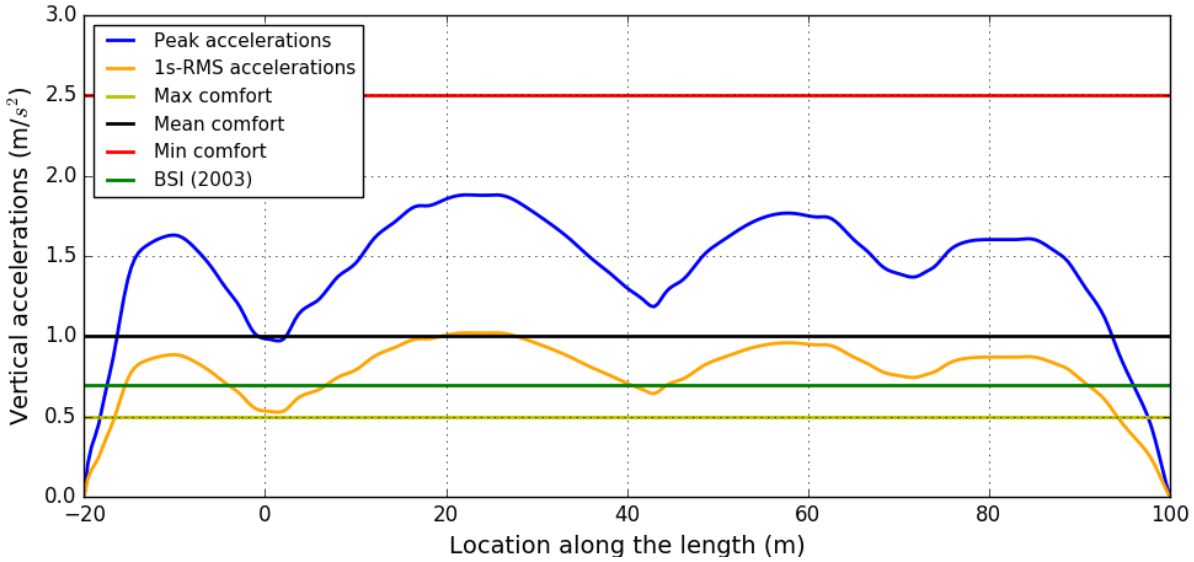
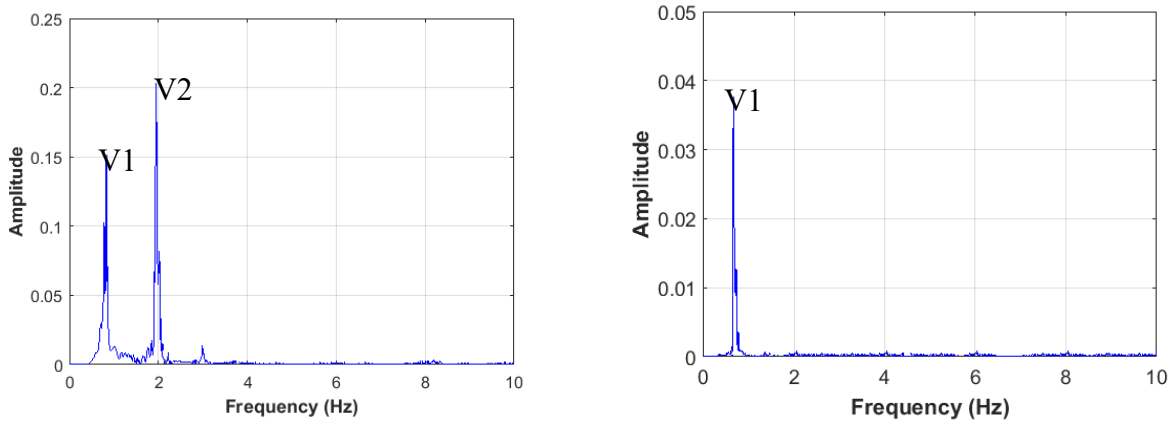


Figure 5.12 Peak and 1s-RMS vertical accelerations for a CSF of a span length of 100 m under a pedestrian density of 0.6 ped/m^2 for commuting activities



(a) (b)

Figure 5.13 Frequency domain analysis at (a) at 25 m, and (b) 50 m (L/2) from the pylon for a CSF of a span length of 100 m with one tower under a pedestrian density of 0.6 ped/m^2 for commuting activities in the vertical direction

Figure 5.14 shows the lateral accelerations along the length. Here, these accelerations correspond to a minimum comfort level, and lock-in effects are expected (generating accelerations than those

shown herein). Figure 5.15 shows the frequency domain analysis for a CSF with a span length of 100 m. The frequency of the critical mode in the lateral direction of the footbridge is 0.80 Hz, which corresponds to the first lateral mode (see mode L1 in Table 5.2).

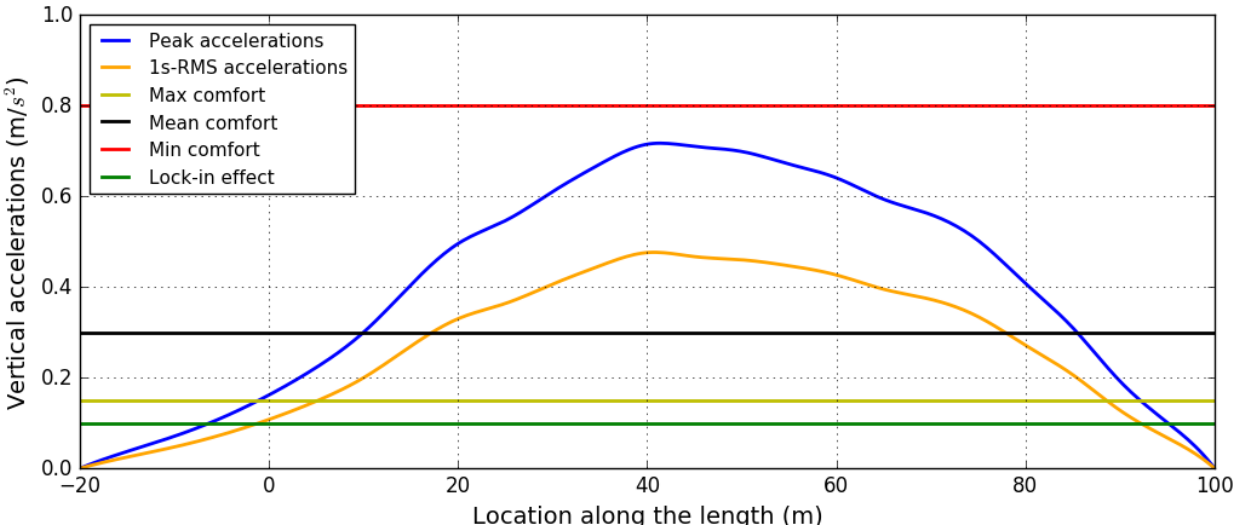
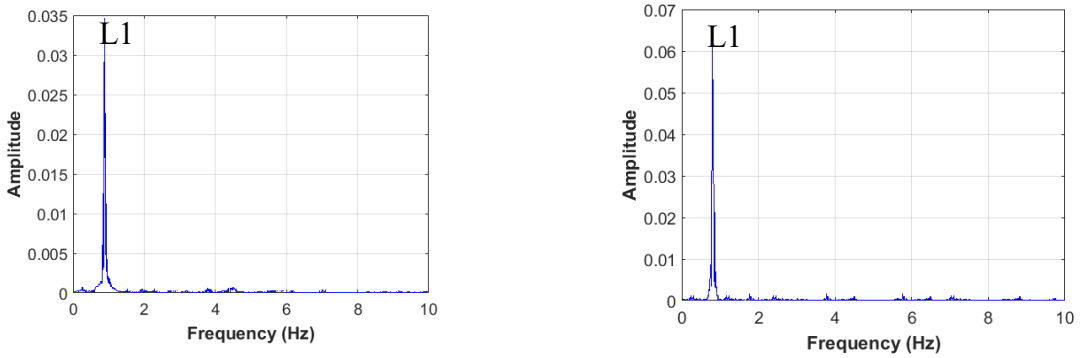


Figure 5.14 Peak and 1s-RMS lateral accelerations for a cable-stayed footbridge with a span length of 100 m under a pedestrian density of 0.6 ped/m^2 for commuting activities



(a) (b)

Figure 5.15 Frequency domain analysis at (a) at 25 m, and (b) 50 m (L/2) from the pylon in the lateral direction for a cable-stayed footbridge with a span length of 100 m with one tower under a pedestrian density of 0.6 ped/m^2 for commuting activities

Figure 5.16 shows the vertical and lateral accelerations for commuting and leisure activities for a cable-stayed footbridge with a span length of 100 m. The maximum comfort level is achieved in

the vertical direction for a pedestrian density of 0.2 ped/m^2 when leisure activities are carried out. In the lateral direction, the mean and maximum comfort level is achieved; however, as the lock-in effect is not avoided in any scenario, the response when using tuned mass dampers will be analysed in Section 5.4.

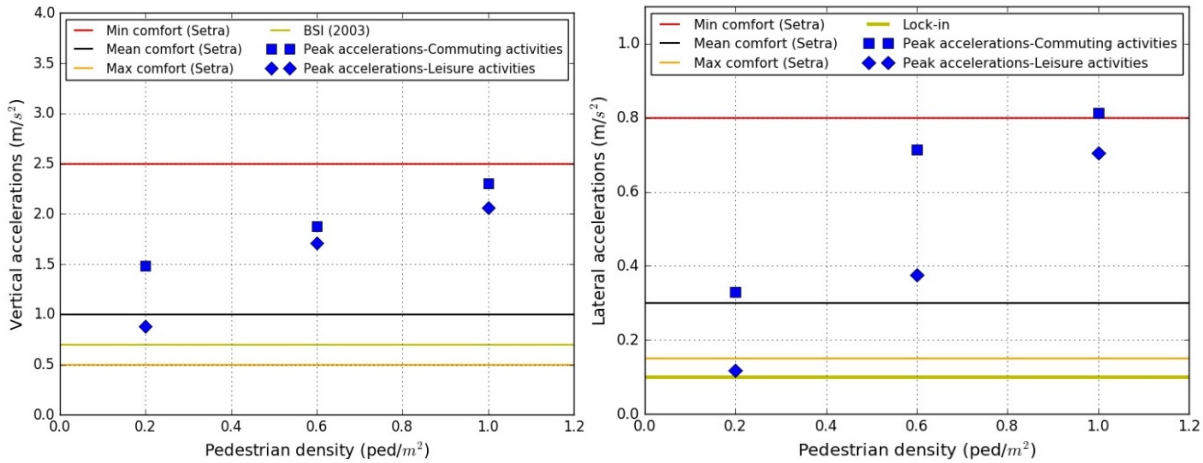


Figure 5.16 Maximum vertical and lateral peak accelerations for cable-stayed footbridges with a span length of 100 m under different pedestrian densities for commuting and leisure activities

5.3.3 Parametric studies with a span length of 150 m

Figure 5.17 shows the vertical accelerations along the length for a CSF with a span length of 150 m. These accelerations correspond to a mean comfort level. Following a similar analysis as in the previous cases, a study was made in the frequency domain for cable-stayed footbridges with a span length of 150 m. Figure 5.18 illustrates the frequency domain analysis in the vertical direction for this cable-stayed footbridge. The frequency of the critical mode in the vertical direction of the footbridge is 1.83 Hz, which corresponds to the third vertical mode (see mode V3 in Table 5.3).

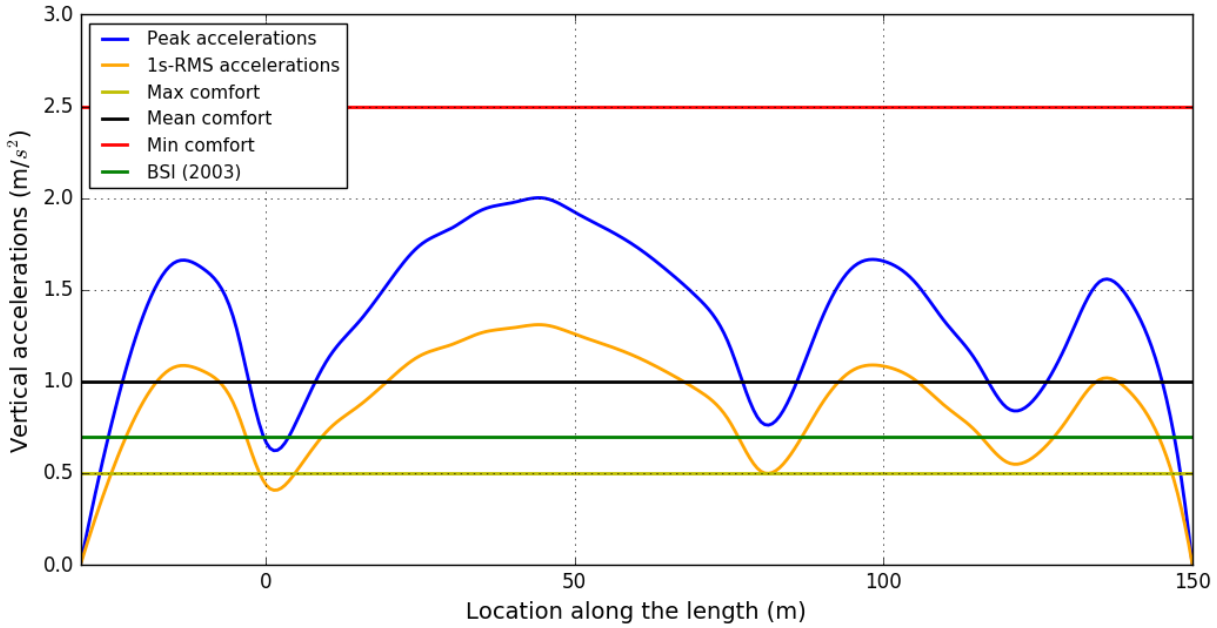
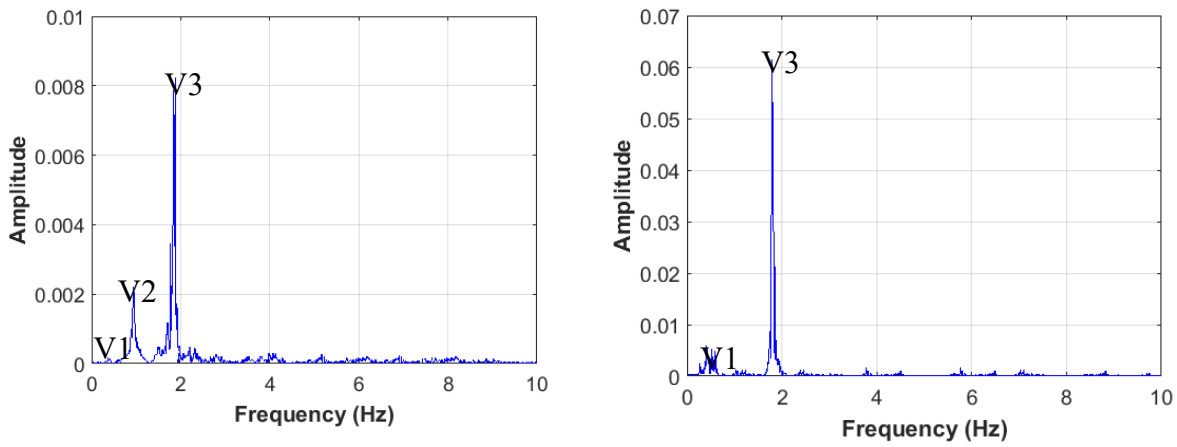


Figure 5.17 Peak and 1s-RMS vertical accelerations for a CSF of a span length of 150 m under a pedestrian density of 0.6 ped/m^2 for commuting activities



(a) (b)

Figure 5.18 Frequency domain analysis at (a) 45 m, and (b) 75 m (L/2) from the pylon in the vertical direction for a cable-stayed footbridge with a span length of 150 m with one tower under a pedestrian density of 0.6 ped/m^2 for commuting activities

Figure 5.19 shows the lateral accelerations along the length. Here, these accelerations correspond to a minimum comfort level, and lock-in effects are expected (generating accelerations than those shown herein). Figure 5.20 shows the frequency domain analysis for a CSF with a span length of

150 m. The frequency of the critical mode in the lateral direction of the footbridge corresponds to the first lateral mode (see mode L1 in Table 5.3).

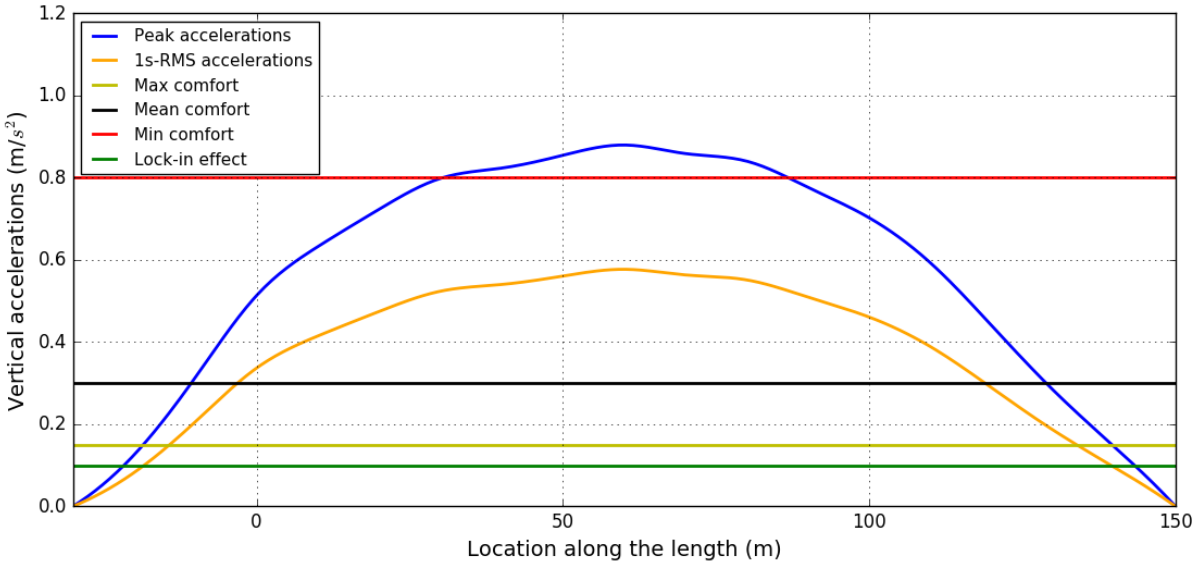
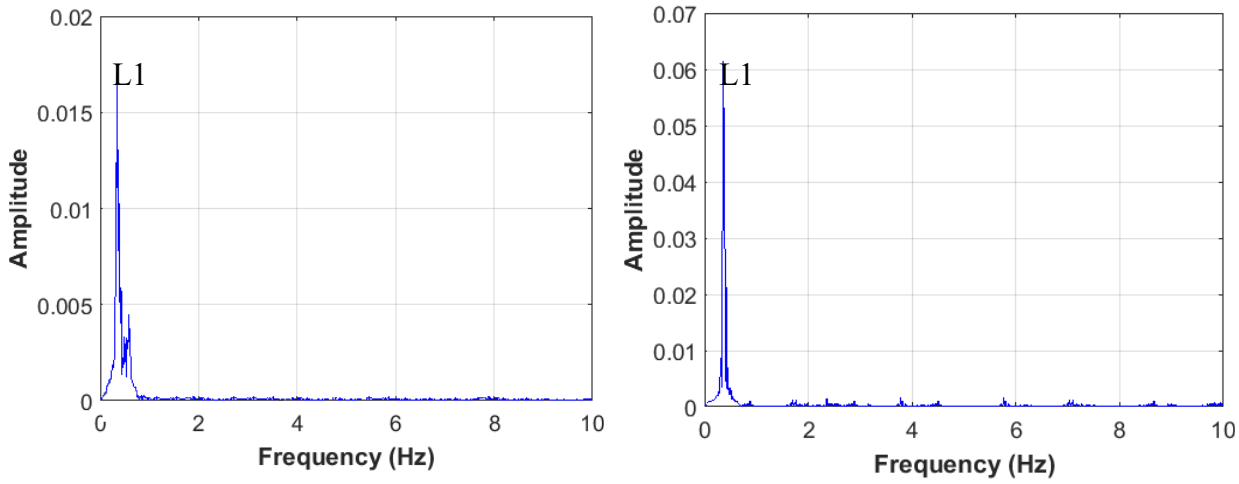


Figure 5.19 Peak and 1s-RMS lateral accelerations for a cable-stayed footbridge with a span length of 150 m under a pedestrian density of 0.6 ped/m^2 for commuting activities



(a) (b)

Figure 5.20 Frequency domain analysis at (a) 45 m and, (b) 75 m (L/2) from the pylon in the lateral direction for a cable-stayed footbridge with a span length of 150 m with one tower under a pedestrian density of 0.6 ped/m^2 for commuting activities

The accelerations in the vertical and lateral direction for commuting and leisure activities are shown in Figure 5.21. The maximum comfort level is not achieved in any of these cases, and the lock-in effect is not avoided in the lateral direction. From Figure 5.21, it is clear that there is a very strong dependence upon both the pedestrian densities and pedestrian activities, in vertical and lateral accelerations. Based on the strong dependence to these parameters, any design recommendations, even at preliminary stage, should considers the pedestrian densities and pedestrian activities.

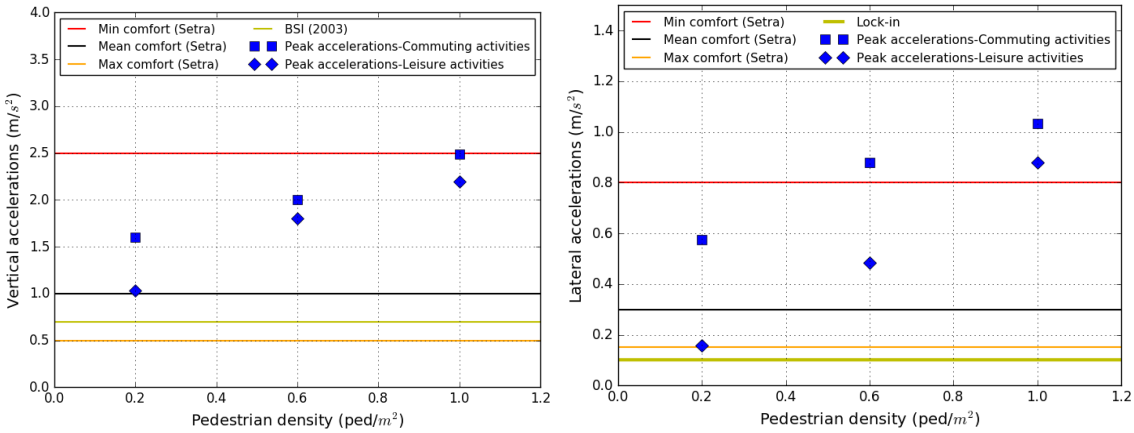


Figure 5.21 Maximum vertical and lateral peak accelerations for cable-stayed footbridges with a span length of 150 m under different pedestrian densities for commuting and leisure activities

5.4 Cable-stayed footbridges with an I-shaped pylon with tuned mass dampers

5.4.1 Parametric studies for 50 m span cable-stayed footbridges

After carrying out an initial dynamic analysis, shown in Section 5.3.1, several cases where the accelerations exceeded the vibration limits were identified. As a result, on further analysis, the impact of employing one or multiple TMDs to mitigate the human-induced vibrations is investigated. Following a systematic procedure to include tuned mass dampers (Section 3.7), the structural modal frequencies and the modal shapes were obtained, with the aim to identify potential critical modes which can be in the range of pedestrian vertical and lateral frequencies. In addition,

the frequency domain of the accelerations to be mitigated was obtained, in order to identify the frequencies of the modes with larger contributions in the response.

Figure 5.22 and Figure 5.23 show the peak vertical and lateral accelerations. These figures consider tuned mass dampers for a cable-stayed footbridge with a span length of 50 m under a pedestrian density of 0.6 ped/m^2. The TMD in the vertical direction is located at 18 m from the pylon (antinode of the vertical mode 2), and in the lateral location is located at 20 m from the pylon (antinode of the lateral mode 1). The vertical accelerations correspond to a mean comfort with a TMD mass ratio of 0.05, and to maximum comfort with a TMD mass ratio of 0.07. The lateral accelerations correspond to a maximum comfort avoiding the lock-in effect with a TMD mass ratio of 0.03 (Figure 5.23).

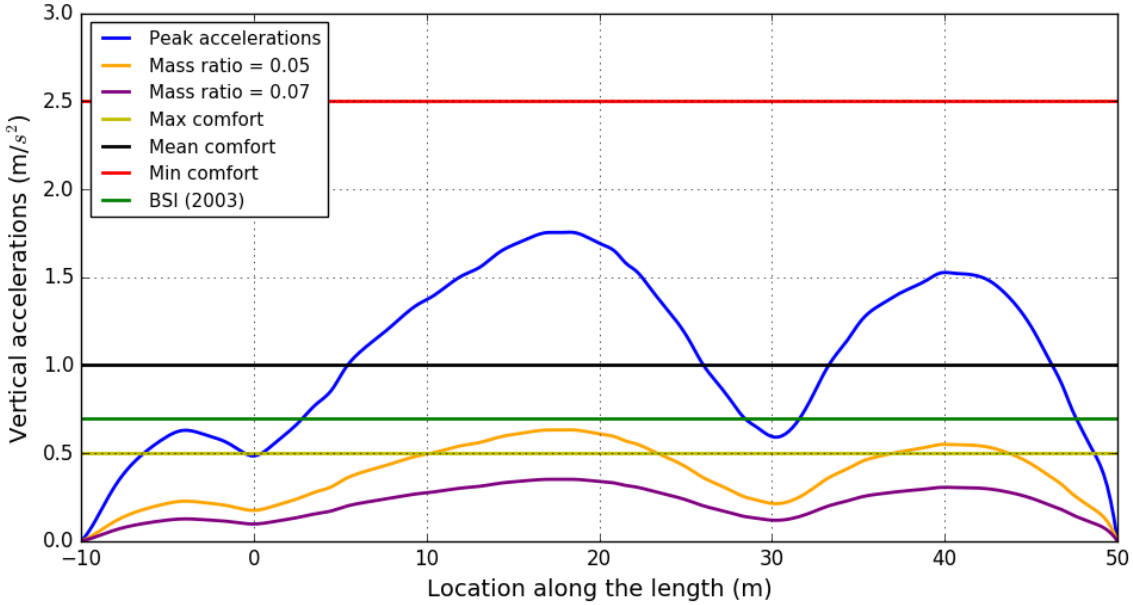


Figure 5.22 Peak vertical accelerations for a cable-stayed footbridge with a span length of 50 m under a pedestrian density of 0.6 ped/m^2 when different TMD mass ratios (0.05 and 0.07) are employed for commuting activities

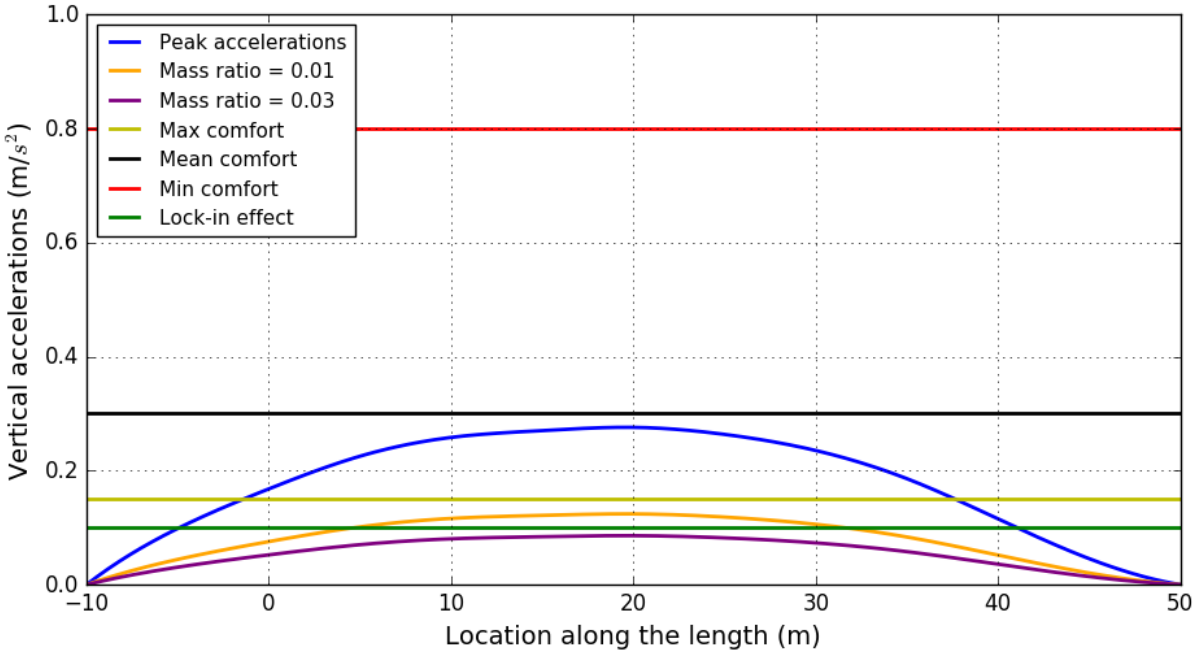
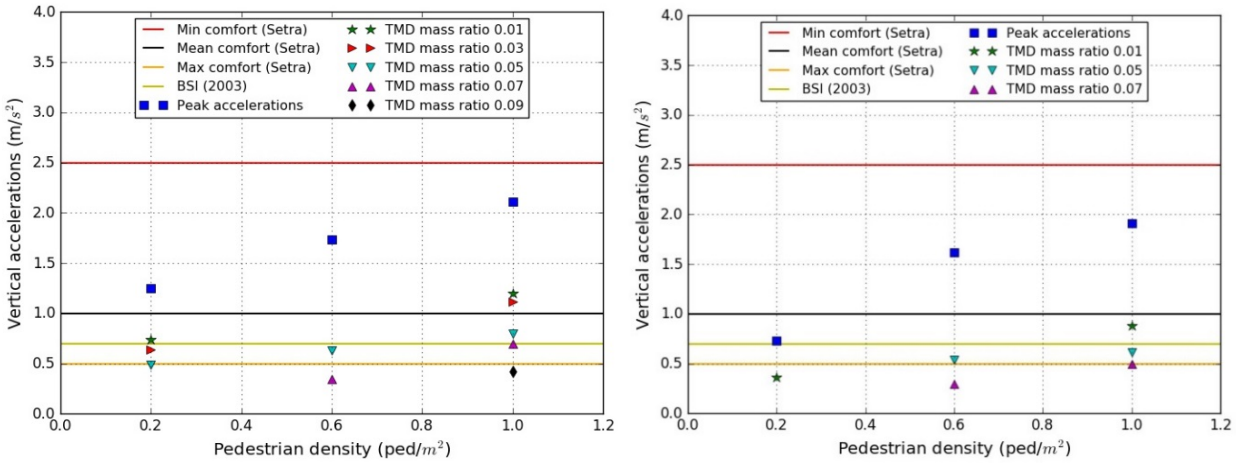


Figure 5.23 Peak lateral accelerations for a cable-stayed footbridge with a span length of 50 m under a pedestrian density of 0.6 ped/m^2 when different TMD mass ratios (0.01 and 0.03) are employed for commuting activities

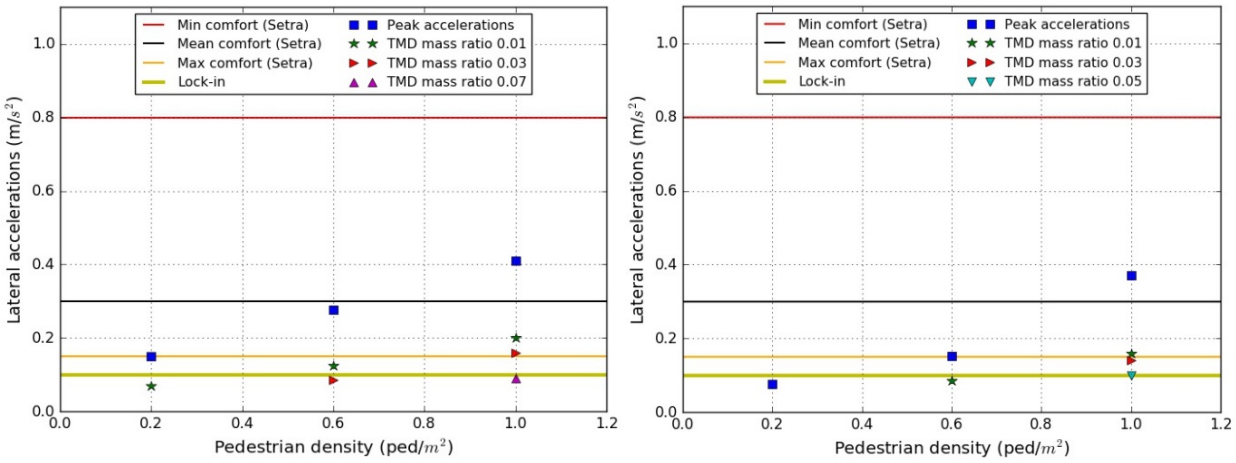
Figure 5.24 displays the required TMD mass ratio according to the different comfort levels, and for different design scenarios (pedestrian densities) in the vertical direction. By implementing a TMD with a mass ratio ranging from 0.01 to 0.09, the accelerations were significantly reduced (TMD efficiencies up to 75 %). The mean comfort level for commuting activities in the vertical direction can be achieved with a TMD mass ratio ranging from 0.01 to 0.07, depending on the pedestrian densities. In case a maximum comfort level in commuting activities is required, the necessary TMD mass ratio varies from 0.05 to 0.09. For leisure activities, the TMD mass ratio to achieve the mean comfort level varies from 0.01 to 0.05, and to achieve the maximum comfort level, it varies from 0.01 to 0.07, depending on the pedestrian densities.



(a) (b)

Figure 5.24 Peak vertical accelerations for cable-stayed footbridges with a span length of 50 m under pedestrian densities of 0.2, 0.6 and 1.0 ped/m^2 when different TMD mass ratios are employed for (a) commuting and (b) leisure activities

To avoid the lock-in effect for commuting activities, the range for the TMD mass ratio varies from 0.01 to 0.07, depending on the pedestrian densities (Figure 5.25 (a)). For a pedestrian density of 0.2 ped/m^2 for leisure activities, the maximum comfort is achieved, and the lock-in is avoided without the necessity of supplemental damping devices. A tuned mass damper with a mass ratio ranging from 0.01 to 0.05 is required to avoid the lock-in effect for CSF under pedestrian densities of 0.6 and 1.0 ped/m^2 (Figure 5.25 (b)).



(a) (b)

Figure 5.25 Peak lateral accelerations for cable-stayed footbridges with a span length of 50 m under pedestrian densities of 0.2, 0.6 and 1.0 ped/m^2 when different TMD mass ratios are employed for (a) commuting and (b) leisure activities

5.4.1.1 Location of the TMD

The maximum reduction of the dynamic response in the vertical direction is achieved when the tuned mass damper is located at 28.0 m ± 11 % from the left support (see Table 5.4 and red dots # 3 to 7 in Figure 5.26). This location corresponds to the maximum nodal coordinates of those modal shapes with a larger contribution (see mode V2 in Table 5.1). By locating the TMD towards the support sections, there is no benefit in reducing the accelerations, as the TMD is not tuned to any frequency (Table 5.4).

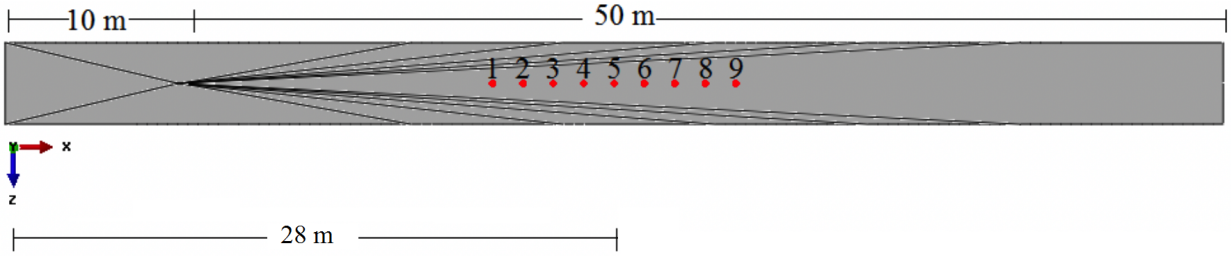


Figure 5.26 Plan view for a CSF with a span length of 50 with one tower where the red dot #5 corresponds to the nodal coordinates of those modal shapes with a larger contribution (V2) in vertical direction located at 28 m from the left support

TMD according Figure 5.26	Location of the TMD from the left support(m)	Accelerations with TMD	TMD efficiency (%)
1	22.0	1.178	32%
2	23.5	0.864	50%
3	**25.0**	**0.465**	**73%**
4	**26.5**	**0.374**	**78%**
5	**28.0**	**0.347**	**80%**
6	**29.5**	**0.363**	**79%**
7	**31.0**	**0.496**	**71%**
8	32.5	0.932	46%
9	34.0	1.246	28%

Table 5.4 Peak vertical accelerations and TMD efficiency along the deck for a CSF with a span length of 50 m with one tower under pedestrian densities of 0.6 ped/m^2 for commuting activities when a TMD (μ= 0.07) is located at different abscises along the length

On the contrary, regarding the dynamic response in the lateral direction, the maximum reduction is achieved when the tuned mass damper is located at 25.0 m ± 5 % from the pylon (see Table 5.5 and red dots # 4, 5, and 6 in Figure 5.27). This location corresponds to the maximum nodal coordinates for the modal shape whose frequency has the largest amplitude in the representation of the frequency domain (see mode L1 in Table 5.1). If the TMD is located towards the support sections, the lock-in effect is not avoided (accelerations > 0.10 m/s^2).

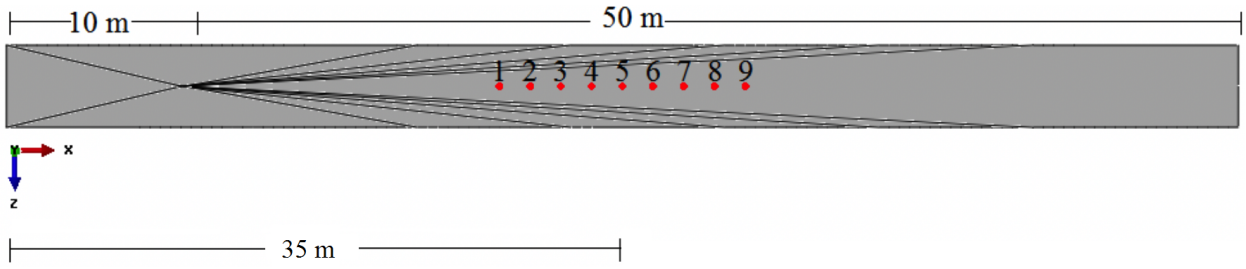


Figure 5.27 Plan view for a CSF with a span length of 50 m with one tower where the red dot # 5 corresponds to the nodal coordinates of those modal shapes with a larger contribution in the lateral direction (L1) located at 25 m (L/2) from the pylon

TMD according Figure 5.27	Location of the TMD from the pylon (m)	Accelerations with TMD	TMD efficiency (%)
1	15.0	0.219	21%
2	17.5	0.192	30%
3	20.0	0.141	51%
4	**22.5**	**0.101**	**63%**
5	**25.0**	**0.086**	**69%**
6	**30.0**	**0.102**	**63%**
7	30.0	0.142	51%
8	32.5	0.192	30%
9	35.0	0.218	21%

Table 5.5 Peak lateral accelerations and TMD efficiency along the deck for a CSF with a span length of 50 m with one tower under pedestrian densities of 0.6 ped/m^2 for commuting activities when a TMD (μ= 0.03) is located at different abscises along the length

5.4.1.2 Reduction of internal forces when a TMD is deployed

By implementing a TMD, the accelerations were significantly reduced (maximum efficiency = 80%). In addition, the TMD also reduces the internal forces by mitigating the dynamic response

(see Figure 5.28). The dynamic amplification factor (DAF) of the sagging and hogging moment are 2.18 and 1.96, respectively. After the implementation of a TMD, the DAFs are reduced to 1.63 and 1.47, respectively. Sagging bending moments (generating tensile stresses at the soffit) are positive. The static response is the envelope of a static load with the same magnitude as the pedestrian weight that could act at any location along the length.

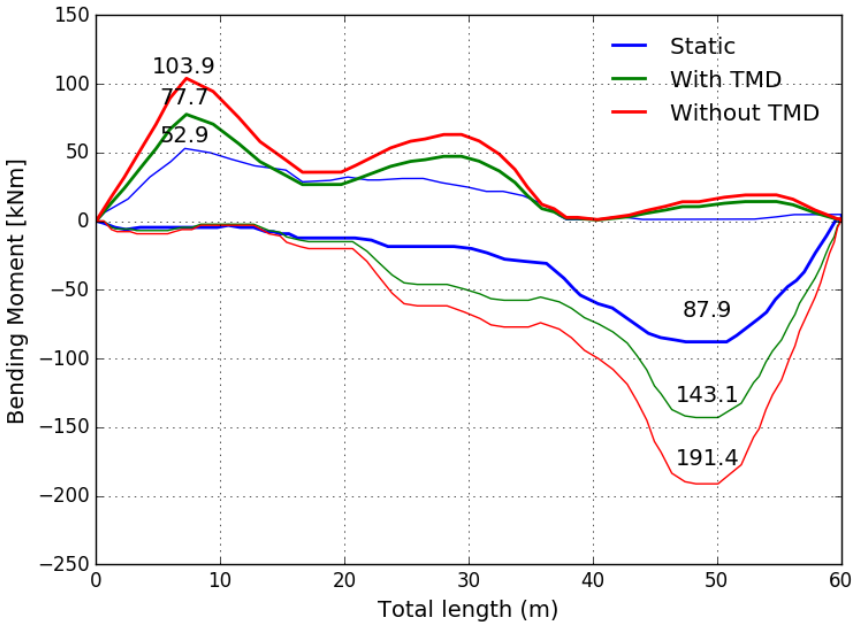


Figure 5.28 Sagging and hogging bending moments along the length before and after a TMD (μ= 0.05) was employed at 18 m from the pylon in a 50 m span cable-stayed footbridge considering a pedestrian density of 0.6 ped/m^2 for commuting activities

5.4.2 Parametric studies for 100 m span cable-stayed footbridges

After checking that the cable-stayed footbridge with a span length of 100 m does not achieve the maximum comfort without supplemental damping devices, the effect of employing tuned mass dampers in different locations with different properties is studied herein. In some cases, due to geometrical constraints, more than a single TMD may be required. Therefore, analyses with more than one tuned mass dampers are considered.

Table 5.6 shows the different cases using tuned mass dampers that were analysed in the cable-stayed footbridge with a span length of 100 m. The analysis of these cases provided a better

understanding of the TMD's efficiency depending on its location. Figure 5.29 shows the vertical modes #1 and #2 and where the maximum displacement (the location where the dampers were placed) is at each mode.

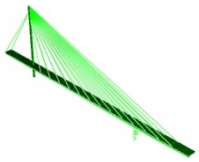
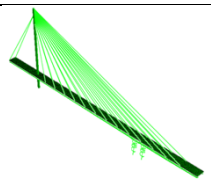
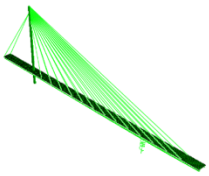
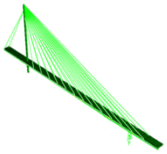
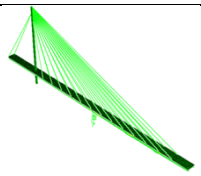
		
Case a: 1 TMD at mode V1 located at 71.5 m from the pylon ($\mu = 0.10$) TMD efficiency = 37%	**Case b:** 2 TMDs (1 TMD at mode V1 and the second one 1.0 m distance from mode V1) ($\mu = 0.05$ each one) TMD efficiency = 40%	**Case c:** 2 TMDs in V2 located at 81.5 m from the pylon (max displacement) ($\mu = 0.10$ each one) TMD efficiency = 84 %
		
Case d: 1 TMD at mode V2 located at 81.5 m from the pylon (max displacement) ($\mu = 0.10$) TMD efficiency = 75%	**Case e:** 1 TMD at mode V2 located at 41.5 m from the pylon (not max displacement) ($\mu = 0.10$) TMD efficiency = 52%	

Table 5.6 Location where the tuned mass dampers were employed for the parametric studies for a CSF with a span length of 100 m

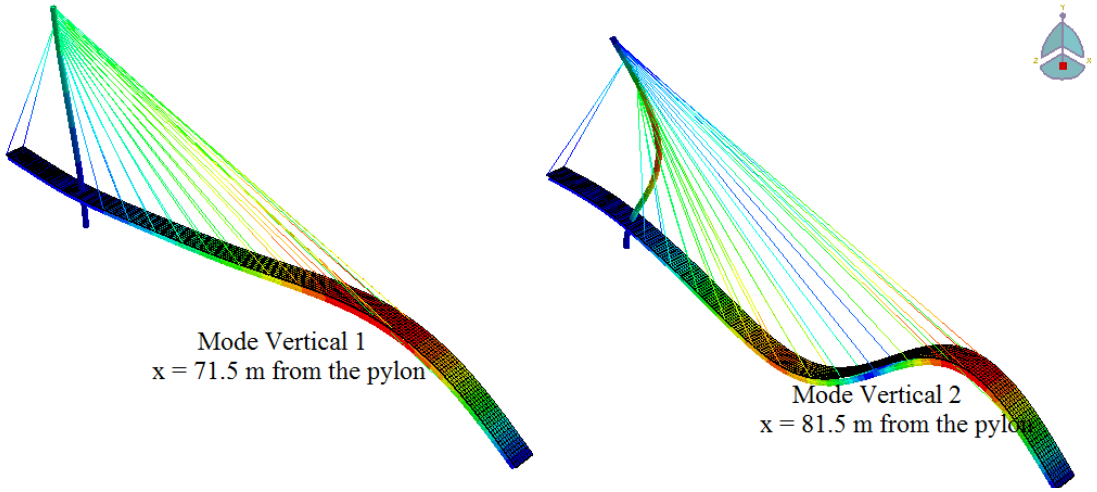


Figure 5.29 Vertical modes 1 and 2 for a cable-stayed footbridge with a span length of 100 m

Figure 5.30 shows the effect of the TMDs in the reduction of the dynamic response. The largest TMD efficiencies are achieved when one TMD (case d, 75% TMD efficiency) or two TMDs (case c, 84% TMD efficiency) are employed at the maximum nodal coordinates for the modal shape that dominates the response, i.e., the second vertical mode. If the TMD is not located at this position the efficiency decreases significantly (TMD efficiency of 37% in case a). One TMD at the maximum displacement of Mode 2 (case d) is enough to achieve the maximum comfort level. Therefore, there is no point in doing overdesign (case c). Moreover, the reduction in accelerations is around 9% for larger increments of mass in the TMD (from case d to case c).

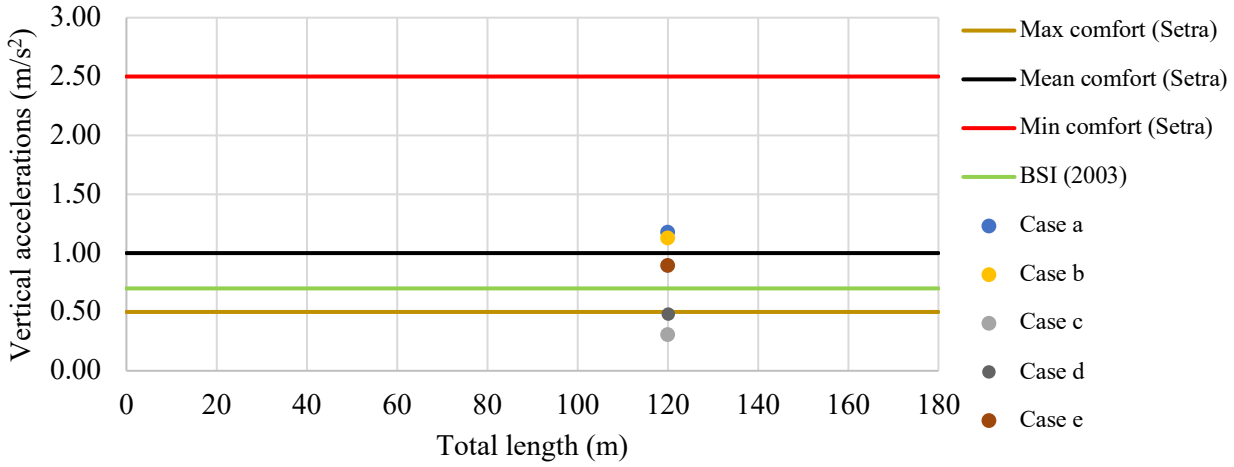
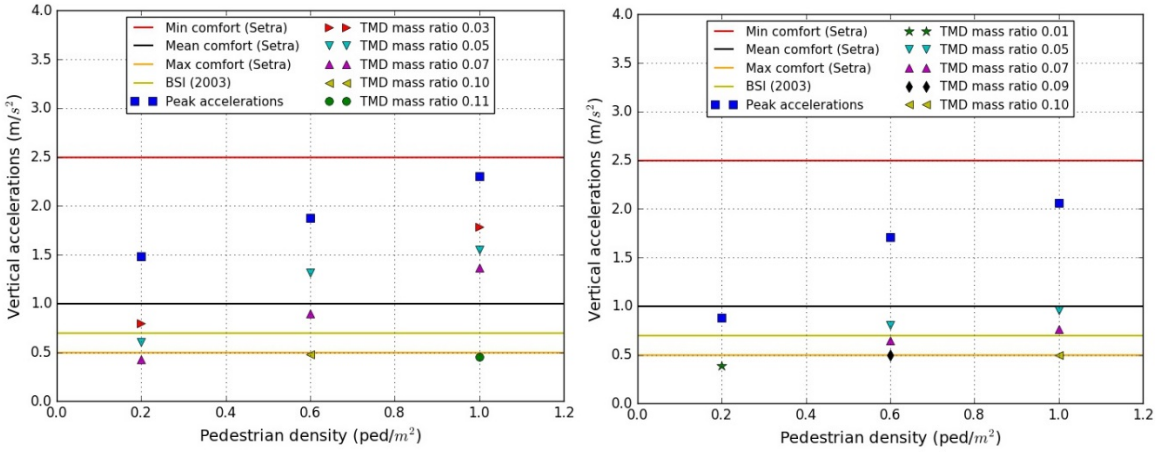


Figure 5.30 Maximum vertical peak accelerations for a CSF with a span length of 100 m when a TMD was employed in different locations based on Table 5.6 for a pedestrian density of 0.6 ped/m^2 for commuting activities

This part will show design recommendations in footbridges with a span length of 100 m under commuting and leisure activities for different pedestrian densities with and without tuned mass dampers. Figure 5.31 shows the different TMD mass ratios that are required in the dampers to achieve minimum, mean, or maximum comfort level. For commuting and leisure activities in the vertical direction, a TMD with a mass ratio ranging from 0.03 up to 0.11 is required to achieve the maximum comfort level.

In the cases where the TMD mass is bigger than 6000 kg, the effect of splitting it into two (halving the mass m, the stiffness k and the damping c, and maintaining the TMD frequency and damping ratio) is analysed. For preliminary designs, the technical sheet of the TMDs of Maurer Sohne claims that up to 5000 kg is the most common TMD mass. Afterwards, the effect is analysed in terms of the reduction of the accelerations and efficiency of the devices. For commuting activities under a pedestrian density of 0.2 ped/m^2, the efficiency whilst using two TMDs (each one of a mass of 4000 kg) was 72%. The acceleration obtained was 0.415 m/s^2. For a pedestrian density of 0.6 ped/m^2, the TMD efficiency was 76 %, which gives an acceleration of 0.460 m/s^2, and for a pedestrian density of 1.0 ped/m^2, the vertical acceleration was 0.4375 m/s^2, which means a TMD efficiency of 81 %. In the case of the cable-stayed footbridge under a pedestrian density of 1.0

ped/m^2 in leisure activities, the mass of the TMD was split into two dampers of 5000 kg each one. In this case, the vertical acceleration was 0.473 m/s^2, which means a TMD efficiency of 77%. The average of the differences before and after split the mass is less than 1% (distance between dampers 0.5 m). These vertical accelerations show the significant effect that TMD or TMDs can have on the reduction of the acceleration. Therefore, the use of damper devices where the maximum comfort level is not achieved is relevant for a preliminary design for cable-stayed footbridges. This analysis confirms that the TMD efficiency is not affected when a single TMD is split into two when these devices are installed at the location of the maximum displacement amplitude.

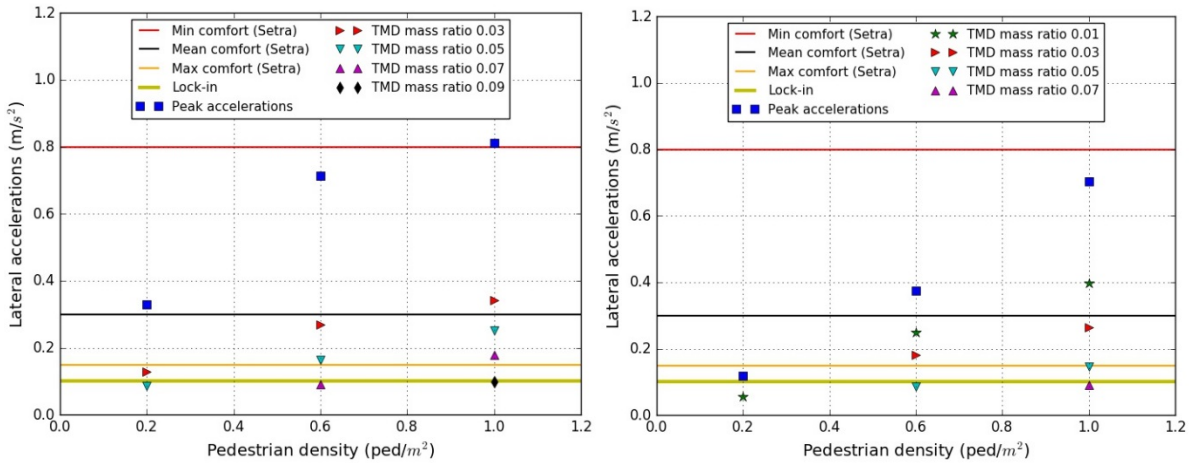


(a) (b)

Figure 5.31 Peak vertical accelerations for cable-stayed footbridges with a span length of 100 m under pedestrian densities of 0.2, 0.6 and 1.0 ped/m^2 when different TMD mass ratios are employed for (a) commuting and (b) leisure activities

Based on the evaluation of the lateral accelerations, the lock-in effect is not avoided for all the cases, when no supplemental damping is provided. Figure 5.32 shows the required TMD mass ratio to avoid this effect (from 0.05 to 0.09 for commuting activities, and from 0.01 to 0.07 for leisure activities). It is pertinent to increase the TMD mass ratio when the pedestrian density increases. The average of the TMD efficiency is 78%. For commuting and leisure activities, the mass of the damper is less than 6000 kg. Hence, it is not required to analyse the effect of splitting this mass, except for the case when the bridge is under a pedestrian density of 1.0 ped/m^2 for commuting activities which corresponds to a minimum comfort level. In this case, the effect of splitting one damper of 8000 kg in two dampers of 4000 kg each one was analysed. After

performing this analysis, the maximum peak lateral accelerations drop from 0.813 to 0.098 m/s^2 when is employed one TMD (μ=0.09), and to 0.099 m/s^2 when two TMDs (μ=0.045 each) are employed. Therefore, it is possible to locate one or two dampers to assure a large efficiency of the TMD system (TMD efficiencies up to 88%) and the fulfilment of the maximum comfort level whilst avoiding the lock-in effect.

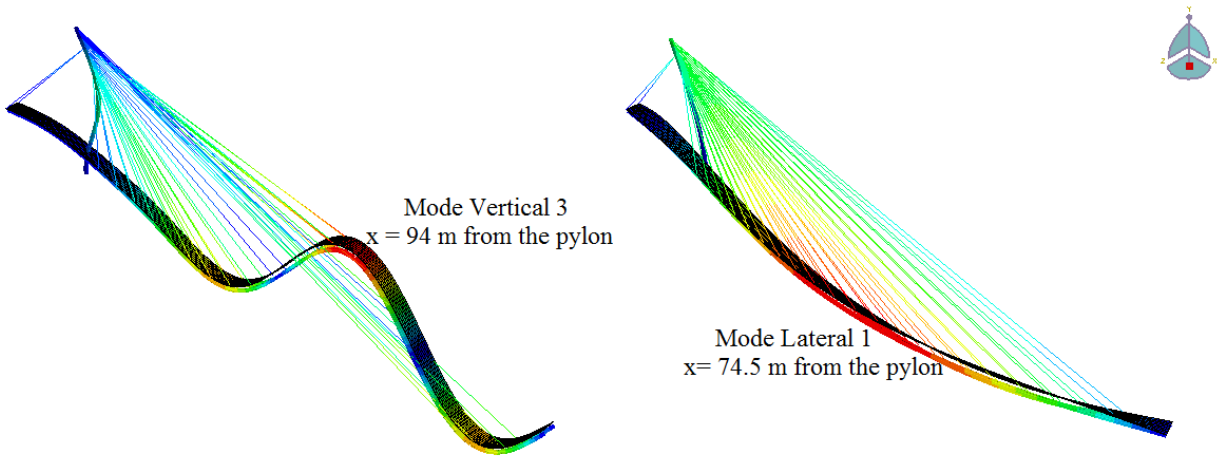


(a) (b)

Figure 5.32 Peak lateral accelerations for cable-stayed footbridges with a span length of 100 m under pedestrian densities of 0.2, 0.6 and 1.0 ped/m^2 when different TMD mass ratios are employed for (a) commuting and (b) leisure activities

5.4.3 Parametric studies for 150 m span cable-stayed footbridges

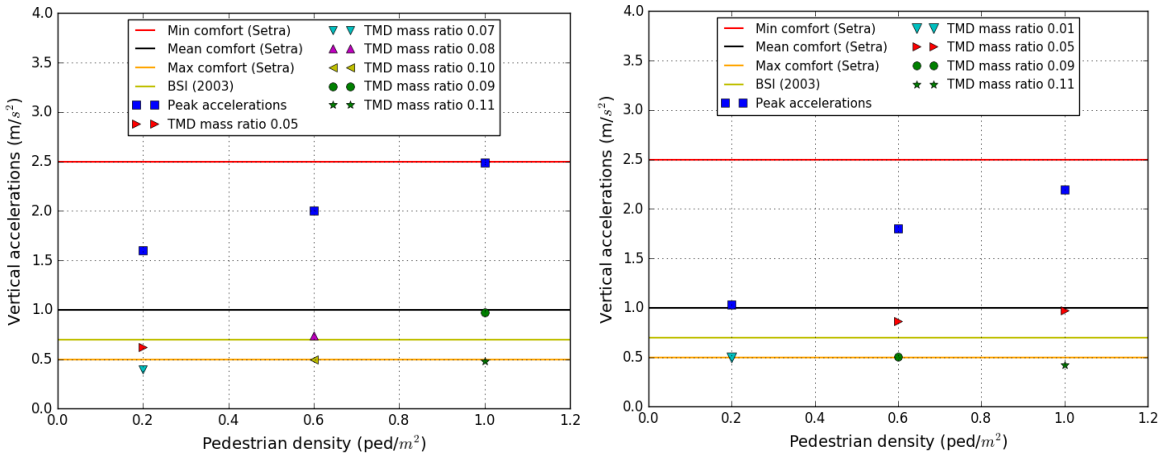
Following the same pattern of the previous cases, tuned mass dampers were employed to investigate if the accelerations exceeded the vibration limits when the span length is 150 m. The TMD location was obtained after the frequency domain analysis (Section 5.3.3). Figure 5.33 shows the location where the TMDs were employed in the vertical and lateral direction.



(a) (b)

Figure 5.33 Maximum nodal coordinates for modal shapes with a larger contribution in the critical acceleration where the TMDs were located in (a) vertical and (b) lateral direction

Figure 5.34 shows the vertical acceleration after the TMD was placed for different activities and pedestrian densities. Tuned mass dampers with different mass ratios were evaluated when the span length is 150 m for commuting and leisure activities to give design recommendations. Different TMD mass ratios are required to achieve the mean and maximum comfort level for commuting and leisure activities. The mean comfort level for commuting activities can be achieved with a TMD mass ratio of 0.05, 0.08, and 0.09 for 0.2, 0.6, and 1.0 ped/m^2, respectively. If the maximum comfort level is required, the necessary TMD mass ratio is 0.07, 0.10, and 0.11 depending on the pedestrian densities. The maximum comfort level can be achieved with a TMD mass ratio of 0.01 for leisure activities under a pedestrian density of 0.2 ped/m^2. For 0.6 ped/m^2, it is required a TMD mass ratio of 0.05 and 0.09 if a mean and maximum comfort level is required, respectively. On top of this, for a pedestrian density of 1.0 ped/m^2, a TMD with a mass ratio of 0.05 and 0.11 is required to achieve mean and maximum comfort level. The TMD efficiency in the mitigation of vibration under pedestrian loads is approximately 73% for commuting and leisure activities.



(a) (b)

Figure 5.34 Peak vertical accelerations for cable-stayed footbridges with a span length of 150 m under pedestrian densities of 0.2, 0.6 and 1.0 ped/m^2 when different TMD mass ratios are employed for (a) commuting and (b) leisure activities

Tuned mass dampers were evaluated for lateral accelerations to provide maximum comfort level according to the Setra guideline whilst the lock-in effect is being avoided (Figure 5.35). The TMD mass ratio varies from 0.06 to 0.10 for commuting activities and from 0.01 to 0.08 for leisure activities. For the latter, the TMD mass ratio is smaller than for the commuting activities because the accelerations that are obtained for commuting activities are higher in comparison to the other activities. For instance, when the pedestrian density is 0.6 ped/m^2, the maximum peak lateral acceleration for commuting activities is 0.879 m/s^2. Regarding leisure activities, this value is 0.484 m/s^2 without tuned mass dampers. After employing these devices, the TMD mass ratio to achieve the maximum comfort level avoiding the lock-in effect is 0.08 for commuting and 0.06 for leisure activities.

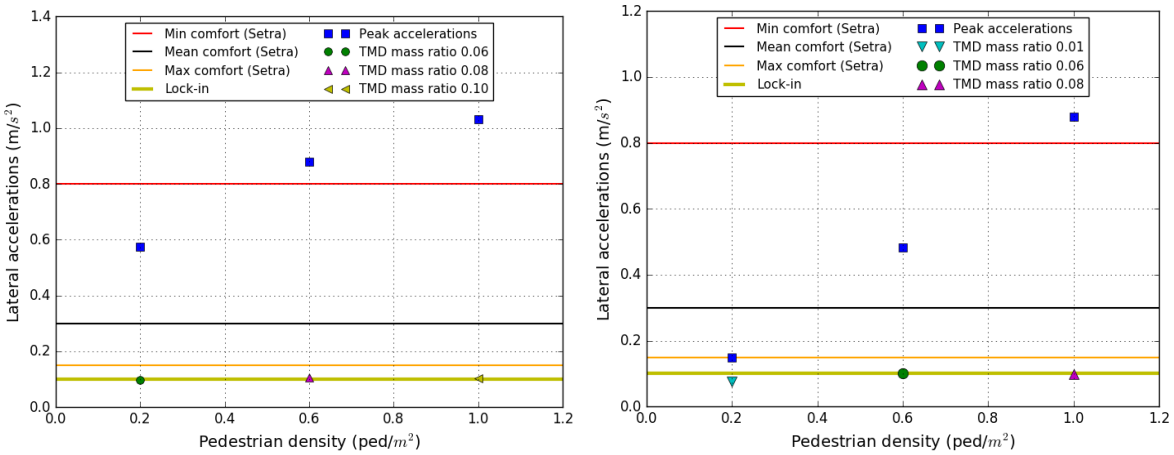


Figure 5.35 Peak lateral accelerations for cable-stayed footbridges with a span length of 150 m under pedestrian densities of 0.2, 0.6 and 1.0 ped/m^2 when different TMD mass ratios are employed for (a) commuting and (b) leisure activities

5.5 Parametric analysis with H-, and A-shaped pylons

This section shows a parametric study of the dynamic response in the vertical and lateral direction for cable-stayed footbridges with different pylon shapes (H, and A). These pylon shapes are very common, because of structural and aesthetical considerations. Ramos-Moreno (2015) demonstrated that changing the pylon shape affected the dynamic response in the vertical and lateral direction, without tuned mass dampers. In the vertical direction the additional contribution of torsional modes T1 and T2 for the H-shaped pylons gives a larger dynamic response in comparison of the I- and A-shaped pylon (Figure 5.36 (c)). On the contrary, in the lateral direction, there is more risk of a resonance effect occurs when an I- and A-shaped pylon are employed (Figure 5.36 (b)). Therefore, in this direction, the dynamic response decreases with an H-shaped pylon. However, the dynamic response using an A- or an H- shaped pylon does not fulfil the serviceability criteria. Thus, the relevance of these shapes combining the implementation of tuned mass dampers in the dynamic response is analysed herein.

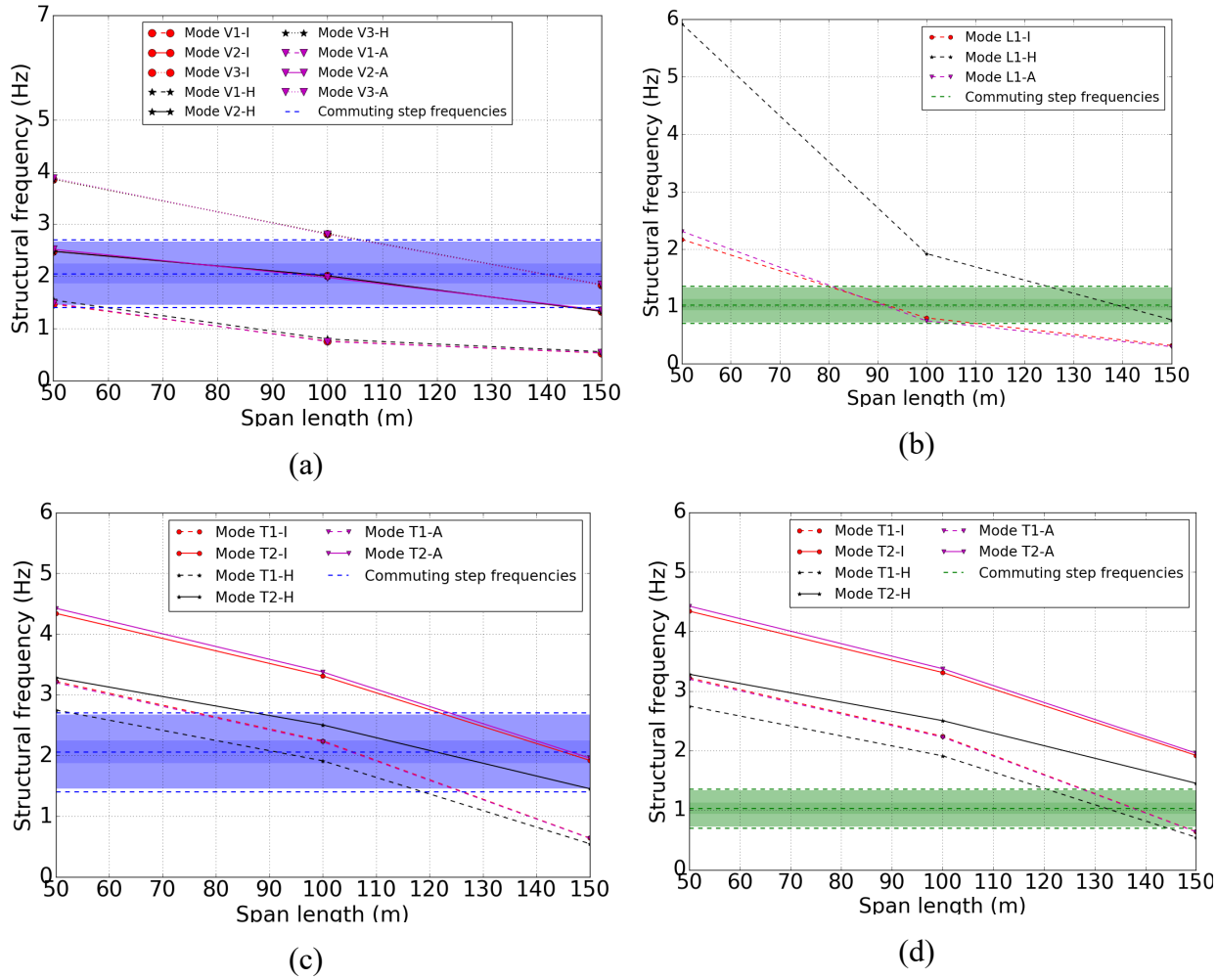


Figure 5.36 Structural (a) vertical, (b) lateral and (c and d) torsional frequencies versus the span length in cable-stayed footbridges with different pylon's shapes under a pedestrian density of 0.6 ped/m^2 for commuting activities

5.5.1 Dynamic response in the vertical direction

From Figure 5.37 to Figure 5.39, the vertical accelerations in the deck are presented for different pylon shapes. A wide range of vertical accelerations was obtained according to the different pedestrian densities (0.2, 0.6, 1.0 ped/m^2) and pedestrian activities (commuting and leisure). It is worth to mention that the accelerations for the I- and A-shaped pylon are very similar with differences smaller than 12% leading to minimum comfort levels. The H-shaped pylon leads to larger vertical accelerations, with the minimum comfort being exceeded for pedestrian densities

of 1.0 ped/m^2. These results show a clear tendency in terms of performance, with the I-shaped pylons better than the A-shaped pylons, and these in turn better than the H- shaped pylons. Nevertheless, the difference in the accelerations is not large enough to have implications in terms of comfort levels. Moreover, similar tuned mass dampers that were employed for an I-shaped pylon (Figure 5.24, Figure 5.31, and Figure 5.34) can be used herein for a cable-stayed footbridge with an A-shaped pylon to achieve mean and maximum comfort. However, these dampers are not large enough to minimize the dynamic response when an H-shaped pylon is employed. To achieve the mean and maximum comfort level for a CSF with a span length of 50 m using an I-shaped pylon, TMD mass ratios ranging from 0.02 to 0.11, and from 0.01 to 0.09 for commuting and leisure activities are required, respectively. For a span length of 100 m, TMD mass ratios ranging from 0.04 to 0.12 (commuting activities) and from 0.02 to 0.11 (leisure activities) are required. When the footbridge has a span length of 150 m, TMD mass ratios ranging from 0.08 to 0.13 for commuting activities and from 0.02 to 0.12 for leisure activities are required.

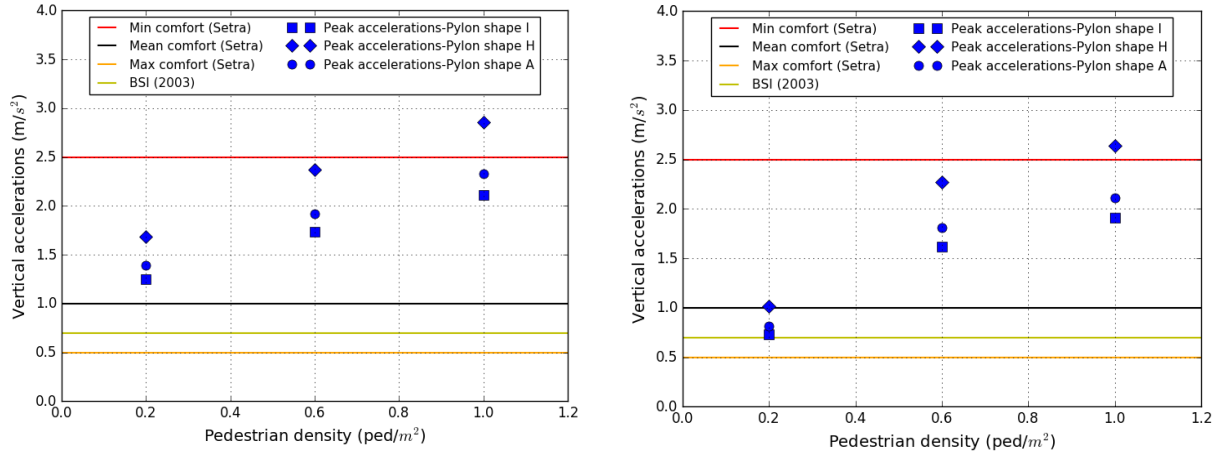
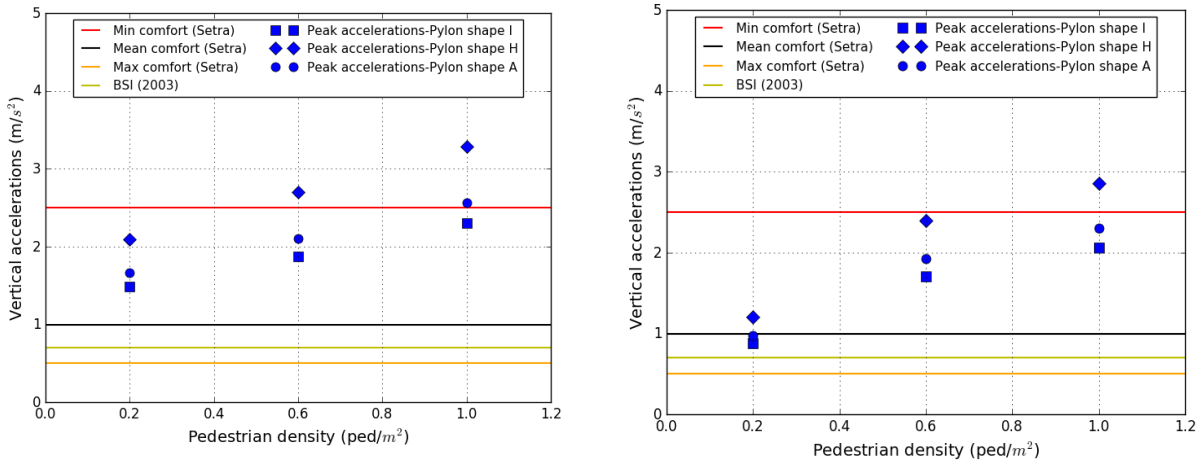
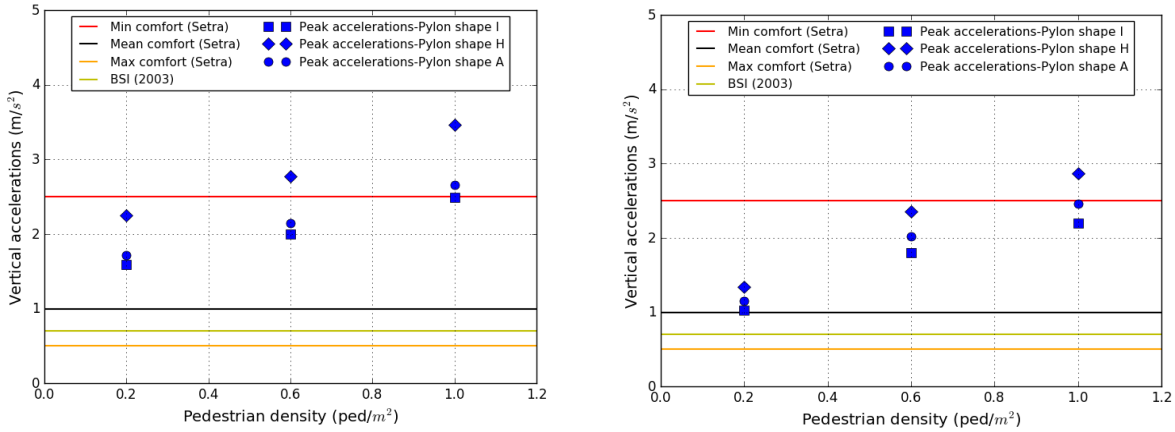


Figure 5.37 Vertical peak accelerations (m/s^2) for a cable-stayed footbridge with a span length of 50 m for (a) commuting and (b) leisure activities for different pylon shapes



(a) (b)

Figure 5.38 Vertical peak accelerations (m/s^2) for a cable-stayed footbridge with a span length of 100 m for (a) commuting and (b) leisure activities for different pylon shapes



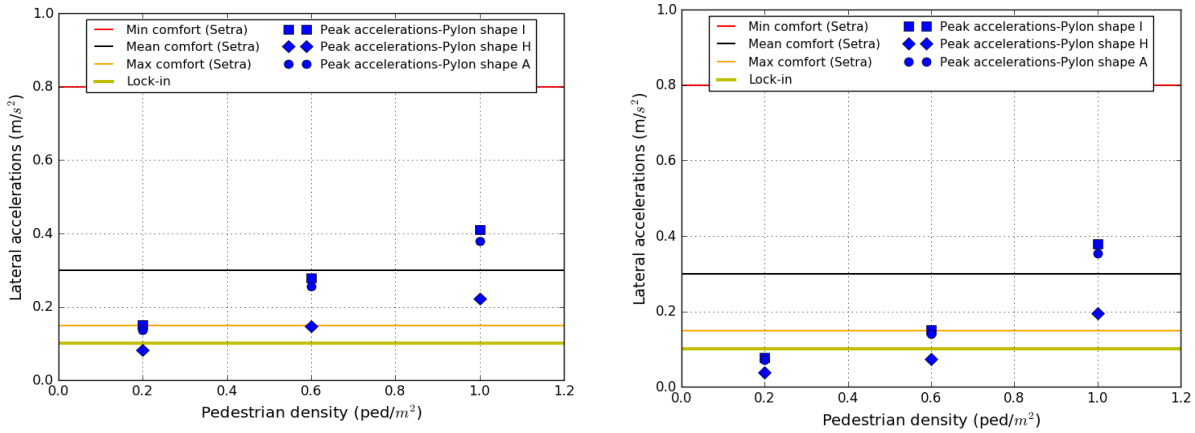
(a) (b)

Figure 5.39 Vertical peak accelerations (m/s^2) for a cable-stayed footbridge with a span length of 150 m for (a) commuting and (b) leisure activities for different pylon shapes

5.5.2 Dynamic response in the lateral direction

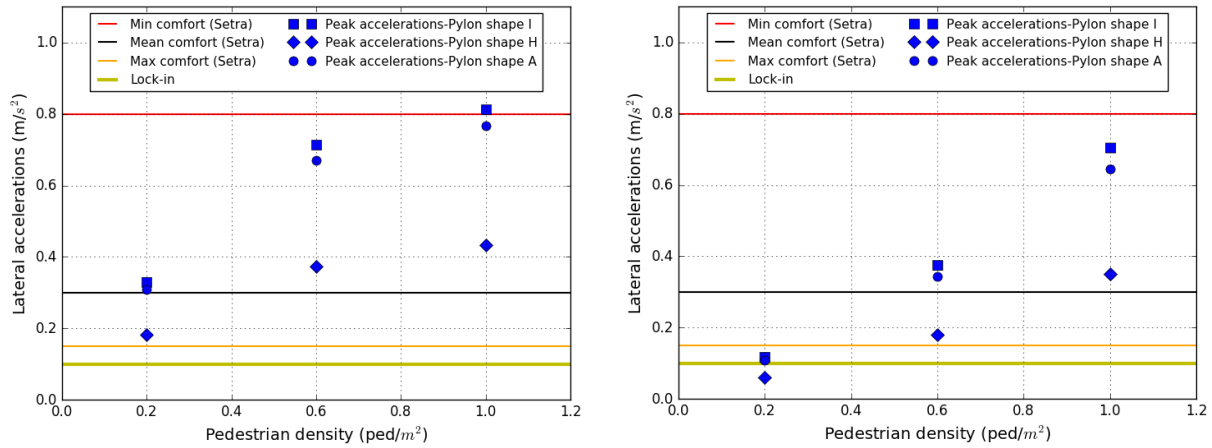
Lateral accelerations analyses are carried out in cable-stayed footbridges with different pylon shapes. These lateral accelerations are shown in Figure 5.40 to Figure 5.42. The maximum lateral accelerations in the deck when the I- or A-shaped pylons are used are very similar, as previously observed for vertical accelerations. Nevertheless, the H- shaped pylons lead to the smallest lateral accelerations (with reductions of the lateral accelerations of up to 47% in comparison to the A-

and I- shaped pylon), contrary to what was observed for vertical accelerations. These results show that the shape of the pylon also has an impact in the lateral accelerations. The TMD mass ratio to fulfil the lock-in effect for a CSF with an H-shaped pylon for commuting activities varies from 0.01 to 0.05 for 0.2 ped/m^2, from 0.02 to 0.07 for a pedestrian density of 0.6 ped/m^2, and from 0.06 to 0.09 for a pedestrian density of 1.0 ped/m^2 depending on the span length (50, 100 or 150 m). In the case of leisure activities, a TMD mass ratio up to 0.07 is required to ensure the achievement of the maximum comfort criteria whilst avoiding the lock-in effect.



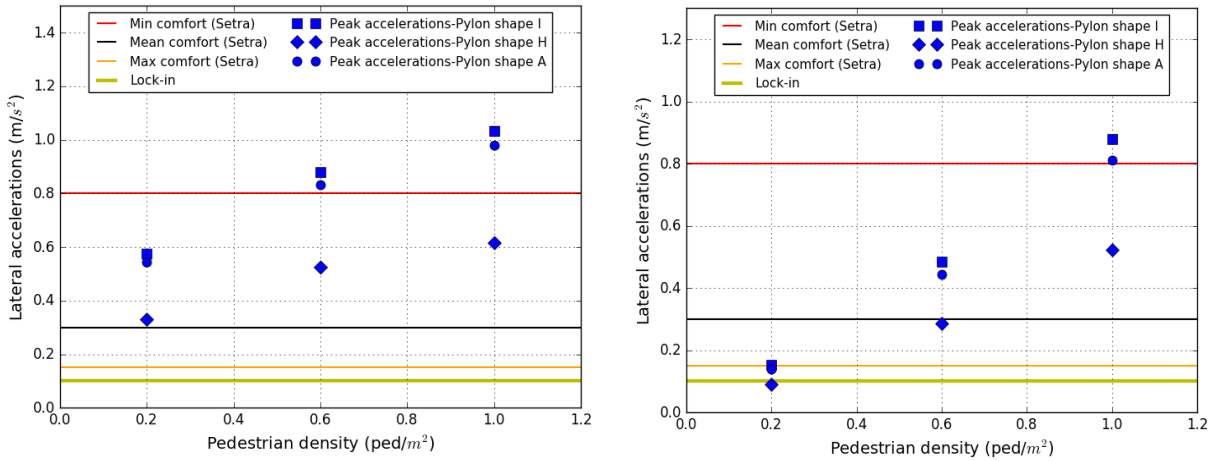
(a) (b)

Figure 5.40 Lateral peak accelerations (m/s^2) for a cable-stayed footbridge with a span length of 50 m for (a) commuting and (b) leisure activities for different pylon shapes



(a) (b)

Figure 5.41 Lateral peak accelerations (m/s^2) for a cable-stayed footbridge with a span length of 100 m for (a) commuting and (b) leisure activities for different pylon shapes

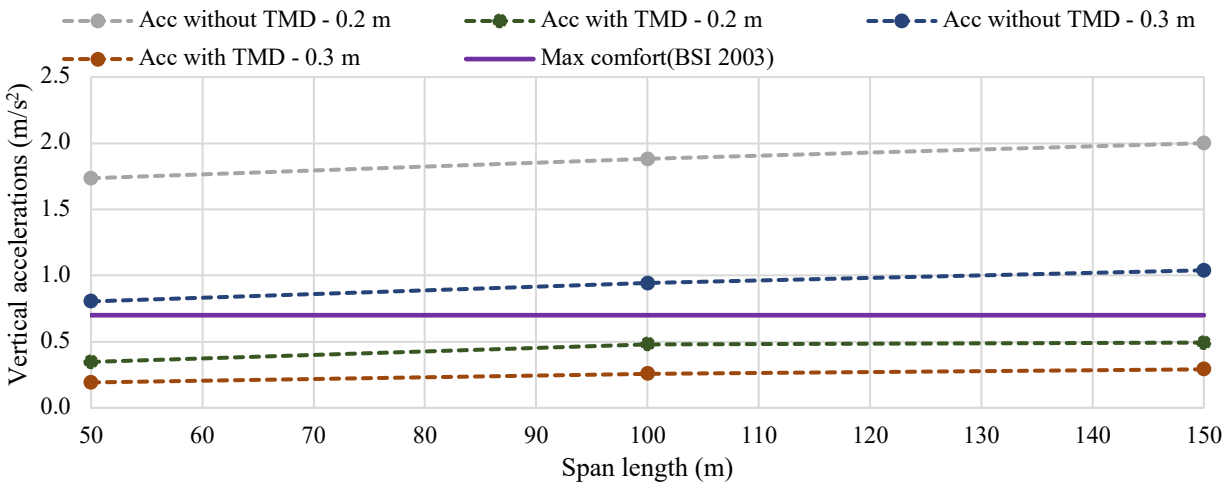


(a) (b)

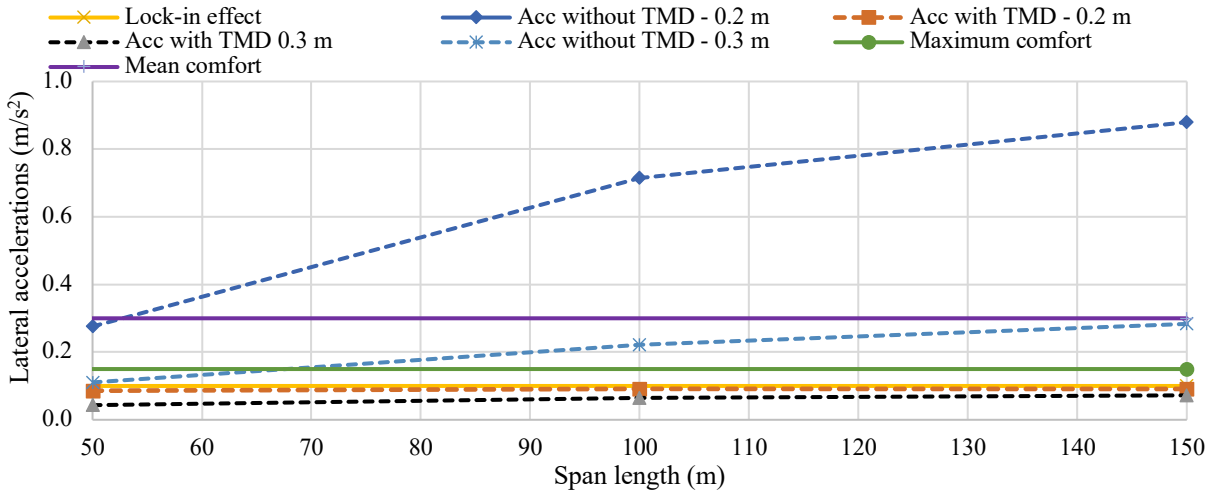
Figure 5.42 Lateral peak accelerations (m/s^2) for a cable-stayed footbridge with a span length of 150 m for (a) commuting and (b) leisure activities for different pylon shapes

5.6 Cost analysis

A comparative cost study between implementing TMD or increasing the slab thickness in the vertical direction is included herein. The unit costs considered are shown in (Table 4.2) updated by 7.3% to reflect the cumulative effects of inflation since these costs were published. The TMDs considered in this analysis have a mass of 600, 1200, 3200, and 4600 kg, a tuning range from 1.4 to 2.8 Hz, a damping ratio from 10 to 15%, and a maximum displacement range of ±40 mm, whose units cost are 7500, 10800, 18500, and 23500 sterling pounds, respectively. These were provided by MAURER supplier (Benicke, 2019). Other costs are not considered herein, as the aim is comparing the relative deck material cost for both design alternatives. Maurer recommends one TMD replacement in 100 years, including two maintenance sessions (Benicke, 2017); therefore, it has been considered one TMD for this cost study (Section 4.3.3). A deck depth of 0.2 m or 0.3 m does not fulfil the serviceability criterion in the vertical and lateral direction without TMDs (Figure 5.43 (a) and (b)). Therefore, TMDs have been implemented for both slab thickness.



(a)



(b)

Figure 5.43 (a) Vertical and (b) lateral peak accelerations according to the span length for CSF with one tower with a slab depth of 0.2 and 0.3 m for pedestrian densities of 0.6 ped/m^2 (commuters)

The cost analysis (see Figure 5.44) has been performed for cable-stayed footbridges with a span length of 50, 100 and 150 m for deck depths of 0.2 and 0.3 m, considering the design scenario of pedestrian densities of 0.6 ped/m^2 (commuters). When TMDs are being used, the smallest material cost is achieved for deck depths of 0.2 m (an average of 11% cheaper than for 0.3 m with TMDs).

Besides, there would be additional savings in other structural members such as tower, cables, bearings, abutments and foundations.

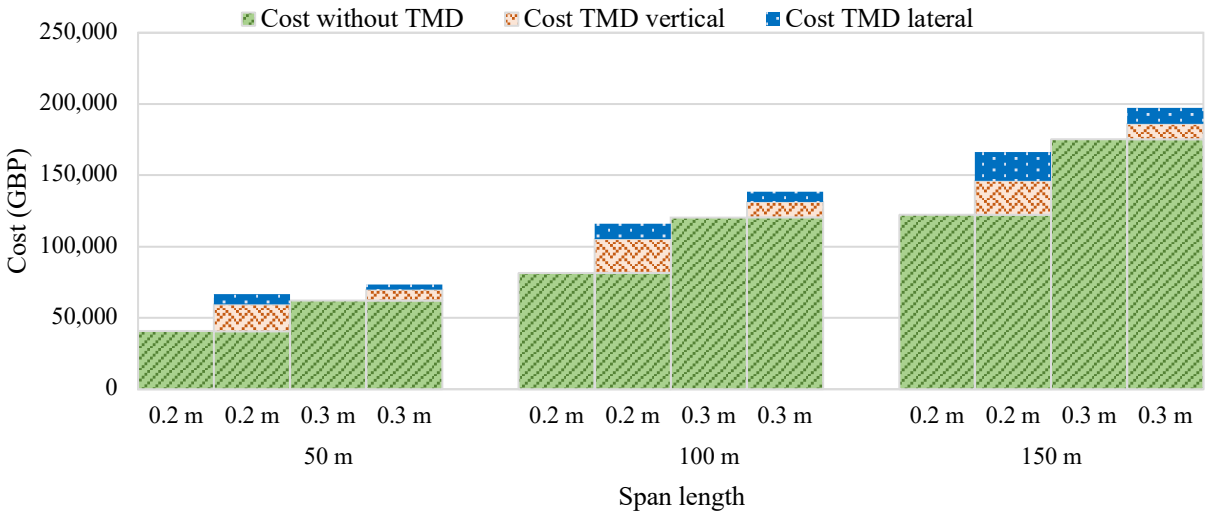


Figure 5.44 Cost analysis for different slab thickness (0.2 and 0.3 m) when one TMD is employed in the design of cable-stayed footbridges with 50, 100 and 150 span lengths with pedestrian densities of 0.6 ped/m^2 (commuters)

5.7 Main conclusions and design recommendations

In this section, design recommendations are given for cable-stayed footbridges with the most common pylon shapes (I-, A- and H-shaped pylon). These recommendations can be employed to estimate the vertical and lateral accelerations for different span lengths, pedestrian densities and pedestrian activities with and without TMDs. The main conclusions and design recommendations are outlined as follows:

Modes dominating the response

- The accelerations in vertical and lateral direction linearly increase when the span length increases. When the span length increases the frequencies decrease, which can lie near the step frequency of pedestrians, amplifying the response, and even causing discomfort to users. The step frequencies where resonant effects can appear corresponds to a range from

1.45 to 2.67 Hz. In the lateral direction, this range varies from 0.73 to 1.34 Hz (half of the vertical frequencies).

- The modes dominating the response, in terms of accelerations, are related to the span length (Table 5.7). These modes can be confirmed through a frequency domain analysis at different locations along the span length.

Tower shape	Direction of the response	Modes	Range of span lengths (m)
I, A, H	Vertical	V1, V2	50 - 60
		V2	60 - 100
		V2, V3	100-150
I, A	Torsion – Vertical	T1	50 - 120
		T2	120 - 150
H		T1	50 – 90
		T2	90 - 150
I, A, H	Lateral	L1	50 - 150
I, A, H	Torsion - Lateral	T1	50 -150

Table 5.7 Structural vertical, lateral and torsional modes dominating the response in cable-stayed footbridges with different pylon's shapes under a pedestrian density of 0.6 ped/m^2 for commuting activities based on Figure 5.36

Dynamic response expected without TMDs

The characteristics of the benchmark cases have been chosen as representative from a database of built structures. Therefore, the dynamic response of these benchmark cases could be expected in similar footbridges. Thus, these graphs can be used in preliminary designs to estimate the accelerations according to the purpose of the bridge, such as rural, suburban, or urban routes (BSI, 2008) without any calculations. Figure 5.45 to 5.47 show the vertical and lateral accelerations for CSFs with a slab depth of 0.2 m for the envelope of commuting and leisure activities as a function of the span length. The accelerations expected without TMDs are outlined as follows:

For vertical direction according to the envelope of I-, A-, and H-shaped pylons

- For this direction, regardless of the span lengths and pedestrian densities, a maximum comfort level is not achieved.
- For span lengths from 50 to 150 m, a minimum comfort for pedestrian densities of 0.2 ped/m^2 is achieved.
- For span lengths up to 70 m, a mean comfort for pedestrian densities of 0.6 ped/m^2 is achieved. For longer spans, an unacceptable comfort is expected.
- Regardless of the span lengths, an unacceptable comfort for pedestrian densities of 1.0 ped/m^2 is achieved.

For lateral direction according to the envelope of the I-, and A-shaped pylons

- Regardless of the span lengths and pedestrian densities, the lock-in effect is not avoided.
- For span lengths ranging from 50 to 90 m, and 90 to 150 m a mean, and minimum comfort is achieved, respectively (pedestrian densities of 0.2 ped/m^2).
- For span lengths up to 120 m, a minimum comfort for pedestrian densities of 0.6 ped/m^2 is achieved. For longer spans, an unacceptable comfort is expected.
- For span lengths up to 100 m, a minimum comfort for pedestrian densities of 1.0 ped/m^2 is achieved. For span lengths > 100 m, an unacceptable comfort is expected.

For lateral direction according to H-shaped pylon

- For span lengths up to 60 m, the lock-in effect for pedestrian densities of 0.2 ped/m^2 is avoided.
- For span lengths ranging from 60 to 90 m, 90 to 150 m, and > 150 m, a maximum, mean and unacceptable comfort is achieved, respectively (pedestrian densities of 0.2 ped/m^2).
- For span lengths up to 80 m, a mean comfort for pedestrian densities of 0.6 and 1.0 ped/m^2 is achieved.

- For span lengths ranging from 80 to 150 m, a minimum comfort for pedestrian densities of 0.6 and 1.0 ped/m^2 is achieved.

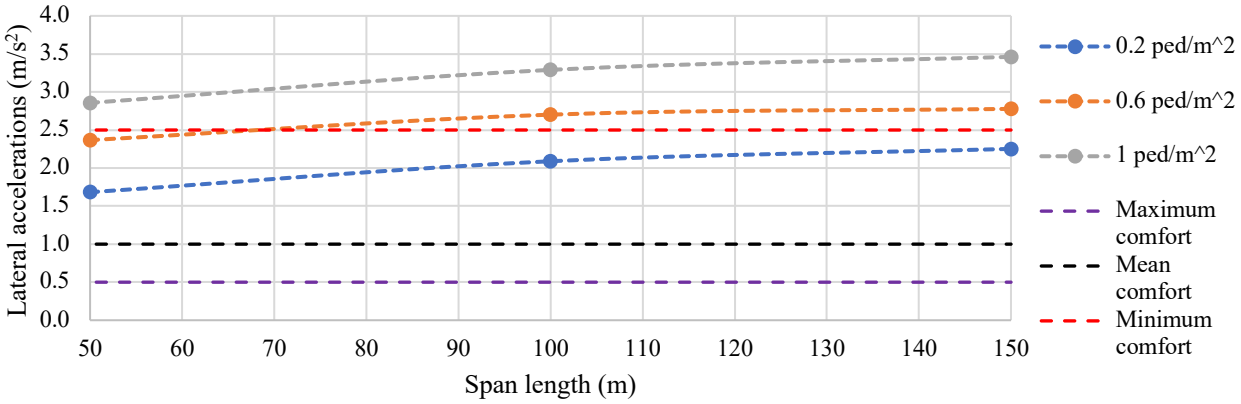


Figure 5.45 Vertical peak accelerations according to the span length for different pedestrian densities without TMDs according to the envelope of the I-, A-, and H-shaped pylons for CSFs with one tower

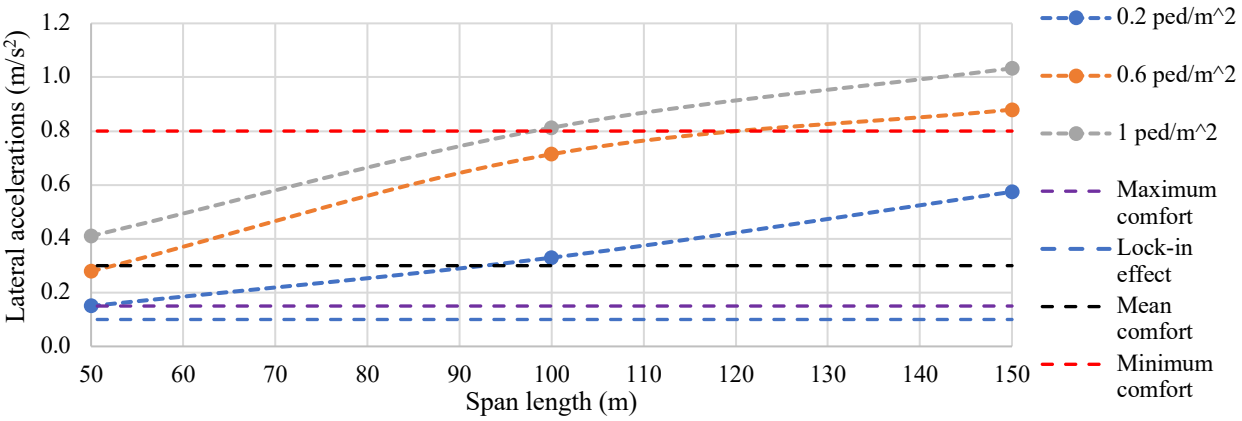


Figure 5.46 Lateral peak accelerations according to the span length for different pedestrian densities without TMDs according to the envelope of the I- and A-shaped pylon for CSFs with one tower

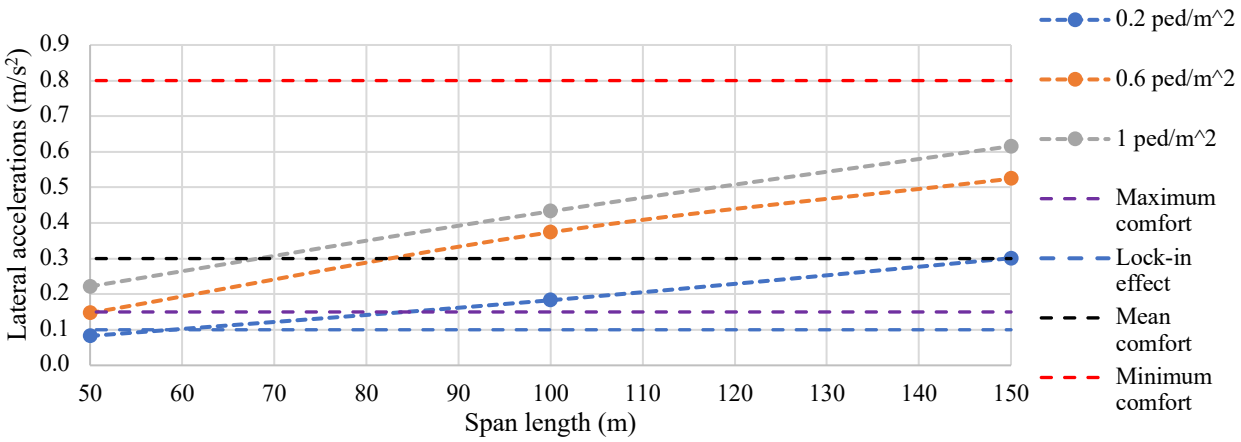


Figure 5.47 Lateral peak accelerations according to the span length for different pedestrian densities without TMDs according to the H-shaped pylon for CSFs with one tower

TMD location

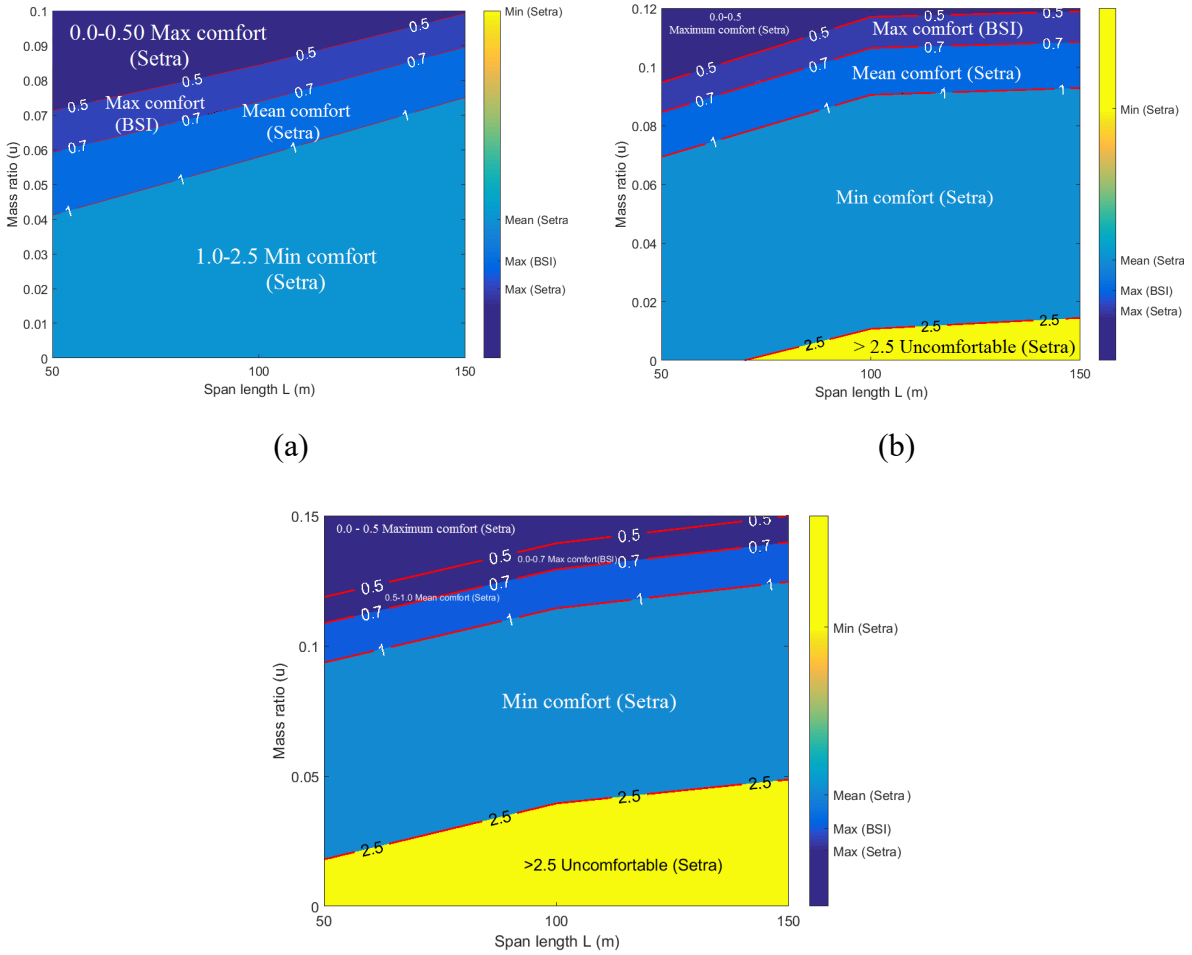
- The greatest TMD efficiency is achieved when the TMD is positioned at the location of the maximum nodal coordinates for the modal shape that dominates the response. At that location, the efficiency of the TMD increases. This location can be identified through the frequency domain analysis.

- In the vertical direction, similar efficiencies of the TMDs are achieved when they are located at the maximum nodal coordinates ± 11 % from that point of those modal shapes with a larger contribution. On the other hand, for the lateral direction, the lock-in effect is avoided if the TMD is located at the maximum nodal coordinates of those modal shapes dominating the response ± 5 % from that point. If the TMD is not employed at this location, the efficiencies are reduced, and the maximum comfort is not achieved in the vertical direction, neither the lock-in effect is avoided in the lateral direction. The implementation of TMDs also reduces the dynamic component of the internal forces, but in a smaller way as it does with the accelerations (approximately 25 % in sagging and hogging BMs).

- TMD efficiencies up to 80% are achieved if the TMDs are positioned at the locations previously mentioned.

Dynamic response and required TMD mass ratios

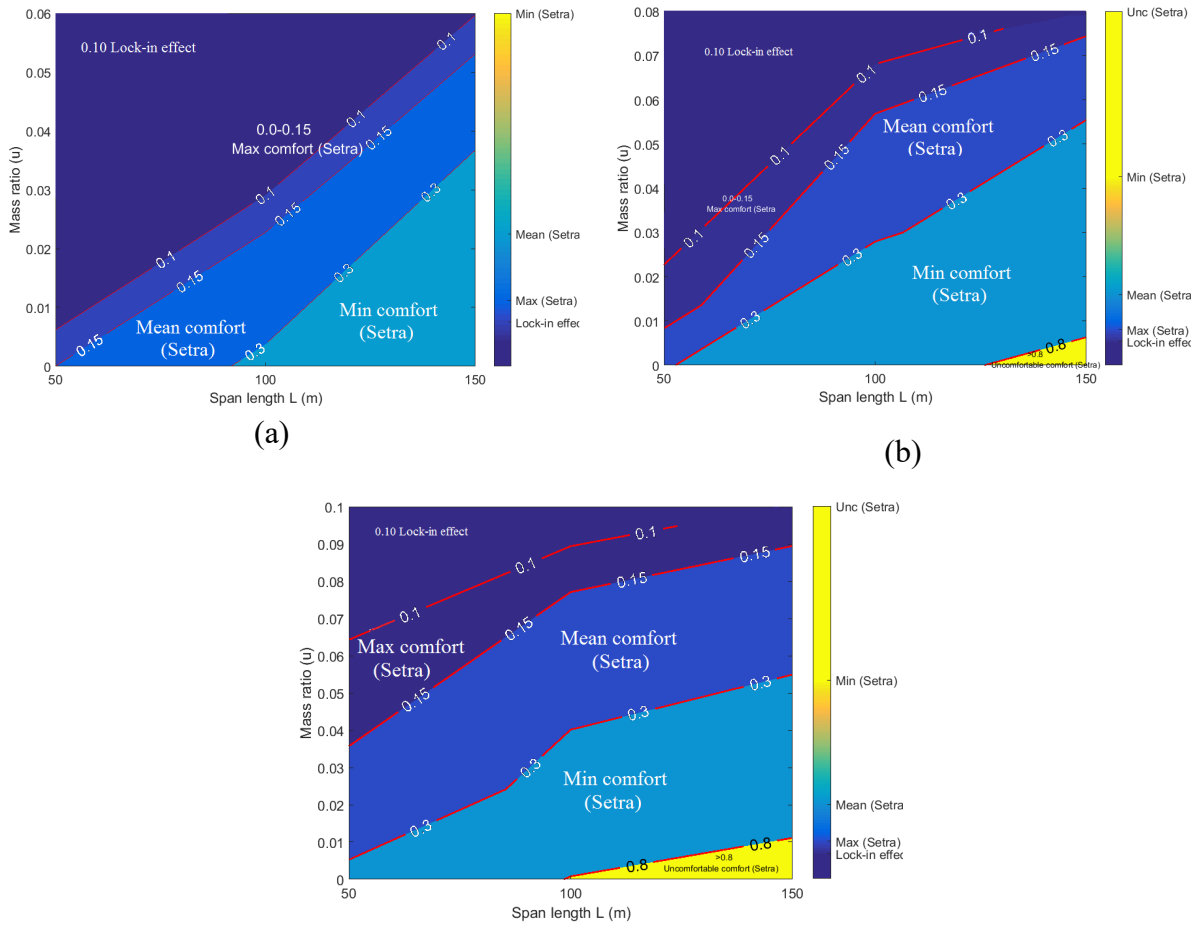
Figure 5.48, Figure 5.49 and Figure 5.50 present the required TMD mass ratio (μ) according to the I-, A- and H-shaped pylons for different pedestrian densities for vertical and lateral accelerations. These graphs show the relationship between the TMD mass ratios according to the peak accelerations, degree of comfort and span lengths. It is evident that the larger is the span length the larger are the accelerations. Therefore, a higher TMD mass ratio is required.



(a) (b)

(c)

Figure 5.48 Vertical peak accelerations and comfort levels for different TMD mass ratios (μ), active in the vertical direction, and for different span lengths under pedestrian densities of a) 0.2, b) 0.6 and c) 1.0 ped/m^2 according to the envelope of the I- A, and H-shaped pylons for CSFs with one tower



(a) (b)

(c)

Figure 5.49 Lateral peak accelerations and comfort levels for different TMD mass ratios (μ), active in the lateral direction, and for different span lengths under pedestrian densities of a) 0.2, b) 0.6 and c) 1.0 ped/m^2 according to the envelope of the I- and A-shaped pylons for CSFs with one tower

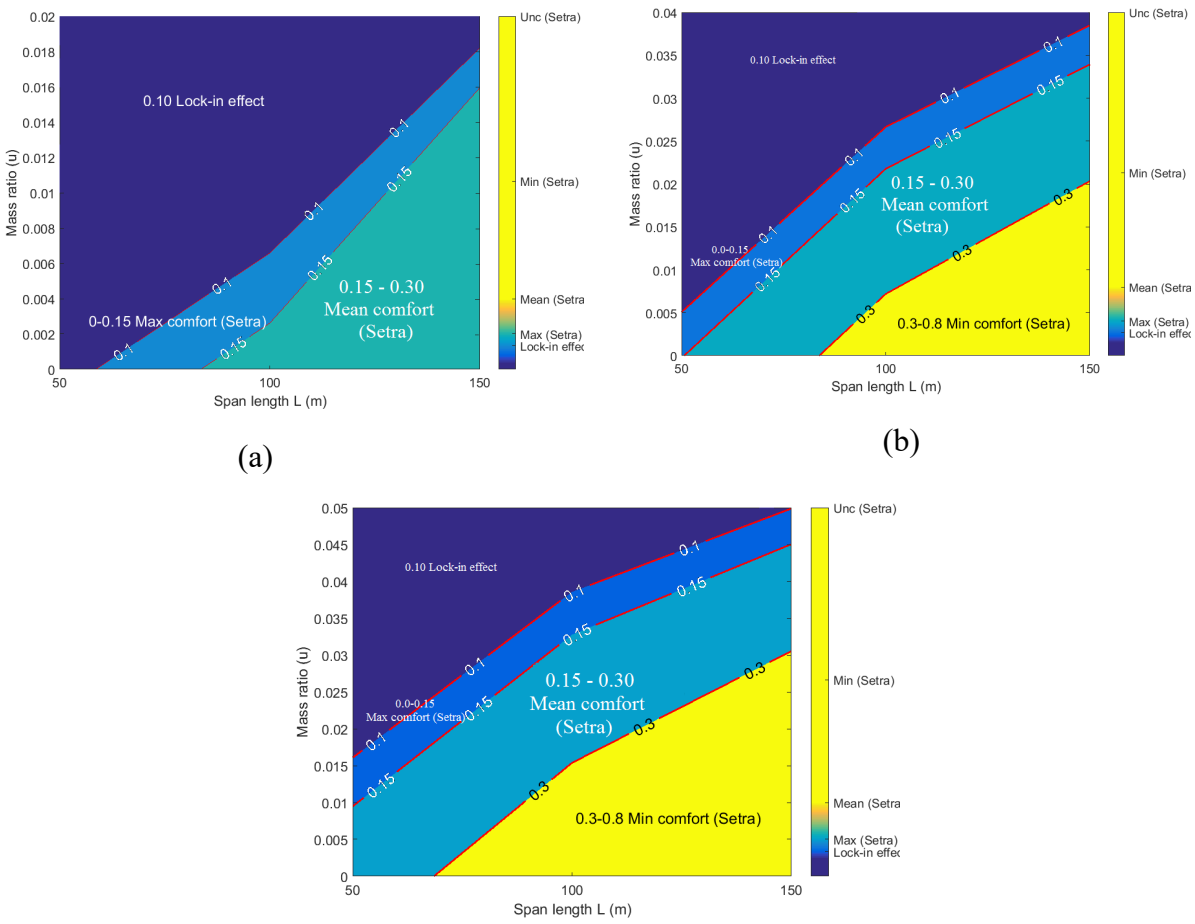


Figure 5.50 Lateral peak accelerations and comfort levels for different TMD mass ratios (μ), active in the lateral direction, and for different span lengths under pedestrian densities of a) 0.2, b) 0.6 and c) 1.0 ped/m^2 according to the H-shaped pylon for CSFs with one tower

The dynamic response with TMDs that could be expected in similar structures are outlined as follows:

- The most cost-effective solution is to install tuned mass dampers instead of increasing the slab depth. If the TMD does not need to be replaced throughout the service life, the deck material cost would be smaller to the case with a slab depth of 0.3 m. Although increasing the slab depth effectively reduced the dynamic response in approximately 60 %, it does not

fulfil the maximum comfort. Therefore, tuned mass dampers are still required for slab depth of 0.3 m making a more expensive solution rather than using a slab depth of 0.2 m.

- For lateral accelerations, another way to reduce the response is to use an A-shaped pylon. This is because they have a better performance when both vertical and lateral accelerations are considered. I-shaped pylons are the best ones when considering vertical accelerations but have the worst performance of those assessed when considering the lateral accelerations. On the contrary, H-shaped pylons are the best ones when considering lateral accelerations but have the worst performance of those assessed when considering the vertical accelerations.

Figure 5.51 summarizes the process to implement TMDs in cable-stayed footbridges with one tower. This flowchart could be followed by a designer for preliminary design of footbridges without serviceability problems.

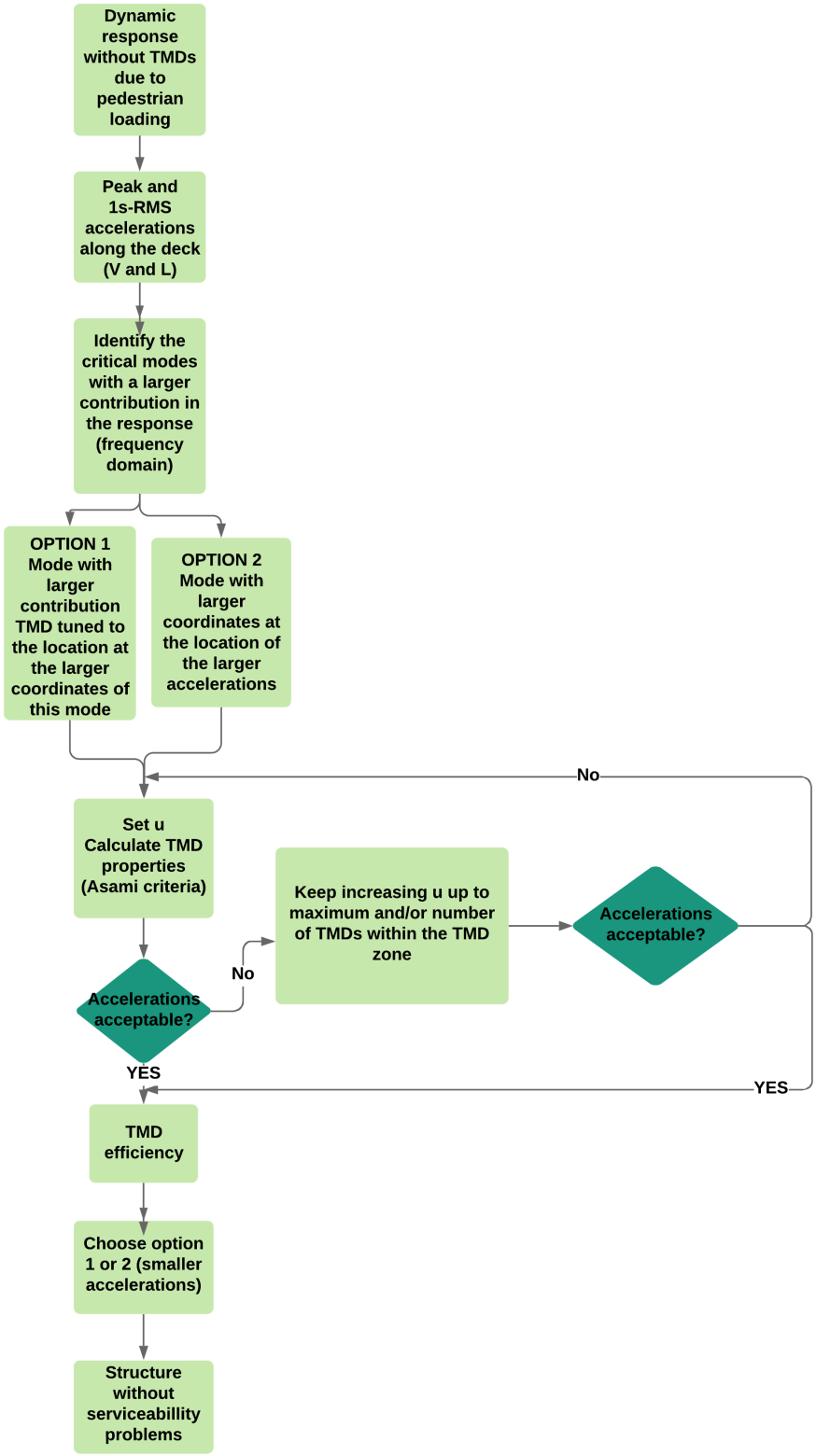


Figure 5.51 TMD implementation: a flowchart to include TMDs in cable-stayed footbridges with one tower

6 Dynamic response of cable-stayed footbridges with two towers

6.1 Introduction

Having a single tower is the most common cable-stayed arrangement for footbridges, according to the database included in Appendix B. However, around 25% of the footbridges are constructed with two towers and it is a common feature for longer bridges. This chapter focuses on the evaluation of the dynamic response for cable-stayed footbridges with two towers with and without tuned mass dampers, following a similar structure to that in Chapter 5. The dynamic response in the vertical and lateral direction for commuting and leisure activities for different pedestrian densities (0.2, 0.6, and 1.0 ped/m^2) is evaluated. In addition, different pylon shapes are considered herein. These footbridges were also studied by Ramos-Moreno (2015), without implementing supplemental damping devices, highlighting that the serviceability limit state (SLS) of vibration was not satisfied by modifying the geometrical material properties, suggesting that further studies implementing tuned mass dampers were necessary as the only possible way to achieve an appropriate serviceability in these bridges.

Thus, Section 6.2 describes the geometry and modal analysis of the cable-stayed footbridges with two towers for different span lengths. Section 6.3 shows the dynamic response under pedestrian loading without tuned mass dampers in the vertical and lateral direction. Section 6.4 provides understanding about the behaviour with tuned mass dampers and defines the required TMD mass ratio to mitigate the human-induced vibrations in cable-stayed footbridges with different span lengths.

Section 6.5 shows the impact on the dynamic response when different pylons shapes are employed. Section 6.6 shows a comparative cost study between implementing TMD or increasing the slab thickness as a measure to fulfil maximum comfort. Finally, Section 6.7 presents the conclusions and design recommendations where the accelerations can be estimated regarding the pedestrian densities, the activities (commuting and leisure) and the degree of comfort level (minimum, mean, or maximum) for different span lengths.

6.2 Benchmark case for cable-stayed footbridges with two pylons

6.2.1 Modelling characteristics

The main geometric characteristics of this type of footbridge were chosen based on an exhaustive analysis of the characteristics of footbridges that are already built and are operating around the world (Annex B). For this research, three main spans (L), which are 50, 100, and 150 m and two side spans of 10, 20, and 30 m, which corresponds to 0.2 L, are evaluated. The characteristics of the structural materials are shown in Section 3.3.2. The depth of the concrete slab is 0.2 m, and the deck width is 4 m. The steel girder depth is 0.3 m, the thickness of the flanges is 80 mm, and the web thickness is 25 mm. The deck is rigidly fixed to the pylon. The main characteristics of this benchmark footbridge are shown in Figure 6.1. These characteristics are included in the numerical model for further parametric studies.

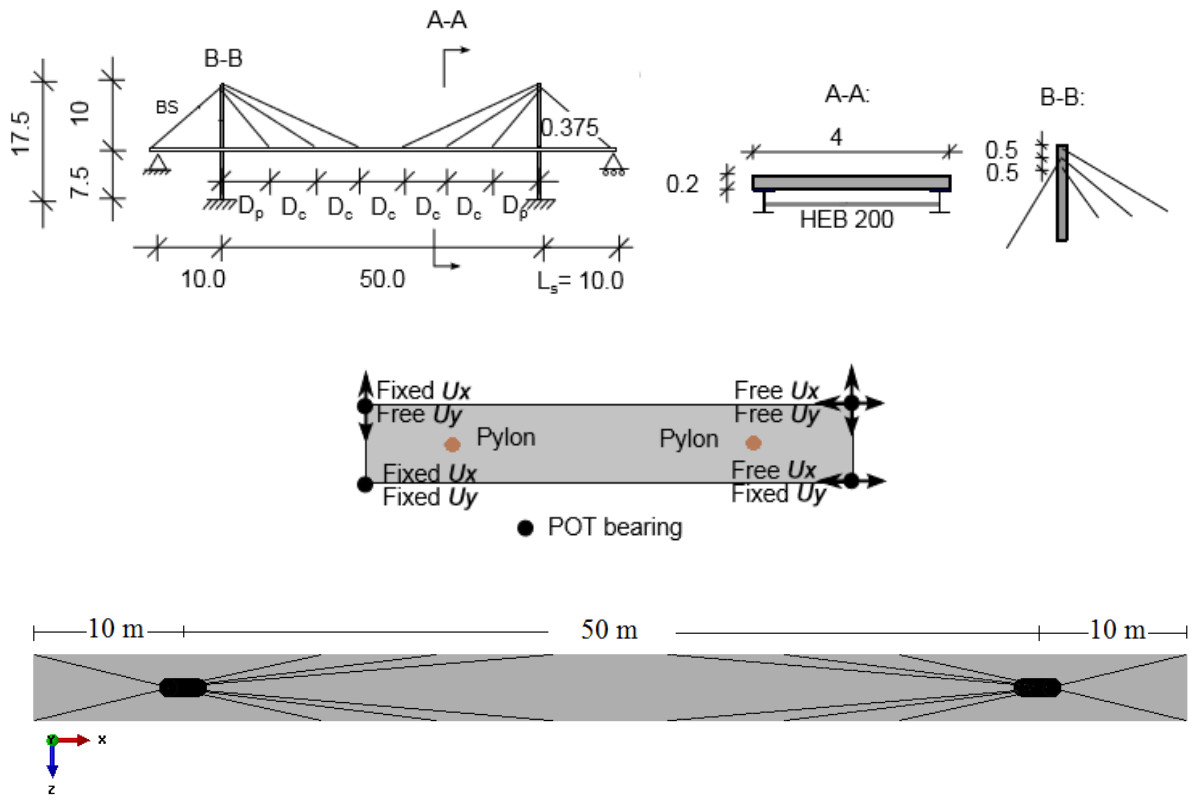
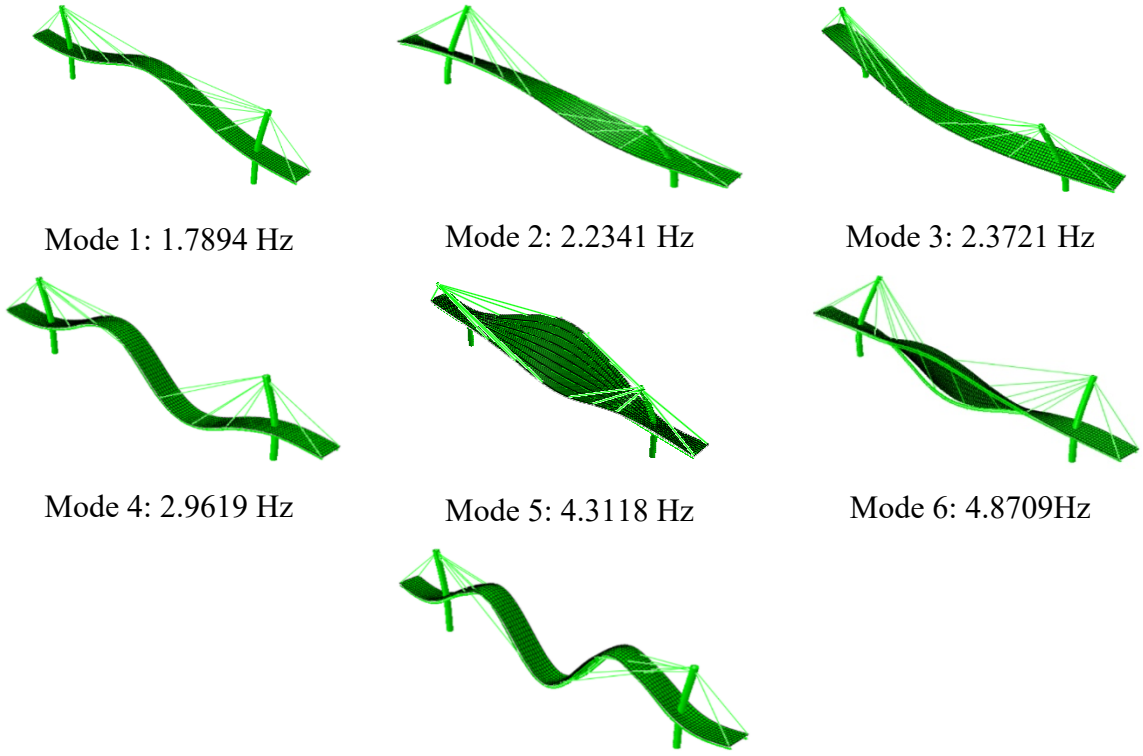


Figure 6.1 Geometry, support configurations and plan view of the cable-stayed footbridges with two pylons. Dimensions in meters (m) (Ramos-Moreno, 2015)

6.2.2 Modal analysis

Cable-stayed footbridges have very low frequencies. These can match the pedestrian frequencies, which can result in the amplification of the response (resonance effects), causing discomfort to users. A modal analysis for each span length was performed to check if the frequencies of the cable-stayed footbridges are in the range of the pedestrian frequencies. Figure 6.2, Figure 6.3, and Figure 6.4 show that for cable-stayed footbridges with a span length from 50 to 150 m some of the frequencies are in the range of the pedestrian frequencies. Hence, these footbridges are prone to have serviceability problems induced by resonant effects. Table 6.1, Table 6.2, and Table 6.3 show the modal frequencies (Hz) of 50, 100 and 150 m span cable-stayed footbridges when the bridge is empty and when it is loaded with different pedestrian densities (0.2, 0.6 and 1.0 ped/m^2). The differences between those load cases are smaller than 3% for all the conditions.



Mode 1: 1.7894 Hz | Mode 2: 2.2341 Hz | Mode 3: 2.3721 Hz

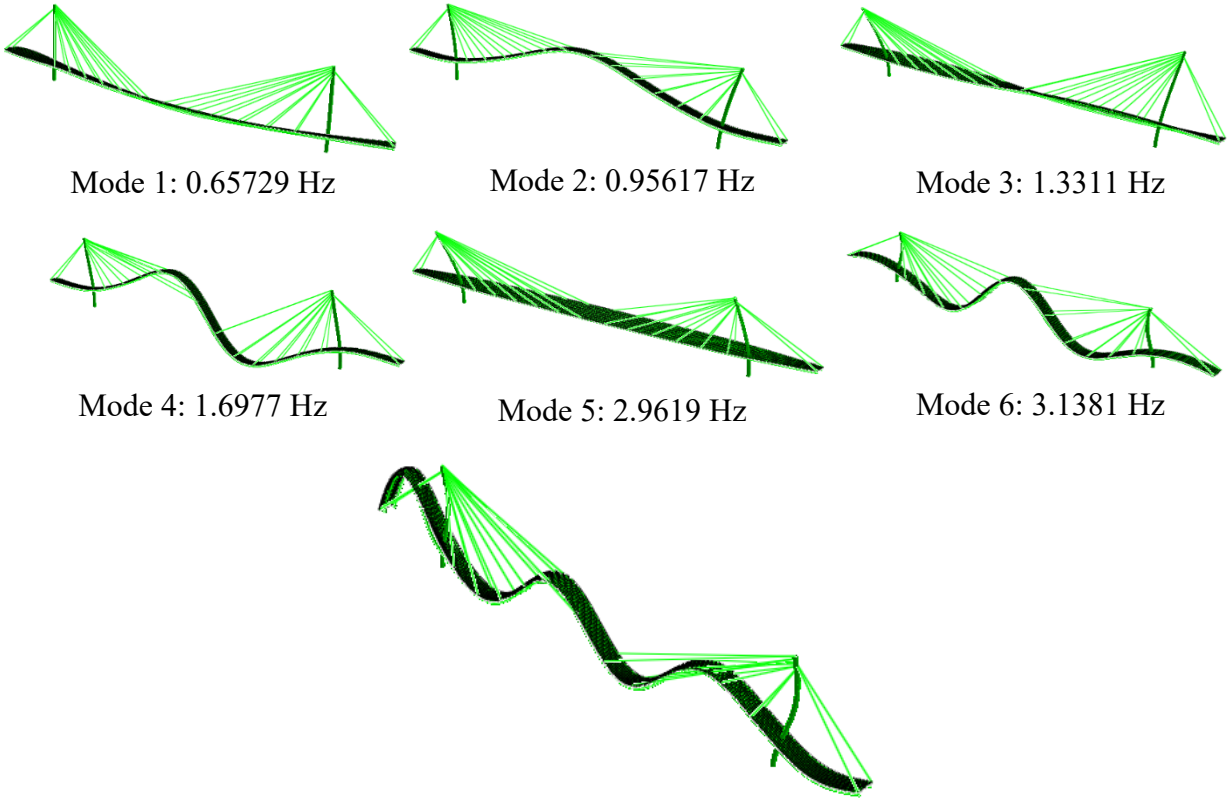
Mode 4: 2.9619 Hz | Mode 5: 4.3118 Hz | Mode 6: 4.8709Hz

Mode 7: 4.9791 Hz

Figure 6.2 Modal frequencies of 50 m span cable-stayed footbridge with two towers considering a pedestrian density of 0.6 ped/m^2

Mode	Mode shape description	Footbridge empty	0.2 ped/m^2	0.6 ped/m^2	1.0 ped/m^2
1	V1	1.82	1.80	1.79	1.75
2	T1	2.29	2.24	2.23	2.21
3	L1	2.41	2.39	2.37	2.35
4	V2	2.99	2.98	2.96	2.90
5	T2	4.36	4.34	4.31	4.29
6	T3	4.91	4.90	4.87	4.85
7	V3	5.02	5.01	4.98	4.90
Maximum differences in relation to empty structure			0.59%	1.15%	2.43%

Table 6.1 Frequencies (Hz) of 50 m span cable-stayed footbridge with two towers when the bridge is empty and when it is loaded with different pedestrian densities



Mode 1: 0.65729 Hz

Mode 2: 0.95617 Hz

Mode 3: 1.3311 Hz

Mode 4: 1.6977 Hz

Mode 5: 2.9619 Hz

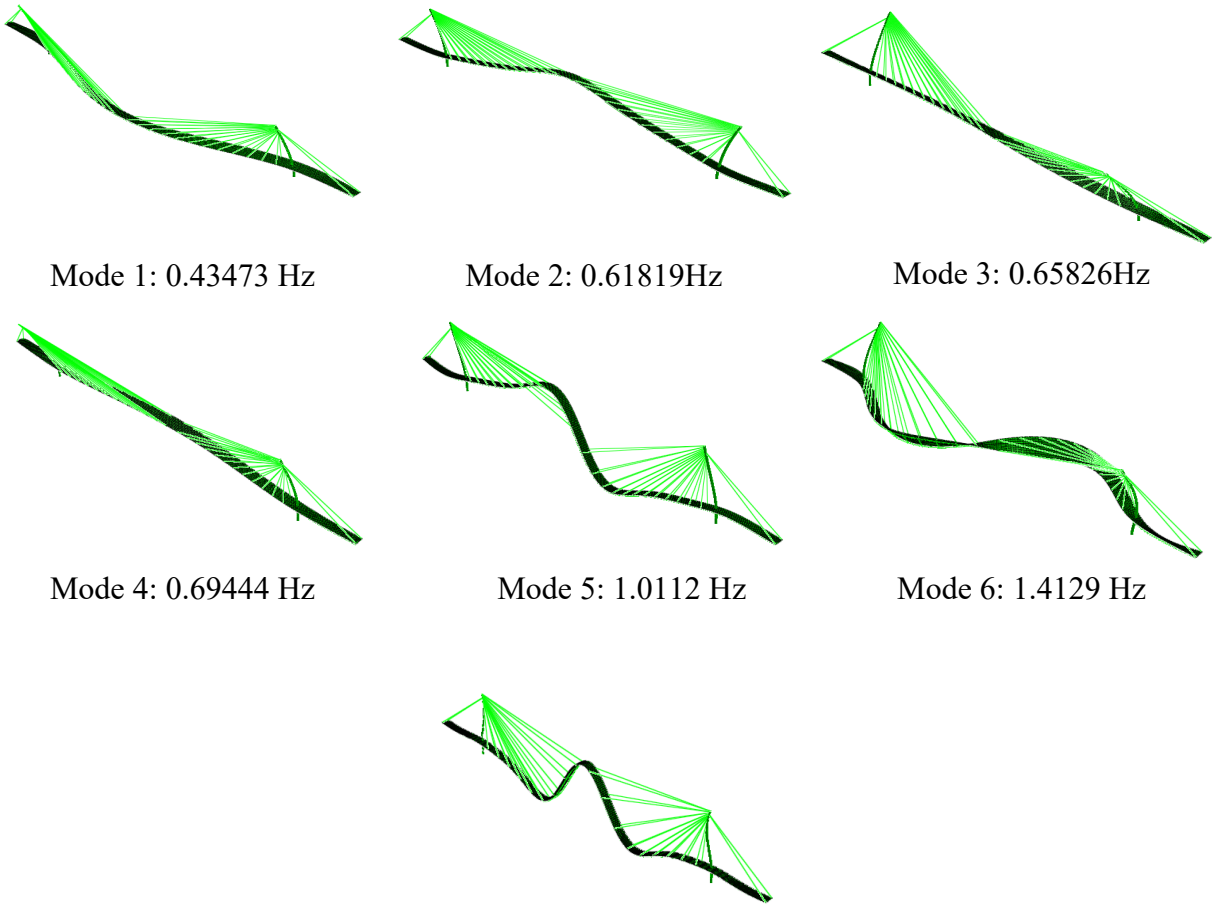
Mode 6: 3.1381 Hz

Mode 7: 3.4997

Figure 6.3 Modal frequencies of cable-stayed footbridges with a span length of 100 m with two towers considering a pedestrian density of 0.6 ped/m^2

Mode	Mode shape description	Footbridge empty	0.2 ped/m²	0.6 ped/m²	1.0 ped/m²
1	L1	0.66	0.63	0.66	0.64
2	V1	0.98	0.96	0.96	0.97
3	T1	1.35	1.34	1.33	1.31
4	V2	1.73	1.71	1.70	1.71
5	T2	2.98	3.16	2.96	2.89
6	V3	3.15	3.16	3.14	3.00
7	V4	3.55	3.52	3.50	3.48
Maximum differences in relation to empty structure			0.46%	2.09%	2.59%

Table 6.2 Frequencies (Hz) of 100 m span cable-stayed footbridge with two towers when the bridge is empty and when it is loaded with different pedestrian densities



Mode 1: 0.43473 Hz Mode 2: 0.61819Hz Mode 3: 0.65826Hz

Mode 4: 0.69444 Hz Mode 5: 1.0112 Hz Mode 6: 1.4129 Hz

Mode 7: 2.0391 Hz

Figure 6.4 Modal frequencies of cable-stayed footbridges with a span length of 150 m with two towers considering a pedestrian density of 0.6 ped/m^2

Mode	Mode shape description	Footbridge empty	0.2 ped/m^2	0.6 ped/m^2	1.0 ped/m^2
1	L1	0.50	0.49	0.47	0.46
2	V1	0.65	0.64	0.62	0.61
3	T1	0.69	0.67	0.66	0.66
4	L2	0.71	0.70	0.69	0.70
5	V2	1.03	1.02	1.01	0.99
6	T2	1.42	1.41	1.41	1.40
7	V3	2.05	2.04	2.04	2.03
Maximum differences in relation to empty structure			1.06%	2.80%	3.14%

Table 6.3 Frequencies (Hz) of 150 m span cable-stayed footbridge with two towers when the bridge is empty and when it is loaded with different pedestrian densities

6.2.3 Distribution of step frequencies of the pedestrians

Cable-stayed footbridges are slender structures prone to vibrate under walking pedestrians which step frequencies can lie near the structural frequencies of the structure. Therefore, the pedestrian step frequencies need to be represented in a realistic way to ensure an accurate estimation of the response. Figure 6.5 shows the distribution of pedestrian frequencies for commuting (blue) and leisure (red) activities. Three pedestrian densities are considered: 0.2, 0.6 and 1.0 ped/m^2. The distribution of step frequencies is similar for span lengths of 50, 100 and 150, whilst it varies with the pedestrian density. The larger variance is for lower pedestrian densities which is explained by the lower number of pedestrians crossing the bridge. While when the pedestrian densities increase the variance is reduced due to the higher number of pedestrians (crowd modelling) which are forcing each other to walk in a similar manner. In addition, the step frequencies can lie near the structural frequencies, which can increase the dynamic response (resonance effects). The range of vertical and lateral frequencies that can be excited by commuting activities is shown in Figure 6.6 (a) and (b), between the blue and green dashed lines, respectively. The influence of the torsional frequencies in the vertical and lateral direction are represented in Figure 6.6 (c) and (d), respectively.

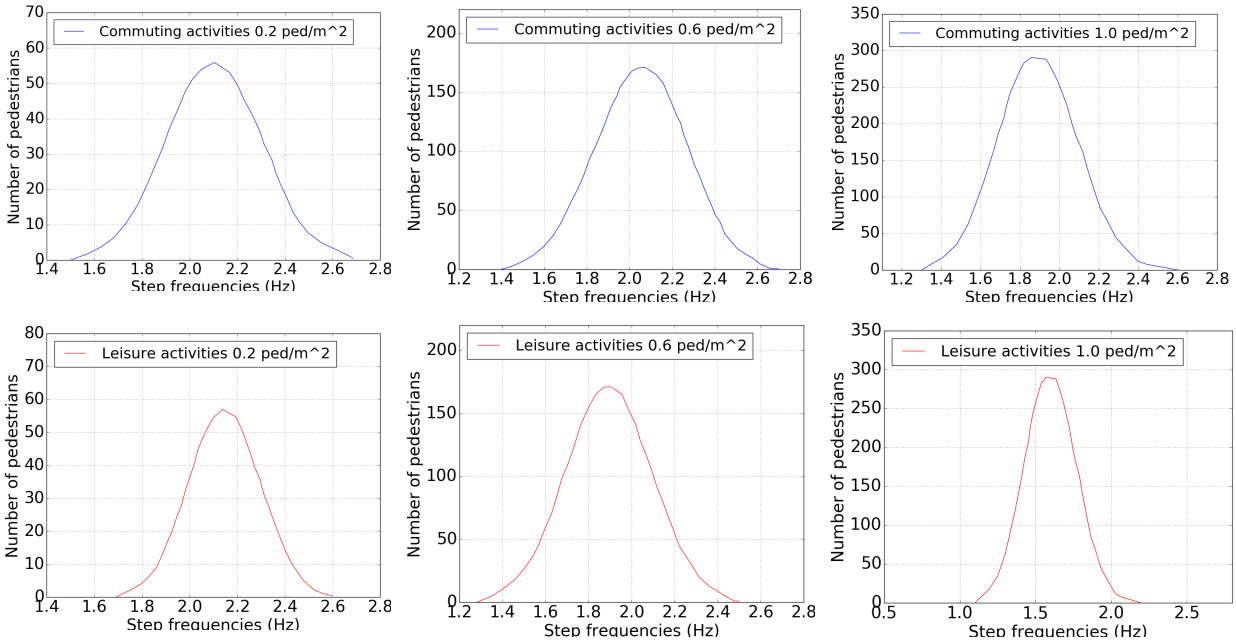


Figure 6.5 Distribution of pedestrian frequencies for commuting (blue) and leisure (red) activities for pedestrian densities of 0.2, 0.6 and 1.0 ped/m^2 in a 50 m span cable-stayed footbridge with two towers

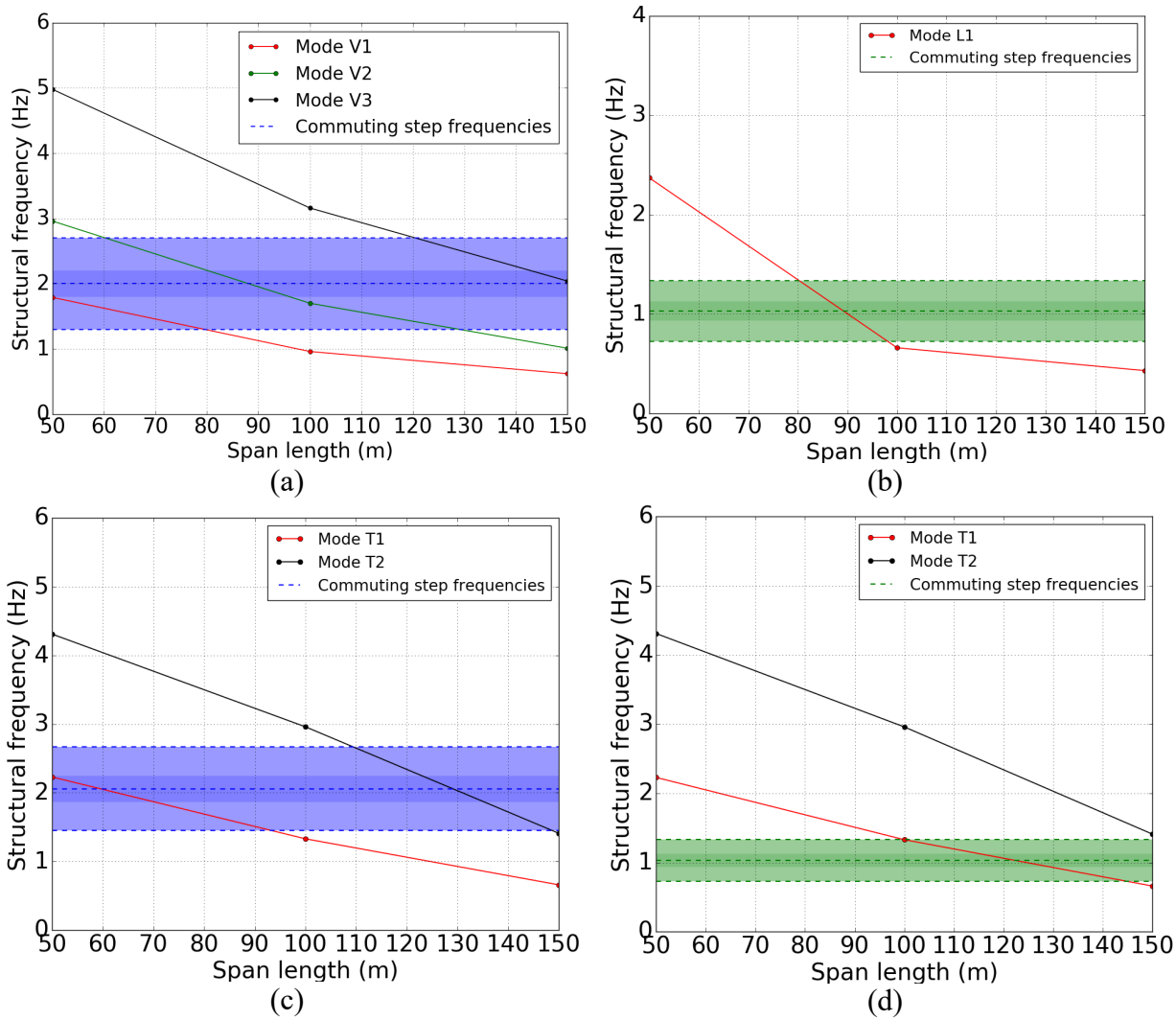


Figure 6.6 Structural (a) vertical, (b) lateral and (c, d) torsional frequencies versus the span length in cable-stayed footbridges with two towers under a pedestrian density of 0.6 ped/m^2 for commuting activities

6.3 Cable-stayed footbridges with an I-shaped pylon without tuned mass dampers

6.3.1 Parametric studies with a span length of 50 m

In this section, the vertical and lateral accelerations along the span length in cable-stayed footbridges with a 50 m span will be presented, where two activities are being studied: commuting

and leisure. In the vertical and lateral direction, the maximum responses, in terms of accelerations, are located at approximately 25 m from the pylon, i.e. at mid-span (Figure 6.7 and Figure 6.8). This distance corresponds to the antinode of the first vertical and lateral mode (see mode V1 and L1 in Table 6.1). The analysis in the frequency domain shows the high contribution of these modes V1 and L1 with frequencies of 1.79 and 2.37 Hz, respectively (Figure 6.9 and Figure 6.10). Mode vertical 1 (V1), and lateral 1 (L1) are critical because these modes are in the range where frequencies can be excited by pedestrians in both directions (Figure 6.6). Furthermore, there are also contributions of torsional modes T1 (Figure 6.6 (c) and (d)).

Figure 6.8 indicates that the lateral accelerations do not achieve the maximum comfort level and that the lock-in effect is not avoided (Lateral accelerations > 0.10 m/s^2). In cases where the maximum comfort level is not achieved, tuned mass dampers will be employed to analyse their effect on the mitigation of the dynamic response.

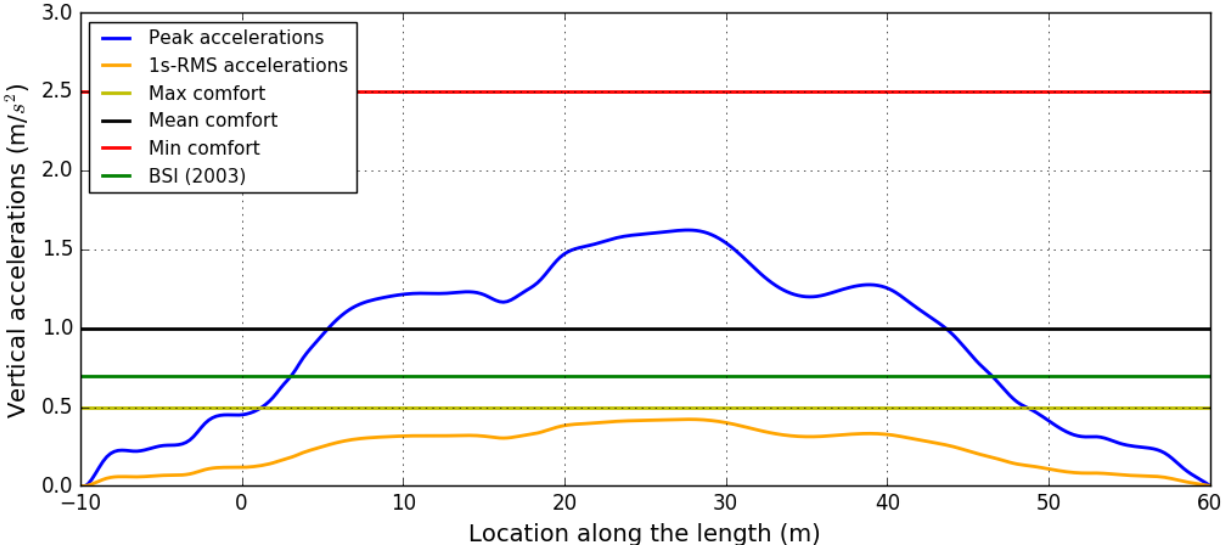


Figure 6.7 Peak and 1s-RMS vertical accelerations for a CSF of a span length of 50 m with two towers under a pedestrian density of 0.6 ped/m^2 for commuting activities

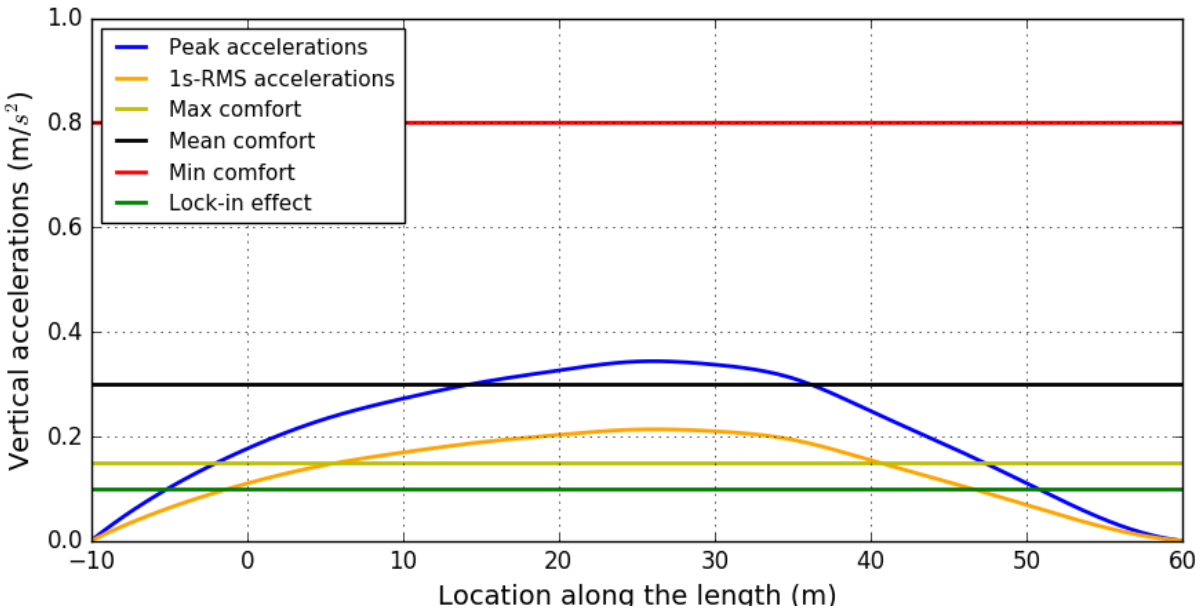
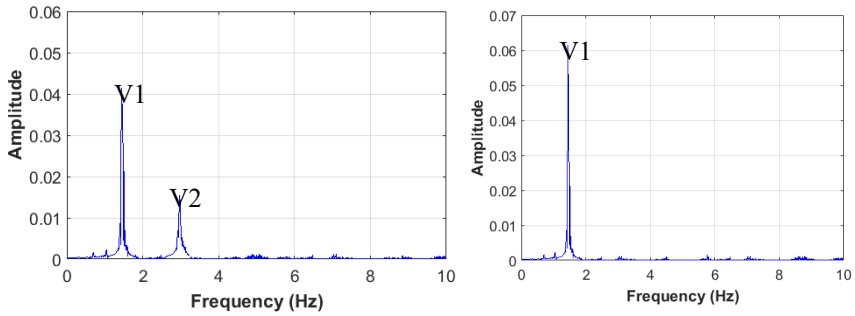
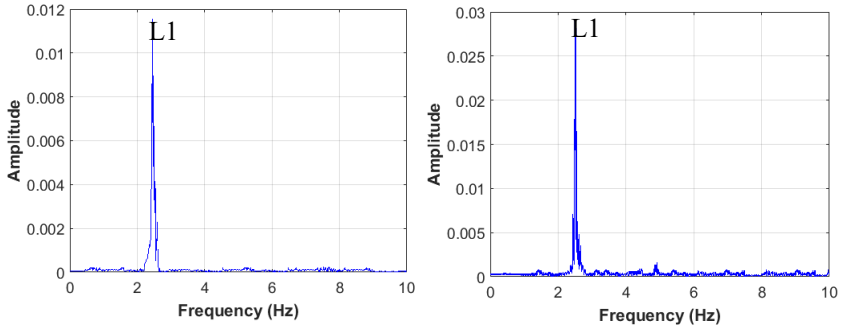


Figure 6.8 Peak and 1s-RMS lateral accelerations for a CSF with a span length of 50 m with two towers under a pedestrian density of 0.6 ped/m^2 for commuting activities



(a) (b)

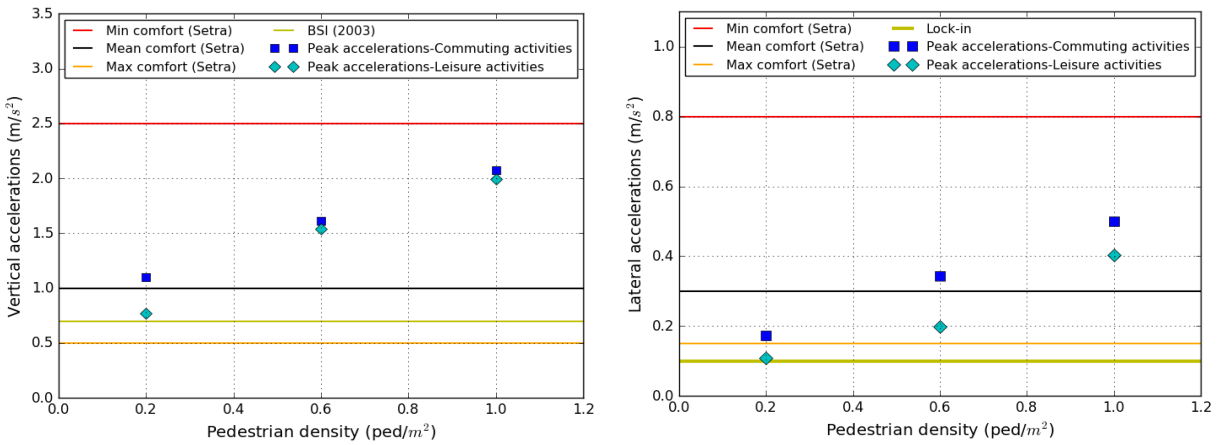
Figure 6.9 Frequency domain analysis at (a) 12.5 m (L/4) and (b) 25.0 m (L/2) from the pylon for a CSF of a span length of 50 m with two towers under a pedestrian density of 0.6 ped/m^2 for commuting activities in the vertical direction



(a) (b)

Figure 6.10 Frequency domain analysis at (a) 12.5 m (L/4) and (b) 25.0 m (L/2) from the pylon for a CSF of a span length of 50 m with two towers under a pedestrian density of 0.6 ped/m^2 for commuting activities in the lateral direction

Figure 6.11 shows the accelerations for different pedestrian densities in the vertical and lateral direction. The vertical accelerations for both activities do not lead to the maximum comfort level. In the lateral direction, the acceleration achieves the maximum comfort level, and only the lock-in effect is slightly avoided when the pedestrian density is 0.2 ped/m^2 for leisure activities (Figure 6.11 (b)). Otherwise, when the pedestrian densities increase, the acceleration also increases, which could cause discomfort to pedestrians (minimum comfort level). Greater differences in the lateral direction among commuting and leisure activities are because for the former, the pedestrian step frequencies are walking with an average lateral frequency of 1.0 Hz which is equivalent to the step frequencies of 2.0 Hz (Figure 6.5). Therefore, the first lateral mode is highly excited by pedestrians in commuter traffic rather than in leisure activities.



(a) (b)

Figure 6.11 Maximum (a) vertical and (b) lateral peak accelerations at mid-span for cable-stayed footbridges with a span length of 50 m for commuting and leisure activities

6.3.2 Parametric studies with a span length of 100 m

Figure 6.12 shows the vertical peak and 1s-RMS acceleration along the span length for commuting activities for a CSF with a span length of 100 m. The comfort level corresponds to a minimum comfort. According to the analysis in the frequency domain in the vertical direction under a pedestrian density of 0.6 ped/m^2 (Figure 6.14), the frequency of the critical mode of the footbridge is 1.70 Hz, which corresponds to the second vertical mode (see mode V2 in Table 6.2). In addition, the mode V2 is in the range where vertical frequencies can be excited by pedestrians. Therefore, this mode is the one that has a larger contribution to the accelerations along the deck (Figure 6.14 (a)), with the exception of the locations closer its modal-shape node at mid-span. However, the maximum accelerations are located at mid-span owing the contribution of the third vertical mode V3 (Figure 6.14 (b)). In the lateral direction, the accelerations correspond to an unacceptable comfort, where the accelerations are above 0.8 m/s^2 (Figure 6.13). In this direction, the critical mode corresponds to the first lateral mode L1 (Figure 6.15). Moreover, there is a contribution of mode T1. This is shown in Figure 6.6 (b) and (d).

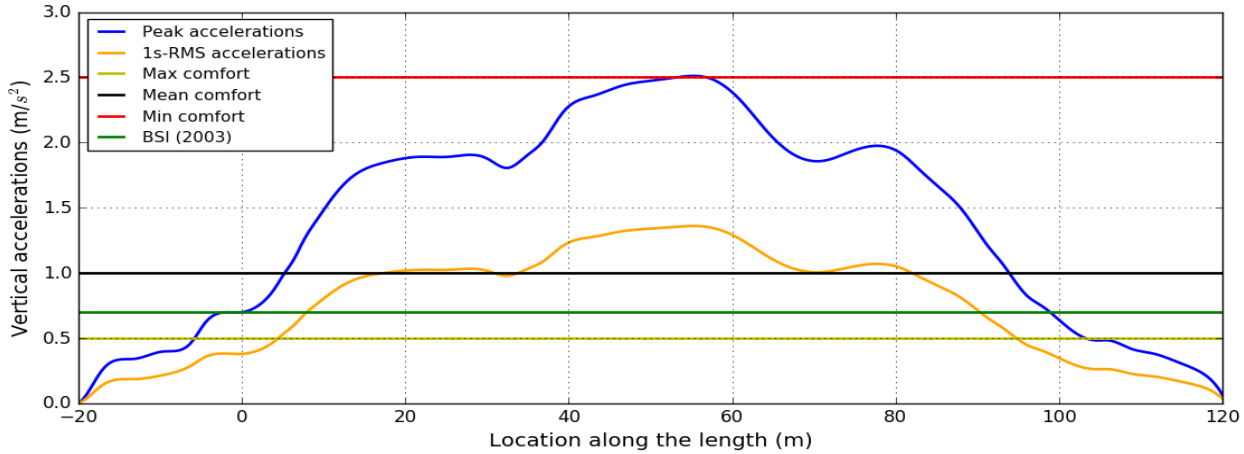


Figure 6.12 Peak and 1s-RMS vertical accelerations for a CSF of a span length of 100 m with two towers under a pedestrian density of 0.6 ped/m^2 for commuting activities

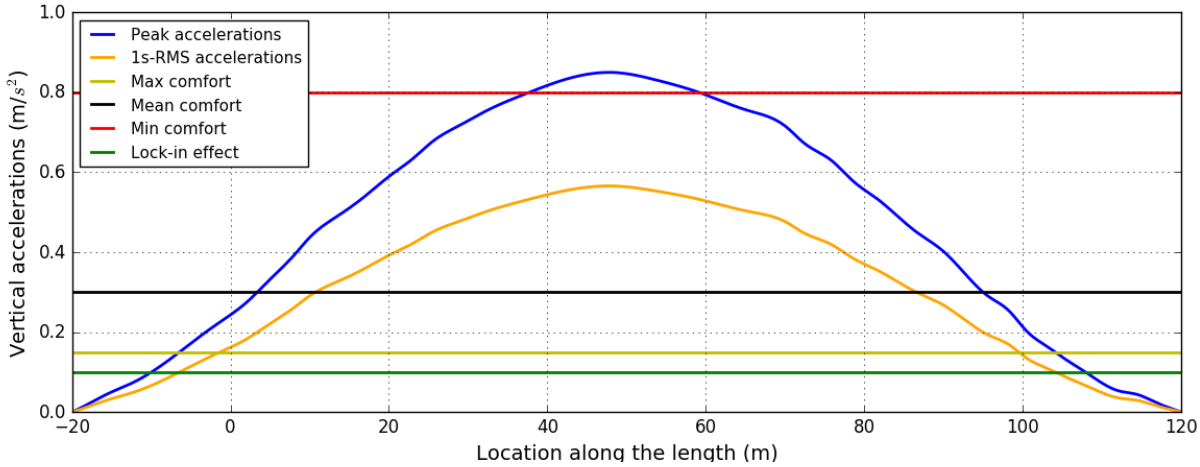
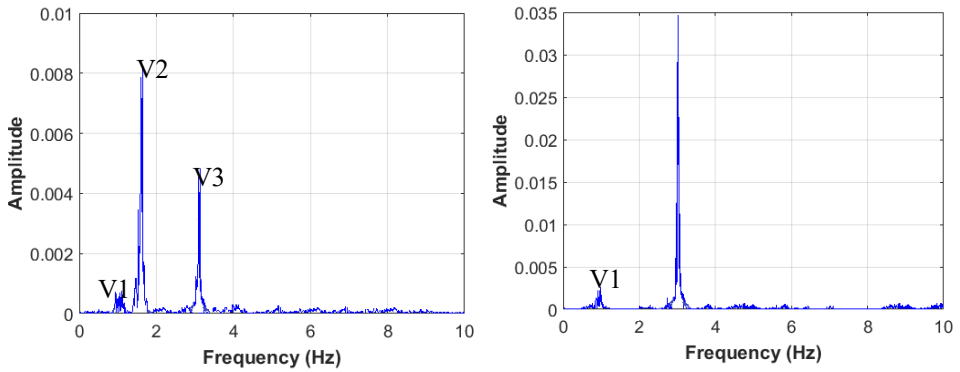


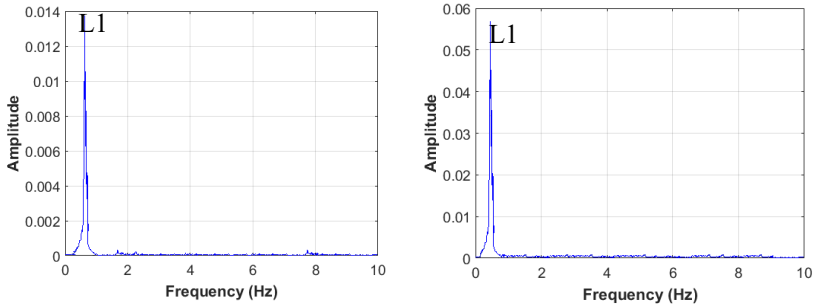
Figure 6.13 Peak and 1s-RMS lateral accelerations for a CSF of a span length of 100 m with two towers under a pedestrian density of 0.6 ped/m^2 for commuting activities

V3



(a) (b)

Figure 6.14 Frequency domain analysis at (a) 25 m (L/4) and (b) 50 m (L/2) from the pylon for a CSF of a span length of 100 m with two towers under a pedestrian density of 0.6 ped/m^2 for commuting activities in the vertical direction

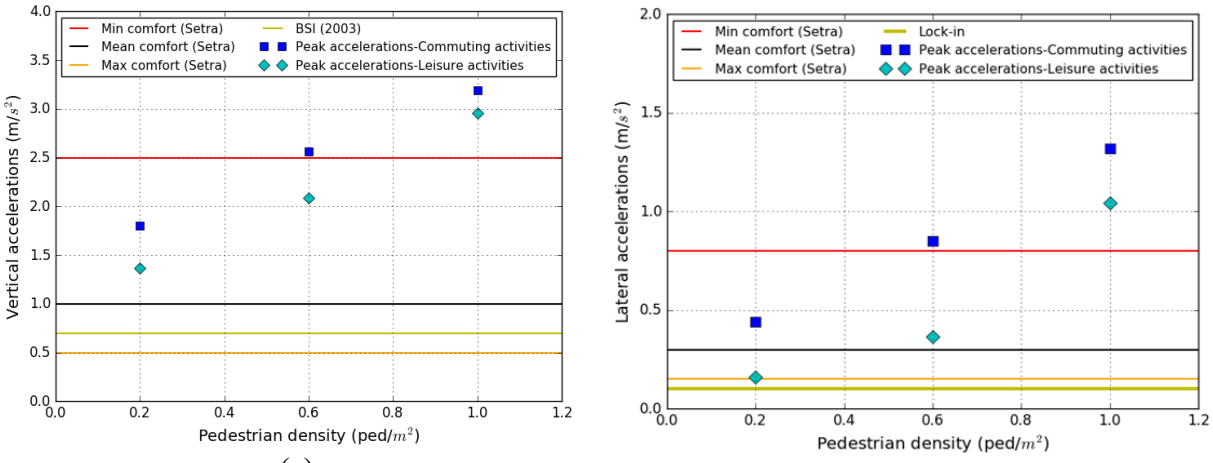


(a) (b)

Figure 6.15 Frequency domain analysis at (a) 25 m (L/4) and (b) 50 m (L/2) from the pylon for a CSF of a span length of 100 m with two towers under a pedestrian density of 0.6 ped/m^2 for commuting activities in the lateral direction

Figure 6.16 shows the vertical and lateral accelerations for different pedestrian densities (0.2, 0.6, and 1.0 ped/m^2) for a cable-stayed footbridge with a span length of 100 m. The same activities were considered here, as they were previously mentioned. Regarding the vertical direction, the accelerations range from mean to an unacceptable degree of comfort (accelerations higher than 1.0 m/s^2). An unacceptable comfort level is obtained for pedestrian densities of 0.6 and 1.0 ped/m^2 for commuting activities and 1.0 ped/m^2 for leisure activities.

In the lateral direction, for any of the pedestrian densities, the lock-in effect is not avoided, and the comfort level varies from mean to unacceptable (Figure 6.16 (b)). For this reason, a thoughtful evaluation regarding the use of tuned mass dampers in the dynamic response should be considered. This will assess the fulfilment of the maximum comfort level in both vertical and lateral direction, avoiding serviceability problems.



(a) (b)

Figure 6.16 Maximum (a) vertical and (b) lateral peak accelerations at mid-span for cable-stayed footbridges with a span length of 100 m with two towers for commuting and leisure activities

6.3.3 Parametric studies with a span length of 150 m

Figure 6.17 and Figure 6.18 show the vertical and lateral accelerations along the length under pedestrian densities of 0.6 ped/m^2 for commuting activities. These accelerations correspond to an unacceptable comfort level. Figure 6.19 and Figure 6.20 show the frequency domain analysis in the vertical and lateral direction for this cable-stayed footbridge. The frequency of the critical mode in the vertical and lateral direction of the footbridge is 2.04 and 0.47 Hz, which corresponds to the third vertical mode (V3) and the first lateral mode (L1), respectively (Table 6.3). According to the frequency domain analysis in the vertical and lateral direction, these modes are critical because they are in the range where frequencies can be excited by pedestrians (Figure 6.6 (a) and (c)). Besides, the T2 mode also has a contribution in both directions (Figure 6.6 (c) and (d)).

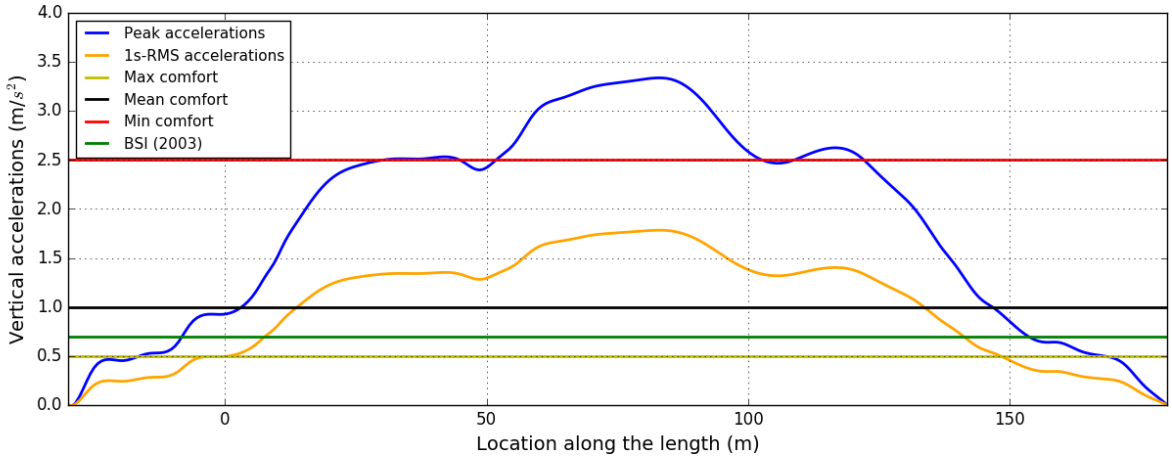


Figure 6.17 Peak and 1s-RMS vertical accelerations for a CSF of a span length of 150 m with two towers under a pedestrian density of 0.6 ped/m^2 for commuting activities

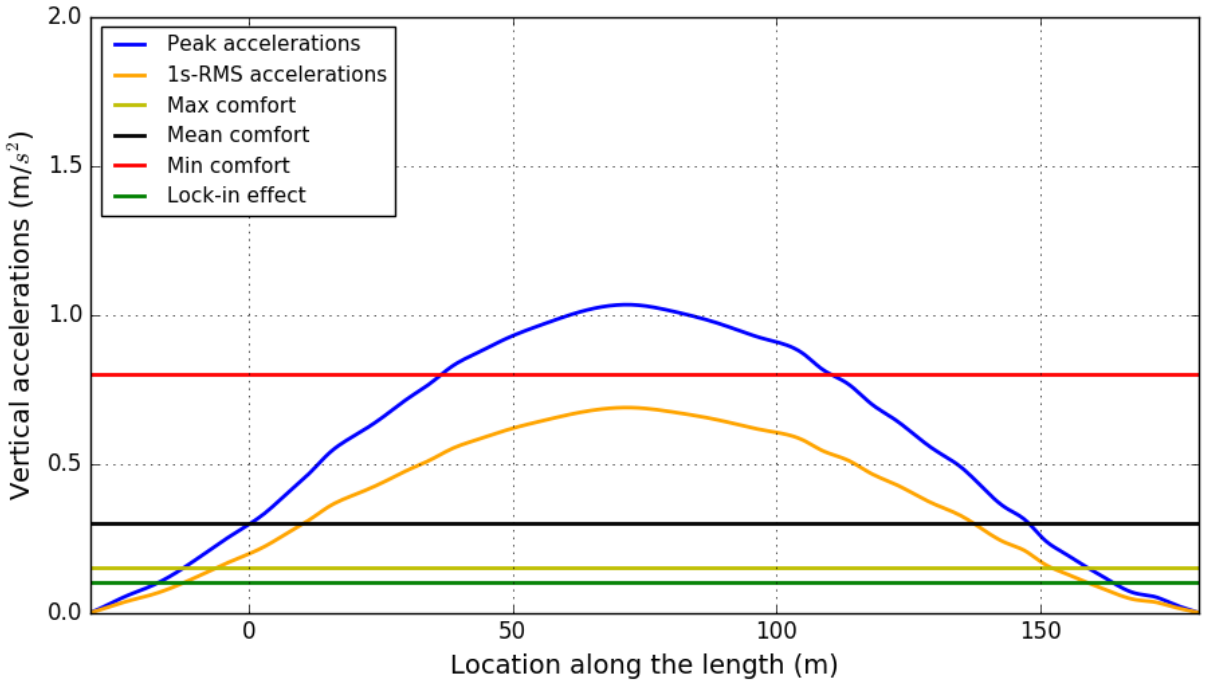
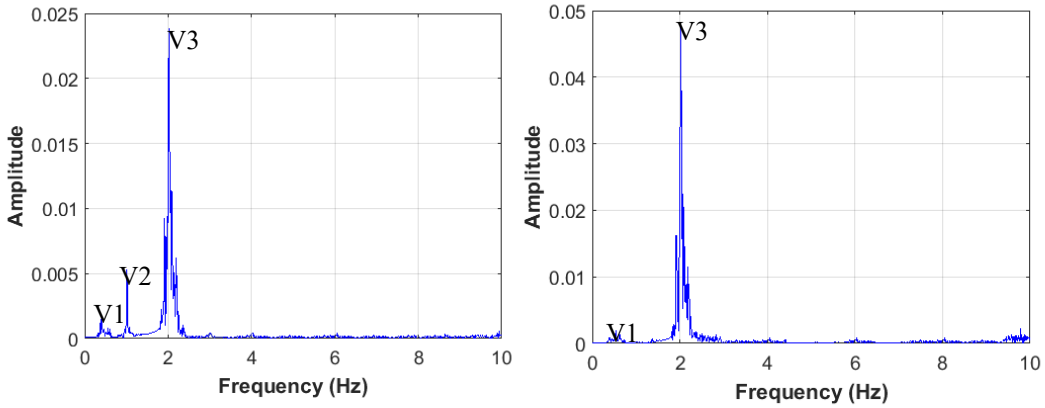
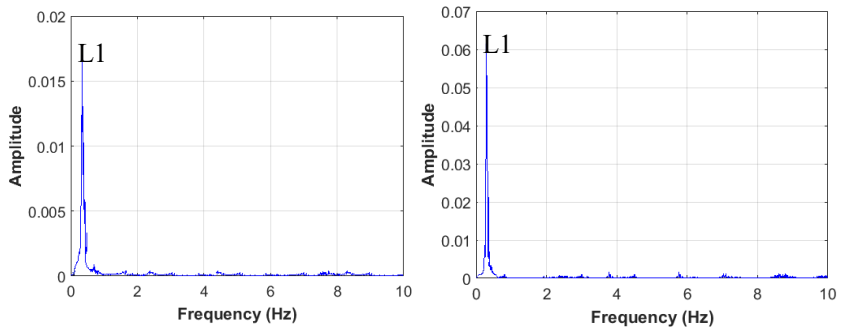


Figure 6.18 Peak and 1s-RMS lateral accelerations for a CSF with a span length of 150 m with two towers under a pedestrian density of 0.6 ped/m^2 for commuting activities



(a) (b)

Figure 6.19 Frequency domain analysis at (a) 37.5 (L/4) and (b) 75.0 m (L/2) from the pylon for a CSF of a span length of 150 m with two towers under a pedestrian density of 0.6 ped/m^2 for commuting activities in the vertical direction

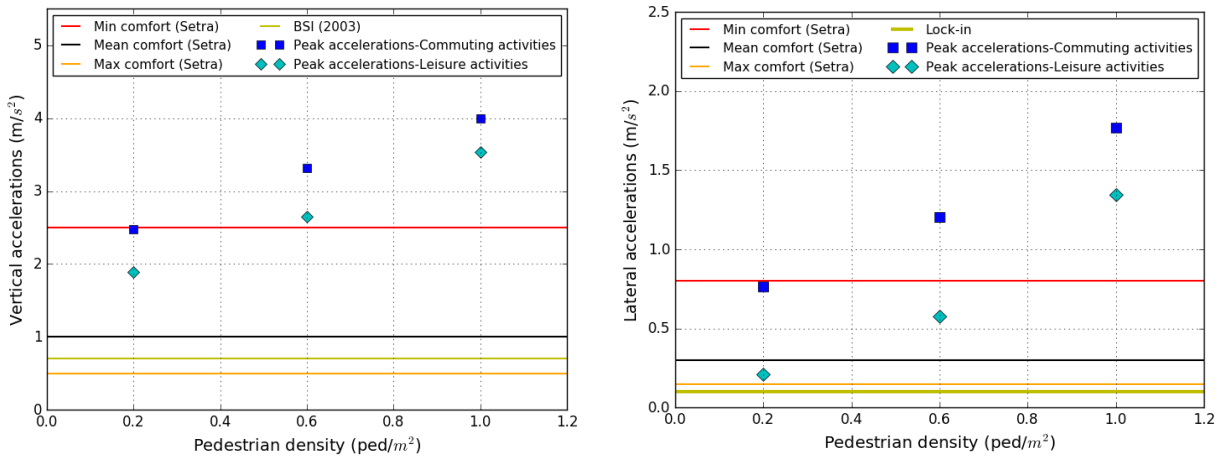


(a) (b)

Figure 6.20 Frequency domain analysis at (a) 37.5 (L/4) and (b) 75.0 m (L/2) from the pylon for a CSF of a span length of 150 m with two towers under a pedestrian density of 0.6 ped/m^2 for commuting activities in the lateral direction

Figure 6.21 (a) shows that the vertical accelerations for commuting and leisure activities range from minimum to uncomfortable comfort. A minimum comfort level is achieved even for low pedestrian densities (0.2 ped/m^2).

In the lateral direction, the accelerations correspond to a comfort level from minimum to uncomfortable for commuting activities and from mean to uncomfortable for leisure activities (Figure 6.21 (b)). For all of the pedestrian densities, the lock-in effect is not avoided. After this evaluation, it can be highlighted that mitigating the dynamic response to get an acceptable comfort level, which can be maximum or mean and avoiding the lock-in effect in the lateral direction, is required. In the next section, the effect of considering different alternatives for the mitigation of the dynamic response will be evaluated.



(a) (b)

Figure 6.21 Maximum (a) vertical and (b) lateral peak accelerations at mid-span for cable-stayed footbridges with a span length of 150 m with two towers for commuting and leisure activities

6.4 Cable-stayed footbridges with an I-shaped pylon with tuned mass dampers

After noticing that the maximum comfort is not achieved in most of the cases for this type of footbridges with a span length of 50, 100 and 150 m, tuned mass dampers are employed. This section will show a variation of TMD's characteristics in order to achieve a mean or maximum comfort level. After performing a frequency domain analysis in the previous section, the nodal coordinates for the modal shape whose frequency has the largest amplitude is selected as the position where the TMD will be located (Section 3.7.1).

6.4.1 Parametric studies with a span length of 50 m

The evaluation of the location of the TMD in the vertical and lateral direction is analyzed herein. In the vertical direction, the maximum reduction of the dynamic response is achieved when the damper is located at 35 m from the left support (i.e., at mid-span). This is the location where the maximum vertical accelerations were registered, and also the location where the critical mode V1 has its anti-node. Moreover, high efficiencies of the TMD are achieved when the TMD is tuned with this mode (V1) and shifted along the span by ±10.0 % of the span length from mid-span (see Table 6.4 and red dots # 3,4,5,6 and 7 in Figure 6.22). This may be convenient for design purpose,

when the location is not convenient at mid-span due to the existence of other structural elements. Otherwise, the efficiency is reduced. This location corresponds to the vibrational frequency that has the greater modal coordinate in this direction (V1 in Figure 6.9). In the lateral direction, the TMD needs to be employed at the location which corresponds to the modal-shape anti-node of the critical mode in this direction, which is also where the maximum lateral accelerations are registered (L1 in Figure 6.10). Similar TMD efficiencies can be achieved if the TMD is shifted from mid-span ±5.0 % of the span length, but the lock-in effect would start to be induced, although the accelerations are almost identical to the threshold of 0.1 m/s^2, and therefore this effect can be neglected (Table 6.5).

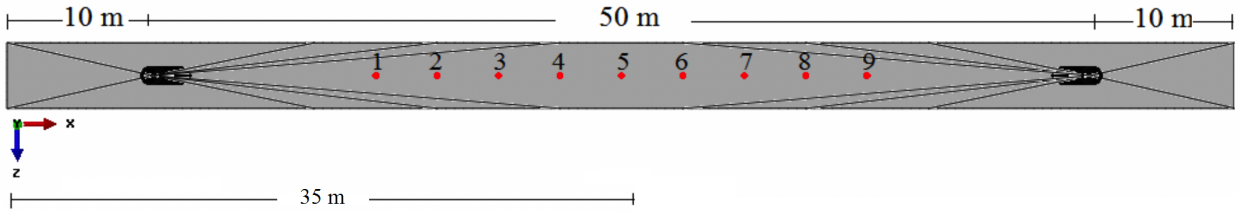


Figure 6.22 Plan view for a CSF with a span length of 50 m with two towers where the red dot #5 corresponds to the nodal coordinates of those modal shapes with a greater contribution (V1) located at 25.0 m (L/2) from the pylon

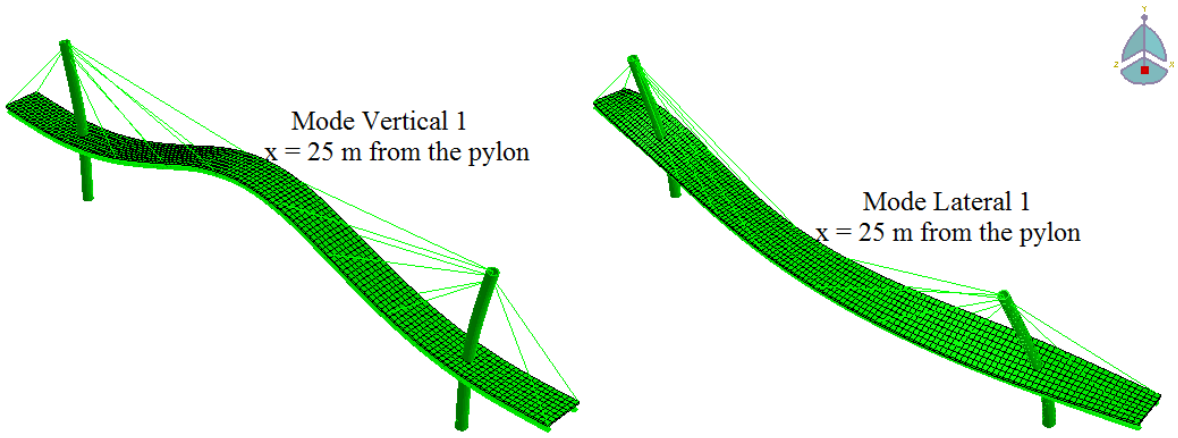
TMD according Figure 6.22	Location of the TMD from the left support /span length (m)	Accelerations with TMD	TMD efficiency (%)
1	0.30	1.032	36%
2	0.35	0.770	52%
3	**0.40**	**0.504**	**69%**
4	**0.45**	**0.460**	**72%**
5	**0.50**	**0.419**	**74%**
6	**0.55**	**0.460**	**72%**
7	**0.60**	**0.505**	**69%**
8	0.65	0.770	52%
9	0.70	1.031	36%

Table 6.4 Peak vertical accelerations and TMD efficiency along the deck for a CSF with a span length of 50 m with two towers under pedestrian densities of 0.6 ped/m^2 for commuting activities when a TMD (μ= 0.06) is located at different abscises along the length

TMD according Figure 6.22	Location of the TMD from the left support /span length (m)	Accelerations with TMD	TMD efficiency (%)
1	0.30	0.247	28%
2	0.35	0.206	40%
3	0.40	0.147	57%
4	**0.45**	**0.116**	**66%**
5	**0.50**	**0.099**	**71%**
6	**0.55**	**0.115**	**66%**
7	0.60	0.147	57%
8	0.65	0.204	40%
9	0.70	1.245	28%

Table 6.5 Peak lateral accelerations and TMD efficiency along the deck for a CSF with a span length of 50 m (L/2) with two towers under pedestrian densities of 0.6 ped/m^2 for commuting activities when a TMD (μ= 0.03) is located at different abscises along the length

Figure 6.23 shows where the vertical and lateral TMDs were located after carried out the analyses to choose the optimum location for the device in the vertical and lateral direction. In practice, they cannot be located at the same location, but it has been shown before that there is a certain flexibility to establish the location along the length while maintaining its efficiency. In the vertical direction, when a TMD mass ratio of 0.06 is employed for commuting activities, the TMD efficiency is 74% (Figure 6.24). This fulfils a maximum comfort level. In addition, the lateral accelerations avoid the lock-in effect when a TMD mass ratio of 0.03 is employed (Figure 6.25).



(a) (b)

Figure 6.23 Maximum nodal coordinates for modal shapes dominating the response where the tuned mass damper is located in the vertical and lateral direction for a cable-stayed footbridge with a span length of 50 m with two towers

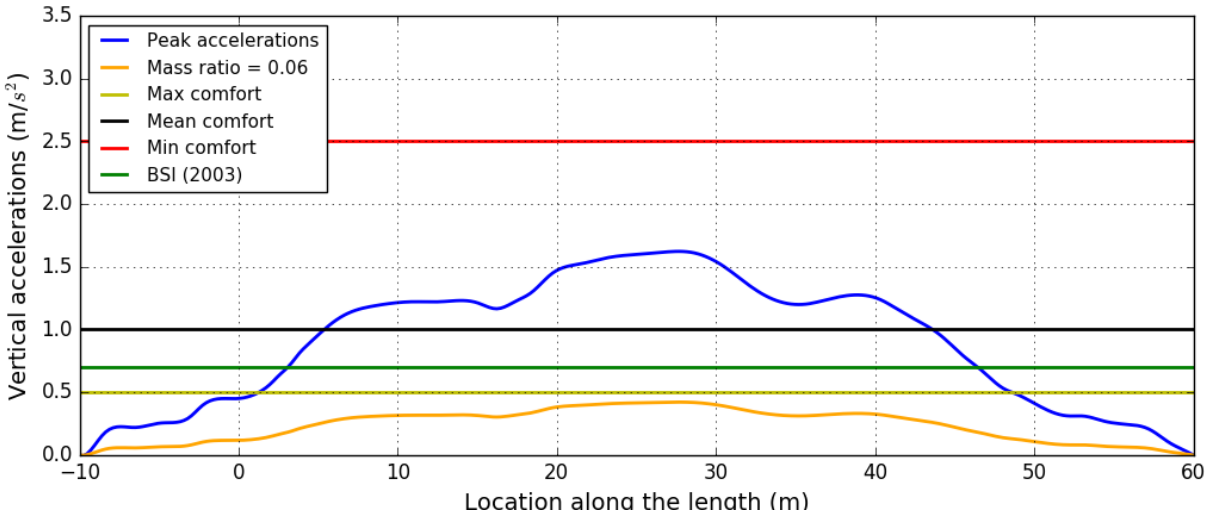


Figure 6.24 Peak vertical accelerations for a cable-stayed footbridge with a span length of 50 m with two towers under a pedestrian density of 0.6 ped/m^2 when a TMD (μ= 0.06) located at 25 m (L/2) from the pylon is employed for commuting activities

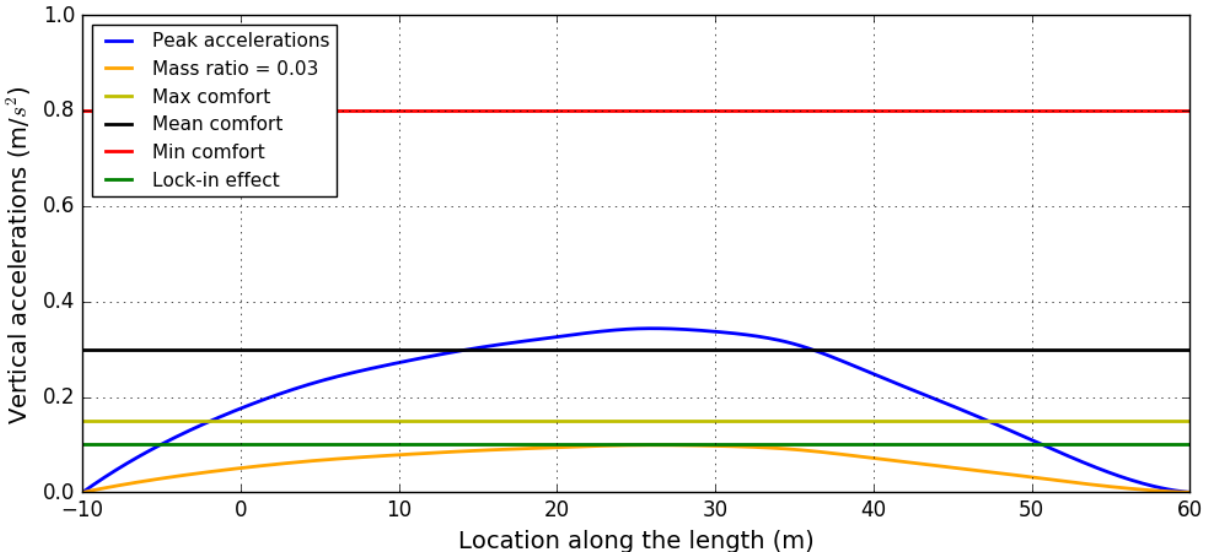


Figure 6.25 Peak lateral accelerations for a cable-stayed footbridge with a span length of 50 m with two towers under a pedestrian density of 0.6 ped/m^2 when a TMD (μ= 0.03) located at 25 m (L/2) from the pylon is employed for commuting activities

Figure 6.26 shows the TMD's mass ratio to mitigate the human-induced vibrations for a range of pedestrian densities according to the comfort level. The TMD mass ratio in vertical direction

ranging from 0.03 to 0.07 for commuting activities and from 0.01 to 0.07 for leisure activities. The more significant TMD efficiency is achieved when the device is located at the maximum nodal coordinates for the modal shape whose frequency has the largest amplitude (Table 6.4). At this location, the comfort level increases as long as the TMD mass ratio is chosen correctly. For instance, for a TMD mass ratio of 0.06 when the pedestrian density is 1.0 ped/m^2, the TMD efficiency for commuting activities is 69% with a mean comfort level. Besides, for a TMD mass ratio of 0.07, the TMD efficiency increases 8%, achieving a maximum comfort level. Likewise, to what occurs for commuting activities, for leisure activities, the TMD efficiency increases from 65% (mean comfort level) to 73% (maximum comfort level). Given that the characteristics of this bridge were obtained as representative of the built cable-stayed footbridges with two towers, these graphs may be useful for preliminary design to have an indication of the supplemental damping that is required in similar footbridges structures.

In the lateral direction, the maximum comfort level avoiding the lock-in effect for commuting activities can be achieved with TMD mass ratios of 0.01, 0.03, and 0.07, for 0.2, 0.6, and 1.0 ped/m^2, respectively (Figure 6.27 (a)). On the other hand, for leisure activities in the lateral direction, a TMD mass ratio of 0.01 and 0.06, for 0.6 and 1.0 ped/m^2, respectively, is required (Figure 6.27 (b)). For these cases, the TMD reduced the dynamic response up to 81%. For instance, for leisure activities, the maximum peak lateral accelerations drop from 0.404 to 0.079 m/s^2 when using a TMD mass ratio of 0.06 (TMD efficiency of 80%).

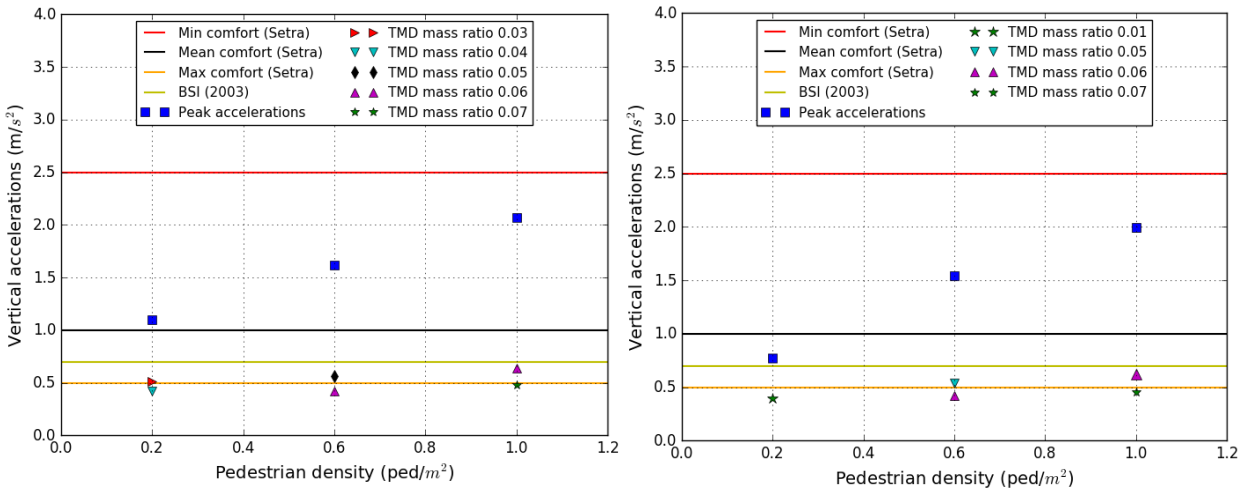


Figure 6.26 Peak vertical accelerations for cable-stayed footbridges with a span length of 50 m with two towers under pedestrian densities of 0.2, 0.6 and 1.0 ped/m^2 when different TMD mass ratios are considered for (a) commuting and (b) leisure activities

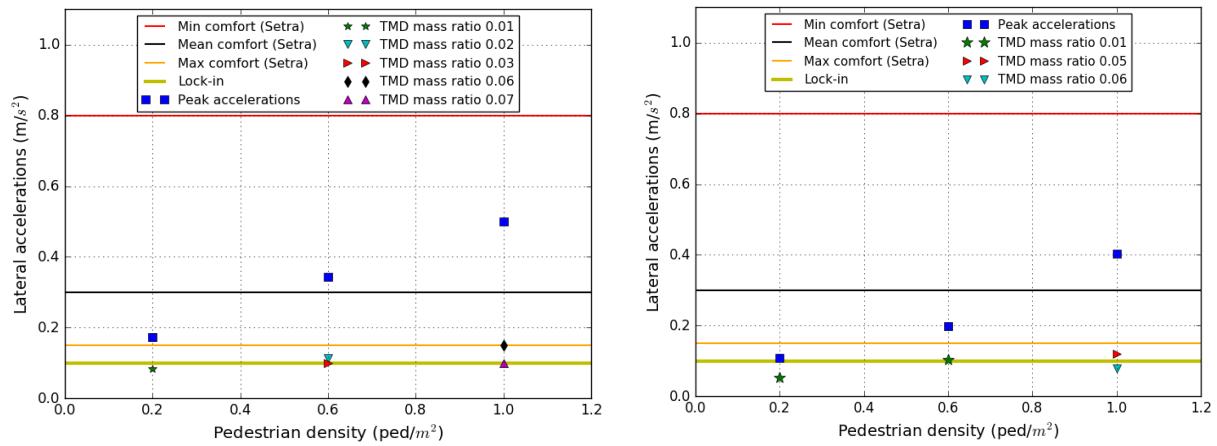


Figure 6.27 Peak lateral accelerations for cable-stayed footbridges with a span length of 50 m with two towers under pedestrian densities of 0.2, 0.6 and 1.0 ped/m^2 when different TMD mass ratios are considered for (a) commuting and (b) leisure activities

6.4.1.1 Reduction of internal forces when a TMD is deployed

At resonance, when L = 25 m from the pylon, the dynamic amplification factor (DAF) of the bending moments at mid-span is 2.21. Nevertheless, the implementation of a TMD reduces the total, and the dynamic bending moments by 27 and 37% respectively, reducing the DAF to 1.62. The static bending moment induced by the weight of the pedestrians is also represented.

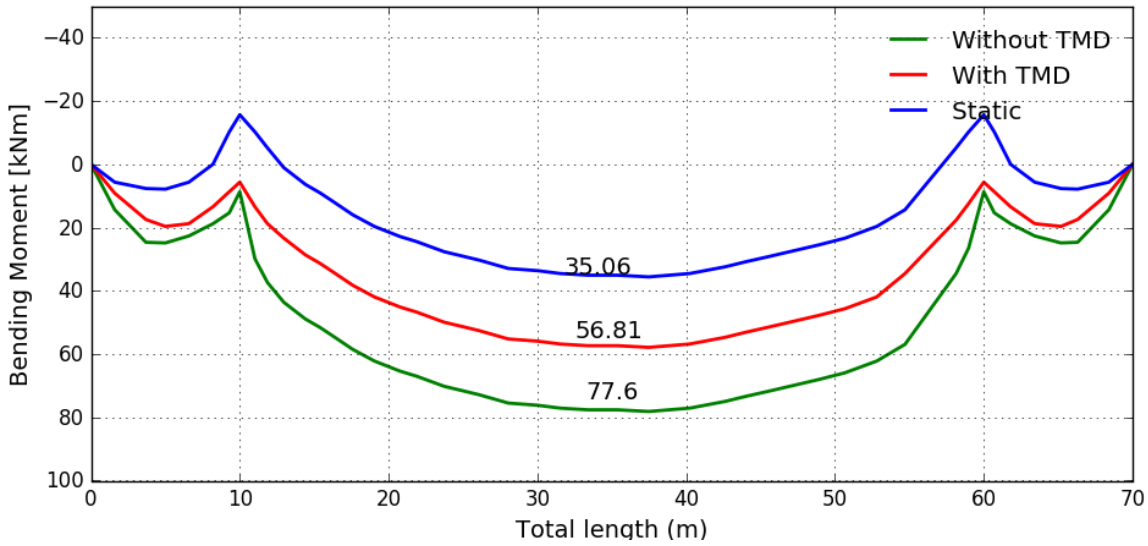
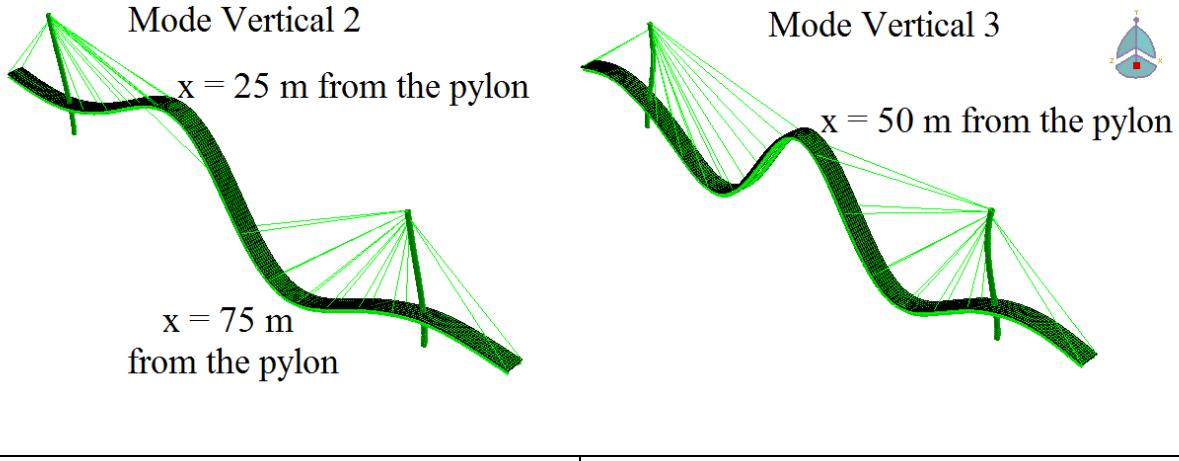


Figure 6.28 Sagging bending moments along the length before and after a TMD (μ= 0.06) is employed at 25 m (L/2) from the pylon in a 50 m span cable-stayed footbridge with two towers considering a pedestrian density of 0.6 ped/m^2 for commuting activities

6.4.2 Parametric studies with a span length of 100 m

After checking that the cable-stayed footbridge with a span length of 100 m does not achieve the maximum comfort without tuned mass dampers, the effect of employing TMDs to reduce these accelerations are studied herein. Two options are considered, locating a TMD to reduce the vibrations induced either by the critical mode V2, or by the mode V3 that generated the largest accelerations along the deck. Table 6.6 shows two cases that were analysed using tuned mass dampers in the cable-stayed footbridge with a span length of 100 m. After the TMD's implementation, the largest TMD efficiency is achieved when two TDMs (Case a) are employed at the maximum nodal coordinates for the modal shape that dominates the response, i.e., the second

vertical mode V2 (Figure 6.14). If the TMD is not located at this position, the efficiency decreases significantly. This is because it is not tuned to the frequency that dominates the response. For instance, the case b) in Table 6.6 where the TMD efficiency is of 38%. Besides, as the Mode Vertical 3 is not the mode that dominates the response, the mass is smaller in comparison of V2 (Table 6.6). Therefore, tuned mass dampers should be tuned and located at the maximum displacement of the mode that dominates the response (Figure 6.29).



Case a: 2 TMDs tuned and located at mode V2 (Total μ = 0.11, modal mass 191623 kg) TMD efficiency = 82%	**Case b:** 1 TMD tuned and located at mode V3 (μ = 0.11, modal mass 150870 kg) TMD efficiency = 38%

Table 6.6 Location where the tuned mass dampers were employed for the parametric studies for a CSF with two towers with a span length of 100 m

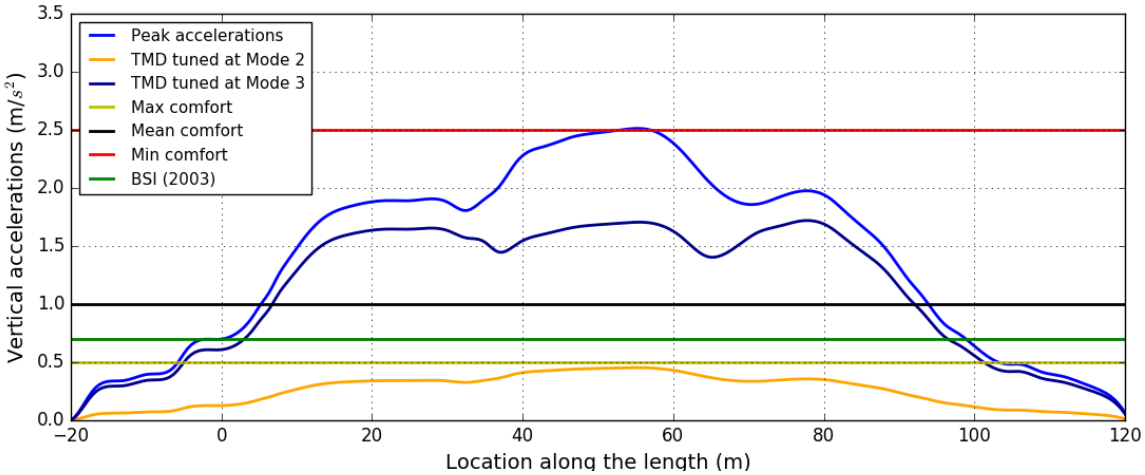
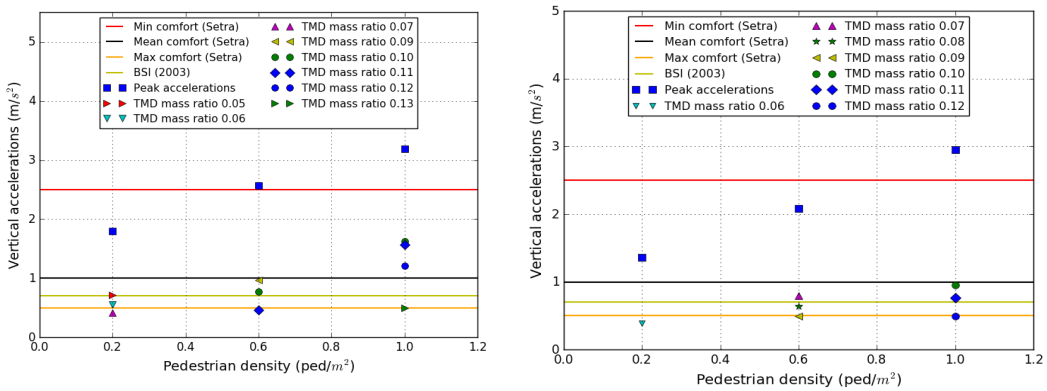


Figure 6.29 Peak vertical accelerations for a cable-stayed footbridge with a span length of 100 m with two towers under a pedestrian density of 0.6 ped/m^2 for commuting activities when TMDs are employed according to Table 6.6

Figure 6.30 shows the effect in the accelerations after employing the TMDs in the vertical direction with different mass ratio's values. Notice that the dynamic response is highly reduced. For instance, when it is evaluated a pedestrian density of 0.2 ped/m^2 for commuting activities, the maximum peak accelerations drop from 1.799 to 0.414 m/s^2. This occurs when a total TMD mass ratio of 0.07 (TMD efficiency approximately 77%) is used for the analysis. Similar efficiencies have been observed for leisure activities (TMD efficiency of up to 83%).

However, for commuting and leisure activities under 1.0 ped/m^2, higher mass ratios are necessary. For both circumstances, the case of using more than two TMDs located at the maximum nodal displacement ±10.0 % instead of a unique device is also analysed. For instance, for commuting activities, the total TMD mass corresponds to 28.265 kg, where the TMD mass ratio is equal to 0.13, with a modal mass of 217.423 kg. Therefore, an analysis considering four and six dampers were performed, with 7.066 kg and 4.711 kg, respectively. After performing this analysis, a maximum comfort level is achieved, obtaining accelerations below 0.5 m/s^2. The maximum comfort level is achieved for all the cases, either when bigger dampers are used or when the TMD is split into smaller ones. Nevertheless, it is essential to highlight that handling TMDs with bigger mass (more than 6.000 kg) becomes more complicated due to logistic reasons (shipment) and operational problems at the site (installation) (Benicke, 2017). Therefore, it is still necessary to

evaluate an alternative solution to provide recommendations where smaller devices are considered. Ramos-Moreno (2015) demonstrated that increasing the slab depth is the most efficient way of reducing the deck accelerations, without implementing supplemental damping devices. Therefore, the implementation of damping devices will be combined with additional slab depth.



(a) (b)

Figure 6.30 Peak vertical accelerations for cable-stayed footbridges with a span length of 100 m with two towers under pedestrian densities of 0.2, 0.6 and 1.0 ped/m^2 when different TMD mass ratios are considered for (a) commuting and (b) leisure activities

Figure 6.31 shows the dynamic analysis when the slab depth is increased from 0.2 to 0.3 m. The dynamic response is reduced approximately 65% from minimum or unacceptable comfort to mean comfort level. As these accelerations do not achieve the maximum comfort level, in the next part will be included an analysis of employing tuned mass dampers for these cases.

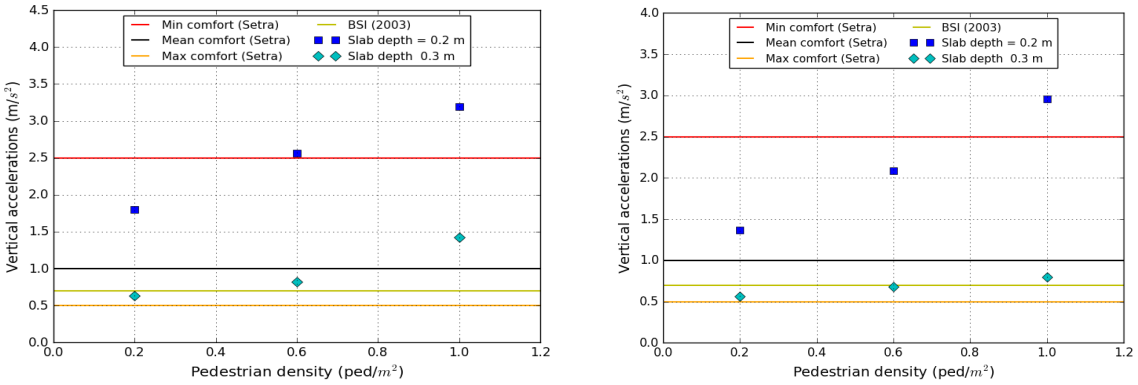


Figure 6.31 Comparison of the vertical peak accelerations using a slab depth of 0.2 and 0.3 m for cable-stayed footbridges with a span length of 100 m with two towers using different pedestrian scenarios for a) commuting and b) leisure activities

There was a high reduction in the accelerations after the slab depth was increased. However, for some of these cases, they do not achieve the maximum comfort level. For this reason, the additional effect of using tuned mass dampers in the vertical direction for commuting and leisure activities for the cases where the comfort level is not maximum is analysed (Figure 6.32). The maximum comfort level for commuting activities is achieved by including tuned mass dampers with a TMD mass ratio ranging from 0.01 to 0.03 into the analysis. This provides the maximum comfort level according to the Setra guideline, with a reduction of approximately 56%. For leisure activities, a TMD mass ratio among 0.01 to 0.02 is required to achieve maximum comfort level.

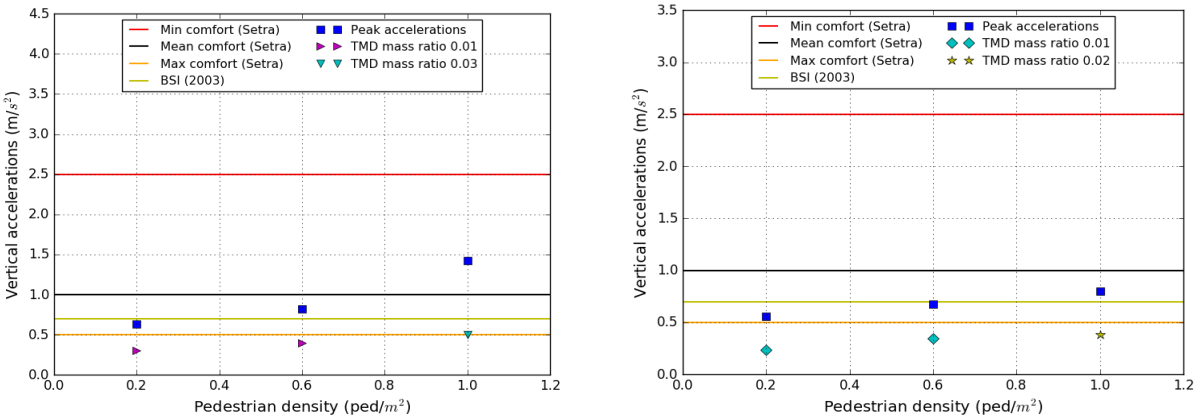
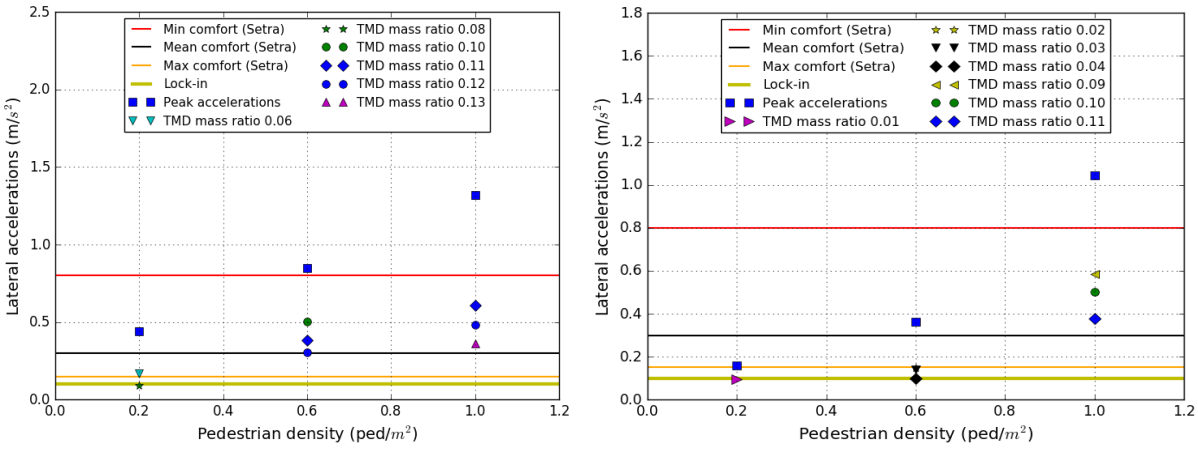


Figure 6.32 Vertical peak accelerations with tuned mass dampers using a slab depth of 0.3 m for cable-stayed footbridges with a span length of 100 m with two towers using different pedestrian scenarios for (a)commuting and (b) leisure activities

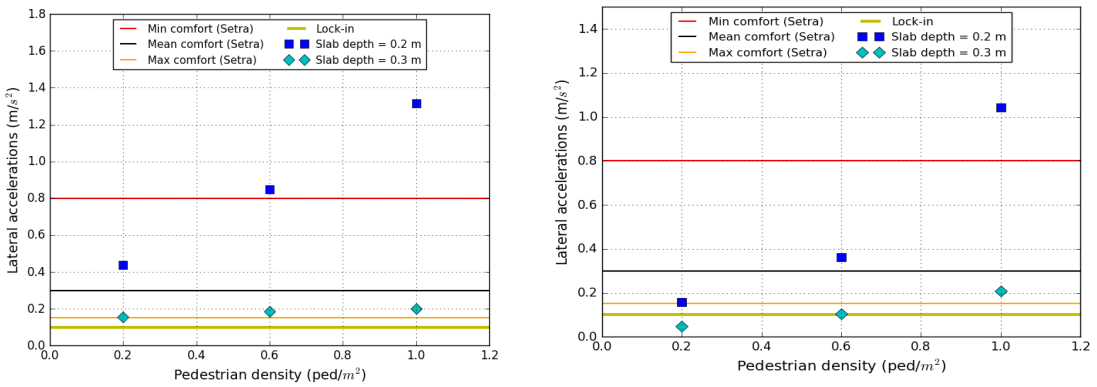
Figure 6.33 shows that the comfort level for lateral accelerations when a slab depth of 0.2 is employed varies from minimum to uncomfortable for commuting and leisure activities. For this reason, the effect on the dynamic response when one tuned mass damper is employed in the first lateral mode was evaluated. After this implementation, the lock-in effect is avoided for pedestrian densities of 0.2 ped/m^2 in commuting and leisure activities, and for 0.6 ped/m^2 in leisure activities. The maximum comfort for pedestrian densities of 1.0 ped/m^2 for commuting activities and leisure activities is not achieved (accelerations > 0.30 m/s^2), although the TMD mass ratio is more than 0.11 (TMD mass = 14735 kg). For handling reasons, it is necessary to analyse different possible solutions to choose a feasible solution to mitigate the dynamic response. The effect of splitting one tuned mass damper into two (halving the mass m, the stiffness k, and the damping c, and maintaining the TMD frequency and damping ratio) in the first lateral mode is analysed. As expected, it was observed that splitting one TMD does not have any impact on the TMD system efficiency.



(a) (b)

Figure 6.33 Peak lateral accelerations for cable-stayed footbridges with a span length of 100 m with two towers under pedestrian densities of 0.2, 0.6 and 1.0 ped/m^2 when different TMD mass ratios are considered for (a) commuting and (b) leisure activities

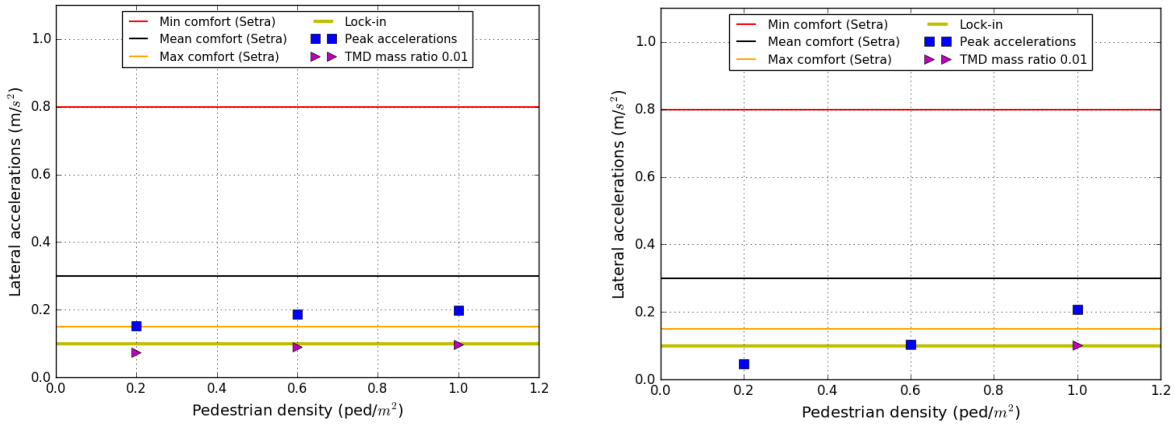
It has been observed that in the lateral direction the serviceability criteria corresponded to mean or minimum comfort level. In most of these cases, there is a potential risk of the pedestrians locking-in or synchronizing with the vibrations of the structure in the lateral direction. This happened even when bigger tuned mass dampers (TMD's mass > 10.000 kg) were employed. Therefore, an alternative solution to achieve the maximum comfort level will be evaluated herein. The alternative considered here is combining the implementation of TMDs and increasing the slab depth from 0.2 to 0.3 m (Figure 6.34). From these figures, it can be observed that the dynamic response is reduced by approximately 75% when the slab is increased so that increasing the slab depth is an optimal solution to reduce the unstable lateral accelerations.



(a) (b)

Figure 6.34 Comparison of the lateral peak accelerations using a slab depth of 0.2 and 0.3 m for cable-stayed footbridges with a span length of 100 m with two towers using different pedestrian scenarios for a) commuting and b) leisure activities

The high reduction in the dynamic response when the slab depth is increased from 0.2 to 0.3 m is essential to note. However, in most of these cases, the serviceability criteria do not correspond to the maximum comfort level. For these cases, tuned mass dampers (Figure 6.35) were employed to avoid the lock-in effect and to achieve the maximum degree of comfort level. With a slab depth of 0.3 m, the TMD mass ratio required to achieve the maximum comfort level avoiding the lock-in effect is 0.01 for commuting and leisure activities.

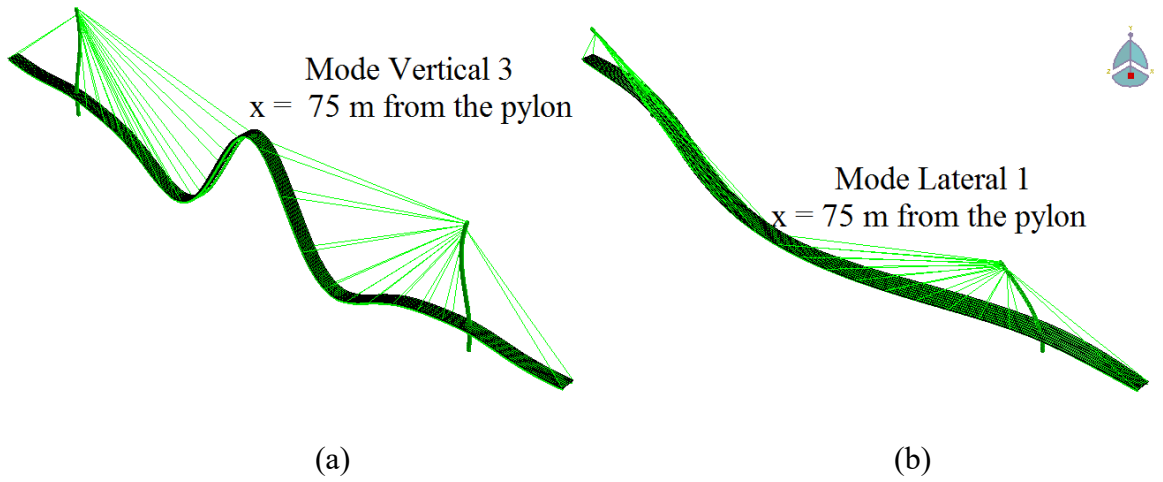


(a) (b)

Figure 6.35 Lateral peak accelerations with tuned mass dampers using a slab depth of 0.3 m for cable-stayed footbridges with a span length of 100 m with two towers using different pedestrian scenarios for (a) commuting and (b) leisure activities

6.4.3 Parametric studies with a span length of 150 m

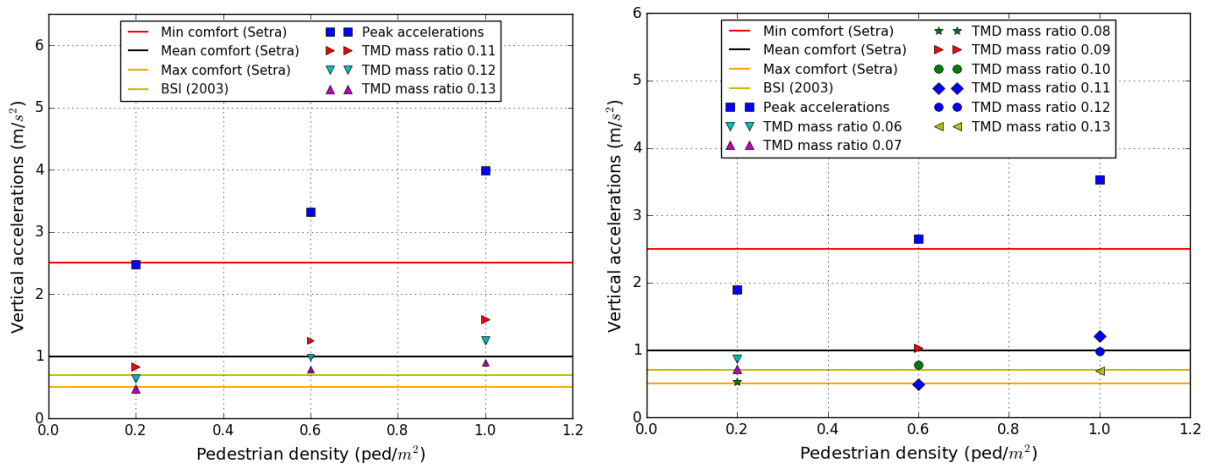
Once it was found that the accelerations do not achieve the maximum comfort level without supplemental damping devices, the effect of using TMDs with different mass ratios, as well as the combined effect of implementing TMDs and increasing the slab depth, is assessed. The TMD is located at the maximum nodal coordinates for the modal shape that dominates the response, V3 in vertical (see Figure 6.6 (a) and Figure 6.19) and L1 in lateral (see Figure 6.6 (b) and Figure 6.20) and are tuned to the frequencies of these particular modes (Figure 6.36).



(a) (b)

Figure 6.36 Maximum nodal coordinates for modal shapes with a larger contribution in the critical acceleration for the (a) third vertical mode (V3) and, the (b) first lateral mode (L1)

Figure 6.37 shows representative information of the tuned mass dampers that are necessary depending on which degree of comfort level is required in the vertical direction for commuting and leisure activities. The mean comfort level for commuting activities is achieved by employing a TMD mass ratio ranging from 0.11 to 0.13. It is also worth noting that for leisure activities, a TMD mass ratio ranging from 0.06 to 0.12 is required to achieve a mean comfort level. A maximum comfort level can be achieved for 0.2 ped/m^2 for commuting and leisure activities with a TMD mass ratio of 0.13 and 0.08, respectively, and for 0.6 ped/m^2 in leisure activities is necessary a TMD mass ratio of 0.11.



(a) (b)

Figure 6.37 Peak vertical accelerations for cable-stayed footbridges with a span length of 150 m with two towers under pedestrian densities of 0.2, 0.6 and 1.0 ped/m^2 when different TMD mass ratios are considered for (a) commuting and (b) leisure activities

A similar procedure is developed for the evaluation of the tuned mass dampers in the lateral direction. For the case of commuting activities, Figure 6.38 (a) shows that although a high TMD mass ratio is employed, the accelerations do not fulfil the maximum comfort level if the bridge is loaded with a pedestrian density of 0.6 and 1.0 ped/m^2. For leisure activities (Figure 6.38 (b)), it is necessary to have a TMD mass ratio of 0.04 and 0.09 to avoid the lock-in effect and to achieve the maximum comfort level for 0.2 and 0.6 ped/m^2; however, for a pedestrian density of 1.0 ped/m^2, a TMD mass ratio of 0.11 is employed, and the lock-in effect is not avoided.

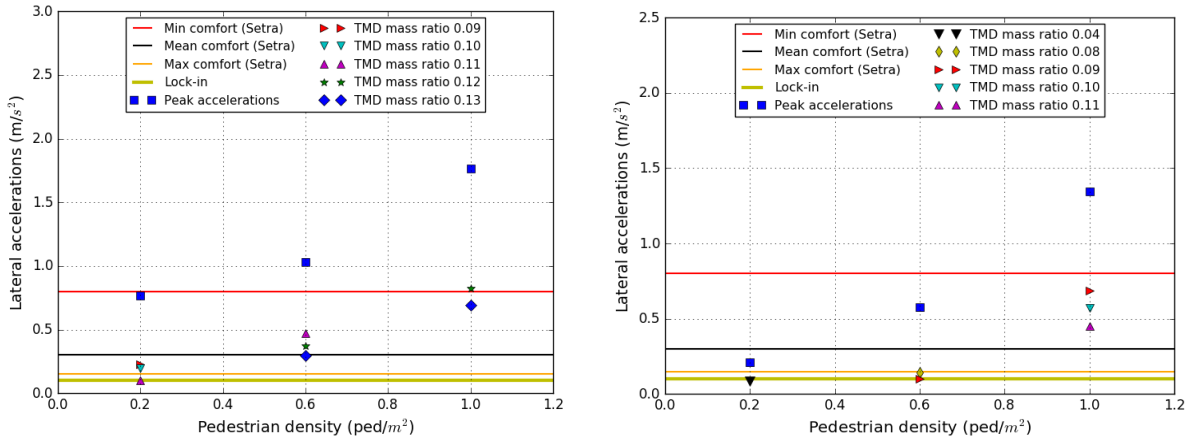
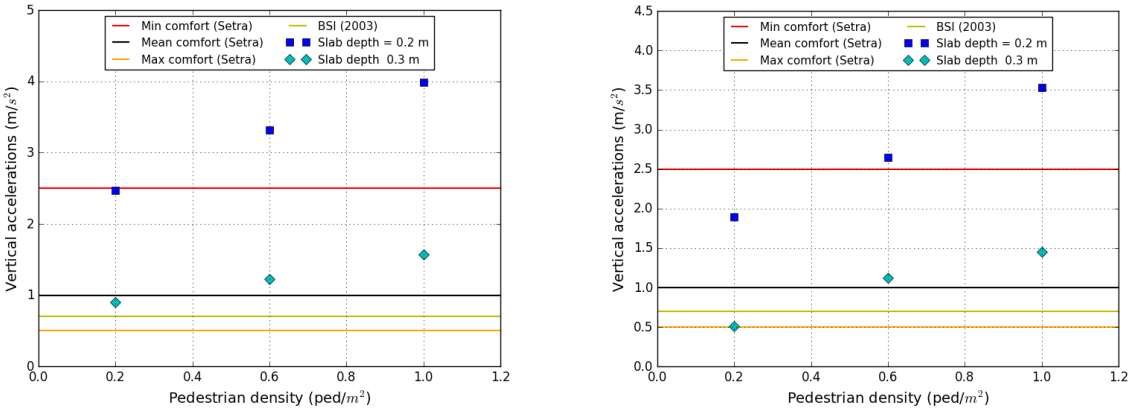


Figure 6.38 Peak lateral accelerations for cable-stayed footbridges with a span length of 150 m with two towers under pedestrian densities of 0.2, 0.6 and 1.0 ped/m^2 when different TMD mass ratios are considered for (a) commuting and (b) leisure activities

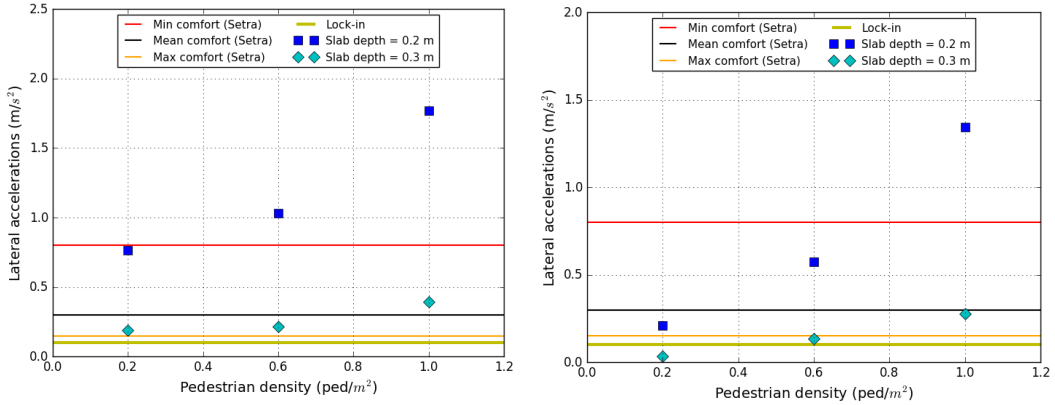
The previous cases show that although a high TMD mass ratio is employed, the maximum comfort level cannot be achieved for most of the cases. Therefore, the influence of changing the slab depth from 0.2 to 0.3 m is evaluated, as recommended by Ramos-Moreno (2015), and it is taken in this case as an additional measure to implementing TMDs. Figure 6.39 (a) depicts the comparison of the vertical accelerations for commuting activities for both slab depths (0.2 and 0.3 m). The high reduction in the dynamic response is noticed when a slab depth of 0.3 m is employed instead of using a slab depth of 0.2 m (approximately 63 %). However, the comfort level for these accelerations is in the range of mean to minimum. Similarly, to this analysis, the accelerations for leisure activities were evaluated (Figure 6.39 (b)). The high TMD efficiency (approximately 62%) can be seen in the reduction of the dynamic response.



(a) (b)

Figure 6.39 Comparison of the vertical peak accelerations using a slab depth of 0.2 and 0.3 m for cable-stayed footbridges with a span length of 150 m with two towers using different pedestrian scenarios for (a) commuting and (b) leisure activities

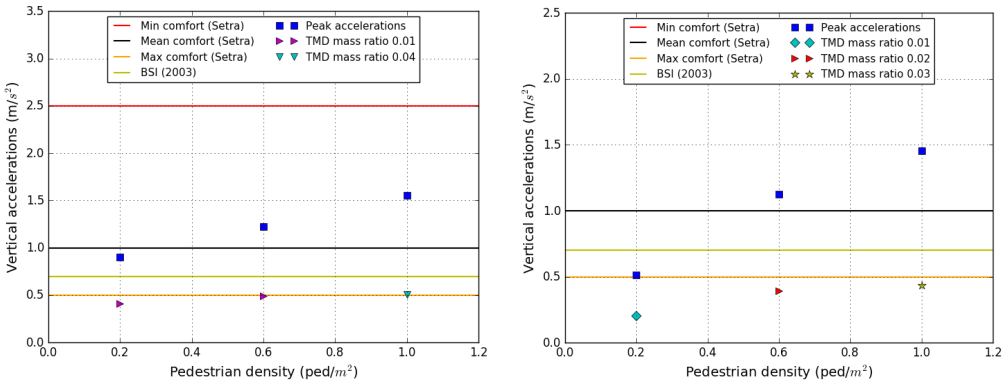
This increase of the slab depth from 0.2 to 0.3 m was also beneficial for the reduction of the lateral accelerations, as the lock-in effect was not avoided for commuting and leisure activities with a slab depth of 0.2 m. A high reduction in the accelerations (TMD efficiency approximately 78%) is achieved with this measure, as shown in Figure 6.40. It is found that the accelerations correspond to a mean comfort level. Therefore, when the slab depth increases, the weight of the structure increases, conveying a reduction of the accelerations.



(a) (b)

Figure 6.40 Comparison of the lateral peak accelerations using a slab depth of 0.2 and 0.3 m for cable-stayed footbridges with a span length of 150 m with two towers using different pedestrian scenarios for (a) commuting and (b) leisure activities

The additional effect of implementing tuned mass dampers in these footbridges with a span length of 150 m and a 0.3 m slab depth is also examined. As shown in Figure 6.41 (a), tuned mass dampers with a mass ratio ranging from 0.01 and 0.04 are required to fulfil the maximum comfort level for commuting activities in the vertical direction (TMD efficiency approximately 62%). From Figure 6.41 (b), the TMD mass ratio required to achieve the maximum comfort level, when considering leisure activities, is 0.01, 0.02, and 0.03 for 0.2, 0.6, and 1.0 ped/m^2, respectively.



(a) (b)

Figure 6.41 Vertical peak accelerations with tuned mass dampers using a slab depth of 0.3 m for cable-stayed footbridges with a span length of 150 m with two towers using different pedestrian scenarios for (a) commuting and (b) leisure activities

For the lateral accelerations, TMDs with a mass ratio ranging from 0.01 to 0.03 for commuting activities and from 0.01 and 0.02 for leisure activities are required. These dampers allow achieving maximum comfort level and avoiding the lock-in effect. Figure 6.42 shows the significant effect of using smaller tuned mass dampers in a cable-stayed bridge with a 0.3 slab depth. Therefore, increasing the slab depth to 0.3 m and simultaneously implementing TMDs leads to solutions where the required TMD masses are within the range of magnitudes provided by suppliers.

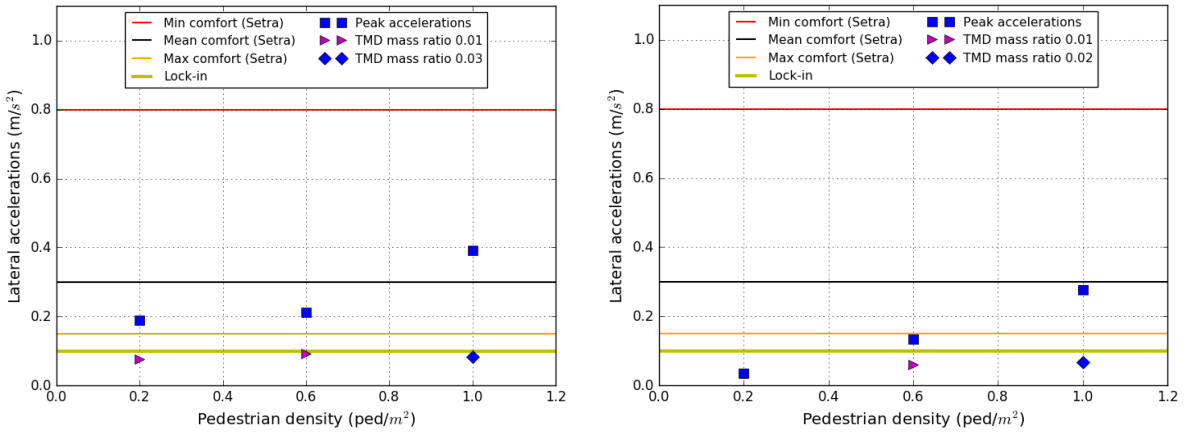


Figure 6.42 Lateral peak accelerations with tuned mass dampers using a slab depth of 0.3 m for cable-stayed footbridges with a span length of 150 m with two towers using different pedestrian scenarios for (a) commuting and (b) leisure activities

6.5 Cable-Stayed footbridges with different pylon's shapes

Different pylon shapes such as H- and A-shaped pylons were analysed to quantify the effect in the dynamic response of using these shapes combined with the implementation of TMDs. Ramos-Moreno (2015) demonstrated that these pylon shapes have a low impact in the vertical direction. Figure 6.43 (a) shows that the frequencies that are excited by pedestrians in the vertical direction are similar for I-, H-, and A-shaped pylons. In this direction, there is a contribution of torsional modes depending on the span length and pylon's shapes. For instance, when an I-shaped pylon is considered for span lengths ranging from 50 to 100 m, there is a contribution of mode T1. Besides, for longer spans, there is also a contribution from mode T2 as it is shown in Figure 6.43 (c). A remarkable benefit in the lateral direction was demonstrated when an A-shaped pylon was employed (Ramos-Moreno, 2015). This benefit is because this shape restricts both lateral and torsional rotations for span lengths up to 150 m. However, for longer spans, there is a contribution from torsional modes T1 (Figure 6.43 (b) and (d)).

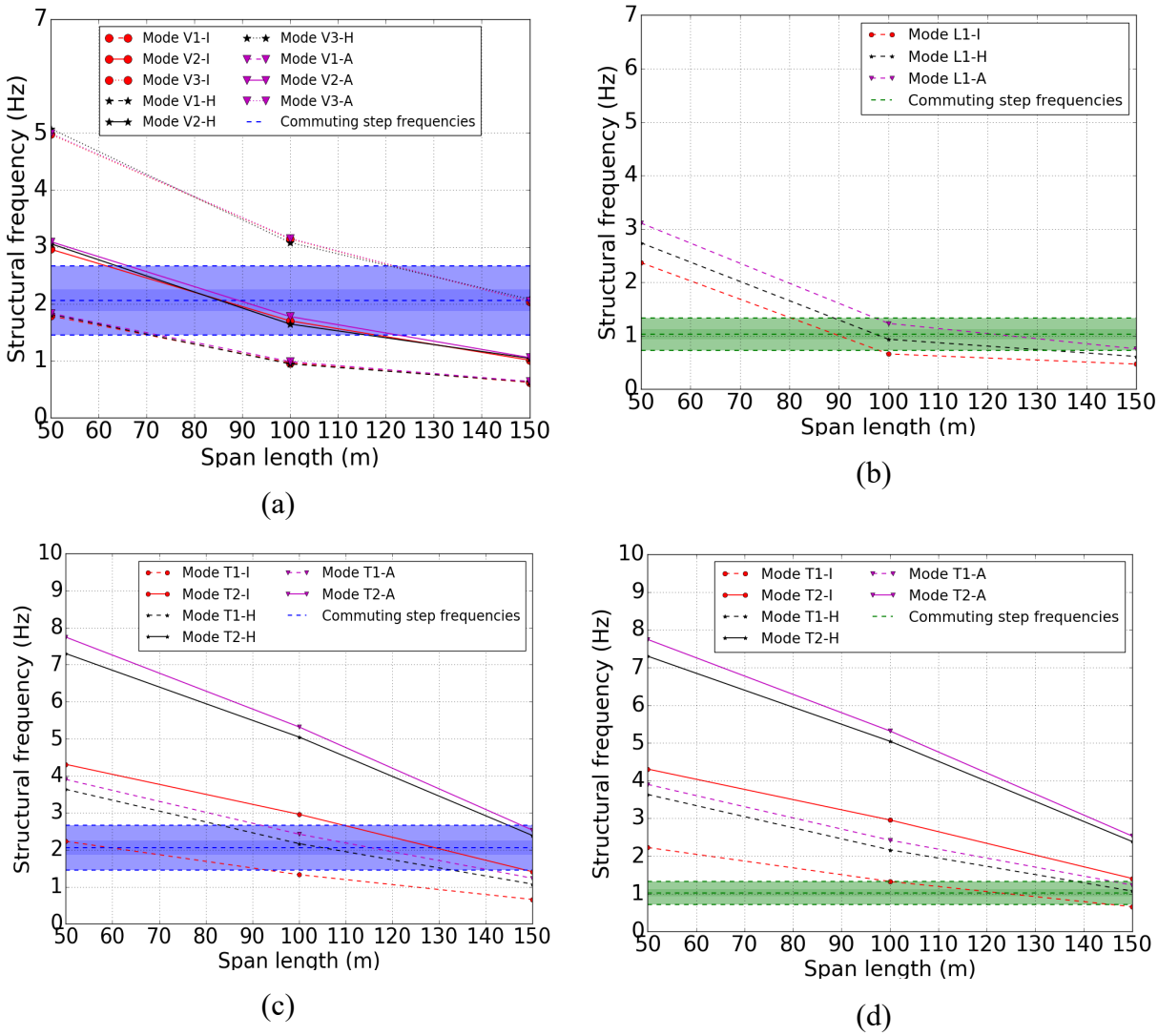
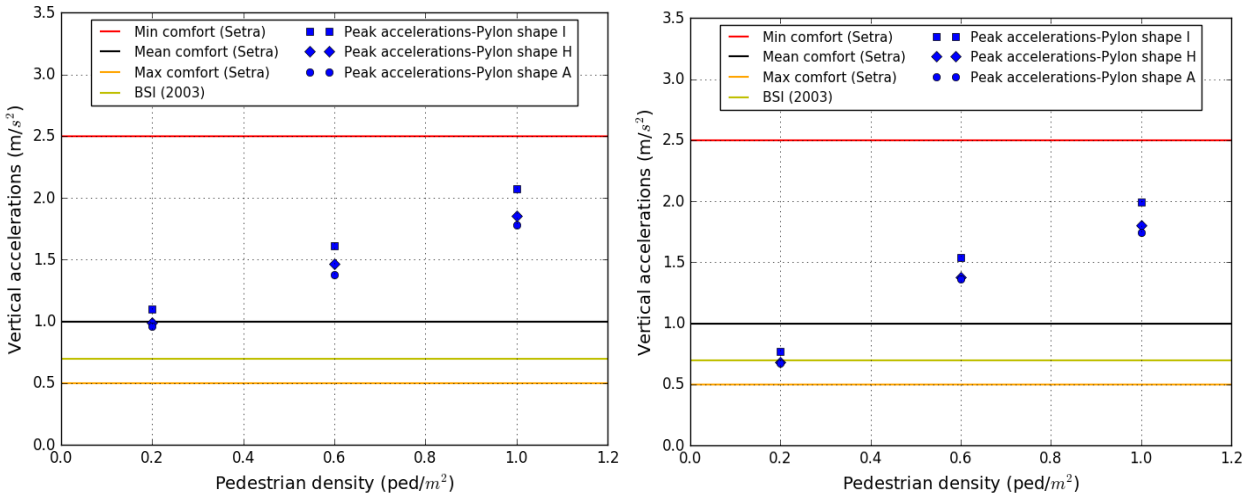


Figure 6.43 Structural (a) vertical, (b) lateral and (c) torsional frequencies versus the span length in cable-stayed footbridges with different pylon's shapes under a pedestrian density of 0.6 ped/m^2 for commuting activities

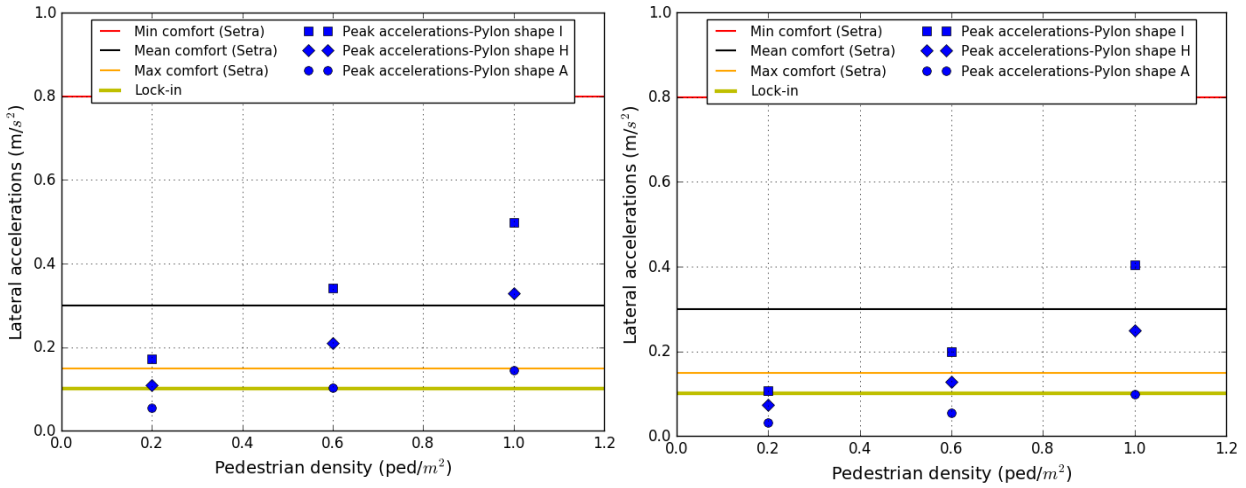
The results obtained using an H- and A-shaped pylons are compared with the previous analysis (I-shaped pylon) for span lengths of 50 m, 100 m, and 150 m. Figure 6.44 shows that the vertical accelerations for H- and A-shaped pylons are approximately 13% smaller in comparison with the I-shaped pylon. Therefore, similar but slightly smaller tuned mass dampers that were employed for an I-shaped pylon can be used herein to achieve a maximum comfort, where the range of the TMD mass ratio goes from 0.03 to 0.08. Nevertheless, the pylon shape has a more significant effect

on the lateral than on vertical accelerations (Figure 6.45). Also, it is worth noticing that when an A-shaped pylon is employed, the lock-in effect is avoided for pedestrian densities of 0.2 and 0.6 ped/m^2. To avoid this effect for a pedestrian density of 1.0 ped/m^2 in commuting activities, a TMD mass ratio of 0.01 is required.



(a) (b)

Figure 6.44 Vertical peak accelerations for cable-stayed footbridges with a span length of 50 m with two towers for (a)commuting and (b) leisure activities using different pylon shapes



(a) (b)

Figure 6.45 Lateral peak accelerations for cable-stayed footbridges with a span length of 50 m with two towers for (a)commuting and (b) leisure activities using different pylon shapes

A similar analysis was performed for a cable-stayed footbridge with a span length of 100 m with different pylon shapes (H- and A-shaped) for vertical and lateral accelerations (Figure 6.46, and Figure 6.47). For commuting and leisure activities with an I-, A-, and H-shaped pylons in the vertical direction, the acceleration varies from minimum to unacceptable. This study helps to quantify the effect that using a different shape (H- and A-shaped pylon) can have in the accelerations instead of using the traditional one (I-shaped). For commuting and leisure activities in the vertical direction, a reduction of approximately 9% is achieved when the H-shaped pylon is employed, and when the A-shaped pylon is used, a reduction of 11% is achieved. For these cases, TMD mass ratios ranging from 0.05 to 0.13 are required to achieve a maximum comfort level.

A similar analysis for the lateral accelerations shows a significant reduction that is achieved when an A-shaped pylon is employed (approximately 65%). Similarly, when an H-shaped pylon is employed, a reduction of approximately 40% is achieved in comparison with an I-shaped pylon. Using a different pylon shape instead of an I-shaped have a great effect on the reduction of the lateral accelerations for cable-stayed footbridges with two towers. For these cases, TMD mass ratios ranging from 0.01 to 0.08 are required to ensure a maximum comfort level avoiding the lock-in effect.

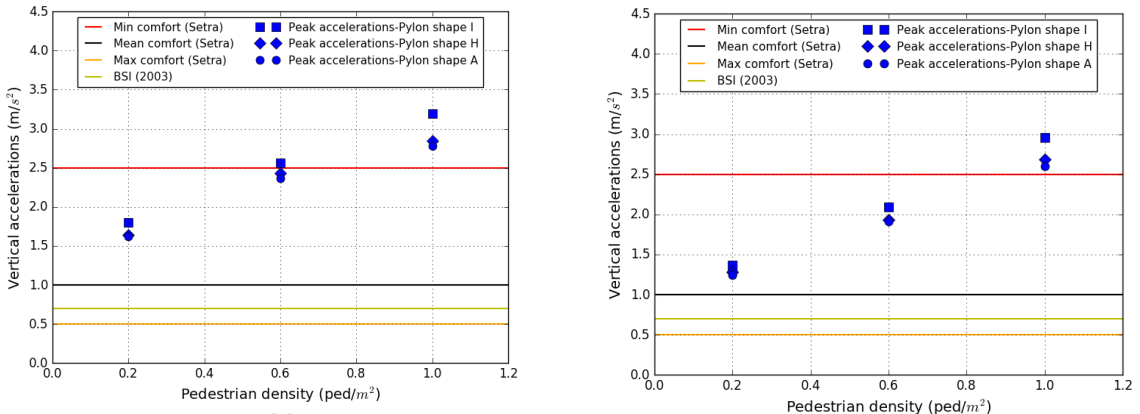
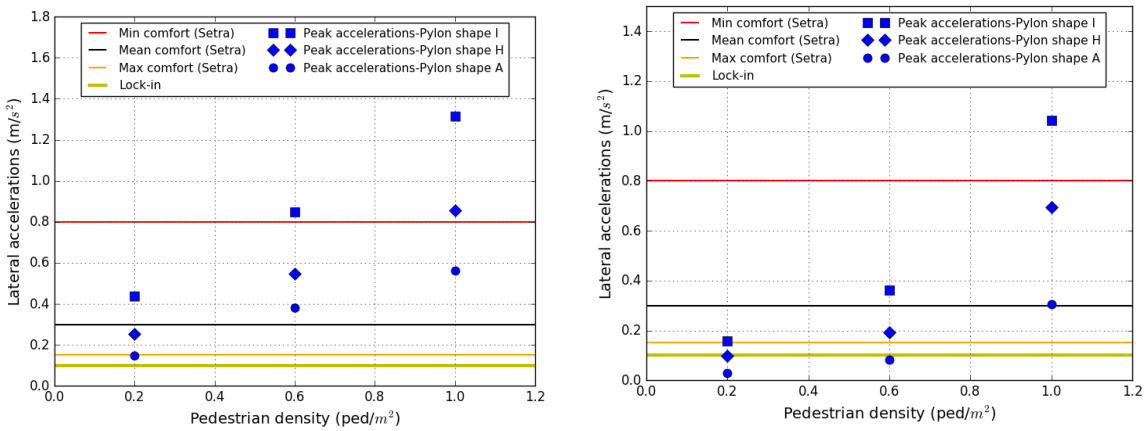


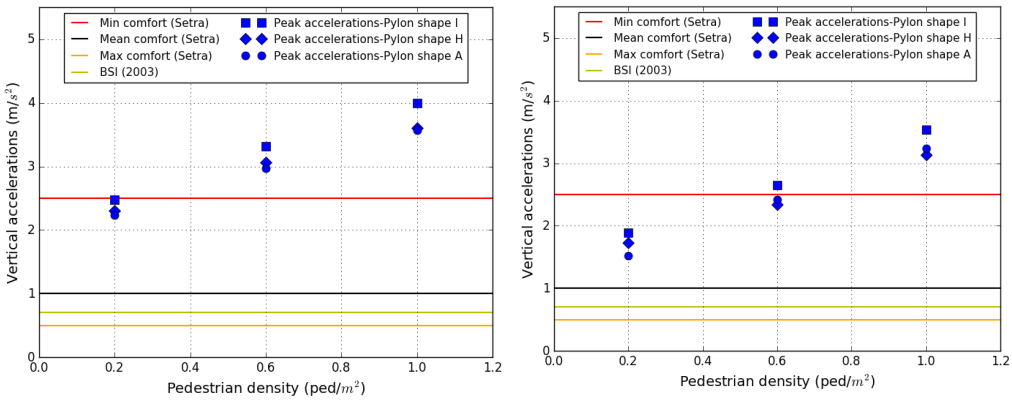
Figure 6.46 Vertical peak accelerations for cable-stayed footbridges with a span length of 100 m with two towers for (a) commuting and (b) leisure activities using different pylon shapes



(a) (b)

Figure 6.47 Lateral peak accelerations for cable-stayed footbridges with a span length of 100 m with two towers for (a) commuting and (b) leisure activities using different pylon shapes

The dynamic response in vertical and lateral direction was performed for cable-stayed footbridges with a span length of 150 m with different pylon shapes, as it was done in the previous cases. These analyses help to gain a better understanding of the effect of changing this structural parameter in the dynamic response using tuned mass dampers. Figure 6.48, and Figure 6.49 show the effect of the H- and A-shaped pylon in comparison to an I-shaped pylon. As in the analysis for a span length of 100 m, a significant reduction in the lateral accelerations can be seen. The TMD mass ratio to fulfil the lock-in effect varies from 0.02 to 0.09.



(a) (b)

Figure 6.48 Vertical peak accelerations for cable-stayed footbridges with a span length of 150 m with two towers for (a) commuting and (b) leisure activities using different pylon shapes

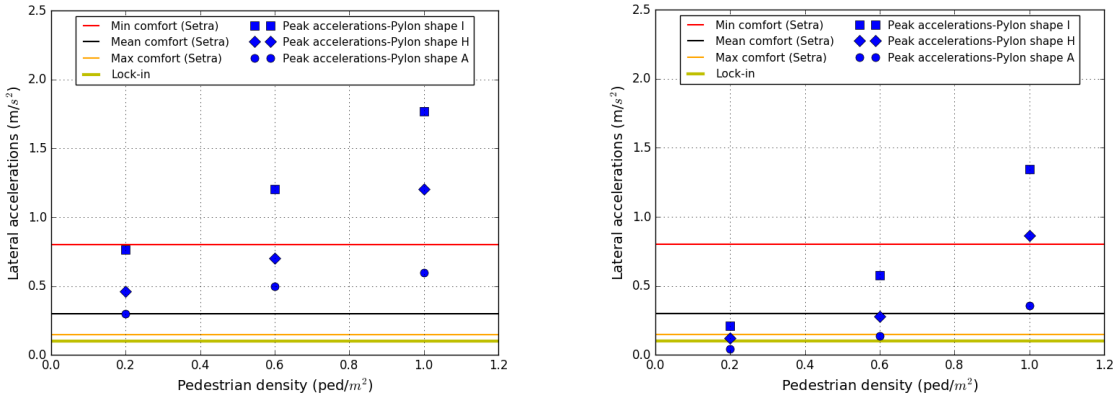
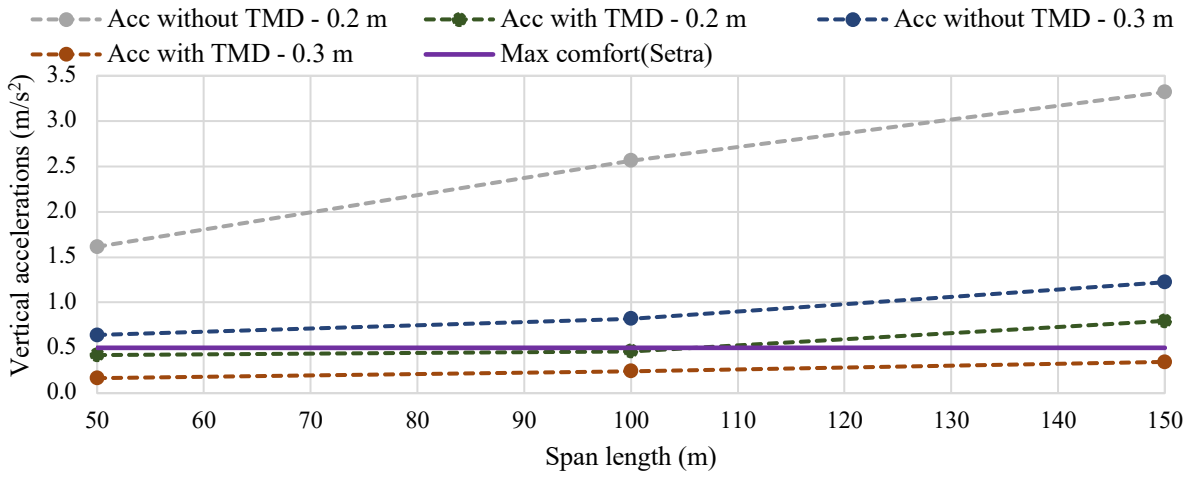


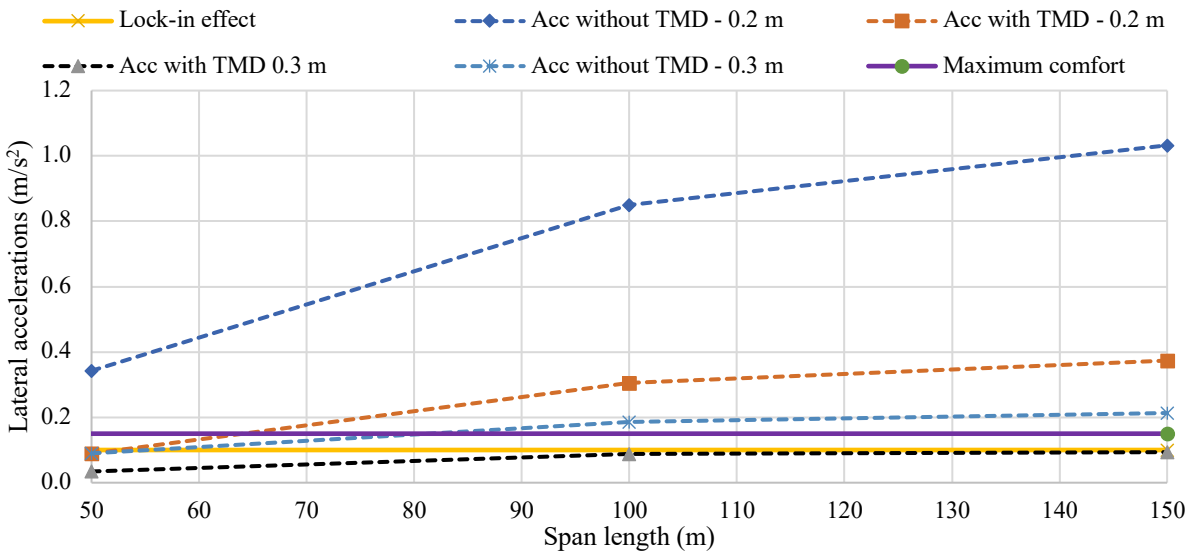
Figure 6.49 Lateral peak accelerations for cable-stayed footbridges with a span length of 150 m with two towers for (a) commuting and (b) leisure activities using different pylon shapes

6.6 Cost analysis

This section shows a comparative cost study between implementing TMD or increasing the slab thickness as a measure to mitigate the human-induced vibrations. The serviceability criterion is not fulfilled when the slab depth is 0.2 or 0.3 m. Therefore, the implementation of TMDs for both depths is considered. When TMDs were implemented, the smallest vertical accelerations were obtained for slab depths of 0.3 m in comparison of the 0.2 m for span lengths up to 100 m. Regardless of the slab depths, a maximum comfort level is achieved for span lengths up to 100 m (Figure 6.50 (a)). However, in lateral accelerations, the lock-in effect is not avoided although a high TMD mass ratio is employed for span lengths longer than 100 m with a slab depth of 0.2 m (Figure 6.50 (b)). For these span lengths, although the price will be higher, the best solution is to increase the slab depth, and then employing smaller TMDs for the cases where is necessary, therefore, vertical and lateral accelerations will fulfil the serviceability criteria (Figure 6.32, 6.35, 6.41, and 6.42). Thus, only footbridges with a slab depth of 0.2 and 0.3 m with a span length of 50 m under pedestrian densities of 0.6 ped/m^2 (commuters) are considered for this cost comparison.



(a)



(b)

Figure 6.50 (a) Vertical and (b) lateral peak accelerations according to the span length for CSF with two towers with a slab depth of 0.2 and 0.3 m for pedestrian densities of 0.6 ped/m^2 (commuters)

For the cost's analysis, only the cost of the slab depth and TMDs are considered. The material costs for this study are shown in Table 4.2. The costs of the TMDs are shown in Table 6.7. For these devices, the tuning range goes from 1.4 to 2.8 Hz, with a damping ratio of 6 to 15% and a maximum displacement range of ± 40 mm.

TMD weight (kg)	Cost rate (2019) in GBP
3500	16500
5000	24500
6500	35049

Table 6.7: TMD cost used in this analysis according to Maurer supplier (Benicke, 2019)

Figure 6.51 shows the cost analyses for different slab thickness (m) in the design of cable-stayed footbridges with a span length of 50 m for pedestrian densities of 0.6 ped/m^2. The most cost-effective solution for a 50 m span length is to install tuned mass dampers instead of increasing the slab depth. If the TMD does not need to be replaced, throughout the service life (Section 4.3.3), the deck material cost would be similar to the case with a slab depth of 0.3 m. However, although increasing the slab depth reduced the dynamic response, an increment of the cost due to other structural members e.g. towers, abutments, towers, cables, etc., will need to be considered.

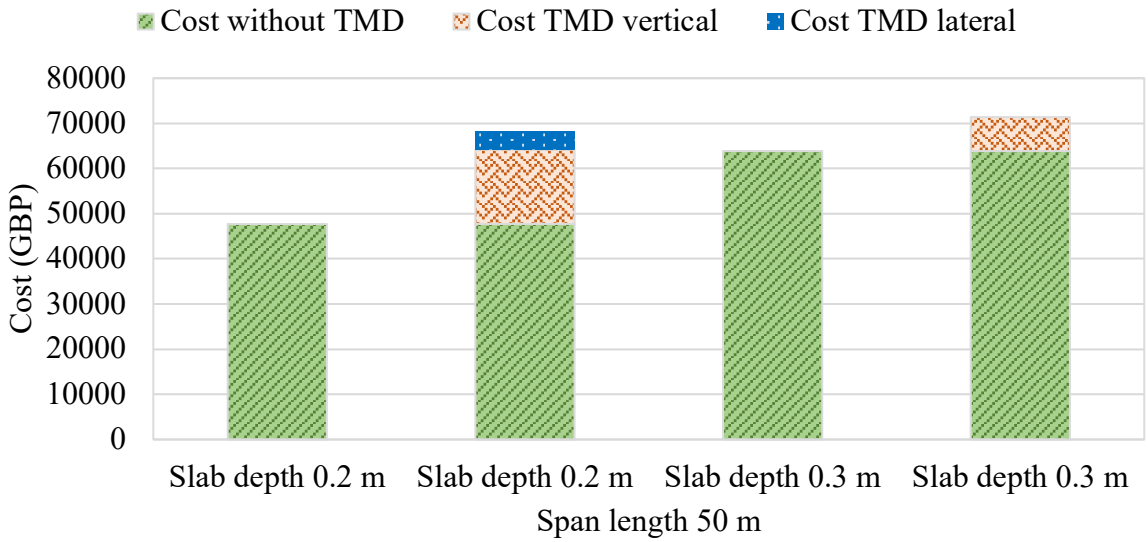


Figure 6.51 Cost analysis for different slab thickness (m) when one TMD is employed in the design of cable-stayed footbridges with a span length of 50 m with two towers for pedestrian densities of 0.6 ped/m^2 (commuters)

6.7 Main conclusions and design recommendations

This section summarises the dynamic response, in the vertical and lateral direction, of cable-stayed footbridges with two pylons, for given spans of 50, 100 and 150 m, with and without TMDs, provides a deeper understanding about the behaviour, and defines a detailed set of recommendations for preliminary designs.
The main conclusions and design recommendations are as follows:

Modes dominating the response

- The vertical frequencies where resonant effects can appear corresponds to a range from 1.5 to 2.7 Hz. In the lateral direction, this range varies from 0.75 to 1.35 Hz (half of the vertical frequencies).
- The modes dominating the response, in terms of accelerations, are related to the span length (Table 6.8). Such situation can be confirmed after a frequency domain analysis at different locations along the span length.

Tower shape	Direction of the response	Modes	Range of span lengths (m)
I, A, H	Vertical	V1	50 - 60
		V1 - V2	60 - 70
		V2	70 - 120
		V3	120 - 150
I	Torsion – Vertical	T1	50 - 100
		T2	> 100
I, A, H		T1	50 - 150
I, A, H	Lateral	L1	50 - 150
I	Torsion - Lateral	T1	50 -150
H, A		T1	50 - 100

Table 6.8 Structural vertical, lateral and torsional modes dominating the response in cable-stayed footbridges with different pylon's shapes under a pedestrian density of 0.6 ped/m^2 for commuting activities based on Figure 6.43

Dynamic response expected without TMDs

The benchmark case bridges selected for this thesis have been chosen as representative from a database of built structures. Therefore, the behaviour of these benchmark cases gives a clear indication that that could be expected in similar structures. Thus, the graphs that are presented in this section, might help the designers, when doing the conceptual design of these footbridges depending on the usage and bridge class such as rural (A), suburban (B), urban routes (C), or primary access (D) (BSI, 2008).

Figure 6.52 to 6.54 show the vertical and lateral accelerations for CSFs with a slab depth of 0.2 m for the envelope of commuting and leisure activities according to the pylon's shapes. The dynamic response expected without TMDs is outlined as follows:

For vertical direction according to the envelope of the I-, A-, and H-shaped pylons

- For this direction, regardless of the span lengths and pedestrian densities, a maximum comfort level is not achieved.
- For span lengths from 50 to 150 m, a mean comfort for pedestrian densities of 0.2 ped/m^2 is achieved.
- For span lengths up to 100 m, a mean comfort for pedestrian densities of 0.6 ped/m^2 is achieved. For longer spans, an unacceptable comfort is expected.
- For span lengths up to 70 m, a mean comfort for pedestrian densities of 1.0 ped/m^2 is achieved. For span lengths, an unacceptable comfort is expected.
- For span lengths > 150 m, the accelerations correspond to an unacceptable comfort, regardless of the pedestrian densities.

For lateral direction according to the envelope of the I-, and H-shaped pylons

- Regardless of the span lengths and pedestrian densities, the lock-in effect is not avoided.

- For span lengths ranging from 50 to 80 m, 80 to 150 m and > 150 a mean, minimum and unacceptable comfort is expected, respectively (pedestrian densities of 0.2 ped/m^2).
- For span lengths up to 90 m, a mean comfort for pedestrian densities of 0.6 ped/m^2 is achieved. For longer spans, an unacceptable comfort is expected.
- For span lengths up to 70 m, a mean comfort for pedestrian densities of 1.0 ped/m^2 is achieved. For span lengths > 70 m, an unacceptable comfort is expected.
- For span lengths > 150 m, the accelerations correspond to a minimum comfort, regardless of the pedestrian densities.

For lateral direction according to the A-shaped pylon

- Regardless of the span lengths and pedestrian densities, the accelerations do not correspond to an unacceptable comfort.
- For span lengths up to 70 m, the lock-in effect for pedestrian densities of 0.2 ped/m^2 is avoided. For longer spans, a mean comfort is expected.
- For span lengths up to 80 m, a mean comfort for pedestrian densities of 0.6 ped/m^2 is achieved. For longer spans, a minimum comfort is expected.
- For span lengths up to 70 m, a mean comfort for pedestrian densities of 0.6 ped/m^2 is achieved. For longer spans, a minimum comfort is expected.

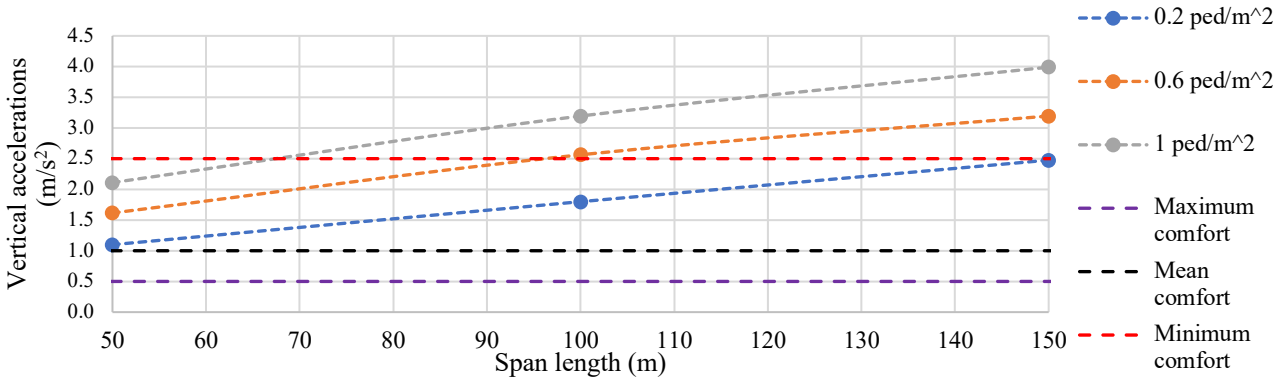


Figure 6.52 Vertical peak accelerations according to the span length for different pedestrian densities without TMDs according to the envelope of the I-, A- and H-shaped pylons for CSFs with two towers

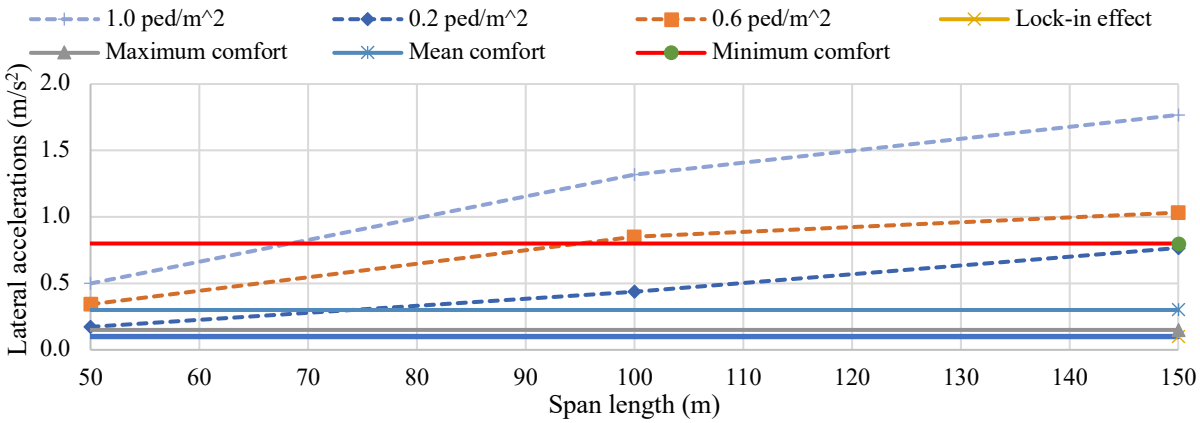


Figure 6.53 Lateral peak accelerations according to the span length for different pedestrian densities without TMDs according to the envelope of the I- and H-shaped pylons for CSFs with two towers

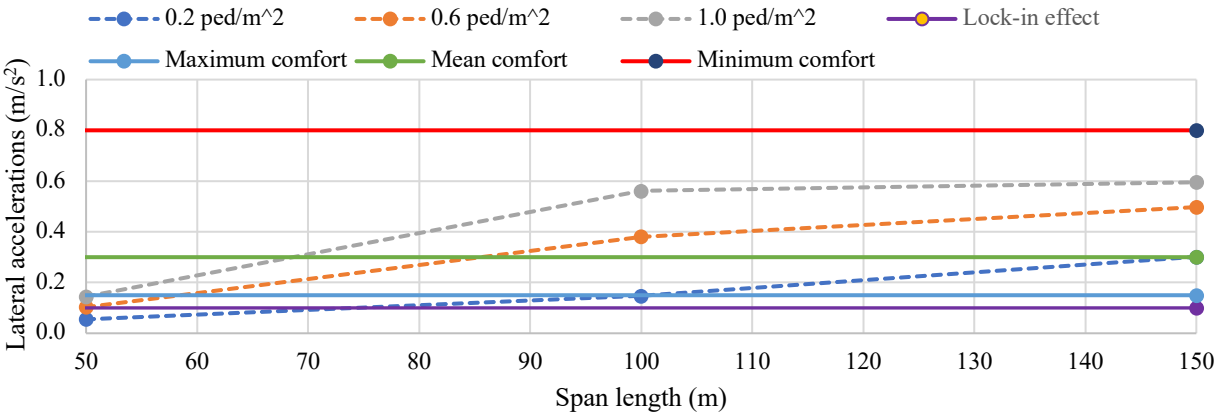


Figure 6.54 Lateral peak accelerations according to the span length for different pedestrian densities without TMDs according to the A-shaped pylon for CSFs with two towers

TMD location

The larger efficiencies of the TMDs, and therefore the larger reduction in the accelerations, are achieved when they are located at the maximum nodal coordinates of those modal shapes dominating the response. The mode that dominates the response can be identified through analyses of the acceleration records in the frequency domain. Furthermore, the implementation of TMDs also reduces the dynamic component of the internal forces i.e. approximately 27 % in sagging BMs for a 50 m span footbridge.

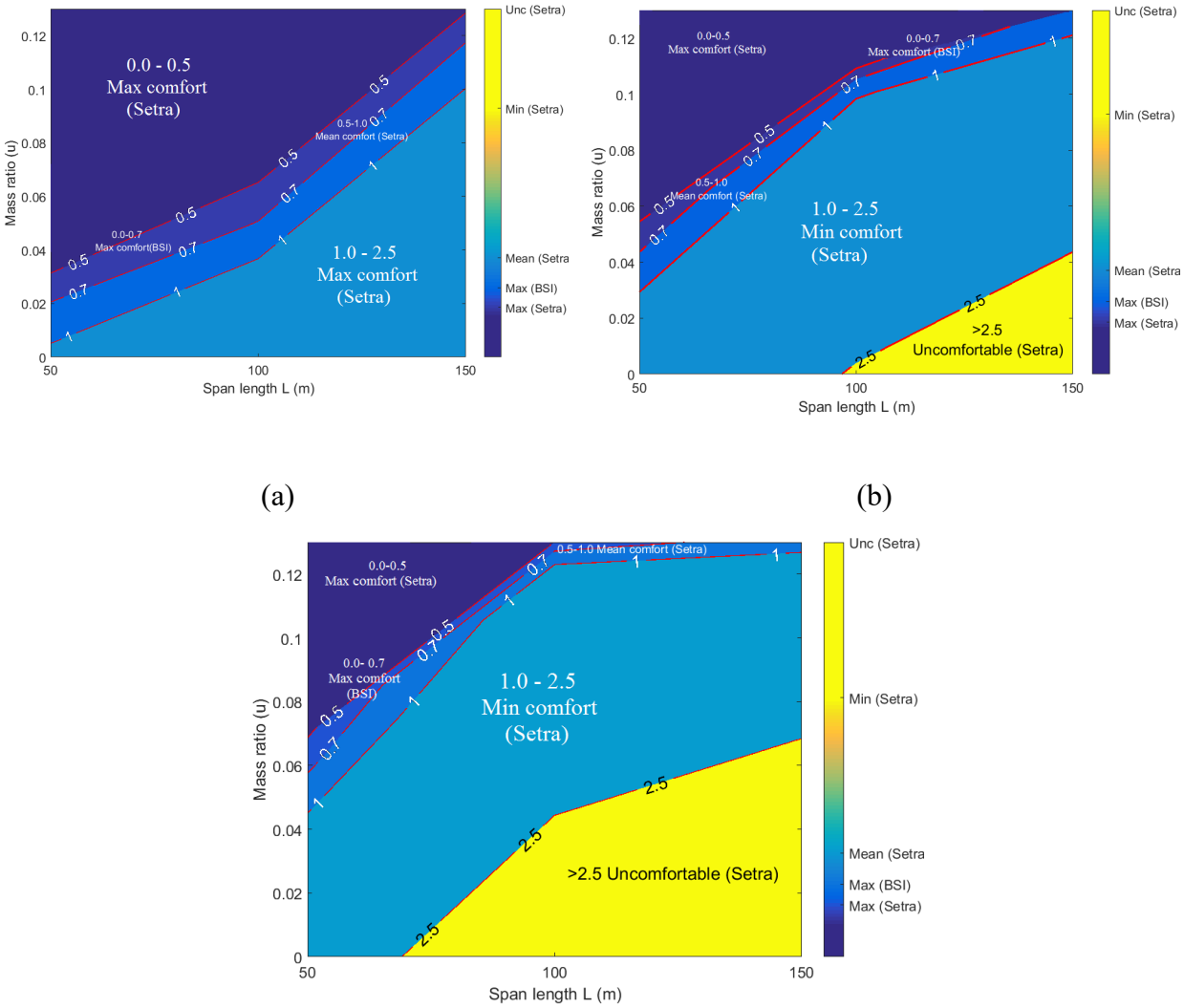
- The TMDs in vertical direction should be tuned to the frequency of the critical mode and located either maximum nodal coordinate of that mode or ± 10% from that point (20% of the span length).

- The TMD in the lateral direction needs to be located at the maximum nodal coordinates for the modal shape whose frequency has the largest amplitude to ensure the high efficiency e.g., first lateral mode L1. Similar efficiencies are achieved if the TMD is located at ± 5% from mid-span (± 10% of the span).

- TMDs efficiencies up to 74% are achieved if the TMDs are employed at the locations previously mentioned.

Dynamic response and required TMD mass ratios

Figure 6.55, Figure 6.56, and Figure 6.57 show the required TMD mass ratio according to the I-, A- and H-shaped pylons for different pedestrian densities. These graphs show the relationship between the required TMD mass ratios (μ), according to peak vertical and lateral accelerations, degree of comfort, and span lengths.



(a) (b)

(c)

Figure 6.55 Vertical peak accelerations and comfort levels for different TMD mass ratios (μ), active in the vertical direction, and for different span lengths under pedestrian densities of a) 0.2, b) 0.6 and c) 1.0 ped/m^2 according to the envelope of the I-, A- and H-shaped pylons for CSFs with two towers

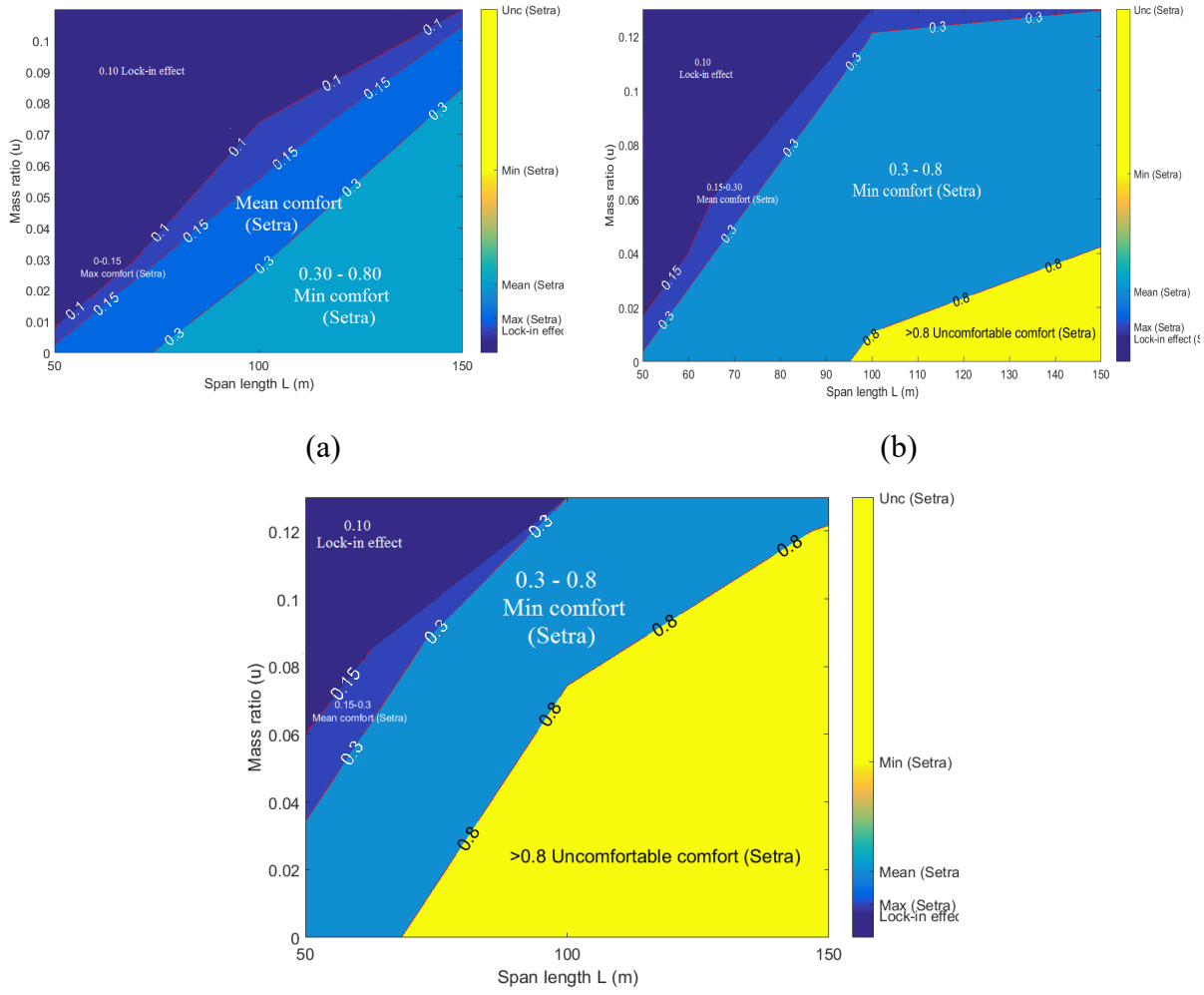


Figure 6.56 Lateral peak accelerations and comfort levels for different TMD mass ratios (μ), active in the lateral direction, and for different span lengths under pedestrian densities of a) 0.2, b) 0.6 and c) 1.0 ped/m^2 according to the envelope of the I- and H-shaped pylons for CSFs with two towers

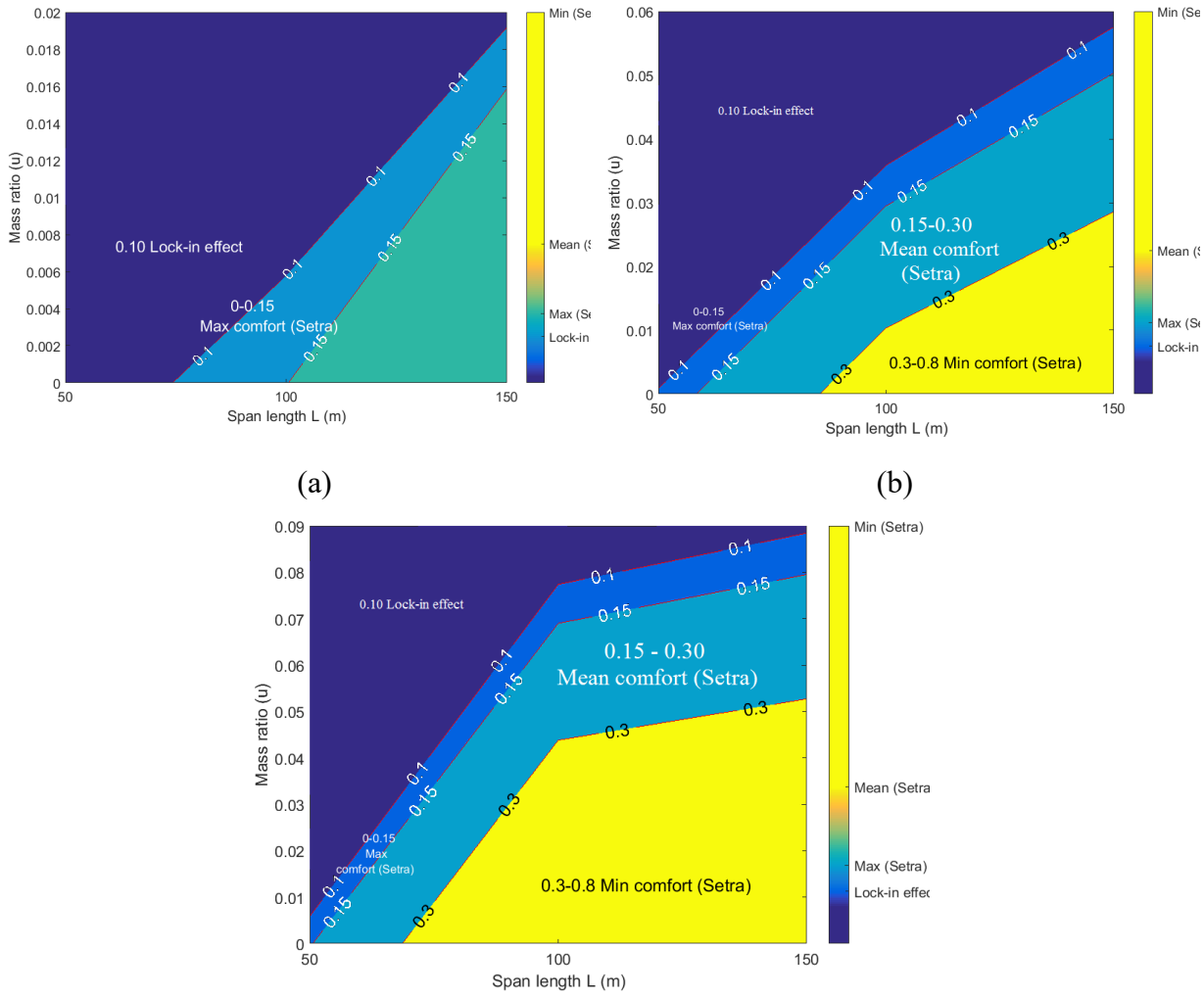


Figure 6.57 Lateral peak accelerations and comfort levels for different TMD mass ratios (μ), active in the lateral direction, and for different span lengths under pedestrian densities of a) 0.2, b) 0.6 and c) 1.0 ped/m^2 according to the A-shaped pylon for CSFs with two towers

The dynamic response with TMDs that could be expected in similar structures are outlined as follows:

- For lateral accelerations, the lock-in effect is not avoided for CSFs with a span length longer than 100 m under pedestrian densities higher than 0.6 ped/m^2 according to the

envelope of I- and H-shaped pylons. Therefore, for these pedestrian densities, an option could be to consider employing an A-shaped pylon or to increase the slab depth.

- For main spans of 50 m, if a service life of 100 years is considered for the TMDs, the best cost-effective solution is to employ a slab with a minimum depth (0.2 m for the benchmark cases considered in this thesis) and mitigate the excessive accelerations by implementing TMDs. For longer spans, the previous solution leads to excessively large TMDs that are difficult to materialise in practice applications. Therefore, for spans longer than 100 m, the practical solution would be to locate the largest TMDs tuned with the critical modes, at the locations where these modes have the larger modal coordinates, and then, provide the additional mitigation by increasing the slab depth up to the required magnitude to guarantee the required comfort levels.

The following flowchart summarizes the process that could be followed by a designer in order to choose the optimum location and number of tuned mass dampers (Figure 6.58). This flowchart is similar to the one showed in Chapter 5. However, this includes the cases where the maximum size and number of TMDs with the maximum efficiency are reached.

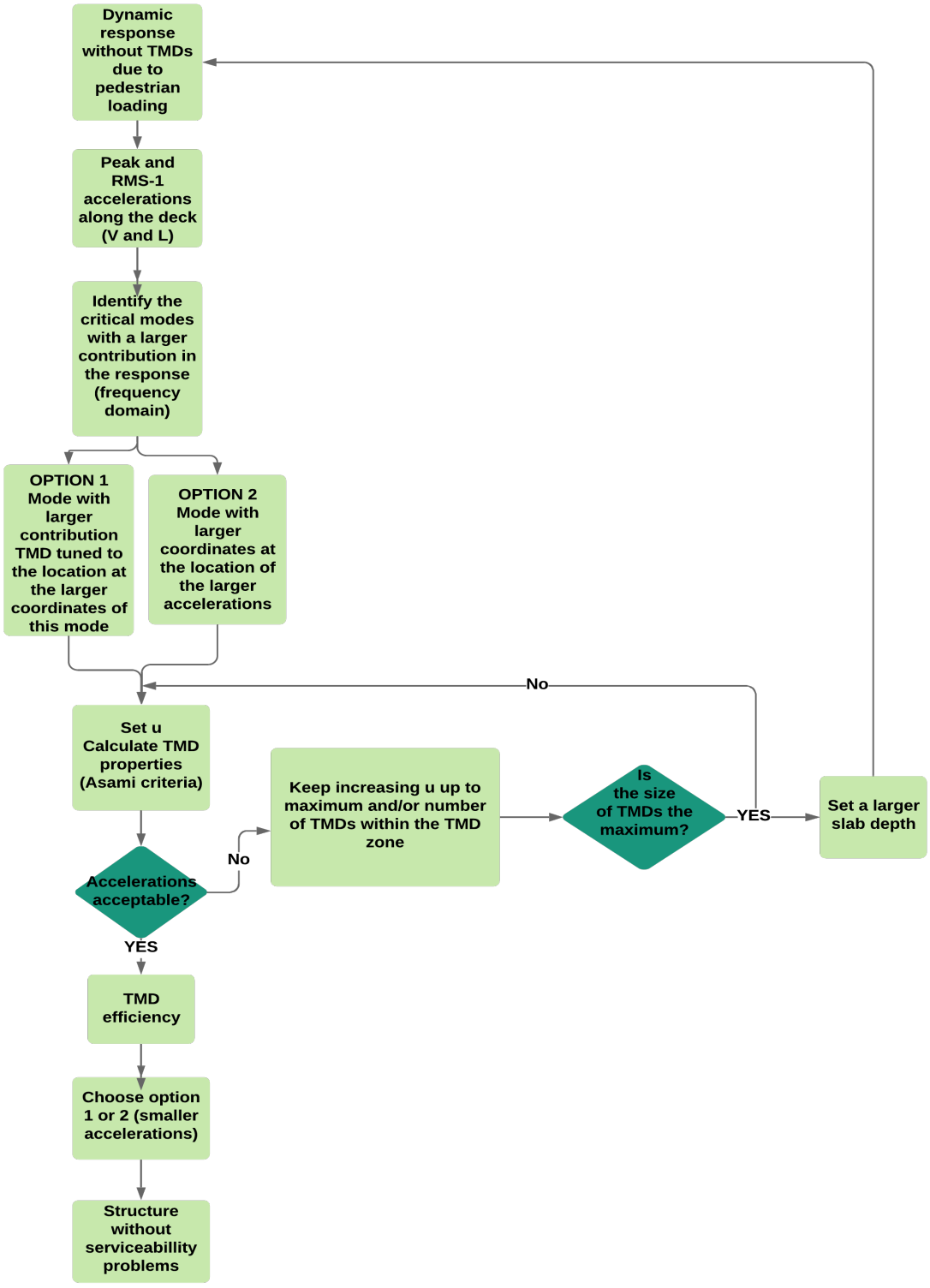


Figure 6.58 TMD implementation: a flowchart to include TMDs in cable-stayed footbridges with two towers

7 Conclusions and further research work

In this final chapter, the main findings of the thesis are presented. Besides, the areas for future research are highlighted.

7.1 Conclusions

In this work, numerical studies on the dynamic response in two footbridges typologies, girder and cable-stayed, were carried out. These numerical models considered scenarios with and without tuned mass dampers under a probabilistic pedestrian load model (including pedestrian intra-variability, and pedestrian-pedestrian interaction within the crowd flow). As design recommendations on how to consider these devices at the design stage to achieve a maximum degree of comfort are scarce, a reliable guidance is required to facilitate the construction of footbridges in order to avoid serviceability problems. Thus, the main objectives of this research work were to investigate and to present design recommendations regarding the use of tuned mass dampers in girder and cable-stayed footbridges. This is to allow an efficient design whilst avoiding serviceability problems. The benchmark cases footbridges have been chosen as representative from a database of built structures. Therefore, the structural behaviour of these cases with and without tuned mass dampers give a clear understanding of the response expected in similar structures.

The main findings and conclusions of this research work are summarized as follows:

Conclusions related to the state of the art and methodology for girder and cable-stayed footbridges

- Despite multiple research studies about how human-induced vibrations in footbridges can be mitigated using supplemental damping devices, a methodology that shows how to implement these devices during the design stage (optimal location and properties) was not

available prior to this thesis. In addition, most of these studies do not consider the non-linearities of the pedestrian actions.

- The duration and number of the numerical simulations are required to ensure a reliable dynamic response without a high dispersion. For the duration of the simulations, initially, the first pedestrians enter the footbridge arriving at the opposite side with the desired pedestrian density. After a while, a steady state response is achieved, and the structure corresponds to a stationary ergodic process. This is when the statistical analysis of multiple data leads to similar results. Then, different durations can be analysed in terms of the time expected for an average pedestrian to cross the bridge (t_{ap}), with the duration measured from the instant when the desired pedestrian density had been already achieved on the structure. Therefore, sensitivity analyses were conducted to choose the duration and the number of simulations. As a result, the dynamic response for girder footbridges converged after 10 simulations for a duration of $3t_{ap}$. For cable-stayed footbridges, the response converged after 6 simulations for a duration of $1t_{ap}$.

- Asami's TMD design criteria led to more efficient TMDs, and therefore higher efficiencies in the reductions in accelerations in the footbridges studied in this work, in comparison to the other criteria available from the literature such as Den Hartog, Krenk or Warburton. This is because the Asami's criterion was set to minimize the accelerations in structures with low damping, such as in footbridges, where the comfort criterion is governed by the accelerations. Therefore, the TMD's properties have been chosen according to Asami's formulations.

Conclusions related to the dynamic response of girder footbridges

In the evaluation of the dynamic response in girder footbridges, a code was developed in Python. In addition, the dynamic response was compared with models developed in Abaqus. For this type of footbridge, Python was chosen as it also has compatibility with the selected FEA package, Abaqus. The dynamic response of girder footbridges under pedestrian loads with and without

TMDs (Chapter 4) has been studied to verify the effectiveness of these devices, as well as to show design recommendations in this type of structures. The main conclusions of this evaluation are:

- There is a clear effect that for certain span lengths, sections, material, and pedestrian's aim of the journey, the serviceability criteria cannot be fulfilled using conventional approaches (such as selecting appropriate values of the geometrical or mechanical properties of the cross-section). In these cases, implementing supplemental damping devices is mandatory. The resonant effects induced when the frequency of the pedestrian loading matches the structural frequencies have been effectively mitigated using tuned mass dampers.

- In the cases where tuned mass dampers are required to mitigate dynamic response, it is necessary to locate them at the maximum nodal coordinates of those modal shapes dominating the response, having a flexibility to choose the location within the $\pm$ 15% of the span length from that point. If the TMD is employed at this location (within the flexibility range defined before), the human-induced vibrations are under the comfort limits, and the TMD have efficiencies of up to 80% (the efficiency of the TMD has been defined in this thesis as the percentage in the reduction of the maximum accelerations when the TMD are implemented). Otherwise, if it is not employed at this location (within the flexibility range defined before), the TMD efficiency is reduced significantly and therefore the serviceability criterion is not fulfilled. Furthermore, the implementation of TMDs also reduces the dynamic component of the internal forces (bending moments are reduced by approximately 31 %).

- An alternative to achieve a maximum comfort level on girder footbridges could be to increase the slab thickness. This conclusion is a generalization, as in most of the cases the impact of increasing the masses is larger than the impact of shifting the frequencies, as a consequence of the increment of the slab thickness. There are obviously the exceptions when the increment in the slab thickness makes the structural frequencies match the pedestrian frequencies inducing a resonant effect. However, it was demonstrated that increasing the slab thickness is not the most cost-efficient way of reducing the dynamic

response. Employing tuned mass dampers is the optimal solution to mitigate the accelerations in girder footbridges is to employ tuned mass dampers.

- Ultra-light footbridges, with cross-sections made of aluminium or glass fibre reinforced polymers and conventional deck span ratios (1/30 and 1/40), do not fulfil the maximum comfort criteria even after implementing multiple TMDs. Therefore, the slenderness and the structural masses must be governed by the dynamic response, losing the lightness achieved by implementing these structural materials.

- Tuned mass dampers can be employed at the design stage to achieve a maximum comfort level. A comprehensive set of graphs of TMDs properties, span length, cross-sections, and pedestrian flow type are given in Chapter 4. These graphs are useful for preliminary designs of girder footbridges.

Conclusions related to the dynamic response of cable-stayed footbridges

The second typology analyzed in this research is the cable-stayed footbridge. The cable-stayed footbridges that have been considered in this research work correspond to the most frequent characteristics that were found in the literature review. These structures correspond to footbridges with one and two towers with a composite section made of a reinforced concrete slab and steel girders, where the main span lengths correspond to 50, 100, and 150 m. Although cable-stayed footbridges with spans of around 150 m are less frequent, it was also considered herein with the aim to analyze whether cable-stayed footbridges with these spans can be constructed without serviceability problems by using tuned mass dampers. It is important to mention that for super long spans, beyond the ranges considered herein, vibrations need to be controlled by additional stay cables anchoring the deck to the ground or by using other structural types and geometrical configurations. For these studies, finite element models in Abaqus considering the stochastic pedestrian load model were developed. The results based on the dynamic analysis of the cable-stayed footbridges are as follows:

- The vertical and lateral accelerations are correlated with the span length. When this parameter is increased, the structural frequencies are reduced. These frequencies can lie near the step frequency of pedestrians, amplifying the response. Therefore, the contribution of some modes in the response can be enhanced due to resonant effects. The modes dominating the dynamic response with different pylon' shapes are shown in Table 5.7 and Table 6.8 for CSFs with one and two towers, respectively. It is worth noticing that the relevance of these modes has been confirmed after a frequency domain analysis of the registers of accelerations along the span length.

- After performing parametric analyses, the maximum peak accelerations and the comfort levels expected in different cable-stayed footbridges without supplemental damping devices have been provided, as a function of the pylon shape, the span lengths, and pedestrian densities (Figures 5.45 to 5.47 and from Figures 6.52 to 6.54 for CSFs with one and two towers, respectively). These figures are very useful to estimate the expected accelerations in similar footbridges at a very early stage of the design.

- The implementation of tuned mass dampers can significantly reduce the accelerations in the vertical and lateral direction and hence avoiding serviceability problems. However, the higher efficiencies depend on the TMD location. In the vertical direction, it is required to locate at the maximum nodal coordinates, having a flexibility to shift them along the span, from that location, by ± 10.0 % and ± 6.0 % of the span length, for CSF with one and two towers, respectively. On the other hand, for the lateral direction, the lock-in effect is avoided if the TMD is located at the maximum nodal coordinates of those modal shapes dominating the response, with a flexibility of locating the TMD ± 5.0 % along the length from that location, regardless the number of towers. Furthermore, the implementation of TMDs also reduces the bending moments by approximately 25 and 27% for CSFs with one and two towers, respectively.

- The relationship between the required TMD mass ratios (μ), according to the peak vertical and lateral accelerations, degree of comfort, span lengths, pylons shapes, pedestrian

densities are defined from Figures 5.48 to 5.50 and Figures 6.55 to 6.57 for CSFs with one and two towers, respectively. These graphs are very useful for preliminary design to expect the level of supplemental damping required, as well as to define the limits of this technology (implementation of TMDs) to control the vibrations within the comfort limits.

- For cable-stayed footbridges with one tower, the most cost-efficient way of reducing the dynamic response is by employing tuned mass dampers instead of increasing the slab depth (recommended by Ramos-Moreno, 2015).

- For cable-stayed footbridges with one tower, an A-shaped pylon are those which have a better performance when both vertical and lateral accelerations are considered. I-shaped pylons are the best ones when considering vertical direction but have the worst performance of those assessed when considering the lateral accelerations. This is because the lateral structural frequencies match the step frequencies of the pedestrians (resonant effects). Contrary, H-shaped pylons are the best ones when considering lateral accelerations but have the worst performance of those assessed when considering the vertical ones. This effect is because of the additional contribution of torsional modes T1 and T2 in comparison of the I- and A-shaped pylons.

- For cable-stayed footbridges with two towers, the most cost-effective solution is to install tuned mass dampers for span lengths of around up to 50 m. For longer spans, the best solution is to increase the slab depth, and then to employ TMDs. This is to guarantee the maximum comfort level in both directions and to avoid the lock-in effect in the lateral direction. Nevertheless, the A-shaped pylon has been identified as another way to reduce the accelerations specifically in the lateral direction. This is because this pylon shape restricts both lateral and torsional rotations.

- Finally, the evaluation of TMDs in this research work has shown that these devices can be implemented at the design stage, as long as the location and properties are chosen correctly. For this implementation, flowcharts of the process that should be followed by a designer

to define the most structural- and cost-efficient configuration, has been included (Figures 5.51 and 6.58). Therefore, this work may be used as a guide for preliminary footbridges design considering TMDs to avoid serviceability problems.

7.2 Future research

Following the research work presented in this thesis, there are still some areas that can be considered as a continuation of the current study. Some of these areas are discussed herein:

- To study the effect of tuned mass dampers in other typologies, e.g. suspension footbridges and under-deck cable-stayed footbridges.

- To perform comprehensive experimental studies to evaluate the damping ratio for footbridges under pedestrian actions. Some researchers and guidelines suggested to not overestimate the structural damping. This is to ensure a conservative analysis of the dynamic response to avoid underestimating the potential dynamic response. However, rigorous and comprehensive experimental studies on the representative and realistic values of the damping ratios for different structural material and different loading conditions would be very beneficial, as it is not available yet.

- To perform further studies of the human-structure synchronization, which is also called the lock-in effect, with the aim to analyse the excitation level that is reached according to the pedestrian's percentage who are synchronized to the structure. Many authors have made different assumptions in relation to the number of pedestrians who are synchronized to the structure. However, so far it is just known that the threshold of the lock-in effect is 0.1 m/s^2. Therefore, it would be relevant to study the effect on the structure and pedestrians when this threshold is reached. This study would be beneficial when considering rare scenarios, with very high pedestrian frequencies, as for verifying the serviceability limit states in frequent scenarios, it would be desirable that the pedestrians would not have to alter the way they walk as a result of the structural vibrations.

- To extend these studies of these bridge typologies considering jumping, running, cycling and vandals' excitations in the pedestrian load model.

- To study the implementation of other types of damping devices (such as viscous dampers, semi-active devices and active dampers) in footbridges to mitigate human-induced vibrations.

Annex A Girder footbridge dataset

#	Name	Country	Year	# of spans	Total length (m)	Deck width (m)	Structural material
1	Bataviabrug	Belgium	2012	-	110.0	5.0	-
2	Tillegemstraat Footbridge	Belgium	2009	-	96.0	4.0	Steel
3	Comenius Bridge	Czech Republic	-	1	61.5	6.0	Steel
4	Iirislahti Bridge	Finland	2009	3	45.0	-	-
5	Stade de France footbridge	France	1998	3	180.0	-	Steel
6	Passerelle des Anges	France	2009	1	67.5	4.0	Concrete
7	Alleebrücke	Germany	2003	4	50.0	-	-
8	Blechensteg	Germany	2006	1	42.0	4.0	-
9	Dahlhausen Footbridge	Germany	1987	2	91.0	3.0	Steel
10	Flöha Footbridge	Germany	2010	3	110.6	3.0	Steel
11	Fußgängerbrücke Lautlingen	Germany	2010	6	97.0	3.2	Textile-reinforced concrete Prestressed concrete
12	Ölhafenbrücke	Germany	2013	5	170.0	-	-
13	Dorsten	Germany	1980	1	59.6	-	Steel
14	Hagelsbrunnenweg Bridge	Germany	2014	1	27.5	3.0	-
15	Schillersteg	Germany	2012	1	27.1	2.5	Timber
16	Margarete Müller-Bull Footbridge	Germany	2011	2	28.5	3.0	Steel
17	Bridge over the River Spree	Germany	2005	3	87.7	6.0	-
18	Bridge over the River Echaz and the B 312	Germany	-	2	50.7	3.4	-
19	Altrheinsteg Albbruck (I)	Germany - Switzerland	-	5	210.0	-	Steel
20	Am Obergraben Bicycle Bridge	Germany - Switzerland	1995	4	72.5	2.8	Steel
21	Bolzano Museum Footbridge	Italy	2008	1	52.0	6.0	Steel
22	Fölkenbach Footbridge	Luxembourg	1974	3	82.0	2.0	Steel
23	Centennial Hall Footbridges	Poland	1926	10	68.0	5.6	Reinforced concrete

#	Name	Country	Year	# of spans	Total length (m)	Deck width (m)	Structural material
24	Forte da Casa Footbridge	Portugal	2014	7	222.3	-	Prestressed concrete
25	Aberfeldy Footbridge	Scotland	1993	3	64.0	-	Fibre-reinforced polymer
26	Lleida pedestrian footbridge 1	Spain	2004	1	38.0	3.0	Fibre-reinforced polymer
27	Pasarela de la Montañita	Spain	2010	2	55.1	-	Steel
28	Pasarela Parque de las Adelfas	Spain	2010	5	157.5	-	Steel
29	Mikel Laboa Footbridge	Spain	2009	3	92.4	3-6.4	Steel
30	Villabona-Zizurkil Footbridge	Spain	2009	2	53.6	-	Steel and wooden deck
31	Birskopfsteg	Switzerland	2012	2	75.5	4.9	Steel
32	Ticino Footbridge	Switzerland	2010	4	159.7	-	-
33	The Rotterdam Central Station footbridge	The Netherlands	2007	6	136.0	-	Composite
34	Almere-Buiten Footbridge	The Netherlands	2008	1	24.0	4.0	Glue laminated timber
35	Castleford Bridge	United Kingdom	2008	7	133.0	4.1	Timber
36	Prince William's Bridge	United Kingdom	2011	1	25.0	2.0	Steel
37	Bradkirk Footbridge	United Kingdom	2009	2	24.0	-	Fibre-reinforced polymer
38	Bellagio bridge	United States	1998	1	46.0	1.5	-
39	Nichols Bridgeway	United States	2009	-	189.0	4.6	Steel

Annex B Cable-stayed footbridge dataset

#	Name	Country	Year	Main span length	Total length	# of pylons
1	Kaisermuhlenbrucke	Austria	1993	80.0	207.0	2
2	René Lavoie Footbridge	Canada	2013	107.0	107.0	1
3	Elbe Pedestrian bridge	Czech Republic	2014	156.0	242.0	2
4	Bridge across D47	Czech Republic	-	59.2	110.5	1
5	Neckar Footbridge	Germany	1973	139.5	252.5	2
6	Nessebrücke	Germany	2006	82.0	123.0	2
7	Passerelle des deux Rives	Germany	2004	177.0	177.0	2
8	Raunheim Footbridge	Germany	2007	130.0	130.0	1
9	Katehaki	Greece	2004	80.0	80.0	1
10	Abrisham Bridge	Iran	2009	67.0	132.9	1
11	Feijenoord	Netherlands	1993	91.0	91.0	1
12	Ruda Slaska	Poland	2000	54.6	61.6	1
13	Krzywykij	Poland	2000	62.4	70.0	1
14	Dunajec River Bridge	Poland – Slovakia	2006	90.0	150.0	1
15	Myakinino Footbridge	Russia	2014	173.0	422.0	2
16	FB over Ibar river	Serbia	2011	120.0	270.0	1
17	Saint Irinej	Serbia	1993	192.5	297.5	2
18	7th Av. Ped. Bridge	South Africa	2010	52.0	-	1
19	Glorias Catalanas	Spain	1974	54.0	97.5	1
20	Voluntariado	Spain	2008	145.0	239.0	1
21	Malecon	Spain	1996	60.0	60.0	1
22	FB over Ticino River	Switzerland	2011	60.0	120.0	1
23	UG1 Footbridge	Turkey	2009	67.0	99.0	1
24	Zabeel Park Footbridge	United Arab Emirates	2005	65.0	65.0	1
25	Golden Jubilee	United Kingdom	2002	50.0	320.0	6
26	Media City	United Kingdom	2011	65.0	83.0	1
27	Christchurch Bridge	United Kingdom	2015	68.0	68.0	1
28	Delta Pond	United States	2010	52.0	104.0	1
29	Reiman Bridge	United States	2001	73.0	87.5	1
30	Ohio and Erie Canalway	United States	2011	65.9	175.5	2
31	Turtle Bay Sundial Bridge	United States	2004	150.0	210.0	1
32	Manzanares	Spain	2008	147.0	-	1

#	Name	Pylon shape	H_{Tp}	h_p	H_i	Inclination	No. cable plans	Cable arrangement
1	Kaisermuhlenbrucke	H	-	-		No	2	Fan mixt
2	René Lavoie Footbridge	A	-	-	-	No	2	Fan mixt
3	Elbe Pedestrian bridge	A	39.2	32.0	7.2	No	2	Fan mixt
4	Bridge across D47	I	25.1	17.8	7.3	No	1	Fan mixt
5	Neckar Footbridge	I	36.4	29.1	7.3	No	1	Fan mixt
6	Nessebrücke	I	15.5	10.5	5.0	Yes, in	2	Fan
7	Passerelle des deux Rives	I	37.0	27.0	10.0	Yes, out	2	Fan
8	Raunheim Footbridge	A	35.0	-	-	Yes, in	2	Fan mixt
9	Katehaki	I	50.0	-	-	Yes, out	1	Harp
10	Abrisham Bridge	A	40.0	-	-	No	2	
11	Feijenoord	A		-	-	Yes, in	2	Fan mixt
12	Ruda Slaska	A	23.7	16.9	6.8	Yes, out	2	Fan mixt
13	Krzywykij	A	21.5	18.0	3.7	Yes, in	2	Fan mixt
14	Dunajec River Bridge	A	27.0	-	-	Yes, in	2	Fan mixt
15	Myakinino Footbridge	A	41.0	-	-	No	2	Fan mixt
16	FB over Ibar river	I	42.8	36.0	6.8	No	1	Harp
17	Saint Irinej	I	40.0		-	No	1	Fan mixt
18	7th Av. Ped. Bridge	I	28.7	20.5	8.2	Yes, out	1	Fan mixt
19	Glorias Catalanas	I	34.1	24.6	9.5	No	1	Harp
20	Voluntariado	I	75.0	-	-	No	1	Fan mixt
21	Malecon	I	15.0	-	-	No	1	Fan mixt
22	FB over Ticino River	A	37.0	28.0	9.0	No	2	Fan
23	UG1 Footbridge		40.0	-	-	No	2	Fan mixt
24	Zabeel Park Footbridge	A	52.0	-	-	No	2	Fan mixt
25	Golden Jubilee	I	28.0	20.0	8.0	No	2	Fan
26	Media City	I	31.0	-	-	Yes, out	1	Fan mixt
27	Christchurch Bridge	I	39.0	-	-	No	2	Fan mixt
28	Delta Pond	H	25.5	18.0	7.5	No	2	Fan mixt
29	Reiman Bridge	I	50.0	-	-	Yes, out	1	Fan mixt
30	Ohio and Erie Canalway	H		14.5	-	No	2	Fan mixt
31	Turtle Bay Sundial Bridge	I	66.0	-	-	Yes, out	1	Harp
32	Manzanares	I	42.0	-	-	No	1	Fan mixt

Annex C Footbridge dataset with supplemental damping devices

#	Name	Country	Year	Structure	Damper device	Length (m)	Structural frequencies (Hz)	Predominant vibration direction
1	Beisbane Kurilpa	Australia	2009	Cable-Stayed footbridge	TMD	470.0	1.8	Lateral
2	Wernstein	Austria	2006	Suspension footbridge	TMD	144	1.2	Vertical
3	Mechelen	Belgium	2012	Steel structure with an L-shaped cross section	TMD	31	3.75	Lateral
4	Alexandra	Canada	2010	Truss bridge with five spans	Viscous damper	563	-	-
5	Panjin Ianhua	China	2015	-	Viscous damper	-	-	-
6	Pilsen	Czech Republic	2003	Cable-Stayed footbridge	TMD	64.8	1.33-2.93	Vertical
7	Langelinie	Denmark	2005	Girder footbridge	TMD	169.8	1.4 - 4.2	Vertical
8	Danish Marine Museum footbridge	Denmark	2013	-	Viscous damper	61	2.2	Vertical
9	Stade de France	France	1997	Girder footbridge	TMD	191.25	1.8- 2.1	Vertical
10	Cavaillon	France	1957	Truss footbridge	TMD	99.4	1.95	Vertical
11	Solferino	France	2000	Arch bridge	TMD	140	0.8-2.2	Lateral & Vertical
12	Noisy-le-Grand	France	1994	Haunched girder bridge	TMD	123.05	1.65	Vertical
13	Montigny-lès-Cormeilles	France	1999	Bow-string arch	TMD	55	2.54	Vertical
14	Footbridge over the Aisne at Soissons	France	-	Suspension footbridge	TMD	60	1.1	Vertical

#	Name	Country	Year	Structure	Damper device	Length (m)	Structural frequencies (Hz)	Predominant vibration direction
15	Bercy Tolbiac	France	2006	Lenticular truss bridge	Tuned liquid dampers	-	-	-
16	Pas-du-lac footbridge at St Quentin	France	1992	Cable-Stayed footbridge	TMD	188	1.38	Vertical
17	Mon-Saint-Martin	France	-	Mixed construction beam footbridge	TMD	23	2.15	Vertical
18	Bundeskanzleramt	Germany	2000	-	TMD	-	1.7 - 3.3	Vertical
19	Forcheim	Germany	2002	Cable-Stayed footbridge	TMD	117.5	1.2 - 2.7	Vertical
20	Freilassing	Germany	2002	Girder footbridge	TMD	-	-	Vertical
21	Dorsten	Germany	1980	Girder footbridge	TMD	59.55	-	Vertical
22	Kassel	Germany	1998	-	TMD	133.2	-	Vertical
23	Bundeskanzleramt	Germany	2000	-	TMD	-	-	Vertical
24	Schwedter Straβe	Germany	1999	Cable-Stayed footbridge	TMD	209	1.9	Vertical
25	Britzer Damm	Germany	2001	Hinged steel arch	TMD	33.8	5.6	Vertical
26	Schwedter StraBe	Germany	1999	Cable-Stayed footbridge	TMD	209	1.9	Vertical
27	Mindem	Germany	-	Suspension footbridge	Telescopic hydraulic dampers	103	-	Lateral & Vertical
28	Duisburg	Germany	1999	Suspension footbridge	Frictional dampers	73.72	-	Lateral
29	Millennium Bridge	Great Britain	2001	Suspension footbridge	TMD + Viscous dampers	370	0.8 - 2.2	Lateral & Vertical

#	Name	Country	Year	Structure	Damper device	Length (m)	Structural frequencies (Hz)	Predominant vibration direction
30	Coventry	Great Britain	2003	-	TMD	-	-	Vertical
31	Port Tawe	Great Britain	2003	Cable-Stayed footbridge	TMD	142	1.1	Lateral
32	Stockton on Tees Northshore	Great Britain	2008	Arch bridge	TMD	180	0.8 - 2.5	Lateral & Vertical
33	Barberino di Mugello	Italy	2002	-	TMD	-	1.6 - 2.3	Vertical
34	The Ponte del Mare in Pescore	Italy	2010	Cable-Stayed footbridge	TMD	466	-	-
35	T-Bridge	Japan	1989	Cable-Stayed footbridge	Tuned liquid dampers	179	0.93	Lateral
36	Aratsu	Japan	1988	Cable-Stayed footbridge	TMD	345	-	-
37	Mjomnesundet	Norway	1996	Girder footbridge	TMD	-	0.8	Vertical
38	Sun You	South Korea	2002	Arch bridge	TMD	120	0.75 - 2	Lateral & Vertical
39	"Zabia Kladka"	Poland	2004	-	TMD	-	1.2 - 1.5	Vertical
40	Pedro and Inés	Portugal	2006	Arch footbridge	TMD	110	0.85	Lateral & Vertical
41	Changi Airport Footbridge	Singapore	2003	Arch footbridge	TMD	140	0.9	Lateral
42	Abandoibarra	Spain	-	-	TMD	-	1.85 - 2.78	Vertical
43	Bagers Bro	Sweden	-	Truss footbridge	TMD + Viscous dampers	37	-	-
44	Rümlang	Switzerland	1992	Cable-Stayed footbridge	TMD	45	2	Vertical
45	Jatujak	Thailand	-	Truss footbridge	MTMD	33.6	-	Vertical

#	Name	Country	Year	Structure	Damper device	Length (m)	Structural frequencies (Hz)	Predominant vibration direction
46	Capital Gate Tower Footbridge	UAE	2010	-	TMD	-	3.5	Vertical
47	YAS Marina Hotel Footbridge	UAE	2009	-	TMD	-	1.8 - 2.7	Vertical
48	Ridgefield NWR	USA	2014	-	Viscous damper	-	-	-
49	Atlanta Botanical Garden (walkway)	USA	2008	-	Viscous damper	-	-	-
50	Cumberland River Pedestrian Bridge	USA	2007	Girder footbridge	TMD	144.7	-	-
51	Spring Mountain Road Pedestrian Bridges	USA	2005	-	Tuned liquid dampers	-	-	-
52	Bellagio Bally	USA	1998	Girder footbridge	TMD	46 m	1.7 - 2.2	Vertical

References

Abaqus, 2014. *Dassault Systemes Simulia Corp.*. Abaqus v. 6.14-2: Analysis User's Guide - Online Documentation.

Andriacchi, T., Ogle, J. & Galante, J., 1977. Walking speed as a basis for normal and abnormal gait measurements. *Journal of biomechanics,* 10(4), pp. 261-268.

Asami, T., Nishihara, O., and Baz, A. (2002). "Analytical solutions to Hinfinity and H2 optimization of dynamic vibration absorbers attached o damped linear systems." J. Vib. Acoust., 124(2), 284–295.

Bachmann, H., 1992. Vibration upgrading of gymnasia, dance halls and footbridges. *Structural Engineering International,* 2(2), pp. 118-124.

Bachmann, H. & Ammann, W., 1987. *Vibrations in structures: induced by man and machines.* 3 ed. Zurich: IABSE.

Bachmann, H. & Weber, B., 1995. Tuned Vibration Absorbers for "Lively" Structures. *Structural Engineering International,* 5(1), pp. 31-36.

Bauby, C. & Kuo, A., 2000. Active control of lateral balance in human walking. *Journal of biomechanics,* 33(11), pp. 1433-1440.

BBC, 2019. *What is the UK's inflation rate?*. [Online] Available at: https://www.bbc.co.uk/news/business-12196322.

Benicke, O., 2017. *Email to Natividad Leonor Garcia Troncoso, 30 November*.

Benicke, O., 2019. *Email to Natividad Leonor Garcia Troncoso, 20 October*.

Blanchard, J., Davies, B. L. & Smith, J. W., 1977 . *Design criteria and analysis for dynamic loading of footbridges.* In: Symposium on Dynamic Behaviour of Bridges. Ed. by Transport and Structures Department Road Research Laboratory Bridge Design Division, Crowthorne, Berkshire, UK.

Bocian, M., Macdonald, J. & Burn, J., 2012. Biomechanically inspired modelling of pedestrian-induced forces on laterally oscillating structures. *Journal of Sound and Vibration,* 331(16), pp. 3914-3929.

Bourne, S., 2013. Prestressing: recovery of the lost art. *Structural Engineering, Volume 91(2),* pp.12-22.

Breman, C., Stuit, H. & Snijder, B., 2011. *Dynamic Analysis of the Rotterdam Central Station Footbridge.* Footbridge 2011, Fourth International Conference, Wroclaw, Poland.

Breukleman, B., Gamble, S., Kottenlenberg, J. & Haskett, T., 2002. *Footbridge damping systems: a case study.* Footbridge 2002, Conception et comportament dynamique des passerelles pietonnes, Paris, France.

Brownjohn, J., P. Fok, M. R. & Omenzetter, P., 2004. "Long span steel pedestrian bridge at Singapore Changi Airport - Part 2: Crowd loading tests and vibration mitigation measures". *In: The Structural Engineer ,* Volume 82, p. 7.

Brownjohn, J. P. A. & Omenzetter, P., 2004. Canadian Journal of Civil Engineering. *A spectral density approach for modelling continuous vertical forces on pedestrian structures due to walking,* 31(1), pp. 64-77.

BSI, 2003. *BS EN 1991-2:2003.* UK National Standard implementation of Eurocode 1: Actions on structures - Part 2: Traffic loads on bridges: BS. London, UK: British Standards Institution.

BSI, 2008. *NA to BS EN 1991-2:2003.* UK National Annex to Eurocode 1: Actions on structures. Part 2: Traffic loads on bridges: BS. London, UK: British Standards Institution.

BSI, 2009. *BS EN 1993-2:1997.* Eurocode 3: Design of steel structures. Part 2: Steel bridges: BS. London, UK: British Standards Institution.

BSI, 2009. *BS EN 1995-1:2004.* Eurocode 5: Design of timber structures. Part 1-1: General-common rules and rules for buildings: BS. London, UK: British Standards Institution.

BSI, 2010a. *BS EN 1993-1:2004.* Eurocode 3: Design of steel structures. Part 1-1: General rules and rules for buildings: BS. London, UK: British Standards Institution.

BSI, 2010b. *BS EN 1999-1-1:2004.* Eurocode 9: Design of aluminium structures. Part 1-1: General structural rules: BS. London, UK: British Standards Institution.

BSI, 2010c. *BS EN 338:2009.* Structural timber. Strength classes: BS. London, UK: British Standards Institution.

BSI, 2011. *BS EN 1992-1:2004.* Eurocode 2: Design of concrete structures. Part 1-1: General rules and rules for buildings: BS. London, UK: British Standards Institution.

Butz, C. et al., 2007. *Advanced load models for synchronous pedestrian excitation and optimised design guidelines for steel footbridges.* European Commission: Research Fund for Coal and Steel.

Cadei, J. & Stratford, T., 2002. *The design, construction and in-service performance of the all-composite Aberfeldy footbridge.* Advanced Polymer Composites for Structural Applications in Construction. ICE Publishing, Southampton, UK.

Caetano, E., Cunha, Á., Magalhães, F. & Moutinho, C., 2010a. Studies for controlling human-induced vibration of the Pedro e Inês footbridge, Portugal. Part 1: Assessment of dynamic behaviour. *Engineering Structures,* 32(4), pp. 1069-1081.

Caetano, E., Cunha, Á., Moutinho, C. & Magalhães, F., 2010b. Studies for controlling human-induced vibration of the Pedro e Inês footbridge, Portugal. Part 2: Implementation of tuned mass dampers. *Engineering Structures,* 32(4), pp. 1082-1091.

Caetano, E. & Cunha, A., 2014. *Vibration mitigation of footbridges: case studies.* London, UK, Footbridge 2014 - Past, Present and Future.

Caetano, E., Cunha, A. & Martins, L., 2011. *Assessment of running pedestrian induced vibrations on a stress-ribbon footbridge.* Footbridge 2011, Fourth International Conference, Wroclaw, Poland.

Caetano, E., Cunha, A. & Moutinho, C., 2007. *Implementation of passive devices for vibration control at Coimbra footbridge.* Porto, In Proceedings of the 2nd International Conference on Experimental Vibration Analysis for Civil Engineering Structures.

Camara, A. & Ruiz-Teran, A. M., 2015. "Multi-mode traffic-induced vibrations in composite ladder-deck bridges under heavy moving vehicles". *Journal of Sound and Vibration,* Vol. 355, pp. 264–283, DOI: 10.1016/j.jsv.2015.06.026.

Carroll, S., Owen, J. & Hussein, M., 2013. Reproduction of lateral ground reaction forces from visual marker data and analysis of balance response while walking on a laterally oscillating deck. *Engineering Structures,* Volume 49, pp. 1034-1047.

Charles, P. et al., 2006. *Footbridges Assessment of vibrational behaviour of footbridges under pedestrian loading.* Guideline: SETRA / AFGC.

Clarke, J. L., 1996. *Structural design of polyme composites: EUROCOMP design code and handbook.* Design code. london, UK: European Structural Polymeric Composites Group.

Clough, R. & Penzien, J., 1993. *Dynamics of structures.* Second ed. London: McGraw-Hill.

Collette, F., 2002. *Tuned Mass Dampers for a suspended structure of footbridges and meeting boxes.* Footbridge 2002, Conception Conception et comportament dynamique des passerelles pietonnes, Paris, France.

Dallard, P. et al., 2001. “The London Millennium Footbridge”. *In: The Structural Engineer,* 79(22), pp. 17–33.

Danbon, F. & Grillaud, G., 2005. *“Dynamic behaviour of a steel footbridge. Characterisation and modelling of the dynamic loading induced by a moving crowd on the Solferino footbridge in Paris”.* In: Footbridge 2005, Second International Conference, Venice, Italy.

Daniel, Y., Lavan, O. & Levy, R., 2011. Multiple-tuned mass dampers for multimodal control of pedestrian bridges. *Journal of Structural Engineering,* 138(9), pp. 1173-1178.

Živanović, S., Feltrin, G., Mottram, J. & Brownjohn, J., Vibration Performance of Bridges Made of Fibre Reinforced Polymer. In: Catbas F. (eds) Dynamics of Civil Structures. *2014,* Volume 4, pp. 155-162.

Živanović, S., Pavic, A. & Reynolds, P., 2005. "Vibration serviceability of footbridges under human-induced excitation: A literature review". *In: Journal of sound and vibration,* 279(1), pp. 1-74.

Živanović, S., Pavic, A. & Reynolds, P., 2006. Modal testing and FE model tuning of a lively footbridge structure. *Engineering Structures,* 28(6), pp. 857–868.

Živanović, S., Pavic, A. & Reynolds, P., 2007. “Probability-based prediction of multi-mode vibration response to walking excitation”. *Engineering Structures 29 (6),* pp. 942–954.

Feldmann, M., Heinemeyer, C. & Lukic, M., 2008. *Human-induced vibration of steel structures,* HIVOSS.

fib, 2006. *fib Bulletin 32: Guidelines for the design of footbridges,* Guideline: International Federation for Structural Concrete.

Fiebig, W., 2010. Reduction of Vibrations of Pedestrian Bridges Using Tuned Mass Dampers (TMD). *Archives of Acoustics,* 35(2), pp. 165–174.

Fujino, P., Pacheco, B., Nakamura, S. & Warnitchai, P., 1993. "Synchronization of human waking observed during lateral vibration of a congested pedestrian bridge". *Earthquake Engineering and Structural Dynamics,* 22(9), pp. 741-758.

Fujino, Y. & Siringoringo, D., 2015. A Conceptual Review of Pedestrian-Induced Lateral Vibration and Crowd Synchronization Problem on Footbridges. *Journal of Bridge Engineering,* 21(8), p. C4015001.

Garcia-Troncoso, N., Ruiz-Teran, A. & Stafford, P., 2017. *Dynamic response of girder footbridges with supplemental damping.* Footbridge 2017, Sixth International Conference, Berlin, Germany.

Gierke, H. & Goldman, D., 1988. *Effects of shock and vibration on man,* New York: McGraw-Hill: Shock and vibration handbook, 3rd edition.

Gimsing, N. J. & Georgakis, C. T., 2012. *Cable supported bridges: concept and design.* Ed. by Wiley. Chichester.

Gu, M. C. S. & Chang, C., 2001. Parametric study on multiple tuned mass dampers for buffeting control of Yangpu Bridge. *Journal of Wind Engineering and Industrial Aerodynamics,* 89(11-12), pp. 987–1000.

Hatanaka, A. & Kwon, Y., 2002. *Retrofit of footbridge for pedestrian induced vibration using compact tuned mass damper.* Footbridge 2002, Conception et comportament dynamique des passerelles pietonnes, Paris, France.

Heinemeyer, C. & Feldmann, M., 2008. *European design guide for footbridge vibration.* Footbridge 2008, Third International Conference, Porto, Portugal.

Heinmeyer, C. et al., 2009. *Design of Leightweight footbridges for human induced vibrations.* Italy: FEUP.

Helbing, D., 1998. *A fluid dynamic model for the movement of pedestrians.* Germany: arXiv preprint cond-mat/9805213.

Helbing, D. & Molnar, P., 1995. Social force model for pedestrian dynamics. *Physical review E,* 51(5), p. 4282.

Highways Agency, 2001. *BD37/01 Design Manual for Roads and Bridges, Volume 1, Section 3, Part 14, Department of Transport, Highway and Traffic,* Loads for Highway Bridges: Departmental Standard.

Hilber, H. M., Hughes, T. J. R. & Taylor, R. L., 1977. Improved numerical dissipation for time integration algorithms in structural dynamics. *Earthquake Engineering and Structural Dynamics,* Volume 5, pp. 283-292.

Ingólfsson, E., Georgakis, C. & Jönsson, J., 2012. "Pedestrian-induced lateral vibrations of footbridges: A literature review". *In: Engineering Structures,* Volume 45, pp. 21-52.

ISO, 2005. *ISO 10137:2007.* Basis for Design of Structures Serviceability of Buildings and Pedestrian Structures againts Vibration. ISO, Committee Draft: Geneva: International Organisation for Standards.

Jiménez-Alonso, J. & Sáez Pérez, A., 2015. *Estimating robust optimum parameters of tuned mass dampers using multiobjective genetic algorithms.* Sevilla, España, 3rd International Conference on Mechanical Models in Structural Engineering CMMoST.

Jiménez-Alonso, J., Sáez, A., Caetano, E. & Magalhãe, F., 2016. Vertical crowd-structure interaction model to analyze the change of the modal properties of a footbridge. *Journal of Bridge Engineering,* 21(8).

Jones, R. & Pretlove, A., 1981. TWO CASE STUDIES IN THE USE OF TUNED VIBRATION ABSORBERS ON FOOTBRIDGES. *Structural Engineer. Part b,* 59(2).

Kala, J., Hradil, P., Salajka, V. & Jüttner, V., 2010. *DYNAMIC RESPONSE OF CABLE-STAYED STEEL BRIDGE WITH TUNED MASS DAMPER INSTALLED NUMERICAL AND EXPERIMENTAL APPROACH.* Vilnius, Modern building materials, structures and techniques.

Karásek, P. et al., 2005. *Dynamic behaviour of a steel cable–stayed footbridge damped by TMD.* Paris, Proceedings of the 4th International Conference on Structural Dynamics–EURODYN 2005 (pp. 521-526).

Keller, T. et al., 1996. Relationship between vertical ground reaction force and speed during walking, slow jogging, and running. *Clinical Biomechanics,* 11(5), pp. 253-259.

Kobori, T. & Kajikawa, Y., 1974. Ergonomic evaluation methods for bridge vibrations. *Proceedings of the Japan Society of Civil Engineers,* 1974(230), pp. 40–41.

Krenk, S., Brønden, A. & Kristensen, A., 2005. *Placement and tuning of resonance dampers on footbridges.* Footbridge 2005, Second International Conference, Venice, Italy.

Labonnote, N., Rønnquist, A. & Malo, K., 2013a. Experimental evaluations of material damping in timber beams of structural dimensions. *Wood Science and Technology,* 47(5), p. 1033–1050.

Li, Q. et al., 2010. Crowd-induced random vibration of footbridge and vibration control using multiple tuned mass dampers. *Journal of Sound and Vibration,* 329(19), pp. 4068–4092.

Low, A., 2008. *Design for dynamic effects in long span footbridges.* Proceedings of Footbridge 2008, Third International Conference, Porto, Portugal.

Macdonald, J., 2009. Lateral excitation of bridges by balancing pedestrians. *Proceedings of the Royal Society a-Mathematical Physical and Engineering Sciences,* 465(2104), pp. 1055-1073.

Marano, G., Quaranta, G. & Greco, R., 2009. Multi-objective optimization by genetic algorithm of structural systems subject to random vibrations. *tructural and Multidisciplinary Optimization,* 39(4), pp. 385–399.

Matlab, 2015. *The MathWorks, Inc.* Matlab R2015a: v. 8.5.0.

Matsumoto, Y., Nishioka, T., Shiojiri, H. & Matsuzaki, K., 1978. Dynamic design of footbridges. *IABSE proceedings,* Volume 2, pp. 21-52.

Meinhardt, C., 2008. *Application of Tuned Mass Dampers for Bridge Decks.* Footbridge 2008, Third International Conference, Porto, Portugal.

Meinhardt, C., Dressen, O. & Dalmer, F., 2008. *Increase of the structural damping due to the application of tuned mass dampers TMD subject to the footbridge construction.* Footbridge 2002, Conception Conception et comportament dynamique des passerelles pietonnes, Paris, France.

Meinhdart, C., Newland, D., Talbot, J. & Taylor, D., 2017. *Vibration performance of London's Millennium.* 24th International congress on sound and vibration, London, United Kingdom.

Mercier, H. et al., 2012. *Vibration problems in structures: practical guidelines.* Vol. 3 ed. Practical Guidelines: Birkhäuser.

Mevada, H. & Patel, D., Experimental determination of structural damping of different materials. *In: 12th International Conference on Vibration Problems.* ICOVP, 2015.

Miguel, L., Fadel Miguel, L. & Lopez, R., 2014. A firefly algorithm for the design of force and placement of friction dampers for control of man-induced vibrations in footbridges. *Optimization and Engineering,* 16(3), p. 633–661.

Mohebbi, M., Shakeri, K., Ghanbarpour, Y. & Majzoub, H., 2013. Designing optimal multiple tuned mass dampers using genetic algorithms (GAs) for mitigating the seismic response of structures. *Journal of Vibration and Control,* 19(4), p. 605–625.

Moutinho, C., Cunha, A. & Caetano, E., 2007. Implementation of an active mass damper to control vibrations in a lively footbridge. *In III Eccomas Thematic Conference on Smart Structures And Materials,* July.pp. 1-18.

Nakamura, S., 2004. "Model for lateral excitation of footbridges by synchronous walking". *In: Journal of Structural Engineering-Asce ,* 130(1), p. 32–37.

Nakamura, S. & Fujino, Y., 2002. Lateral vibration on a pedestrian cable-stayed bridge. *Structural Engineering International,* 12(4), pp. 295-300.

Nakamura, S. & Kawasaki, T., 2006. Lateral vibration of footbridges by synchronous walking. *Journal of Constructional Steel Research,* 62(11), p. 1148–1160.

Oliveira, C., 2014. Fundamental frequencies of vibration of footbridges in Portugal: from in situ measurements to numerical modelling. *Shock and Vibration,* Volume 2014, p. 22.

Pachi, A. & Ji, T., 2005. Frequency and velocity of people walking. *Journal of Structural Engineer,* 83(3), p. 5.

Pedersen, L. & Frier, C., 2010. Sensitivity of footbridge vibrations to stochastic walking parameters. *Journal of Sound and Vibration,* 329(13), pp. 2683-2701.

Pizzimenti, A. D. & Ricciardelli, F., 2005. *"Experimental evaluation of the dynamic lateral loading of footbridges by walking pedestrians".* 6th European Conference on Structural Dynamics EURODYN 2005, Ed. by C. Soize and G. Schueller. Paris, France.

Racic, V. & Brownjohn, J., 2011. Advanced Engineering Informatics. *Stochastic model of near-periodic vertical loads due to humans walking,* 25(2), pp. 259-275.

Ramos, C., Ruiz-Teran, A. & Stafford, P., 2014. *Footbridge response: Improved understanding through probabilistic interpretation.* Footbridge 2014 - Past, Present and Future, London, UK.

Ramos, C., Ruiz-Teran, A. & Stafford, P., 2017. *Serviceability response of a benchmark cable-stayed footbridge: Comparison of available methods' prediction.* Footbridge 2017, Sixth International Conference, Berlin, Germany.

Ramos, C., Ruiz-Teran, A. & Stafford, P., 2019. *Impact of stochastic representation of pedestrian actions on serviceability response.* ICE proceedings (submitted).

Ramos-Moreno, C., 2015. *DESIGN OF CABLE-STAYED FOOTBRIDGES UNDER SERVICEABILITY LOADS.* A thesis submitted to Imperial College London for the degree of Doctor of Philosophy ed. London: Imperial College London. Full text available at Imperial College London open-access research repository (https://spiral.imperial.ac.uk/handle/10044/1/58244).

Rose, J. & Gamble, J., 1994. Human Walking. *London: Williams & Wilkins,* 43c(2nd ed.), pp. 112-115.

Sahnaci, C. & Kasperski, M., 2005. *Random loads induced by walking.* In: 6th European Conference on Structural Dynamics EURODYN 2005. Ed. by C. Soize and G. Schueller., Paris, France, pp. 441–446.

Schubert, S., Gsell, D., Steiger, R. & Feltrin, G., 2010. Influence of asphalt pavement on damping ratio and resonance frequencies of timber bridges. *Engineering Structures,* 32(10), pp. 3122-3219.

Seiler, C., Fischer, O. & Huber, P., 2002. *Semi-active MR dampers in TMD's for vibration control of footbridges, Part 2: numerical analysis and practical realisation.* Footbridge 2002, Conception Conception et comportament dynamique des passerelles pietonnes, Paris, France.

Setareh, M. & Hanson, R., 1992. Tuned mass dampers to control floor vibration from humans. *Journal of Structural Engineering,* 118(3), pp. 741-762.

Soong, T. & Dargush, G., 1997. *Passive energy dissipation systems in structural engineering.* Illustrated ed. Wiley.

Strasky, J., 2011. Stress Ribbon and Cable-supported Pedestrian Bridges. In: S. Edition, ed. *Stress Ribbon and Cable-supported Pedestrian Bridges.* ICE Publishing, pp. 155-169.

Structurae, 2015. *Structurae: International database for civil and structural engineers,* url: http://structurae.net.

Tilly, G., Cullington, D. & Eyre, R., 1984. Dynamic behaviour of footbridges. *IABSE,* Volume 26, pp. 12-24.

Townsend, M., 1985. Biped gait stabilization via foot placement. *Journal of biomechanics,* 18(1), pp. 21-38.

Tubino, F. & Piccardo, G., 2015. Tuned Mass Damper optimization for the mitigation of human-induced vibrations of pedestrian bridges. *Meccanica,* 50(3), pp. 809–824.

Umashankar, K. S., Abhinav, A., Gangadharan, K. V. & Vijay, D., 2009. Damping behaviour of cast and sintered aluminium. *ARPN Journal of Engineering and Applied Sciences,* 4(6), pp. 66-71.

Van Nimmen, K., Lombaert, G., De Roeck, G. & Van den Broeck, P., 2014a. Vibration serviceability of footbridges: Evaluation of the current codes of practice. *Engineering Structures ,* Volume 59, pp. 448–461.

Van Rossum, G. & L., D. F. L., 2010. *The Python Language Reference.* Python Software Foundation, 2010.

Venuti, F. & Bruno, L., 2007. An interpretative model of the pedestrian fundamental relation. *Comptes Rendus Mécanique,* 335(4), pp. 194-200.

Warburton, G., 1982. Optimum absorber parameters for various combinations of response and excitation parameters. *Earthquake Engineering & Structural Dynamics,* 10(3), pp. 381-401.

Weber, B. & Feltrin, G., 2010. Assessment of long-term behavior of tuned mass dampers by system identification. *Engineering structures,* 32(11), pp. 3670-3682.

Wells, M. & Clash, P., 2008. Footbridges. In: *ICE Manual of Bridge Engineering.* London: Thomas Telford Ltd, pp. 459-484 .

Wheeler, J., 1982. Prediction and Control of Pedestrian Induced Vibration in Footbridges. *Journal of the Structural Division-Asce,* 108(ST9), pp. 2045-2065.

Yamaguchi, H. & Harnpornchai, N., 1993. Fundamental characteristics of Multiple Tuned Mass Dampers for suppressing harmonically forced oscillations. *Earthquake Engineering & Structural Dynamics,* 22(1), pp. 51–62.

Yang, X., 2009. *Firefly algorithms for multimodal optimization.* Berlin Heidelberg, Springer, pp. 169-178.